GEOLOGIJA

2015 | št.: **58/2**

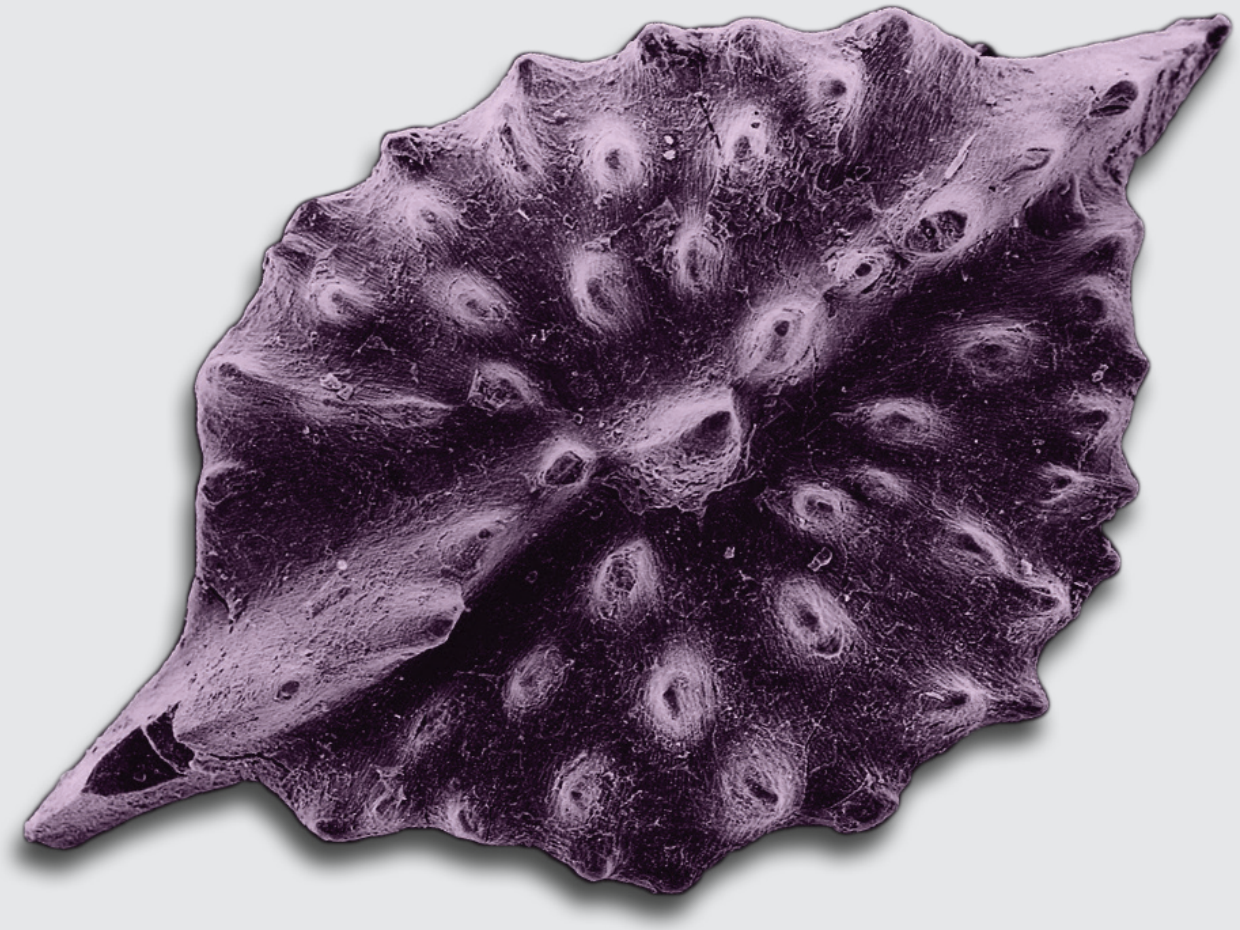

Geološki zavod Slovenije
Geological Survey of Slovenia

ISSN
Tiskana izdaja / Print edition: 0016-7789
Spletna izdaja / Online edition: 1854-620X

GEOLOGIJA

58/2 – 2015

GEOLOGIJA	2015	58/2	105-269	Ljubljana

GEOLOGIJA
ISSN 0016-7789

Izdajatelj: Geološki zavod Slovenije, zanj direktor Miloš Bavec
Publisher: Geological Survey of Slovenia, represented by Director Miloš Bavec
Financirata Javna agencija za raziskovalno dejavnost Republike Slovenije in Geološki zavod Slovenije
Financed by the Slovenian Research Agency and the Geological Survey of Slovenia

Vsebina številke 58/2 je bila sprejeta na seji Uredniškega odbora, dne 21. 12. 2015.
Manuscripts of the Volume 58/2 accepted by Editorial and Scientific Advisory Board on December 21, 2015.

Naslov uredništva / Editorial Office: GEOLOGIJA Geološki zavod Slovenije / Geological Survey of Slovenia
Dimičeva ulica 14, SI-1000 Ljubljana, Slovenija
Tel.: +386 (01) 2809-700, Fax: +386 (01) 2809-753, e-mail: urednik@geologija-revija.si
URL: http://www.geologija-revija.si/

GEOLOGIJA izhaja dvakrat letno. / GEOLOGIJA is published two times a year.
GEOLOGIJA je na voljo tudi preko medknjižnične izmenjave publikacij. /
GEOLOGIJA is available also on exchange basis.

Izjava o etičnosti
Izdajatelji revije Geologija se zavedamo dejstva, da so se z naglim naraščanjem števila objav v svetovni znanstveni literaturi razmahnili tudi poskusi plagiatorstva, zlorab in prevar. Menimo, da je naša naloga, da se po svojih močeh borimo proti tem pojavom, zato v celoti sledimo etičnim smernicam in standardom, ki jih je razvil odbor COPE (Committee for Publication Ethics).

Publication Ethics Statement
As the publisher of Geologija, we are aware of the fact that with growing number of published titles also the problem of plagiarism, fraud and misconduct is becoming more severe in scientific publishing. We have, therefore, committed to support ethical publication and have fully endorsed the guidelines and standards developed by COPE (Committee on Publication Ethics).

Baze, v katerih je Geologija indeksirana / Indexation bases of Geologija: Scopus, Directory of Open Access Journals, GeoRef, Zoological Record, Geoscience e- Journals, EBSCOhost

Cena / Price

Posamezni izvod / Single Issue	Letna naročnina / Annual Subscription
Posameznik / Individual: 15 €	Posameznik / Individual: 25 €
Institucija / Institutional: 25 €	Institucija / Institutional: 40 €

Tisk / Printed by: Tiskarna Formatisk d.o.o.

Slika na naslovni strani: konodont *Foliella gardenae* (Staesche) iz spodnjetriasnih plasti blizu Tržiča. (Kolar-Jurkovšek, T. & Jurkovšek, B., članek v tej številki)

Cover page: conodont *Foliella gardenae* (Staesche) from Lower Triassic strata near Tržič. (Kolar-Jurkovšek, T. & Jurkovšek, B., paper in this issue)

GEOLOGIJA *58/2*, 105-269, Ljubljana 2015

VSEBINA – CONTENTS

GEOLOGIJA *58/2*, 109–110 Ljubljana 2015
http://dx.doi.org/10.5474/geologija.2015.000

Uvodnik

Spoštovane bralke, spoštovani bralci!

V naslednjem letu se založniku Geologije Geološkemu zavodu Slovenije obeta velik jubilej. Minilo bo sedemdeset let odkar je tedanja slovenska vlada ustanovila našega predhodnika Geološki zavod Ljubljana. V dolgem, zanimivem, raznolikem in konec koncev na srečo niti ne pretirano burnem življenju se je Geološki zavod utrdil na položaju osrednje državne inštitucije na področju geologije, ki povezuje temeljne in aplikativne raziskave, strokovno in razvojno delo.

Jubilej bomo uporabili kot možnost za pogled naprej in za utrditev položaja našega javnega raziskovalnega zavoda na mestu, ki ga zavzema v skladu z njegovim ustanovnim aktom, pa tudi v skladu s primerljivimi geološkimi zavodi v Evropi in po svetu. Kaj je ključna razlika med geološkimi zavodi in znanstvenoraziskovalnimi inštituti s področja geologije? Celovitost obravnavanja državnega ozemlja in skrb za stroko na vseh ravneh; od temeljnega znanstvenoraziskovalnega dela, skrbnega zbiranja znanja in podatkov o geosferi, do njihovega prenosa v družbo na področju javne službe, sodelovanja v procesih izobraževanja v najširšem smislu ter v obliki podpore raznim uporabnim projektom, ki se dotikajo polj geoznanosti. Ni torej naključje, da bomo v naslednjem, jubilejnem letu izdali tudi Atlas geoloških kart Slovenije in knjigo 70 geoloških znamenitosti Slovenije. Napovedujemo tudi vzpostavitev portala e-geologija, ki bo od leta 2016 dalje na spletu prinašal raznolike geološke podatke iz našega bogatega digitalnega arhiva. Rezultati seveda niso samo naši. Ključna sestavina delovanja je dobro sodelovanje z bolj ali manj sorodnimi institucijami doma in v tujini. Na domačih tleh skoraj ni ustanove s področja naše ali sorodnih strok, s katero v dolgoletni zgodovini nismo uspešno sodelovali. Sodelovanje izven državnih meja je bilo že od ustanovitve rdeča nit GeoZS in na mednarodnem področju smo iz leta v leto bolj aktivni. Tudi zato, in ne samo zato, nas je doletela čast, da bomo lahko v naslednjem letu v Ljubljani gostili sestanek najvišjih predstavnikov vseh evropskih geoloških zavodov.

Glede na to, da širše okolje vedno bolj prepoznava pomen in uporabnost geološkega znanja, in glede na to, da so geoznanosti bolj kot kadarkoli sposobne vračati uporabno znanje družbi, se lahko sedanja generacija geologov resnično iskreno zahvali vsem predhodnikom za trdne temelje, na katerih lahko gradimo. V dobršni meri je bilo v Sloveniji v preteklih sedemdesetih letih to znanje zbrano v okviru Geološkega zavoda Slovenije in njegovih predhodnikov.

Geologiji gre torej dobro. Ne samo pri nas. Stoletja analitičnega raziskovalnega dela in desetletja eksplozivnega tehnološkega razvoja že nekaj časa obilno vračajo raziskovalcem in uporabnikom našega znanja. Današnji geološki modeli so iz dneva v dan bolj dovršeni, vseobsegajoči in utemeljeni na širokem naboru temeljnih in tematskih podatkov, razumevanju procesov in vse bolj koherentnih interpretacijah. Pojem geološka karta je dobil nov, razširjen pomen.

Prihodnost je torej svetla in temelji na znanju; ne glede na to, koliko bo besedna zveza »na znanju temelječa družba« modna v prihodnosti, ali včasih le uporaben okrasek kakšnemu nagovoru. Nedvomno bo tudi v prihodnje znanstvenoraziskovalno delo temelj geološke stroke in s tem tudi Geološkega zavoda Slovenije.

Še naprej bomo raziskovalci svoja spoznanja objavljali. Ni pomembno, ali bodo znanstvena dela ovrednotena s črticami, zvezdicami ali čebelicami. Objavljali bomo v dobrih revijah, tudi v takih, kot je v vaših rokah. Geologija je mednarodna revija z mednarodnim uredniškim odborom, obenem pa tudi osrednja slovenska znanstvena revija za širše področje geoloških ved. Od leta 1953 je izšla že v 77 zvezkih, v njej so bila objavljena prenekatera temeljna dela slovenskih geoznanosti. Vsebine člankov se močno prepletajo s sorodnimi vedami, kot so kemija, seizmologija, fizika, biologija ter z nekaterimi tehničnimi vedami. V reviji objavljamo vedno več interdisciplinarnih člankov, v katerih se geološko znanje uporablja za reševanje raznovrstnih drugih naravoslovnih problemov. To je neposreden odsev trenutnega položaja geologije kot ene od ključnih sinteznih znanstvenih področij v naravoslovju.

Tako kot celotna slovenska geološka stroka je tudi revija Geologija z leti vse bolj vpeta v širši prostor in mednarodno priznana. Vključena je v mednarodno bazo DOAJ (Directory of Open Access Journals, http://www.doaj.org/), ki omogoča takojšen prost dostop do celotnih člankov ter iskanje po avtorjih in ključnih besedah. Leta 2011 je Geološki zavod Slovenije postal član mednarodnega založniškega združenja PILA (Publishers International Linking Association). S tem se je založnik vključil v sistem CrossRef, ki je posrednik mednarodnih znanstvenih založnikov in omogoča založnikom, da pridobijo DOI - identifikator digitalnega objekta za vsako izdano publikacijo. Ob tem je revija indeksirana še v GeoRef, Zoological Record, Geoscience e-Journal, COBISS in EBSCO.

Pred koncem naj z vami, spoštovane bralke in spoštovani bralci, podelim še veselo novico o velikem darilu Geologije svojemu založniku ob prihajajočem jubileju. Leta 2015 je bila Geologija sprejeta v SCOPUS, eno najuglednejših svetovnih baz bibliografskih podatkov. To je nedvomno velik uspeh tako aktualnega kot prejšnjih uredništev, za kar se vsem zahvaljujem in jim čestitam, prav tako pa se seveda zahvaljujem tudi avtorjem in recenzentom, ki so s skrbno pripravljenimi prispevki omogočili trajen razvoj naše kvalitetne znanstvene revije.

Naj ob koncu dodam še veliko dobrih želja v prihajajočem, za založnika Geologije jubilejnem letu 2016. Začenja se dobro!

dr. Miloš Bavec, direktor GeoZS

GEOLOGIJA *58/2*, 111–120, Ljubljana 2015
http://dx.doi.org/10.5474/geologija.2015.009

Geochemical investigations of potentially toxic trace elements in urban sediments of Idrija

Geokemične raziskave potencialno strupenih slednih elementov v urbanih sedimentih Idrije

Špela BAVEC

Geological survey of Slovenia, Dimičeva ulica 14, SI–1000 Ljubljana, Slovenia, spela.bavec@geo-zs.si

Prejeto / Received 20. 8. 2015; Sprejeto / Accepted 27. 8. 2015; Objavljeno na spletu / Published online 2. 9. 2015

Key words: Idrija urban area, potentially toxic trace elements, SEM/EDS, urban sediment, Slovenia
Ključne besede: urbano območje Idrije, potencialno strupeni sledni elementi, SEM/EDS, urbani sediment, Slovenija

Abstract

Urban areas and associated human activities (industry, traffic, processes of mining and ore extracting, etc.) have induced anthropogenic emissions of potentially toxic trace elements (PTTE), which can present risk to living organisms and ecosystems in case of enriched levels. An example of such area in Slovenia is the Idrija town, the central part of the second largest Hg mining district in the world, which is heavily contaminated with Hg in all environmental compartments. The knowledge about levels and distribution of other PTTE in Idrija is very limited due to the outstanding Hg related problems. In this study the geochemical investigation of PTTE (As, Cd, Co, Cr, Cu, Mo, Ni, Pb and Zn) was performed in urban stream and road sediments of Idrija town for the first time. In addition, solid phases of PTTE were observed using SEM/EDS and their potential sources were assessed. The results show that the levels of PTTE in urban stream and road sediments are mostly below international guidelines, except for Cu some high values were measured in road sediments. The highest Cu level was determined in the vicinity of a commutator production industry. The associations of Cu with other elements in solid phases are very diverse, which is why the analyses could not reveal the specific source of high Cu levels.

Izvleček

Urbana območja in z njim povezane antropogene aktivnosti (industrija, promet, procesi rudarjenja in predelave rude, itn.) so pospešile antropogene emisije potencialno strupenih slednih elementov, ki lahko v primeru povišanih vrednosti predstavljajo tveganje za žive organizme in ekosisteme. Primer takega območja v Sloveniji je Idrija, osrednji del drugega največjega živosrebrovega rudarskega območja na svetu, ki je močno onesnažen s Hg v vseh segmentih okolja. Zaradi izjemnih problemov v povezavi s Hg je znanje o vsebnostih in porazdelitvi ostalih potencialno strupenih slednih elementov zelo omejeno. V tej študiji smo izvedli geokemično raziskavo potencialno strupenih slednih elementov (As, Cd, Co, Cr, Cu, Mo, Ni, Pb in Zn) v urbanih potočnih in cestnih sedimentih. Poleg tega smo z SEM/EDS metodo opazovali trdne faze potencialno strupenih slednih elementov in ugotavljali njihove potencialne izvore. Rezultati so pokazali, da so vrednosti potencialno strupenih slednih elementov v urbanih potočnih in cestnih sedimentih večinoma pod mednarodnimi smernicami, z izjemo visokih vrednosti Cu v cestnih sedimentih. Najvišja vrednost Cu je bila določena v bližini industrijskega obrata, v katerem proizvajajo komutatorje. Združbe Cu z drugimi elementi v trdnih fazah so zelo pestre, zato z analizo ni bilo možno oceniti specifičnega izvora visokih vrednosti Cu.

Introduction

Trace elements are chemical elements that occur in natural and perturbed systems in small amounts and among others include arsenic (As), cadmium (Cd), cobalt (Co), chromium (Cr), copper (Cu), molybdenum (Mo), nickel (Ni), lead (Pb), and zinc (Zn) (Adriano, 1986) that were investigated in this study. All investigated trace elements are metals, except As, which is a metalloid (Adriano, 1986). Co, Cu, Mo and Zn are essential for the nutrition of higher plants, while Co, Cr, Cu, Mo, Ni and Zn are essential for animal nutrition (Adriano, 1986; Addiscott, 2006). The essential trace elements are those which cannot be substituted by others in their specific biochemical roles and they have a direct negative influence on the organism, if their supply is inadequate (Adriano, 1986; Kabata Pendias & Pendias, 2001). An inadequate supply of trace elements can affect the living organism in two ways: either there is a lack of a trace element in the living organism (deficiency) or an excess of a trace element in the living organism (toxicity). In both cases, the growth of a plant or an animal is abnormal, so it can neither grow nor complete some metabolic cycle (Adriano, 1986; Kabata Pendias & Pendias, 2001). As, Cd and Pb are non-essential, which means that no beneficial function to the living organisms has been recognized yet for them and furthermore, when these elements are

present in sufficient concentrations they become toxic (Adriano, 1986; Kabata Pendias & Pendias, 2001; Addiscott, 2006). As explained above, all investigated elements can potentially cause harm to living beings in explicit conditions, this is why they are also called potentially toxic trace elements (PTTE). The sources of trace elements are primarily natural, such as soil parent materials (rocks) (Adriano, 1986). However, with urban development and associated human activities the anthropogenic sources of trace elements emerged, such as mining, industries and energy production, traffic, agriculture, construction- building materials, landfills and illegal waste dumps, etc. (Wong et al., 2006; Zupan et al., 2008). Anthropogenic influences induced PTTE emissions that often accumulate in earth materials of urban areas (urban materials) (Thornton et al., 2008; Johnson et al., 2011).

An example of contaminated urban materials are urban sediments of Idrija town (Slovenia), in which mercury (Hg) levels are several hundred times increased regarding to the European median for stream sediments due to the past Hg mining and ore processing activities (Bavec et al., 2014). Several natural and anthropogenic identified Hg sources (Čar, 1998; Čar & Terpin, 2005; Gosar & Čar, 2006; Mlakar & Čar, 2009, 2010; Kavčič, 2008) were recognised as sources of Hg in investigated sediments, such as outcrop of rocks containing Hg ore, former ore roasting sites, ore residue dumps and mine ventilation shafts (Bavec et al., 2014). After the Hg production was stopped in 1995, a commutator production industry evolved. In addition, Idrija is nowadays amongst higher urbanized areas in Slovenia that raised new scientific questions about accumulation of other PTTE in urban area of Idrija.

Therefore, in this study the levels of PTTE (As, Cd, Co, Cr, Cu, Mo, Ni, Pb and Zn) in the urban sediments of Idrija were determined and evaluated regarding to the European background for stream sediments and international guidelines. In addition, the solid phases of PTTE were observed and their potential sources were assessed.

Materials and methods

Site description and potential PTTE sources

Idrija town (Fig. 1), where past Hg mining district is situated, consists of a small densely populated centre with highly developed urban infrastructure along the rivers. The main river Idrijca flows through the district in the direction from south to north and has several tributaries (local streams). Another major stream, named Nikova, flows from the west and joins the river Idrijca in the centre of the town. The detailed surface water flow is presented in Fig. 1. For the majority of streams, regulation of natural waterways took place during the development of the town and consequently artificial channels were constructed. In addition, an urban drainage system has been established and runoff is discharged directly into the river Idrijca without any pre-

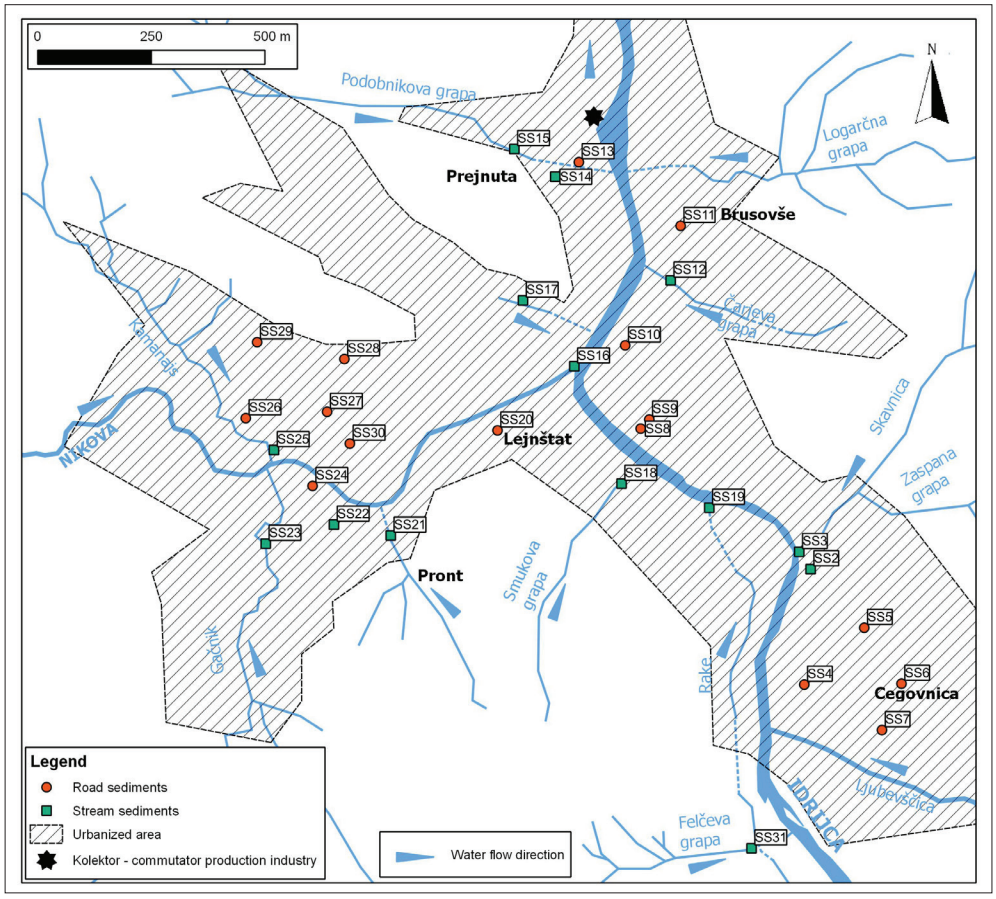

Fig. 1. Sediment sampling locations in the Idrija urban area and near surroundings (modified after Bavec et al., 2014).

treatment (Bavec et al., 2014). In Idrija town, the following trace element sources are recognised, besides local bedrock. There are two main roads following the rivers Idrijca and Nikova, where traffic is denser mostly during rush hours, while in the surroundings traffic is scarce. Ore deposit is monometallic, therefore Hg is the only mineral found in economically important quantities, while other elements occur only in traces or insignificant quantities (Čar, 1998). A commutator production industry is situated in the northern part of the town, where former Hg roasting facilities used to be. The industry started in the year 1963 as a small factory, but developed into a worldwide successful company as it is today (Kolektor, 2014). The biggest wastes in their manufacturing process are plastic and non-ferrous metals, primarily copper (Benčina, 2007).

Urban sediments

In the urban areas the major sites of sediment deposition are: street surfaces, gully pots and storm sewers, rivers, canals, docks and lakes (Fig. 2) (Taylor, 2007). Deposition and storage on street surfaces, gully pots and storm sewers is short term (in the order of days and month), while in canals, docks and on floodplains is longer term (in the order of years to decades, although they are not necessarily permanent due to erosion of floodplain banks and dredging of channels, canals and docks) (Taylor, 2007; Taylor & Owens, 2009).

Road-deposited sediment is the accumulation of particulate matter on street surfaces and it has received considerable attention in recent years, because it can be used to define current diffuse or local deposition of contaminants (Taylor, 2007; Johnson & Demetriades, 2011). Contaminated road sediment affects urban air quality and urban runoff. Gully pots are the first entry point of road runoff into the urban drainage network and are designed to trap some of the sediment carried by the runoff (Taylor & Owens, 2009). The processes acting within gully pots are complex. During runoff events (wet weather processes), denser particles in the water will settle under gravity. However, there is usually a high degree of turbulence within the gully pot, which not only limits the amount of sediment that will settle down, but may also lead to the erosion and resuspension of existing sediment in the pot. Biochemical changes also take place within the gully pot. Most biochemical changes take place during periods between runoff events (dry weather processes) (Taylor & Owens, 2009). Sediments within gully pots are neither wholly subaerial nor subaqueous, but experience both conditions episodically dependent on weather conditions (Taylor, 2007). The sources of road deposited sediments include vehicle exhaust emissions, vehicle tyre and body wear, break lining material, building and construction material, road salt, road paint and pedestrian debris, soil material, plant and leaf litter and atmospheric deposition (Taylor, 2007).

River bottom sediment is a mixture of mineral as well as organic material that is deposited on the bottoms of river channels (Taylor et al., 2008). In case of constant water flow, bottom sediment is often eroded or re-suspended within a channel by flowing water, so the composition of sediment is constantly changing. The sources of river sediments have much larger background than road sediments and include mainly weathering of rock by physical, chemical and biological processes and the actions of wind and rain as mobilizing and transporting agents. The main natural sources of sediment to river are atmospheric dust deposition and wind erosion, mass movement events (landslides, debris flows, etc.) and erosion of soils by water. Within the river corridor, also

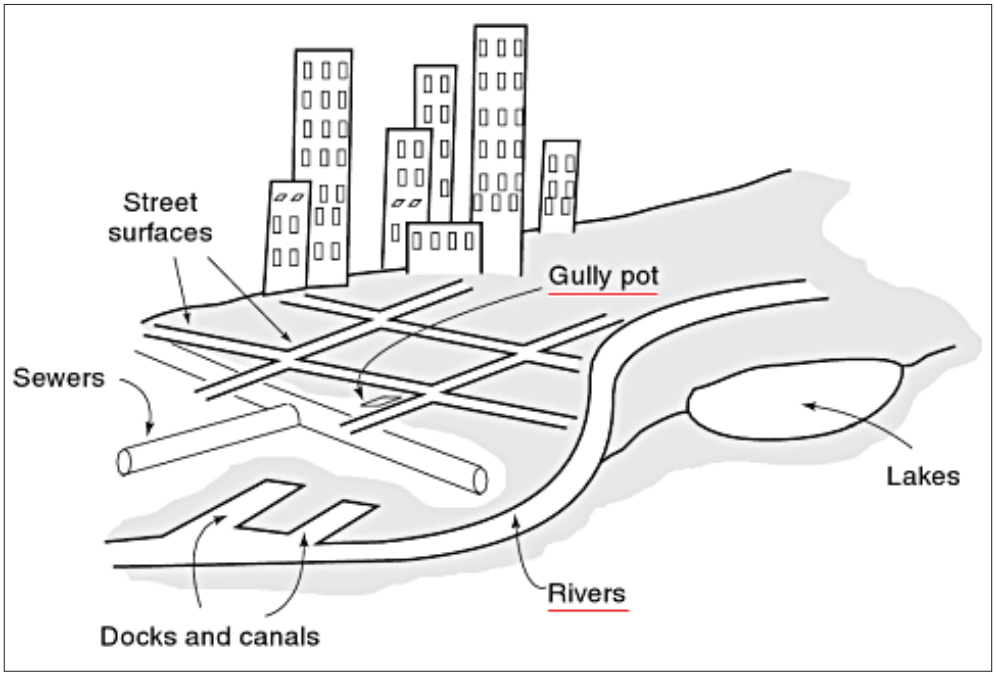

Fig. 2. Sites of sediment deposition in urban areas (after Taylor, 2007). In our study, sediments from gully pots and river channel beds (underlined with red) from Idrija urban area were investigated.

erosion of channel banks, floodplain deposits and resuspension of channel bed sediments contribute to sediment loads. Anthropogenic sources are mines, construction sites, urban road network and mineral and organic material from point sources and industrial sites (Taylor et al., 2008).

Sample collection

On 2.06.2011 two different types of urban sediments were collected - road sediments from gully pots of the urban drainage system (n=16) and active bottom stream sediments from the local streams flowing through the urban area (n=14). Altogether 30 samples were collected and sampling locations (Fig. 1) were spatially defined by a GPS device. The weather was sunny and windy and the last rain event (24-hour rainfall at 7 a.m. = 32.1 mm) was on 28.05.2011 (NMS, 2012). Approximately 1 kg of urban sediment was collected at each sampling site with a scoop and stored in polyethylene bags.

Sample preparation

In the laboratory, dry sieving was performed to collect two grain size fractions (<0.125 and <0.04 mm) for chemical analyses after aqua regia digestion. The preparation of samples for SEM/EDS analysis was performed according to Miler (2012). The sieved samples (n=5), (SS11 (<0.04 mm), SS13 (<0.04 mm & <0.125 mm), SS15 (<0.04 mm) and SS21 (<0.04 mm)) were mounted on a double-sided carbon tape with the surface of 25 mm^2 (the excess was blown off with compressed air) and sputter-coated with a thin layer of gold to achieve conductivity. Samples were analysed in a high vacuum using BSE mode on JEOL JSM 6490LV SEM coupled with Oxford INCA EDS system, comprising Oxford INCA PentaFET3 Si(Li) detector and INCA Energy 350 processing software at accelerating voltage 20 kV and working distance 10 mm. This instrument was used for qualitative chemical point analysis and for microphotographs in backscattered and secondary electron modes. Each analysed metal particle was characterized by its size, morphology and qualitative chemical composition measured by the EDS X-ray point analysis with an acquisition time 60 s. The particle size was determined by measuring their longest dimension using a measuring tool included in the JEOL SEM software.

Chemical analysis after aqua regia digestion

Pseudo-total levels of PTTE were determined with inductively coupled plasma (ICP) mass spectrometry (MS) after aqua regia digestion at AcmeLabs, Canada-Vancouver (accredited under ISO 9001:2008). Certified reference materials (CRM) and replicate samples were used to control the quality analysis and detailed description is provided in Bavec and co-workers (2015).

Scanning Electron Microscopy with Energy Dispersive Spectrometer

Solid phases of PTTE were investigated using the combination of scanning electron microscope (SEM) and energy dispersive spectrometer (EDS). SEM/EDS analysis is useful to observe the morphology, chemical and mineral composition of individual solid particles on the micron level and thus serves as a complementary method to the conventional mineralogical and geochemical methods (Miler & Gosar, 2009a, 2009b, 2012, 2013; Teršič, 2011; Miler, 2012). Backscattered electron (BSE) images in the SEM display compositional contrast that results from different atomic number of elements and their distribution in solid particles, while the EDS enables qualitative and semi-quantitative chemical analyses and it allows to identify the elements that are present in the investigated samples as well as their relative proportions (atomic % for example) (Beane, 2004). The method is particularly effective for investigation of metals due to their chemical properties: metals are electron dense elements with high atomic numbers (Z) and effective electron backscatterers. Consequently they appear visibly bright in a low-Z matrix (Aragon et al., 2000; Bernaus et al., 2005; Miler, 2012). In this study the SEM/EDS analysis was used as a complementary method for investigation of PTTE asscociations in urban sediment particles.

Results and discussion

PTTE levels

The basic statistics of PTTE levels in the road sediment samples and stream sediment samples are presented in Table 1 and Fig. 3. To evaluate the PTTE levels in the studied sediments, the results were compared to the European background median levels (determined after aqua regia) of stream sediments (<0.15 mm) (Salminen et al., 2005) and to The New Dutchlist action values for sediments (MHSPE, 2014) (Table 1, Fig. 3). Median values were selected for comparison, because strong positive skewness, kurtosis (Table 1) and histogram inspection showed that the bulk of values for all elements were clustered around the median on the left side of the histogram.

Box and whisker plots of PTTE levels in urban sediments (Fig. 3) show that for elements As, Cd, Cr, Mo and Zn the ranges of levels are wider and the medians are lower in the stream sediments in comparison to the road sediments for both grain size fractions. For Cu, the ranges of levels are narrower and the medians are lower in the stream sediments in comparison to the road sediments for both grain size fractions. For Ni and Co the ranges of levels and their medians are similar in both types of sediments (road and stream). The differences in basic statistical distribution (As, Cd, Cr, Mo, Zn and Cu) in road and stream sediments suggest that their

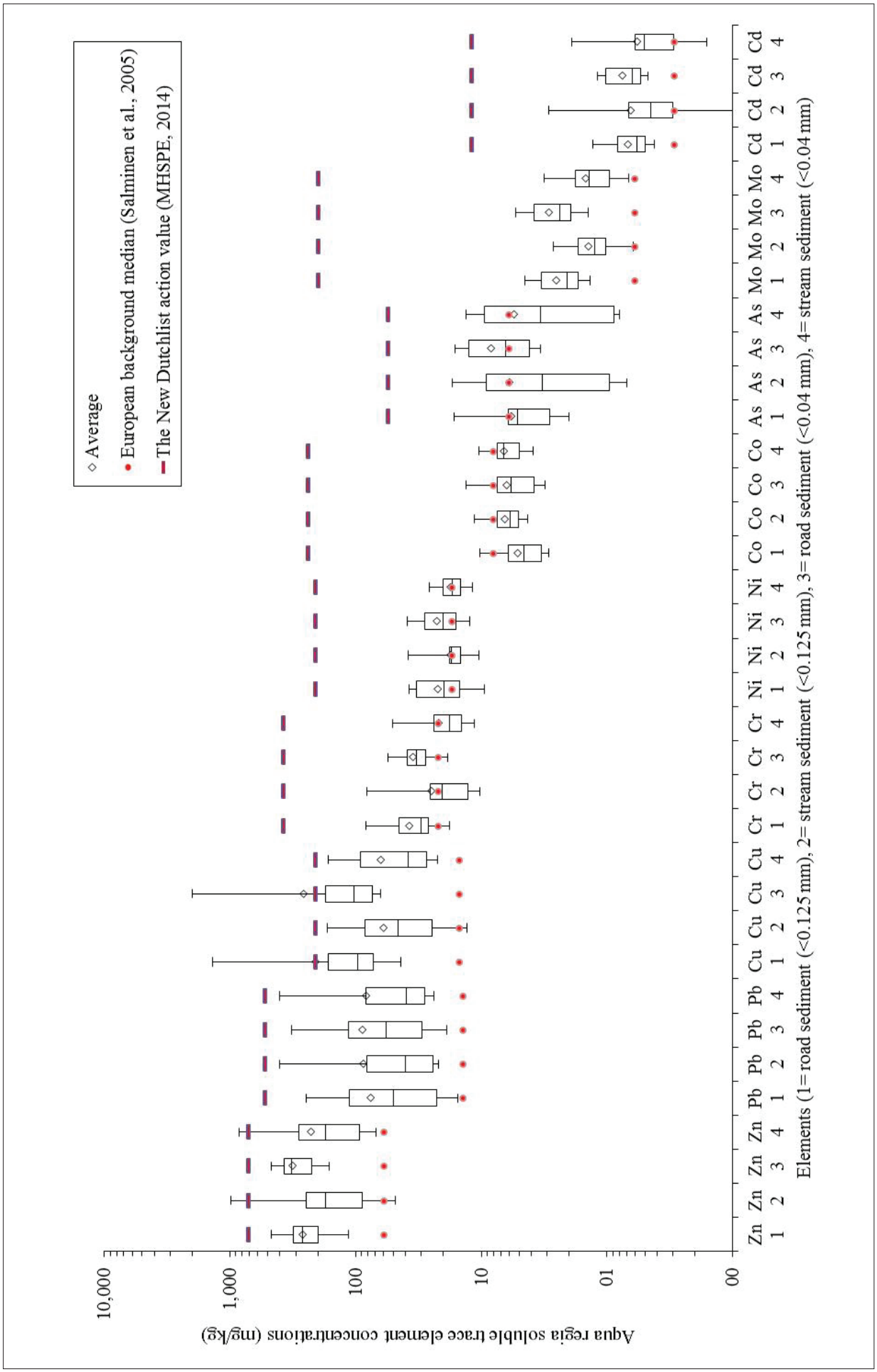

Fig. 3. Box and whisker plots of PTTE levels in urban road sediments (<0.125 mm and <0.04 mm) and stream sediments (<0.125 mm and <0.04 mm) of Idrija together with the European median background concentrations (determined after aqua regia) for sediments (SALMINEN et al., 2005) and The New Dutchlist action values for sediments (MHSPE, 2014)

Table 1. Basic statistics of PTTE levels in road (n=16) and stream sediments (n=16) for grain size fractions <0.125 and <0.04 mm

Element	Unit	LoD	Fraction	Type	x	Md	Ave	Min	Max	s	Skew	Kurt	
As	mg/kg	0.1	<0.125 mm	ROAD	0	5.2	5.7	2	16.5	3.6	1.9	4	6* 55**
				STREAM	0	3.3	5.9	0.7	17.1	5.7	0.9	-0.3	
			<0.04 mm	ROAD	0	6.4	8.3	3.4	16.3	3.4	0.6	-1.2	
				STREAM	0	3.4	5.4	0.8	13.2	4.8	0.4	-1.6	
Cd	mg/kg	0.01	<0.125 mm	ROAD	0	0.6	0.7	0.4	1.3	0.2	1.4	1.5	0.29* 12**
				STREAM	0	0.4	0.6	0.1	2.9	0.7	3.1	10.5	
			<0.04 mm	ROAD	0	0.6	0.7	0.5	1.2	0.5	0.7	-1.1	
				STREAM	0	0.5	0.6	0.2	1.9	0.4	2.5	7.7	
Co	mg/kg	0.1	<0.125 mm	ROAD	0	4.6	5.1	2.9	10.3	2.2	1.3	0.7	8* 240**
				STREAM	0	5.9	6.4	4.3	11.4	1.9	1.3	1.8	
			<0.04 mm	ROAD	0	5.8	6.2	3.1	13.3	3.1	1.1	1.1	
				STREAM	0	6.7	6.5	3.9	10.5	1.9	0.6	-0.2	
Cr	mg/kg	0.5	<0.125 mm	ROAD	0	30.4	37.1	17.9	82.9	17.6	1.4	1.7	22* 380**
				STREAM	0	20.4	24.8	10.3	81.7	18	2.5	7.1	
			<0.04 mm	ROAD	0	32.7	34.7	18.5	55.5	18.5	0.7	0.1	
				STREAM	0	18	21.4	11.4	50.5	10.6	1.9	3.4	
Cu	mg/kg	0.01	<0.125 mm	ROAD	0	96.5	206.8	43.9	1369.5	315.9	3.4	12.4	15* 210**
				STREAM	0	45.8	59.1	13	166.6	40.8	1.4	1.9	
			<0.04 mm	ROAD	0	102.4	254.7	63.8	1988.4	63.8	3.7	14.2	
				STREAM	0	38.2	62.5	22.3	166	43.8	1.3	0.7	
Mo	mg/kg	0.01	<0.125 mm	ROAD	0	2.1	2.5	1.4	4.5	0.9	0.7	-0.7	0.6* 200**
				STREAM	0	1.3	1.4	0.6	2.7	0.6	1	0.7	
			<0.04 mm	ROAD	0	2.4	2.9	1.4	5.3	1.4	0.8	-0.3	
				STREAM	0	1.4	1.5	0.7	3.2	0.6	1.4	2.6	
Ni	mg/kg	0.1	<0.125 mm	ROAD	0	19.9	22	9.4	37.4	9.3	0.6	-1	17* 210**
				STREAM	0	17.2	17.5	10.5	38	6.2	2.7	9	
			<0.04 mm	ROAD	0	20.1	22.2	12.4	39.1	12.4	0.7	-0.2	
				STREAM	0	17.1	17.3	11.8	25.9	3.6	0.7	0.6	
Pb	mg/kg	0.01	<0.125 mm	ROAD	0	50	75	15.4	246.7	65.6	1.6	1.8	14* 530**
				STREAM	0	39.9	85.2	22.1	402.8	104.5	2.4	5.8	
			<0.04 mm	ROAD	0	57.1	87	19	326.4	19	1.9	3.2	
				STREAM	0	39.3	82.1	23.8	401.8	100	2.7	7.5	
Zn	mg/kg	0.1	<0.125 mm	ROAD	0	266.7	258.7	114.4	471.8	86.2	0.5	1	59.5* 720**
				STREAM	0	172.4	222.7	48.1	984.5	228.5	2.9	9.3	
			<0.04 mm	ROAD	0	326.4	313	162.8	471.9	162.8	0.1	-0.8	
				STREAM	0	172.5	224	68.7	848.4	195.9	2.5	7.2	

Md= median; Ave= average; Min= minimum; Max= maximum; s= standard deviation; Skew= skewness; Kurt= Kurtosis; LoD = Limit of detection; x = Number of samples below lower LoD;* the European background median concentration (determined after aqua regia) for stream sediments (<0.15 mm) (Salminen et al., 2005); **The New Dutchlist action value for sediments (MHSPE, 2014)

geochemical distribution is potentially impacted by anthropogenic activities, while not for Ni and Co. The ranges and the medians of levels in different grain size fractions of road and of stream sediments are similar for all investigated PTTE (Fig. 3), which indicates that different grain size fraction (<0.125 mm and <0.04 mm) does not affect the geochemical distribution of PTTE in urban sediments of Idrija.

In comparison to the European background medians for stream sediments (Table 1, Figure 3), As, Co, Cr and Ni levels are not enriched, Mo levels are enriched up to 9 times, Cd levels up to 10 times, Zn levels up to 17 times, Pb levels up to 29 times and Cu levels up to 133 times in urban sediments of Idrija. For these enrichments again anthropogenic influences are possible due to the urban settlement of the investigated area.

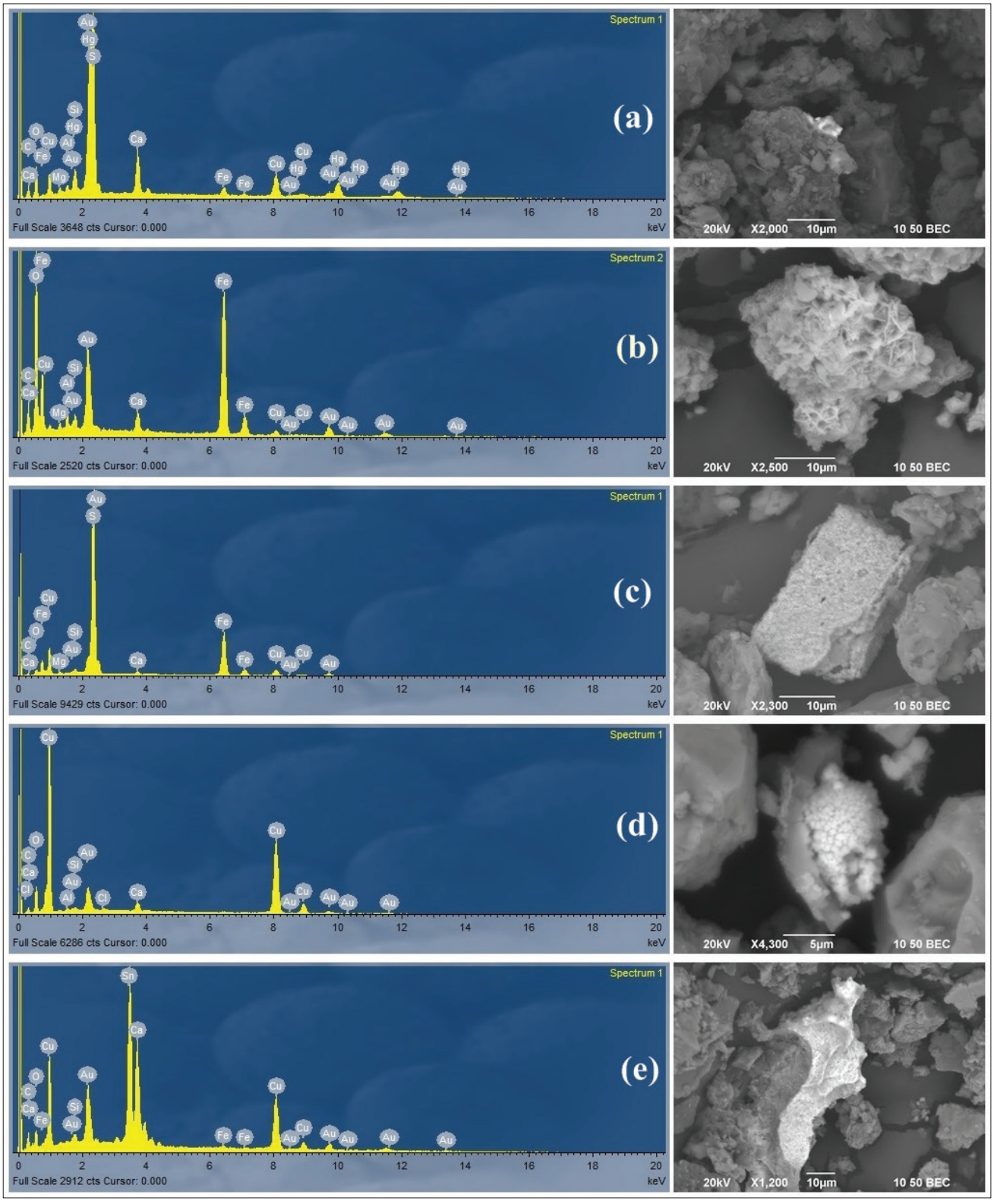

Fig. 4. Particles containing Cu in associations with the following elements: (a) Hg-S-Cu, (b) Fe-O-Cu, (c) Cu-Fe-S, (d) pure Cu (e) Sn-Cu

In comparison to The New Dutchlist action values (MHSPE, 2014) (Table 1, Fig. 3), almost all investigated PTTE are below it, except Cu and Zn. In case of Cu the levels exceed The New Dutchlist action value (210 mg/kg; MHSPE, 2014) in 3 road sediments (SS8, SS13 and SS29). The sample SS8 contains 305 mg/kg of Cu in the grain size fraction <0.125 and 350 mg/kg in the grain size fraction <0.04 mm. The sample SS13 contains 1370 mg/kg of Cu in the grain size fraction <0.125 and 1989 mg/kg of Cu in the grain size fraction <0.04 mm. The sample SS29 contains 434 mg/kg of Cu in the grain size fraction <0.125 and 415 mg/kg of Cu in the grain size fraction <0.04 mm. For the extra high Cu levels that were determined in the sample SS13 (<0.125 & <0.04 mm), two potential sources were observed. First is the vicinity of the manufacturing facilities of the company Kolektor. As already mentioned, the company Kolektor is a commutator production industry, which started in 1963 as a small factory, but developed into a worldwide successful company as it is today. Its manufacturing facilities are located on the right and on the left bank of the river Idrijca in the northern part of Idrija, where Hg ore roasting facilities used to be. Benčina (2007) also mentions that the company uses three types of water: sanitary, cooling and technology. The cooling water that is used for the cooling of the machinery from the production process is collected from the river Idrijca and after use it is returned back into the river Idrijca. The exhaust of cooling water that is released back into the river Idrijca is constantly monitored (Benčina, 2007). Second possible source of Cu is the Hotel Jožef that is situated near the road shaft. The cladding of the hotel consists mainly of an alloy of iron with the addition of copper (Hotel Jožef, 2015). The reason for high Cu enrichments in the samples SS8 and SS29 are unknown. It is possible that there was some current local source of Cu spilled in the road shaft prior to the sampling. In the rest of the road samples Cu levels were low and in the stream sediment samples even lower. Copper enrichments are very local, but this indicates an obvious anthropogenic disturbance. In need of a special attention are sediments from the location SS13, because the concentrations are extremely high. In case the Cu loadings are constant, this could potentially cause negative local disturbance, since the sediments are discharged directly into the river Idrijca without any pre-treatment. In case of Zn the levels exceed The New Dutchlist action value (720 mg/kg; MHSPE, 2014) in one stream sediment (SS22) that contains 984.5 mg/kg of Zn in the grain size fraction <0.125 and 848.4 mg/kg of Zn in the grain size fraction <0.04 mm. The source for high Zn value in the sample SS22 could not have been recognized.

Solid phases of PTTE regarding to SEM-EDS

Using SEM/EDS Cu was the only element abundantly recognized among the investigated elements in PTTE bearing phases, and even Cu particles were abundant in only one sample - SS13, which contained the highest Cu level. Some very interesting Cu associations with elements were observed (Fig. 4). Because of the diversity of Cu mineral phases, both grain size fractions (<0.125 and <0.04 mm) were inspected. Following element associations were recognised:

- Cu with Hg and S in atomic ratio Hg : Cu : S = 4.07 : 4.72 : 8.30 (Fig. 4 example (a)). The size of the particle is 6 µm. This particle is not recognised as any known mineral Hg phase. However, we propose two possible origins of the element associations Hg-Cu-S. Firstly, based on the assumptions that Cu ore is not present in Idrija Hg ore deposit, that current industry (Kolektor) uses Cu-based alloy for the production of commutators for electrical motors (Ule et al., 1994) and that the biggest waste in the manufacturing process of commutator production is primarily copper (Benčina, 2007), it is possible that Hg-Cu-S associations are of secondary origin (anthropogenic). It should be noted that the Hg-Cu-S associations were found in the sediment collected in a gully pot that is situated in the immediate vicinity of the Kolektor manufacturing facilities. Secondly, Drovenik and co-workers (1980) performed spectrochemical analyses of cinnabar and metacinnabar from Idrija ore deposit and found out that they contain from 1 to 200 mg/kg of Cu. Therefore, it is possible that Cu was concentrated in secondary metacinnabar during roasting of cinnabar ore.
- Cu with Fe and O in atomic ratio Cu : Fe : O = 0.50 : 10.35 : 55.52 (Fig. 4 example (b)). This particle is a secondary authigenic (crystalized in situ) iron oxyhydroxide that has a rosette like morphology, which most probably entrapped traces of Cu into the crystals during growth (Cu partially substitutes for Fe in iron oxyhydroxide). Cu has a high tendency to bound to iron oxyhydroxides during low pH conditions. The size of the particle is 32 µm.
- Cu with Fe and S in atomic ratio Cu : Fe : O: S = 2.81 : 12.97 : 14.09 : 29.78 (Fig. 4 example (c)). This mineral phase is probably a product of iron sulfide oxidation and the mineral phase is recognised as an oxyhydroxy sulphate containing Cu (Cu partially substitutes for Fe in partially oxidised pyrite (iron oxyhydroxy sulphate)). The particle size is 32 µm.
- Metallic Cu in atomic ratio Cu = 28.53 (Fig. 4 example (d)). This is a pure copper particle and it is undoubtedly anthropogenic, which is shown by its morphology. The shape of a particle is partialy rounded, composed of micron-sized crystals and it appears hollow. The size of the particle is 14 µm.
- Cu with Sn in atomic ratio Sn : Cu = 13.3 : 13.51 (Fig. 4 example (e)). This is an anthropogenic particle (Sn-Cu alloy), known as bronze. The size of the particle is 82 µm.

A diversity of Cu mineral phases was observed in the sample SS13 and some particles are obviously of anthropogenic origin.

Conclusions

The investigation of levels of potentially toxic trace elements (As, Cd, Co, Cr, Cu, Mo, Ni, Pb and Zn) in urban stream and road sediments revealed that they are mainly within European background and below The New Dutchlist action values, only for Cu local enrichments were discovered in road sediments. Particularly in one road sediment an extremely high Cu level (1989 mg/kg) was determined in the vicinity of a commutator production industry. The Cu particles were inspected by SEM/EDS analysis that revealed a diversity of Cu associations with other elements in solid phases.

Acknowledgments

The presented study was funded by the Slovenian Research Agency (ARRS) in the frame of the research programme Groundwater and Geochemistry (P1-0020), which is performed by the Geological Survey of Slovenia. The author would like to thank Vesna Miklavčič, Msc., director and Martin Kržišnik from Komunala Idrija for advices and good cooperation during sampling of urban sediments, dr. Miloš Miler from Geological survey of Slovenia for guidance, help and advice during SEM/EDS analysis and doc. dr. Mateja Gosar for guidance, help and advice during the whole process of the presented research, which is a part of a comprehensive PhD study, which is presented in a PhD thesis (Bavec, 2015).

References

Adriano, D.C. 1986: Trace elements in the terrestrial environment. Springer-Verlag, New York, Berlin, Heidelberg, Tokyo: 533 p.

Addiscott, J.A. 2006: Soil and Environmental Issues. In: Warkentin B.P. (ed.): Footprints in the Soil: People and Ideas in Soil History, Elsevier Science: 572 p.

Aragaon, A.P., Torres, G.V., Monroy, M.F., Luszczewski, A.K. & Leyva, R.R. 2000: Scanning electron microscope and statistical analysis of suspended heavy metal particles in San Luis Potosi, Mexico. Atmos. Environ, 34: 4103–4112.

Bavec, Š. 2015: Geochemical investigations in Idrija urban area with emphasis on mercury: dissertation thesis. Ljubljana: 190 p.

Bavec, Š., Biester, H. & Gosar, M. 2014: Urban sediment contamination in a former Hg mining district, Idrija Slovenia. Environ Geochem Health, 4/3: 427-439, doi:10.1007/s10653-013-9571-6

Bavec, Š., Gosar, M., Biester, H. & Grčman, H. 2015: Geochemical investigation of mercury and other elements in urban soil of Idrija (Slovenia). J Geochem Explor, 154: 213–223, doi:10.1016/j.gexplo.2014.10.011.

Beane, J. 2004: Using the Scanning Electron Microscope for Discovery Based Learning in Undergraduate Courses. Journal Geos Educ, 52/3: 250–253.

Benčina, T. 2007: The development of environmental design in municipality of Idrija: Graduation thesis. Ljubljana, 113 p. Internet: http://geo.ff.uni-lj.si/pisnadela/pdfs/dipl_200703_tatjana_bencina.pdf (30. 1. 2014)

Bernaus, A., Gaona, X. & Valiente, M. 2005: Characterisation of Almaden mercury mine environment by XAS techniques. J Environ Monit, 7/8: 771–777, doi:10.1039/B502060N.

Čar, J. 1998: Mineralized rocks and ore residues in the Idrija region. In: Miklavčič, V. (ed.): Proceedings of the meeting of researchers entitled: Idrija as a natural and anthropogenic laboratory, Mercury as a major pollutant. Idrija, Mercury mine Idrija, 10–15.

Čar, J. & Terpin, R. 2005: Stare žgalnice živosrebrove rude v okolici Idrije. Idrijski razgledi, 50/1, 80-105.

Drovenik, M., Pleničar, M. & Drovenik, F: 1980: Nastanek rudišč v SR Sloveniji. Geologija, 23/1, 1–57.

Gosar, M. & Čar, J. 2006: Influence of mercury ore roasting sites from 16th and 17th century on the mercury dispersion in surroundings of Idrija. Geologija, 49/1: 91–101, doi:10.5474/geologija.2006.007.

Hotel Jožef 2015: Official website. Internet: http://www.hotel-jozef.si/ (27. 8. 2015)

Johnson, C.C. & Demetriades, A. 2011: Urban Geochemical Mapping: A Review of Case Studies in this Volume. In: Johnson, J.C.C., Demetriades, A., Locutura, J. & Ottesen, R.T. (eds.): Mapping the Chemical Environment of Urban Areas. John Wiley & Sons, West Sussex, UK, 7–27, doi:10.1002/9780470670071.ch2

Johnson, C.C., Demetriades, A., Locutura, J. & Ottesen, R.T. 2011: Mapping the Chemical Environment of Urban Areas. John Wiley & Sons, West Sussex: 616 p.

Kabata-Pendias, A. & Pendias, H. 2001: Trace elements in soils and plants. Boca Raton, FL, CRC Press: 403 p.

Kavčič, I. 2008: Živo srebro: Zgodovina idrijskega žgalništva. Založba Bogataj, Idrija: 352 p.

Kolektor 2014: Offical website of the company. Internet: http://www.kolektor.com/ (31. 1. 2014).

MHSPE 2014: Ministry of Housing, Spatial Planning, and the Environment. The New Dutchlist. Internet: http://www.contaminatedland.co.uk/std-guid/dutch-l.htm. (30. 01. 2014).

Miler, M. 2012: Application of SEM/EDS to environmental mineralogy and geochemistry: dissertation thesis. Ljubljana: 169 p.

Miler, M. & Gosar, M. 2009a: Application of SEM/EDS to environmental geochemistry of heavy metals. Geologija, 52/1, 69-78, doi:10.5474/geologija.2009.008.

Miler, M. & Gosar, M. 2009b: Characterisation of solid airborne particles in urban snow deposits from Ljubljana by means of SEM/EDS. RMZ – Materials and Geoenvironment, 56/3: 266–282.

Miler, M. & Gosar, M. 2012: Characteristics and potential environmental influences of mine waste in the area of the closed Mežica Pb–Zn mine (Slovenia). J. Geochem. Explor., 112: 152–160. doi:10.1016/j.gexplo.2011.08.012.

Miler, M. & Gosar, M. 2013. Assessment of Metal Pollution Sources by SEM/EDS Analysis of Solid Particles in Snow: A case Study of Žerjav, Slovenia. Microscopy and Microanalysis, 19: 1606–1619. doi:10.1017/S1431927613013202.

Mlakar, I. & Čar, J. 2009: Geological map of the Idrija - Cerkljansko hills between Stopnik and Rovte 1:25.000. Ljubljana: Geološki zavod Slovenije.

Mlakar, I. & Čar, J. 2010: Geological structure of the Idrija – Cerkljansko hills: Explanatory Book to the Geological map of the Idrija – Cerkljansko hills between Stopnik and Rovte 1:25.000. Ljubljana: Geološki zavod Slovenije.

NMS 2012: National Meteorological Service of Slovenia. Ministry of Agriculture and Environment: Slovenian Environment Agency. Internet: http://meteo.arso.gov.si/met/sl/archive/ (27. 12. 2012).

Plant, A.J., Korre, A., Reeder, S., Smith, B. & Voulvoulis, N. 2005: Chemicals in the environment: implications for global sustainability. Applied earth sciences (Transactions of the Institution of Mining and Metallurgy Section B), 114/2: 65–97, doi:10.1179/037174505X62857.

Salminen, R., Batista, M.J., Bidovec, M., Demetriades, A., De Vivo, B., De Vos, W., Duris, M., Gilucis, A., Gregorauskiene, V., Halamic, J., Heitzmann, P., Lima, A., Jordan, G., Klaver, G., Klein, P., Lis, J., Locutura, J., Marsina, K., Mazreku, A., O'connor, P.J., Olsson, S.Å., Ottesen, R.T., Petersell, V., Plant, Ja., Reeder, S., Salpeteur, I., Sandström, H., Siewers, U., Steenfelt, A. & Tarvainen, T. 2005: Geochemical Atlas of Europe. Part 1- Background Information, Methodology and Maps. Geological survey of Finland: 526 p.

Taylor, K.G. 2007: Urban Environments. In: Perry, C.T. & Taylor, K.G. Environmentaly Sedimentology. Blackwell, Oxford, 191–222.

Taylor, K.G. & Owens, N.P. 2009: Sediments in urban river basins: a review of sediment-contaminant dynamics in an environmental system conditioned by human activites. J. Soils. Sed., 9/4: 281–303. doi:10.1007/s11368-009-0103-z.

Taylor, K.G., Owens, P.N., Batalla, R.J. & Garcia, C. 2008: Sediment and contaminant sources and transfers in river basins. In: Owens, P.N. (ed.): Sustainable management of sediment resources: sediment management at the river basin scale. Elsevier, 4:83–135, doi:10.1016/S1872-1990(08)80006-2.

Teršič, T. 2010: SEM/EDS analysis of soil and roasting vessels fragments from ancient mercury ore roasting sites at Idrija area. Geologija, 54/1: 31–40, doi:10.5474/geologija.2011.002.

Thornton, I., Farago, M.E., Thums, C.R., Parrish, R.R., Mcgill, R.A.R., Breward, N., Fortey, N.J., Simpson, P., Young, S.D., Tye, A.M., Crout, N.M.J., Hough, R.L. & Watt, J. 2008: Urban geochemistry: research strategies to assist risk assessment and remediation of brownfield sites in urban areas. Environ. Geochem. Health, 30/6: 565–76, doi:10.1007/s10653-008-9182-9.

Ule, B., Kuzman, K., Švetak., D. & Kofol, F. 1994: Cockcroft-Latham Fracture Criterion and Bulk Formability of Copper Base Alloys. Kovine, zlitine, tehnologije, 28/4: 595–600.

Wong, C.S.C., Li, X. & Thornton, I. 2006: Urban environmental geochemistry of trace metals. Environ. Poll., 142/1: 1–16, doi:10.1016/j.envpol.2005.09.004.

Zupan, M., Grčman, H., Hodnik, A., Lobnik, F., Kralj, T., Rupreht, J., Šporar, M., Lapajne, S., Tič, I., Šijanec, V., Gogič, S., Mohorovičič, B., Ilc, R. & Kobal, M. 2008: Raziskave onesnaženosti tal Slovenije. Agencija RS za okolje, Ljubljana: 63 p.

GEOLOGIJA *58/2*, 121–138, Ljubljana 2015
http://dx.doi.org/10.5474/geologija.2015.010

Microfacies characteristics of the Lower Jurassic lithiotid limestone from northern Adriatic Carbonate Platform (central Slovenia)

Sedimentološke značilnosti spodnjejurskega litiotidnega apnenca s severnega roba Jadranske karbonatne platforme (osrednja Slovenija)

Luka GALE[1,2]

[1]University of Ljubljana, Faculty of Natural Sciences and Engineering, Department for Geology; Privoz 11, SI–1000 Ljubljana, Slovenia; e-mail: luka.gale@ntf.uni-lj.si
[2]Geological Survey of Slovenia, Dimičeva ul. 14, SI–1000 Ljubljana; e-mail: luka.gale@geo-zs.si

Prejeto / Received 9. 10. 2015; Sprejeto / Accepted 30. 11. 2015; Objavljeno na spletu / Published online 30. 12. 2015

Key words: Dinaric Carbonate Platform, microfacies analysis, External Dinarides, lithiotid limestone, Podbukovje Formation, Sinemurian, Pliensbachian
Ključne besede: Dinarska karbonatna platforma, mikrofaciesna analiza, Zunanji Dinaridi, litiotidni apnenec, Podbukovška formacija, sinemurij, pliensbachij

Abstract

The lithiotid limestone is characteristic for many Late Sinemurian – Pliensbachian tropical and subtropical carbonate platforms of the Neotethys and the Piemont-Liguria Oceans. On the northern edge of the ancient Adriatic Carbonate Platform (present NW External Dinarides) the lithiotid limestone forms a few hundred kilometres long belt. Sedimentological characteristics of the lithiotid limestone have been recorded in samples taken from three sections located in central Slovenia. Peloids, ooids, aggregate (lump) grains, benthic foraminifera, and micritised bivalve shells (cortoids) are the dominant grains. The microfacies association suggests restricted to open marine interior of a carbonate platform bordered by marginal sand shoals, or an inner ramp setting. Subtidal conditions were occasionally interrupted by emersions.

Izvleček

Litiotidni apnenec je značilna spodnjejurska litološka enota karbonatnega zaporedja številnih tropskih do subtropskih karbonatnih platform z obrobja Neotetide in Piemont-Ligurijskega oceana. Na severnem robu nekdanje Jadranske karbonatne platforme (današnji SZ Zunanji Dinaridi) se litiotidni apnenec razteza v smeri ZSZ-VJV v nekaj sto kilometrov dolgem pasu. Dosedanje poznavanje litiotidnega apnenca dopolnjujem s podrobnim sedimentološkim opisom vzorcev, nabranih v treh profilih na območju Krima v osrednji Sloveniji. Od klastov v apnencu prevladujejo peloidi, ooidi, agregatna zrna, bentoške foraminifere in delno mikritizirane lupine mehkužcev (kortoidi). Faciesna združba kaže na odlaganje v plitvem, nekaj metrov globokem morju razčlenjenem na zaprto laguno, odprto laguno, nakopičenja litiotidnih školjk in ooidne sipine. Podplimske pogoje so prekinjala kratkotrajna obdobja okopnitve vrha platforme, do katerih je pogosteje prišlo v spodnjem pliensbachiju.

Introduction

The Early Jurassic sea-level rise (Hallam, 2001), a gradual recovery of biota after the alleged biocalcification crisis in the latest Triassic (Hautmann et al., 2008; Greene et al., 2012), and, in many cases, extensional tectonics (Ruiz-Ortiz et al., 2004; Šmuc, 2005; Verwer et al., 2009) brought a gradual change from flat, uniformly shallow and skeletal-poor carbonate platforms of the earliest Jurassic (Dozet, 1993; Bucković et al., 2001; Azerêdo et al., 2003; Eren et al., 2002; Barattolo & Romano, 2005; Pomoni-Papaioannou & Kostopoulou, 2008; Wilmsen & Neuweiler, 2008; Bosence et al., 2009; Ogorelec, 2009) into the middle Early Jurassic platforms characterised by the abundance of biota and a variety of facies types (Galli, 1993; Fugagnoli & Loriga Broglio, 1998; Masetti et al., 1998; Blomeier & Reijmer, 1999; Scheibner & Reijmer, 1999; Cobianchi & Picotti, 2001; Fraser et al., 2004; Wilmsen & Neuweiler, 2008). Among the more extensively researched carbonate platforms of the Early Jurassic is also the Adriatic Carbonate Platform (AdCP), a large carbonate platform with an approximate length of 600 km (Dragičević & Velić, 2002; Tišljar et al., 2002; Vlahović et al., 2002, 2005; Čadjenović et al., 2008), positioned in the western part of the Neotethys Ocean (Thierry, 2000; Bosence et al., 2009) (Fig. 1).

One of the most distinct facies types on the AdCP is the Late Sinemurian – Pliensbachian (according to Sabatino et al., 2013 also earliest Toarcian) lithiotid limestone (Buser, 1965;

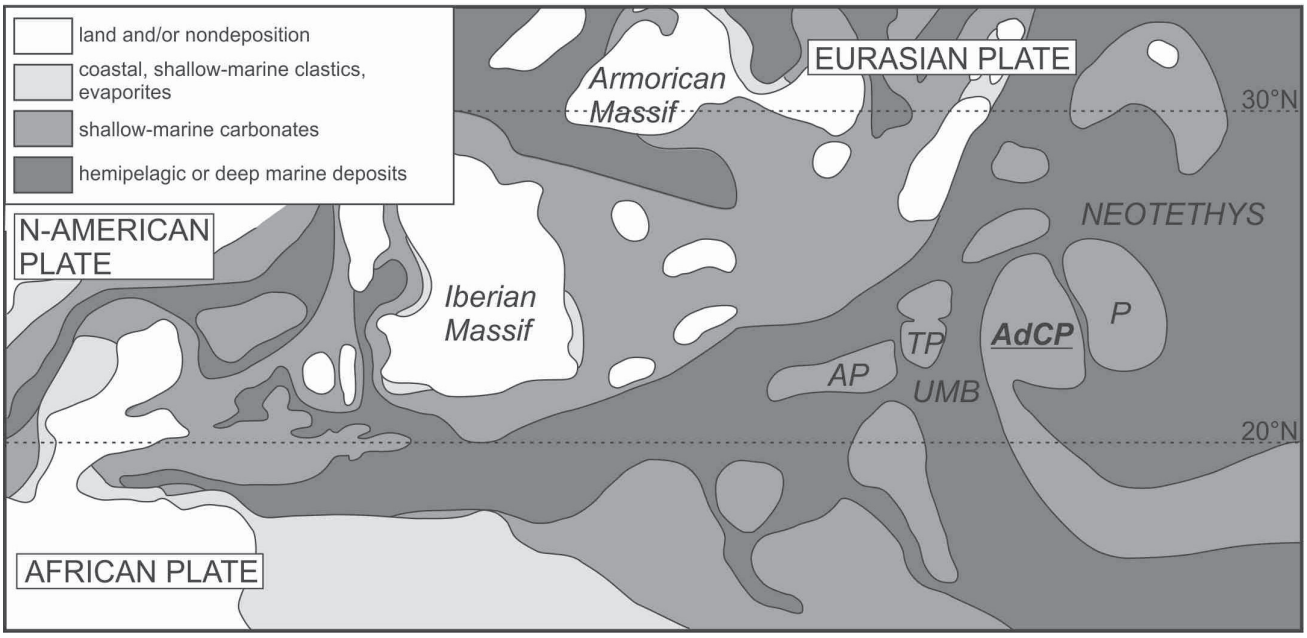

Figure 1. Palaeogeographic map of the western Neotethys for Late Sinemurian. AdCP – Adriatic carbonate platform; AP – Apennine Carbonate Platform; P: Pelagonia; UMB – Umbria Marche Basin; TP – Trento Platform. Modified after Thierry (2000) and Bosence et al. (2009).

Radoičić, 1966; Šribar, 1966; Strohmenger & Dozet, 1991; Dozet, 1992, 1996; Buser & Debeljak, 1996; Debeljak & Buser, 1997; Turnšek & Košir, 2000; Tišljar et al., 2002; Turnšek et al., 2003; Čadjenović et al., 2008; Črne & Goričan, 2008; Martinuš et al., 2012; Gale, 2014). At the northern part of the AdCP, structurally belonging to the north-western External Dinarides (Placer, 1999), the lithiotid limestone extends in over 100 km long belt from Trnovski gozd in the west towards Kočevje and further to the east-southeast (Buser & Debeljak, 1996). The lithiotid limestone was quarried south of Ljubljana and became known as the "Podpeč limestone" (Ramovš, 2000; Štukovnik et al., 2011; Kramar et al., 2015). Dozet named it the Lithiotid Limestone Member of the Podbukovje Formation (Dozet & Strohmenger, 2000) or the Lithiotid Limestone Member of the Predole beds (Dozet, 2009). On the basis of a detailed description of the lithiotid limestone from Trnovski gozd Črne and Goričan (2008) advocated a ramp model for the northern part of the AdCP, gradually passing into the deep-water Slovenian Basin to the north, while previous studies suggested a rimmed carbonate platform model (Buser & Debeljak, 1996).

The aim of this paper is to extend the current knowledge on the lithiotid limestone at the northern edge of the AdCP by giving a detailed description of the lithiotid limestone from the Mt. Krim area (central Slovenia) (Fig. 2). The described sections are subsequently compared with the lithiotid limestone from Trnovski gozd, described in Črne and Goričan (2008). Finally, the question of the platform geometry is discussed.

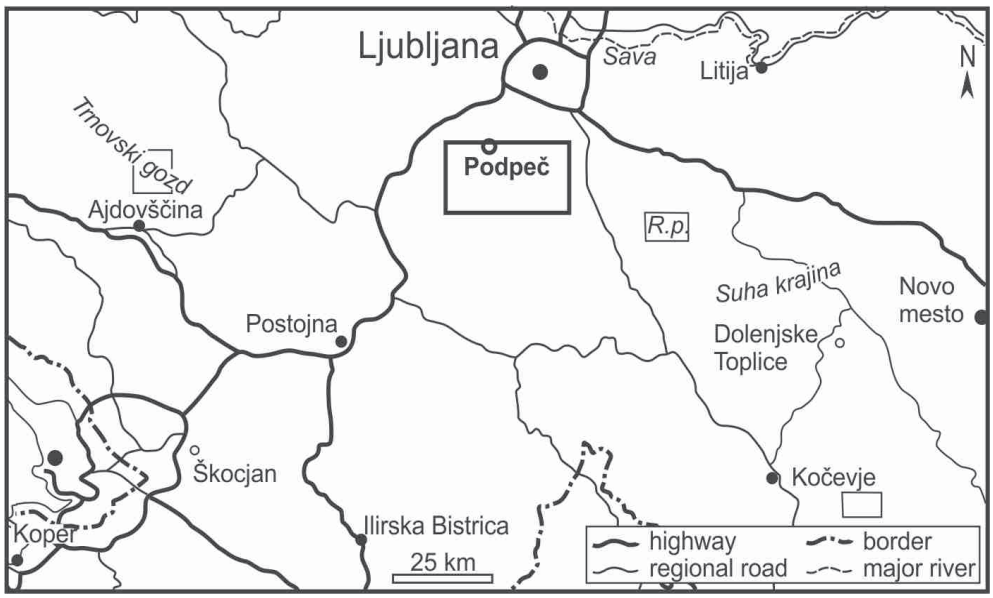

Figure 2. Position of the studied area. Other localities, mentioned in the text (Kovk on Trnovski Gozd, Kočevje, R.p. – Radensko polje), are shown in other rectangles.

Geological setting

The northern part of the AdCP structurally belongs to the External Dinarides, which represent a deformed margin of the Adriatic tectonic microplate. The deformations in the External Dinarides are due to post-Cretaceous collision with the European plate, accompanied by folding and thrusting in SW direction during Late Cretaceous to Paleogene (Placer, 1999; Vrabec & Fodor, 2006; Placer, 2008; Kastelic et al., 2008). The thrust units, from the uppermost to the lowermost, comprise: the Trnovo Nappe, the Hrušica Nappe, the Snežnik thrust block, and the Komen thrust block (Fig. 3). Thrust blocks consist of Late Paleozoic to Middle Triassic clastics and carbonates, followed by carbonates deposited on the AdCP. Towards north, the External Dinarides border the Tolmin thrust unit of the Southern Alps along the South-alpine reverse fault and the Marija Reka fault. The Tolmin thrust unit mostly comprises deep water sediments of the Slovenian Basin, originally extending along the northern margin of the AdCP (Placer, 1999). Thrusts are further cut and displaced by dextral strike-slip faults active since the Pliocene (Vrabec & Fodor, 2006; Kastelic et al., 2008; Kastelic & Carafa, 2012).

The Mt. Krim area structurally belongs to the Hrušica Nappe of the External Dinarides (Placer, 1999). The geological structure of this territory was established by Lipold (1858), Kramer (1905), Vetters (1933), Buser et al. (1967), Buser (1968), and Miler and Pavšič (2008). The Mt. Krim area mostly consists of Upper Triassic to Middle Jurassic shallow water carbonates (Buser et al., 1967; Buser, 1968, 1989; Ogorelec & Rothe, 1993), which today form the southern hilly rim and the southern basement of the younger, post-Pliocene tectonic Ljubljana Moor Basin (Jamšek Rupnik et al., 2015). Mesozoic

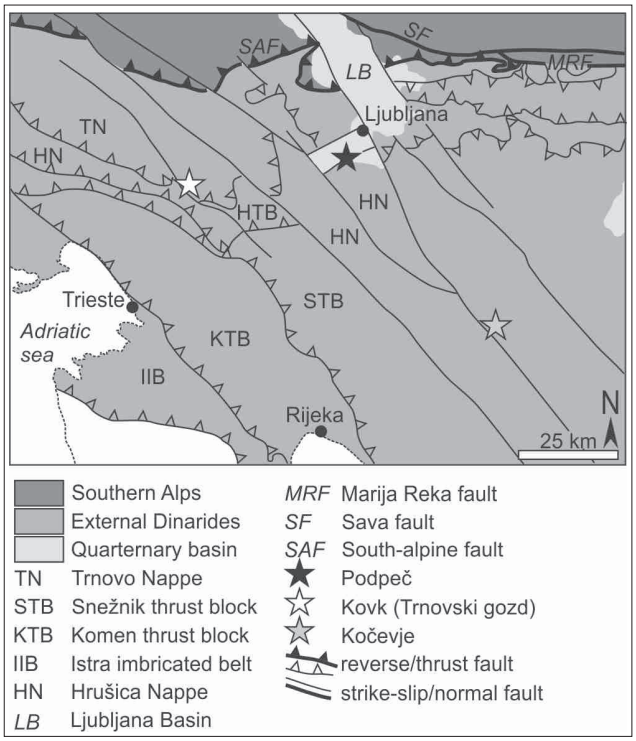

Figure 3. Structural map of the south-western Slovenia. Simplified after Placer (1999).

carbonates are dissected by N-S and WNW-ESE to NW-SE running faults (Buser et al., 1967; Buser, 1968) (Fig. 4).

The Lower Jurassic succession in the Mt. Krim area conformably overlies the Norian-Rhaetian Main Dolomite (Fig. 5), which is characterised by medium to thick-bedded crystalline dolomite, laminated fenestral dolomite and intraclastic breccia, marking cyclically interchanging shallow subtidal, intertidal and supratidal conditions (Ogorelec & Rothe, 1993; Miler et al., 2007; Miler & Pavšič, 2008). The lowermost Jurassic

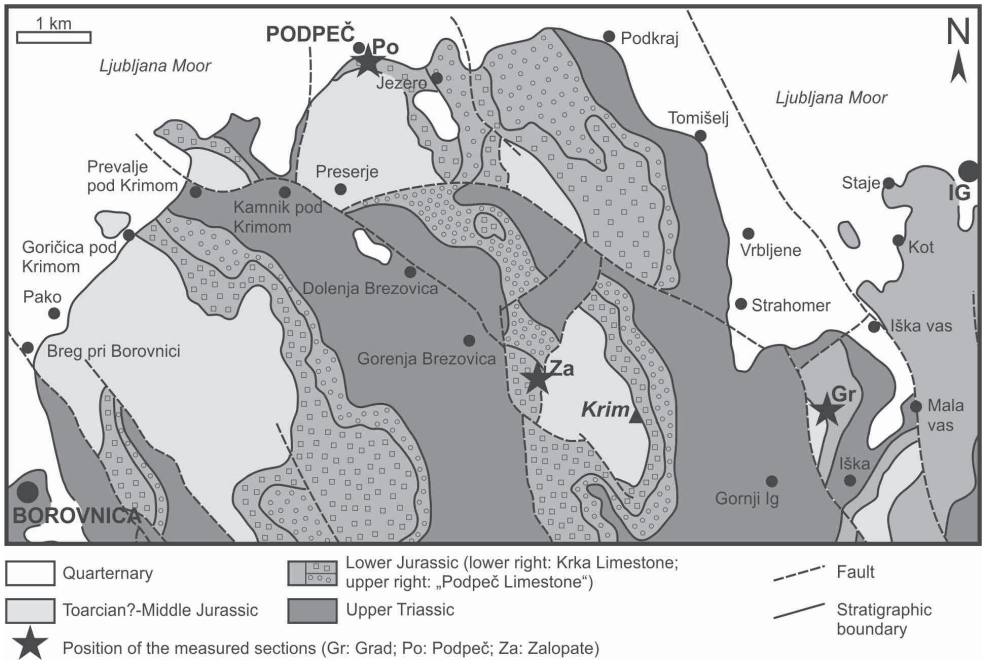

Figure 4. Geologic map of the Mt. Krim area. Modified after Buser et al. (1967) and Buser (1968).

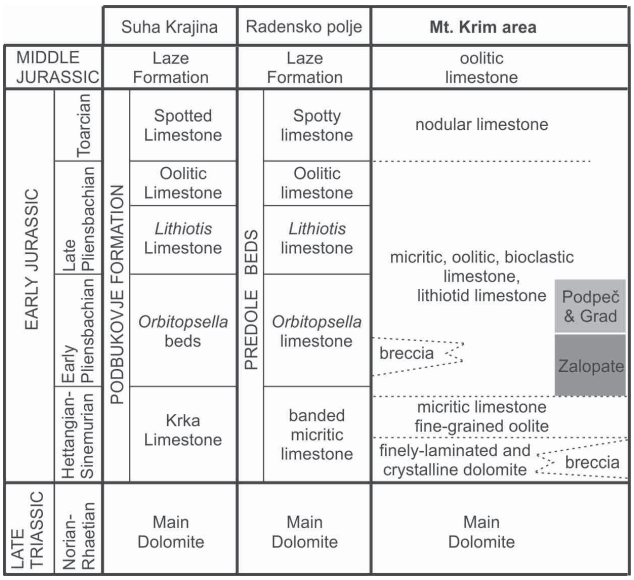

Figure 5. Lower Jurassic lithological succession in the Mt. Krim area, and comparisson to the lithostratigraphic division proposed by Dozet and Strohmenger (2000) for the Suha krajina and by Dozet (2009) for the Radensko polje. The positions of the measured sections are shown with gray rectangles.

(Hettangian-Sinemurian) succession consists of medium to thick-bedded coarsely crystalline dolomite, finely laminated dolomite, bedded micritic, rarely peloidal and oolitic limestone. Emersion surfaces are indicated by red-stained irregular upper bedding planes. This succession also deposited in peritidal and shallow subtidal setting (Miler & Pavšič, 2008; Ogorelec, 2009). Discontinuous, up to several tens of meters thick bodies of mud-supported breccia are locally present (Buser, 1965), as well as up to a meter wide dikes, filled with large angular blocks of dolomite in dolomitised matrix (visible along road cut south of Pijava Gorica). Upwards, oolitic and bioclastic limestone predominates, gradually passing into dark grey to black limestone with lithiotid bivalves, bioclastic packstone, floatstone, ooid packstone and grainstone (Buser & Debeljak, 1996; Miler & Pavšič, 2008). On the basis of lithiotid bivalves and foraminifera, a Late Sinemurian-Pliensbachian age has been determined for the lithiotid limestone (Buser & Debeljak, 1996; Gale, 2014). Discontinuous, but much rarer bodies of black limestone breccia can be laterally found (Buser, 1965), for example west of Jezero. The Lower Jurassic succession ends with the Toarcian thin-bedded, often nodular micritic limestone (A. Košir, pers. com.). The Middle Jurassic succession consists of mostly strongly dolomitised thick succession of oolitic limestone (Buser, 1965, 1968; Miler & Pavšič, 2008).

Material and methods

The facies analysis of the "Podpeč limestone" is based on three detailed sections, namely the Zalopate (45°56'09'' N, 14°27'21'' E), the Podpeč quarry (45°58'22'' N, 14°25'16'' E) and the Grad (45°55'46'' N, 14°30'14'' E) sections (Fig. 4). Bed thickness classification follows Tucker (2001). Altogether, 63 thin sections were investigated and described according to terminology of Dunham (1962), and Embry and Klovan (1971). The proportion of grain types was estimated with the use of comparison charts of Bacelle and Bosellini (1965). Sand-size, roughly spherical homogenous lime-mud particles are termed peloids sensu Friedman (2003). Microfacies (MF) types were compared to Standard Microfacies Types in Flügel (2004).

Description of sections

The Zalopate section (Fig. 6) is 42.5 m thick and consists mostly of grey to black limestone of variable textures. Bed thickness ranges from 6 cm to 320 cm, but thicker beds predominate in the lower part of the section, whereas thin to medium thick beds are more common in the upper half of the section. The texture of the limestone varies from mudstone to floatstone with grainstone

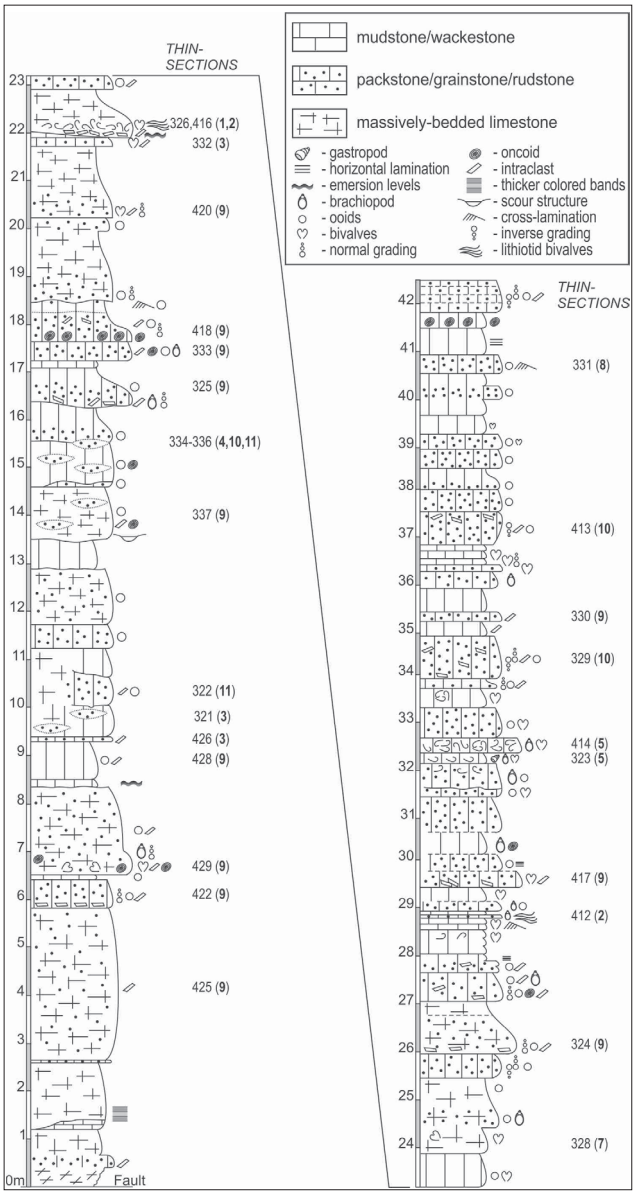

Figure 6. The Zalopate section. This is the lower part of the "Podpeč limestone" s.l. (note the scarcity of lithiotid bivalves). Late Sinemurian – early Early Pliensbachian. Number in brackets denotes the microfacies type.

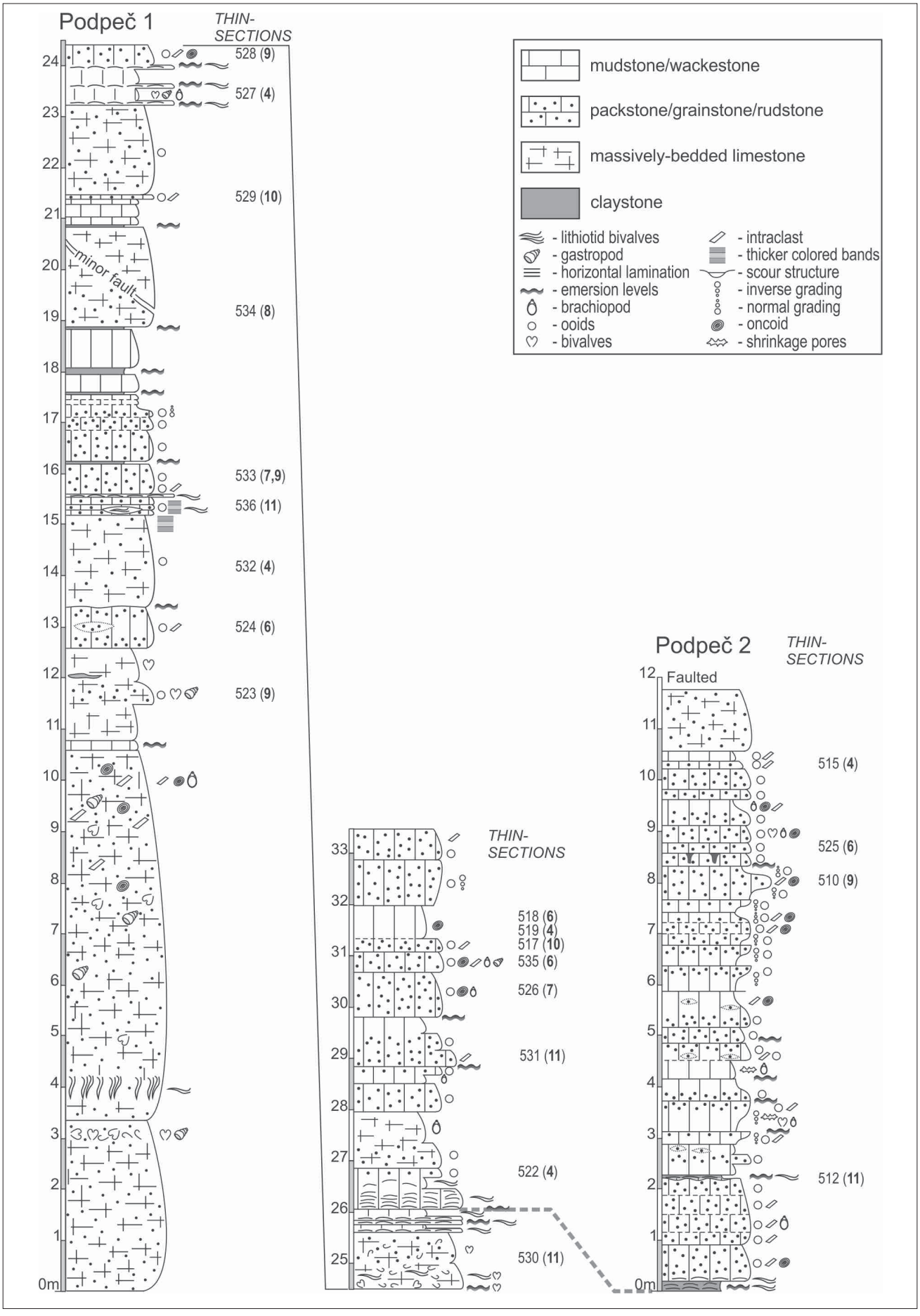

Figure 7. The lithiotid-rich "Podpeč limestone" from the type locality in the Podpeč quarry. Two overlapping sections were measured. Early Pliensbachian. Number in brackets refer to mikrofacies type.

support, often within the same bed, either through grading, or through irregular mixing (at least in part due to bioturbation) and lateral pinching out. Normal grading is the most common sedimentary structure. Some accumulations of fossils (mostly fragmented bivalve shells) can be found at the bottom of beds. Bivalve shells are more commonly dispersed in oolite. Several bedding planes show irregular morphology, reddish colouration, and thin intercalations of red or yellow claystone. Lithiotid bivalves are rare, and only up to 5 cm long, undetermined specimens were found, in one case accumulated above a score structure, cutting through mudstone with birdseyes-type porosity and red clayey surface. Cross-lamination is rarely found in oolitic limestone. The section is placed in the *Orbitopsella primaeva* partial-range zone of Late Sinemurian to early Early Pliensbachian age (Velić, 2007; not into the early Late Sinemurian *Lituosepta recoraensis* zone as stated in Gale, 2014).

In the Podpeč quarry two sections were logged and correlated: Podpeč 1 (33 m thick) and Podpeč 2 (12 m thick) (Fig. 7). Limestone predominates, but up to several centimetres thick intercalations of red claystone are common. The measured section starts with 3 m thick packstone/grainstone with superficial ooids and recrystallised bivalve shells concentrated near the upper bedding plane in a 20 cm thick layer. Grainstone is followed by almost 7 m thick packstone/grainstone with lithiotid bivalves oriented perpendicular to the bedding plane, with commissures oriented upwards (i.e., preserved in toto). A 20 cm thick limestone bed with claystone intercalations follows. Throughout the rest of the section thick to very thick limestone beds predominate. Grey oolitic limestone is the most common lithological type. Dispersed bivalve shells may be present. Gradual transition from oolite into micritic limestone or vice versa is common. Oncoids are frequent in the upper part of the section. Mudstone and wackestone are also present. The latter may contain dispersed, randomly oriented terebratulid brachiopods or megalodontid bivalves. Limestone beds are often separated by red claystone layers, which may be several centimetres thick. Red claystone partings are common near the top of individual beds, and may be present also inside limestone beds. Irregular subvertical pockets filled with yellowish claystone were also found near the top of the measured section (8.5 m above the base of Podpeč 2 section in Fig. 7). Some limestone beds and claystone interlayers contain accumulated shells of lithiotid bivalves oriented parallel to the bedding plane, but often with both valves preserved together. Up to 15 cm large fragments of shells are commonly found eroded from the latter. According to Buser and Debeljak (1996), *Lithioperna scutata* is present in the lower part of the Podpeč quarry succession, whereas *Cochlearites loppianus* appears higher. The section belongs to the Early Pliensbachian *Orbitopsella praecursor* taxon range zone (Gale, 2014).

The Grad section measures 8 m in thickness (Fig. 8). Medium to thick beds predominate, which are internally often heterogenous. Mudstone, wackestone, bioclastic and ooid packstone, floatstone and rudstone with brachiopods and bivalves were determined in the field. Few beds have wavy lower boundaries and chaotic shell accumulations at the bottom, gradually passing into ooid packstone and wackestone. Lithiotid bivalves are present, but shells are randomly distributed and fragmented. The section belongs to the Early Pliensbachian *Orbitopsella praecursor* taxon range zone (Gale, 2014).

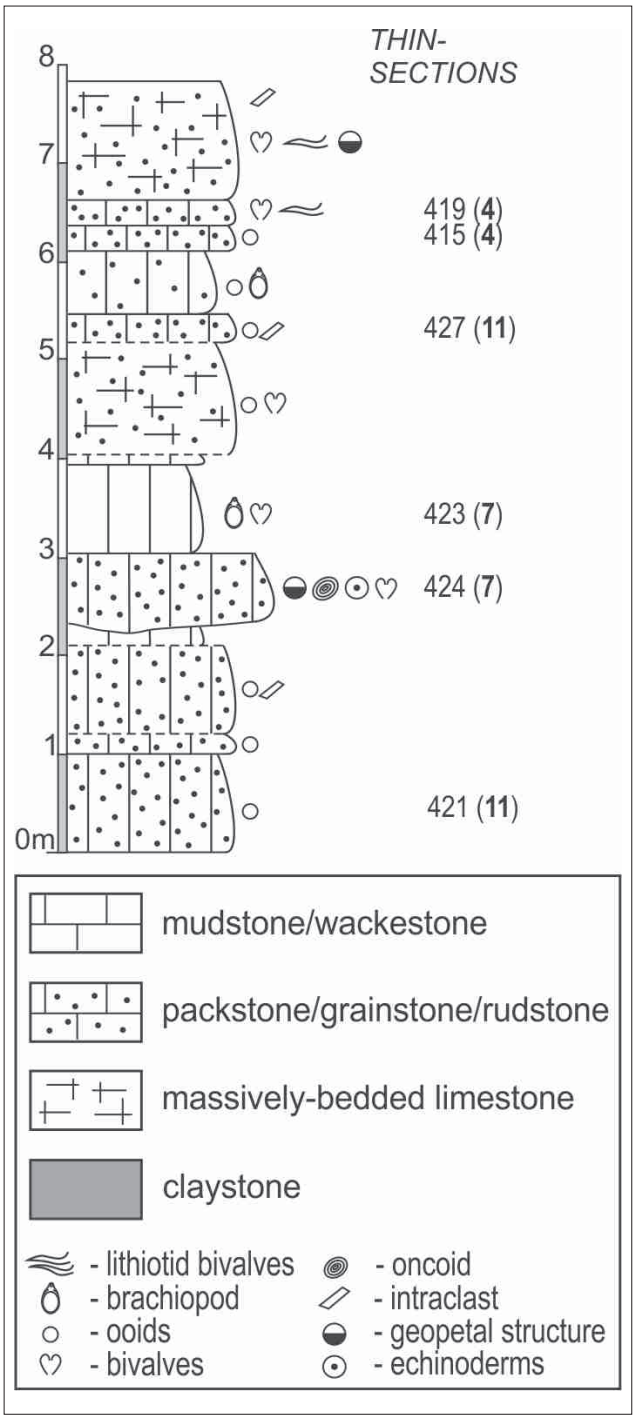

Figure 8. The Grad section of the lithiotid limestone ("Podpeč limestone" s.str.). Early Pliensbachian. Numbers in brackets denote the microfacies type.

Microfacies description

Eleven microfacies (MF) types were recognised, although subtle variations in some of them could lead to several subtypes. Comparison of described MF types with standard microfacies types (SMF) is given in Table 1.

MF 1 – Mudstone

A very common facies type is grey or black micritic limestone in thin to very thick beds. Micritic matrix is devoid of grains. Fenestrae (5 % of the thin section surface) show geopetal fabric formed by crystal silt in the lower and blocky spar in the upper part (Fig. 9.1).

MF 2 – Lithiotid floatstone to rudstone

Lithiotid bivalves are commonly accumulated in several horizons in Grad and Podpeč sections, whereas only up to several centimetres large specimens were recorded in the Zalopate section. Shells comprise up to 50 % of the thin section surface. They are partly neomorphically altered into blocky spar, and retain fibrous outer layer. They are embedded into peloidal wackestone or packstone with some fenestrae (Fig. 9.2–9.3). Small fragments of shells are common and rare benthic foraminifera are present.

MF 3 – Peloidal wackestone-packstone with Thaumatoporella

This MF type was found in thin to medium-thick beds of the Zalopate section. The distinct feature of this microfacies is the abundance of the problematic algae *Thaumatoporella* and a low abundance of benthic foraminifera. The matrix is peloidal-bioclastic wackestone with some fenestrae, and with up to 45 % of grains. Peloids represent 80–90 % of grains. Subordinate are benthic foraminifera (*Meandrovoluta asiagoensis*, *Textularia* sp. and *Siphovalvulina* spp. predominate), mollusc fragments and *Thaumatoporella* thalli. Micritic matrix in places appears clotted (Fig. 9.5).

MF 4 – Peloidal wackestone to packstone

This MF type is similar to MF 3 by the high abundance of peloids, but contains more diverse biota. It was found in medium to very thick beds and is rather common in all sections. Accumulations of lithiotid shells are sometimes present in the lower part of the same beds.

Table 1. Comparison of the determined microfacies (MF) types with Standard Microfacies Types from Flügel (2004).

Described microfacies Type	Standard Microfacies Type (Flügel, 2004)	Occurrence on flat-top platform	Occurrence on ramp
1: Mudstone	SMF 23	FZ 8 (tidal flat)	Inner ramp
2: Lithiotid floatstone to rudstone	SMF 12-Lithiotid	FZ 8 (restricted platform and tidal flat), FZ 7 (open platform)	Inner ramp
3: peloidal wackestone-packstone with *Thaumatoporella*	?SMF 18	FZ 8 (restricted platform; as bar sand channels, sand shoals heaped up by tidal currents in shallow lagoon and bays), FZ 7 (shelf lagoon with open circulation)	Inner ramp
4: Peloidal wackestone to packstone	SMF 16- Non-laminated to SMF 10	FZ 7 (open shelf lagoon) FZ 8 (restricted platform)	Inner ramp
5: Bivalve floatstone to rudstone	SMF 12-Bs	FZ 8 (restricted platform) FZ 7 (open platform)	Open inner ramp
6: Oncoidal-peloidal floatstone	SMF 22	FZ 8 (low-energy part of shallow lagoon and tidal zone)	Middle and outer ramp
7: Coated bioclastic floatstone with peloidal-bioclastic wackestone-packstone matrix	SMF 10	FZ 7 (open shelf lagoon)	Inner ramp
8: Peloidal grainstone	SMF 16-Non-laminated	FZ 8 (shallow platform interior)	Inner ramp
9: Cortoid floatstone to rudstone with peloidal-bioclastic grainstone matrix	(no single analogue; mostly SMF 14)	Shallow platform interior with moderate to high water energy	Inner ramp (shoal)
10: Bimodal poorly to medium sorted ooidal-peloidal grainstone	SMF 17	FZ 7 (shallow open shallow platform)	(very rare)
11: Well sorted ooidal grainstone	SMF 15	FZ 8 (restricted lagoon) FZ 7 (oolitic shoals, tidal bars, beaches)	Inner ramp

Grains represent 40–50 % of the thin section surface, and are well to very well sorted (Fig. 9.6). Peloid size is 0.1–0.15 or 0.2–0.35 mm.

Subangular to well-rounded peloids predominate (60–80 % of clasts; Fig. 9.7). Mollusc fragments (in some thin sections with micritic outlines) and micritic intraclasts represent 5 % of grains each. The rest of the clasts are represented by small benthic foraminifera (*Meandrovoluta* sp., Lagenina), pellets (*Parafavreina* sp.), microproblematica *Thaumatoporella* sp., green algae, echinoderms, and ostracods. Aggregate grains (mature lumps) are very rare. Subangular, sub-elongated mudstone intraclasts (mudchips) are rarely present.

Into microspar recrystallised matrix is bioturbated and contains some fenestrae. Vugs, filled with blocky spar, represent 2.5–5 % of the thin section surface.

MF 5 – Bivalve floatstone to rudstone

Present in medium thick beds, without apparent orientation of shells or with convex side turned downwards.

This MF is characterised by accumulation of up to several milimetres large bivalves and rare gastropods embedded in micritic matrix (Fig. 9.8). Both valves are present, mostly unbroken, without micritic outlines, and positioned oblique or parallel to bedding. The original shell material is replaced by blocky spar. Microcrystalline spar is present at the bottom of some valves, succeeded by blocky spar, suggesting dissolution of shells. Ostracods are very rare.

MF 6 – Oncoidal-peloidal floatstone

This type of microfacies was recorded in thick beds, overlying oolite with intraclasts and passing into ooid-intraclastic packstone to rudstone. It may also form a homogenous texture within individual beds.

This MF is characterised by 20–40 % of 4–12 mm large oncoids with micritic inner structure. Some peloids, small spar crystals, encrusting foraminifera, and microproblematica *Thaumatoporella* are found within the oncoids. A possible partly bored sponge was found in the center of one of the oncoids. Two subtypes may be distinguished on the basis of the matrix surrounding the oncoids.

In the first subtype, oncoids are embedded in packstone matrix (Fig. 10.1). Patches of peloidal grainstone with intergranular drusy mosaic spar are present along the packstone. Grains comprise 50 % of the area. They are poorly sorted, with an average size 0.15 mm. Peloids predominate (80 % of grains) over intraclasts (10 %), foraminifera (4 %), bivalve fragments (3 %), and microproblematica *Thaumatoporella* and *Tubiphytes* (2 %). Gastropods, echinoderms and green algae are very rare. Large lituolid foraminifera are rarely present. Echinoderm plates are overgrown by sintaxial calcite.

In the second subtype, oncoids are embedded in wackestone with patches of packstone (Fig. 10.2). Washed-out patches are rarer (2.5 % of surface), filled with drusy mosaic cement. Peloids are the dominant grain type. Superficial ooids, foraminifera, intraclasts, echinoderms, and serpulid fragments are subordinate.

MF 7 – *Coated bioclastic floatstone with peloidal-bioclastic wackestone-packstone matrix*

Present in medium to very thick beds, in places with erosional lower bedding planes.

Grains measuring 2–5 mm represent up to 25 % of the thin section area (Fig. 10.3–10.4). They consist of bivalve fragments, rarely gastropods, brachiopod shells, and aggregate grains. Fossils are neomorphically altered into mosaic or granular spar. Some are rounded due to abrasion/bioerosion, strongly bored at the surface or have micritic coatings. The supporting matrix is represented by peloidal-bioclastic wackestone-packstone with 30-50 % of grains (Fig. 10.5). These are dominated by peloids (80 % of grains). Common are mollusc shell fragments (10–15 % of grains), which are angular, without micritic outlines. Foraminifera (up to 5 % of grains diverse small and large benthic forms) and echinoderms (2.5 % of grains) are always present, whereas amount of superficial ooids varies (0–5 %). Gastropods (Fig. 10.6), ostracods, dasyclad green algae, and brachiopods are rare to very rare. Almost 2 mm wide stromatactis-like cavities are rarely present, filled with blocky spar.

Remark: This MF could alternatively be assigned to SMF 11 (Coated bioclastic grainstone), occuring in winnowed platform edge sands, rarely in inner- and middle-ramp settings. In Table 1, it is attributed to SMF 10 (Bioclastic packstone and grainstone with worn skeletal grains).

Figure 9. Microfacies types of the Podpeč limestone.

1 – Mudstone with fenestrae, partly filled with crystal silt (arrowhead). Thin section 416.

2 –3 Lithiotid rudstone. Thin section 412.

4 –5 *Thaumatoporella* wackestone-packstone. *Thaumatoporella* thallus is marked with the arrowhead. Thin section 426.

6 –7 Peloidal wackestone to packstone. Thin section 336.

8 – Bivalve rudstone. Thin section 323.

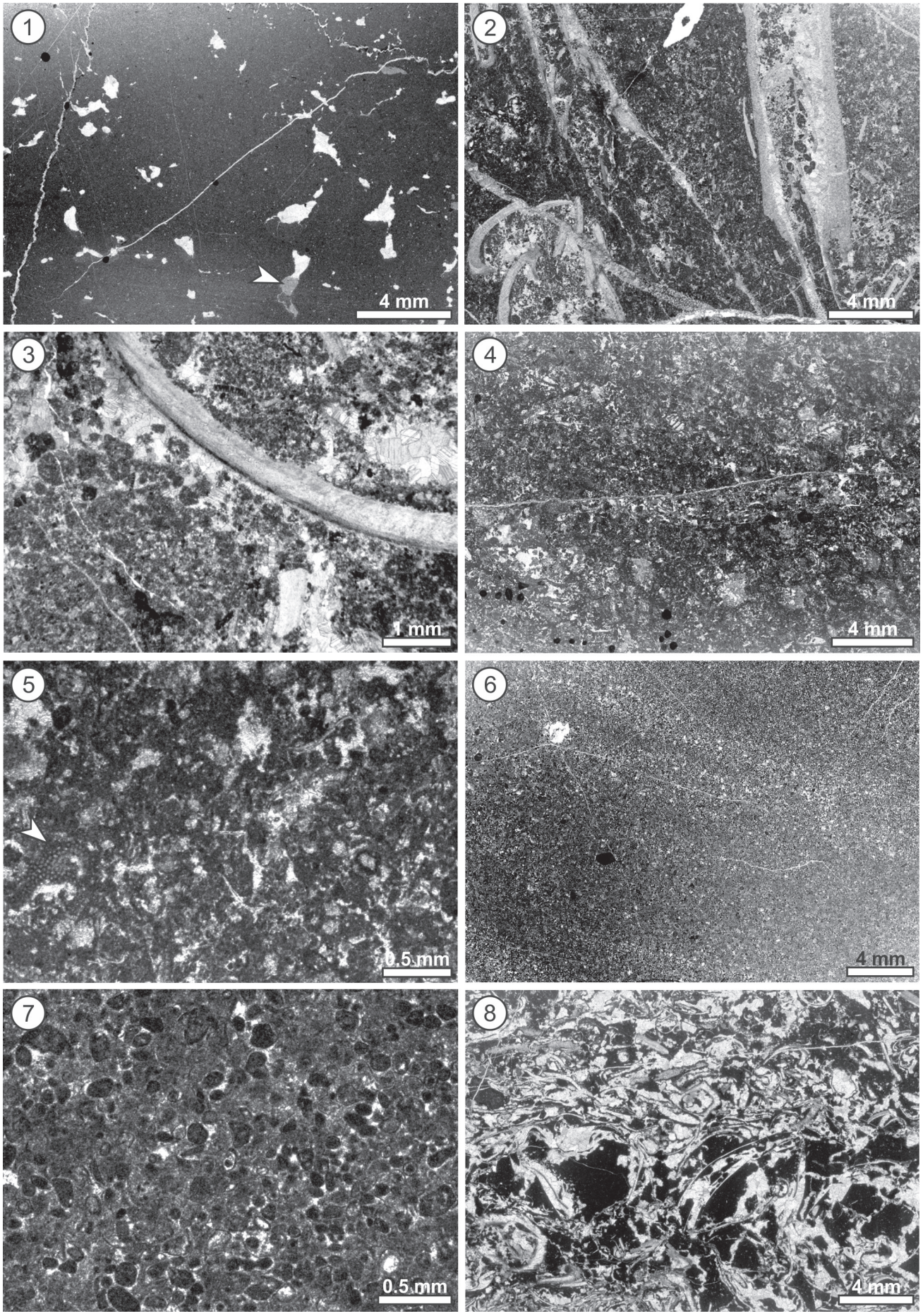
1
4 mm
2
4 mm
3
1 mm
4
4 mm
5
0.5 mm
6
4 mm
7
0.5 mm
8
4 mm

MF 8 – Peloidal grainstone

Present in medium thick beds with cross-lamination, and massive beds.

This MF is distinguished from MF 7 in the smaller amount of clasts larger than 2 mm, and a lack of micritic matrix.

Up to 4 mm large clasts (up to 5 % of the surface) comprise mudstone and wackestone intraclasts, fragmented bivalve shells with microborings on the outer surface, gastropods, and large benthic foraminifera. Clasts are parallel to the bedding and are floating in peloidal grainstone.

Around 50 % of the peloidal grainstone consists of grains. These are well to very well sorted (Fig. 10.7–10.8). Rounded, 0.1–0.2 mm or 0.2–0.35 mm large peloids (in this case "pseudo-ooids") predominate (70 % of clasts). Subordinate are cortoids of small mollusc fragments (10 % of grains), replaced by spar, sub-rounded to angular in shape, and sub-elongated or isometric in form. Superficial ooids (10 % of grains) have nuclei of mollusc fragments, echinoderms or peloids. Echinoderms, foraminifera and lumps comprise each 5 % of grains. Gastropods and calcimicrobes are very rare.

Grains are surrounded by circumgranular bladed spar. The remaining intergranular space is filled with mosaic spar. Sintaxial cement is present around echinoderm plates.

MF 9 – Cortoid floatstone to rudstone with peloidal-bioclastic grainstone matrix

This is a very common microfacies, building medium to very thick beds. The latter are often normally graded, with large bioclasts concentrated in the lower part. Indistinct grading may be present, with rudstone passing into floatstone. Larger bivalve shells are usually parallel to bedding, but variably concave- to convex-upwards. Geopetal structures may be present in gastropod shells. Lamination due to differences in grain size is in places present in the grainstone matrix.

Clasts larger than 2 mm (up to 11 mm in diameter) comprise 10–50 % of the rock volume. They are mostly bivalve shells with micritised outer surfaces and replaced by mosaic spar (Fig. 11.1-11.2). Micritic coatings are also present. Packstone or mudstone matrix clings to some shells. Some large intraclasts with keystone vugs are locally present (Fig. 11.5). A minor part of larger clasts belongs to abraded and on the outside micritised gastropods. Their lumen is filled with packstone or with mudstone. Large benthic foraminifera, calcimicrobe *Cayeuxia*, dasyclad green algae geniculi, echinoderms, and packstone intraclasts represent a smaller amount of large grains.

The described large clasts float in peloidal-bioclastic grainstone (Fig.11.3–11.4). The mean size of peloids is around 0.2 mm, whereas bioclasts measure 0.5–1 mm. Grains are well rounded, sub-elongated to spherical in shape. Peloids or superficial ooids predominate (around 80 % of smaller grains). The rest of the smaller grains are echinoderms (some with micritised outlines), mollusc fragments, benthic foraminifera, dasyclad green algae, brachiopod fragments, and aggregate grains.

Grains are surrounded by fibrous to bladed circumgranular cement. The remaining intergranular space is filled with mosaic spar. Larger vugs and umbrella-type vugs beneath some bivalve shells are filled with drusy mosaic spar. Echinoderms are enclosed in sintaxial cement.

Remark: There is no single SMF type to describe rudstone to floatstone with grainstone matrix. Instead, comparable lithology is interpreted as storm deposit (Pl. 127, fig. 2 in Flügel, 2004; see also Caracuel et al., 2005).

MF 10 – Bimodal poorly to medium sorted ooid-peloidal grainstone

This type of microfacies was recognised in thin beds, in very thick beds with inverse-to-normal grading, or in very thick beds with bivalve accumulations at the base. It was also encountered as lense-shaped accumulations.

Grains represent 60% of the volume and are bimodally distributed (Fig.11.6–11.7). Sorting is poor to moderately good. Grains are in point contacts. Larger grains (diameter 0.3 or 0.5–0.8 mm) are represented by ooids and aggregate grains. Interstices between larger grains are more or less densely filled with smaller ooids (diameter 0.05–0.07 mm) and peloids.

Figure 10. Microfacies types of the Podpeč limestone.

1 – Oncoidal floatstone with packstone matrix. Thin section 524.

2 – Oncoidal floatstone with wackestone matrix. Thin section 518.

3 – Floatstone with packstone matrix. Thin section 328.

4 – Floatstone with dense wackestone matrix. Thin section 424a.

5 – Wackestone matrix of floatstone. Fragmented fossils, ostracods and peloids. Thin section 423.

6 – Gastropod shell replaced by drusy mosaic spar. Crossed nicols. Floatstone with wackestone matrix. Thin section 423.

7 – Peloidal grainstone. Thin section 534.

8 – Peloidal grainstone. Note a small radial ooid (white arrowhead) and spar-replaced bioclasts (black arrowhead), the majority of which have micritic outline. Thin section 331.

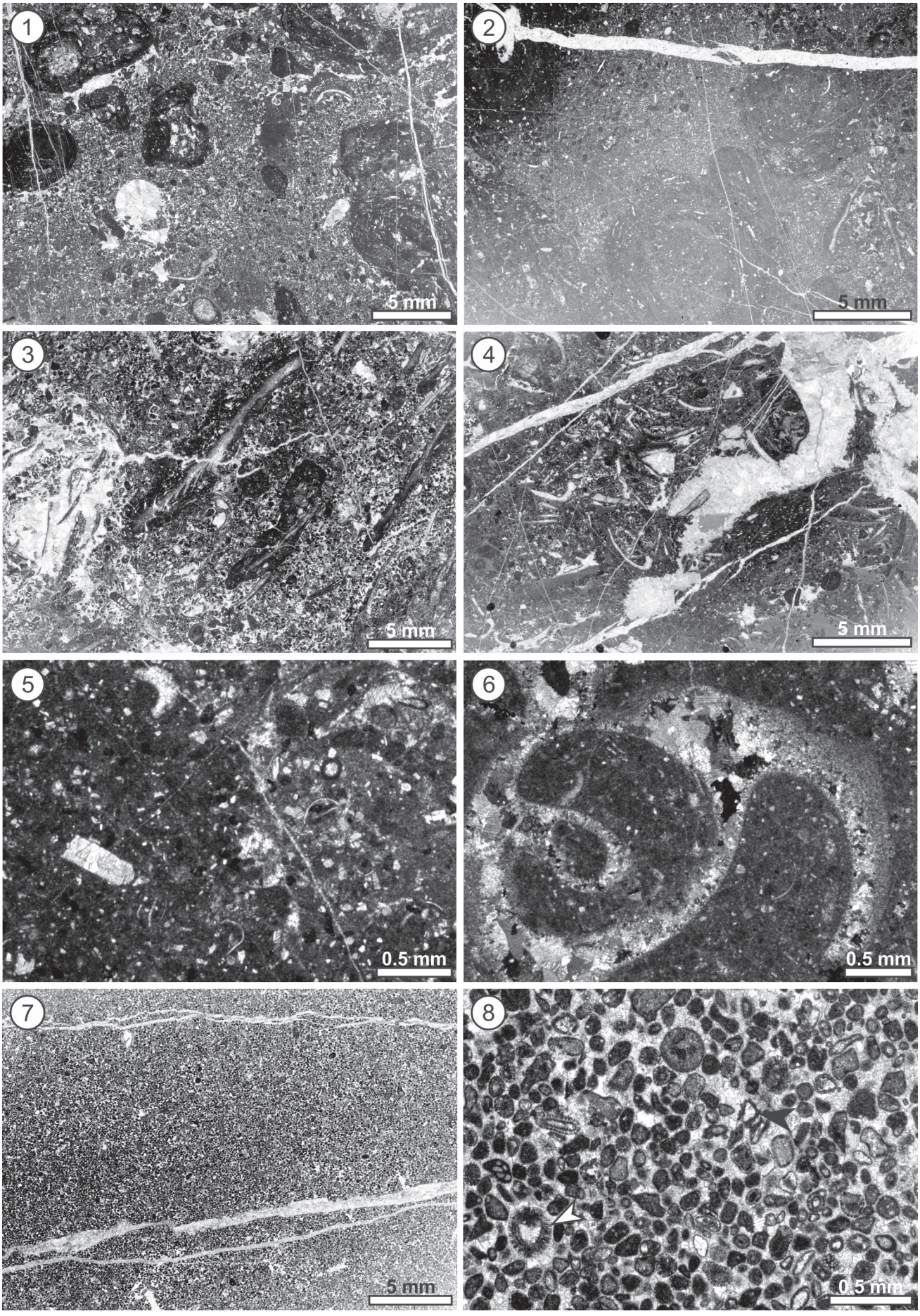
1
5 mm
2
5 mm
3
5 mm
4
5 mm
5
0.5 mm
6
0.5 mm
7
5 mm
8
0.5 mm

Peloids account for 40 % of grains. They are very well rounded and have hazy outlines. They are often grouped into small patches. Aggregate grains (lumps and mature lumps) represent around 30 % of grains. They consist of ooids, bounded by micritic meniscus cement. Spheroidal ooids represent approximately 20 % of grains. They are largely micritised and partly recrystallised; it is thus difficult to distinguish whether they were concentric or radial. Their nuclei include neomorphically altered shell fragments, echinoderm plates, rarely small gastropods, but most are micritic/micritised. The cortex (often micritised) consists of 9–15 or more laminae, each 8–10 μm thick. The cortex/nucleus ratio is 41–56 %. Superficial ooids, formed around large benthic foraminifera, and a few spiny ooids are also present (Fig. 12.1). A minor amount of grains belongs to intraclasts of peloidal packstone. Cortoids (up to 5 % of clasts) are mostly small fragments. Some larger bivalve shell fragments have strongly micritised outer surfaces. Some have uneven micritic coatings. The shells themselves are replaced by spar. Isolated (i.e., not included into ooids) benthic foraminifera are rarely found. Gastropods are rare.

Intergranular space is filled with drusy mosaic spar.

MF 11 – Well-sorted ooid grainstone

This type is present in medium thick beds with slight cross lamination, in thick and very thick beds (also following bivalve shell accumulation at the base), and as lens-like accumulations.

Grains represent 50 % of the volume. Sorting is good to very good (Fig. 12.2–12.3, 12.5). Grains are in point contacts. Two MF 11 subtypes are distinguished on the basis of the prevalent ooids sizes: MF11a with 0.15-0.35 mm (mean size 0.30 mm) large ooids (Figs. 12.2-12.3, 12.5), and MF11b with 0.35-0.55 mm (mean size 0.40 mm) large ooids (Figs. 12.4, 12.6). In places, lamination is visible due to a slight change in grain size and packing (Fig. 12.3). The lamina boundaries may be slightly undulating and sharp (Fig. 12.5).

Ooids are spheroidal and present 95 % of grains (Fig. 12.4). Nuclei are usually micritic, although small benthic foraminifera, mollusc fragments and echinoderm remains are present. As in MF 10, ooids are mostly strongly micritised, but there appears to be fewer (up to nine) laminae in cortices. The ratio cortex:nucleus amounts to up to 45 % for the thickest ooids. Few superficial ooids, formed around shell fragments, foraminifera and echinoderms, are also present. Spiny ooids are very rare, as well as broken and half-moon ooids.

The remaining grains are neomorphically altered shell fragments (mostly free of micritic coating), echinoderms, gastropods, aggregate grains, and very rare green algae, ostracods, and brachiopod fragments. Foraminifera were found only as ooid nuclei.

Grains are rimmed by fibrous to bladed spar (Fig. 12.6), succeeded by drusy mosaic intergranular cement (Fig. 12.4). Sintaxial cement is present around echinoderm plates, and ooids are partly recrystallised. Keystone vugs, filled with drusy mosaic spar are common. Slightly irregular laminae of crystal silt are sometimes present within grainstone (Fig. 12.6).

Discussion

Interpretation of the studied sections

Reddish colouration of upper bedding planes, thin irregular intercalations of claystone and in one case subvertical pipes filled with yellowish claystone correspond to palaeosol and palaeokarst surfaces (Martinuš et al., 2012; see also Buser & Debeljak, 1996), and suggest deposition in a very shallow sea, frequently interrupted by emersions. Spiny ooids are also indicative of vadose conditions (Flügel, 2004). On the basis of the thickest bed (7 m in Podpeč section), and the abundance of paleosol horizons in the Podpeč section, the water depth might have been only a few meters.

Lithiotid bivalves preserved in living position in the lower part of the Podpeč section suggest a short transport of lithiotid shells found in slightly

Figure 11. Microfacies types of the Podpeč limestone.

1 – Bioclastic floatstone-rudstone with peloidal grainstone matrix. Note the neomorphic replacement of mollusc shells by drusy mosaic spar (arrowhead) and the sindepositional pore space beneath the shell, filled by spar (S). Thin section 523.

2 – Bioclastic rudstone with peloidal grainstone matrix. Thin section 429d.

3 – Details of the grainstone matrix. Note the highly micritised bioclasts (B), a large rounded micritic clast (completely recrystallised bioclast?) and a fragment of benthic foraminifera (arrowhead). Thin section 417.

4 – Details of the grainstone matrix. Note the crude lamination due to the difference in grain size and sorting (arrowhead points at the sub-horizontal boundary). Thin section 528.

5 – Large lithified intraclast (peloidal grainstone with large keystone vugs (K) – cemented beachrock) in bioclastic rudstone. Arrowhead points at the intensely cemented intraclast boundary. Thin section 420.

6 – Bimodal poorly to medium sorted ooid grainstone. Note large bivalves (B), keystone vugs (K) partly filled with internal sediment and some aggregate grains (arrowhead). Thin section 413.

7 – Bimodal poorly to medium sorted ooid grainstone. Note crude lamination (laminae running from top left to lower right) suggested by grain density. Thin section 429c, not oriented.

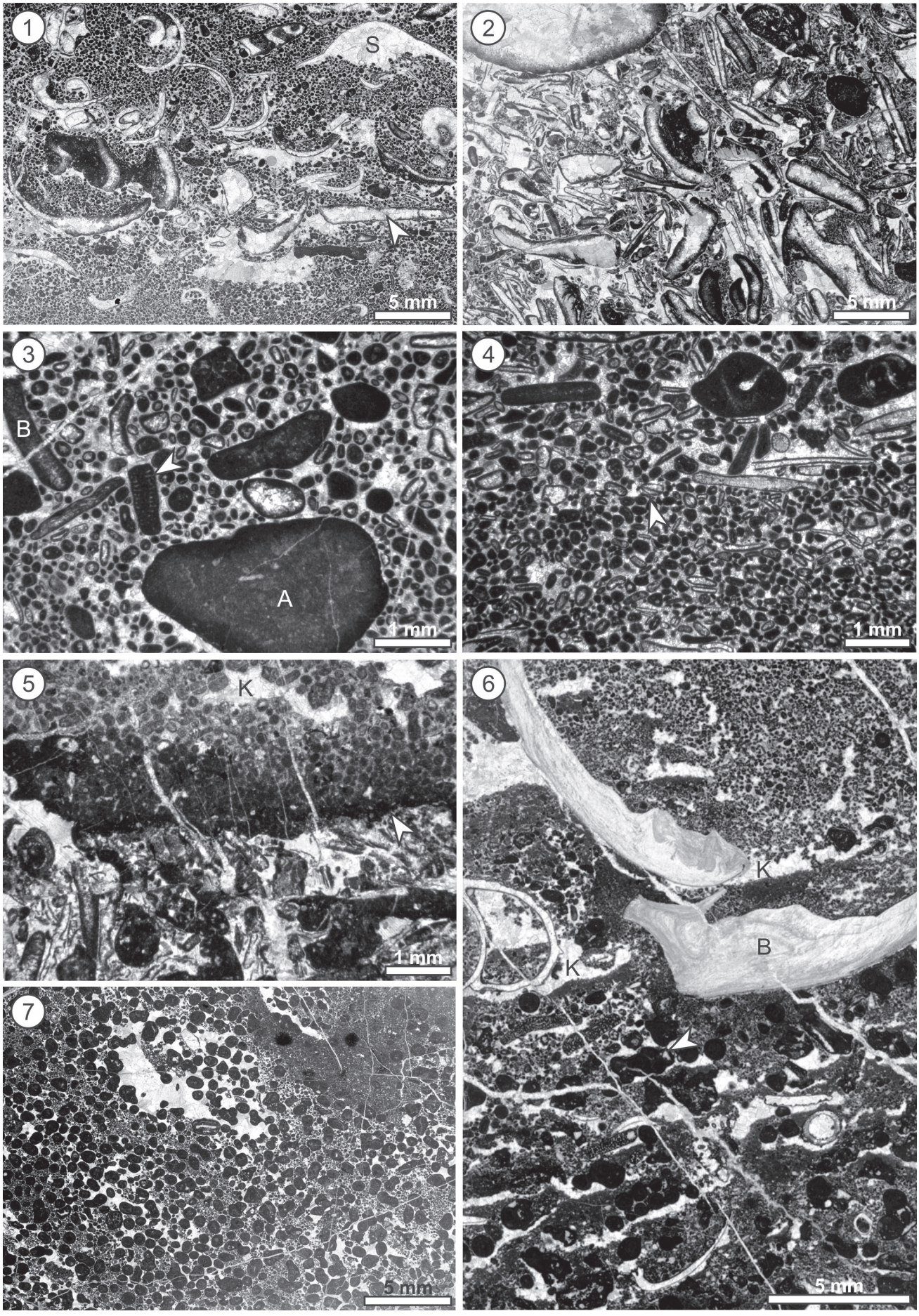
1
S
5 mm
2
5 mm
3
B
A
1 mm
4
1 mm
5
K
1 mm
6
K
B
K
5 mm
7
5 mm

younger claystone beds. It is also possible that accumulations of lithiotid shells in claystone result from subaerial exposure of the entire buildup, resulting in its demise, so these individuals may also be preserved in situ (hence the preservation of both valves).

Birdseyes vugs and cortoids further agree with deposition in a very shallow marine setting (Flügel, 2004). A mixture of high- and low-energy environment and/or events is suggested by the co-presence of ooids and oncoids (turbulent water) and micritic limestone (stagnant water), and is reflected in the mixture of high and low energy microfacies types. Chaotic accumulations of mollusc shells suggest occasional influence of high water-energy events, such as storms (Masetti, 2002; Flügel, 2004).

The microfacies (MF) association agrees with the interpretation of the shallow-marine sedimentary environment (Table 1). Although MF types 1, 2, 3 and 5 were described only from the Podpeč section, and MF 6 only from the Zalopate section, this is attributed to the sampling bias, because only a small proportion of beds were sampled for microscopy.

The northern part of the Adriatic Carbonate Platform

On the basis of several schematic sections, Buser and Debeljak (1996) suggested a rimmed carbonate platform model. They positioned the Podpeč area close to the oolitic margin of the platform. A similar position was envisaged for the Špik section in Trnovski gozd. The ooid-rich margin of the platform is followed landward by a restricted lagoon in which mud-rich limestone with low energy index deposited (Buser and Debeljak, 1996). Dozet (1999) later described lithiotid limestone near Kočevje, where lithiotid-bearing dolomite is intercalated with thin layers of fine-grained intraformational breccia and coal-bearing horizons.

In contrast, Črne and Goričan (2008) suggested the ramp type model on the basis of similarities of the Kovk section with the Rumija in Montenegro. The lithiotid limestone in the Kovk section was divided into three units (Črne and Goričan, 2008). The lowermost of these comprises thick bedded peritidal limestone (subtidal wackestone, rarely packstone, inter- to supratidal fenestral mudstone or fenestral peloidal packstone, rarely peloidal grainstone with few ooids) with lithiotid bivalves. The second subunit consists of peloidal grainstone with ooids, and the third of peritidal wackestone and packstone with bivalves of the lithiotid facies. According to Črne and Goričan (2008), Kovk section belongs to the inner ramp setting.

The herein described association of microfacies types agrees with both interpretations (Table 1), and may correspond to the inner-ramp setting, or to the open and restricted lagoon interior of the rimmed platform model (Flügel, 2004). However, the rimmed platform model is herein preferred due to the following reasons:

(1) cortoids and aggregate grains are more common on a rimmed platform (Flügel, 2004), although they are not excluded from ramps;
(2) a rimmed platform would be more prone to small sea-level falls, and emersions are common in recorded sections, especially in the Podpeč sections;
(3) the ramp model suggests that all known localities of the lithiotid limestone belong to the inner ramp setting (Fig. 13.1); this also suggests that an entire middle and outer ramp are currently missing due to latter thrusting or breaking of the AdCP margin;
(4) the rimmed carbonate platform model on the contrary suggests a more widespread palaeogeographic distribution of localities (Fig. 13.2), and a less drastic post-Cretaceous crust shortening.

Conclusions

The microfacies association recorded in the Late Sinemurian – Pliensbachian lithiotid bivalves-bearing limestone at the northern margin of the Adriatic Carbonate Platform comprises: (1) mudstone, (2) lithiotid floatstone

Figure 12. Microfacies types of the Podpeč limestone.

1 – Bimodal poor to medium sorted ooid grainstone. Note the common aggregate grains (A) and a spiny ooid (S), typical of sands cemented in a vadose environment (see Flügel, 2004, p. 148). Thin section 334.

2 – Well sorted ooid grainstone. Unimodal size distribution of ooids suggests pre-depositional sorting of grains. Note moldic porosity formed through total dissolution of some bivalve shells (black arrowhead). A few cortoids (white arrowhead) and intraclasts (I) are also present. Thin section 322.

3 – Unimodally sorted ooid grainstone with at least four laminae (L1-L4) with blurred boundaries, suggesting changes in water energy conditions. Note normal grading in laminae L3 and L4. Obliquely cut sample. Thin section 335.

4 – Detail of ooid grainstone with a small bivalve. Note circumgranular and intragranular fibrous cement (arrowhead) and the blocky spar (B) filling the remaining inter- and intragranular space. Thin section 421.

5 – Well sorted ooid grainstone. Arrowheads point at wavy boundaries reflecting short-term changes in water energy conditions. Thin section 536.

6 – Lamina within ooid grainstone, where the pore space between grains (oolites, aggregate grains, bivalve fragment with micritic outline) is filled with marine phreatic fibrous circumgranular cement (arrowhead) and crystal silt, suggesting occasional vadose conditions (see Fig. 14.20 in Flügel, 2004). Thin section 427.

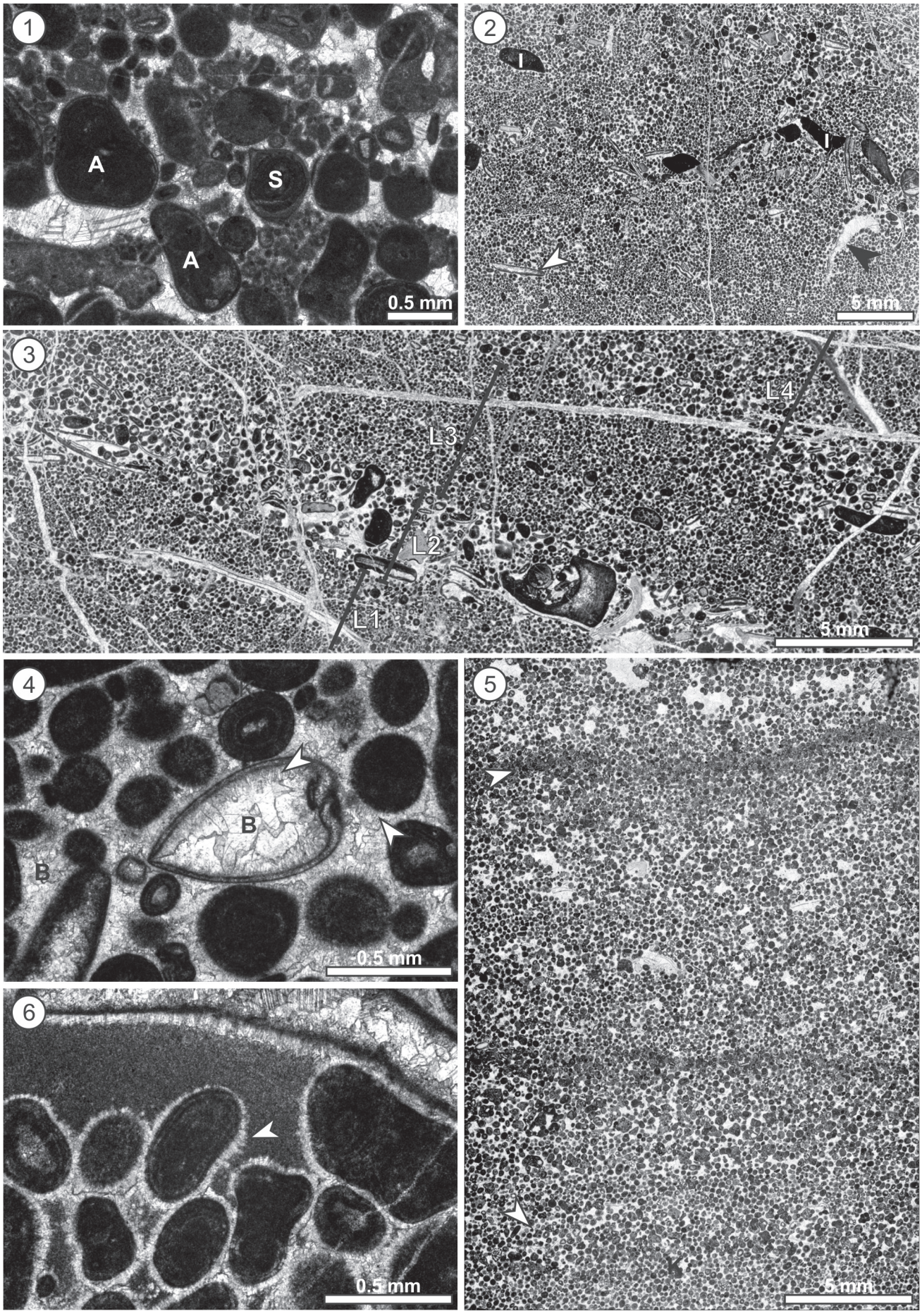
1
A
S
A
0.5 mm
2
I
I
5 mm
3
L4
L3
L2
L1
5 mm
4
B
B
0.5 mm
5
5 mm
6
0.5 mm

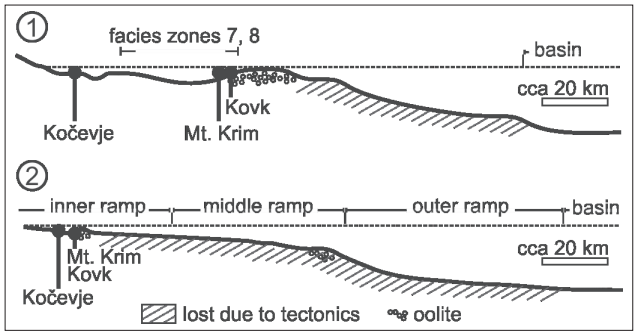

Figure 13. Discussed possible models for the northern part of the Adriatic Carbonate Platform. 1 – Rimmed platform. 2 – Carbonate ramp. Modified after Flügel (2004).

to rudstone, (3) peloidal wackestone-packstone with *Thaumatoporella*, (4) peloidal wackestone to packstone, (5) bivalve floatstone to rudstone, (6) oncoidal-peloidal floatstone, (7) coated bioclastic floatstone with peloidal-bioclastic wackestone-packstone matrix, (8) peloidal grainstone, (9) cortoid floatstone to rudstone with peloidal-bioclastic grainstone matrix, (10) bimodal poorly to medium sorted ooid-peloidal grainstone, and (11) well sorted ooid grainstone.

The most common type of grains are ooids, aggregate grains and various skeletal particles (bivalve shells, large benthic foraminifera). Cortoids are common. Rare spiny ooids indicate occasional vadose conditions, and subaerial exposure surfaces point to occasional emersion. The most common type of cement, present in washed-out patches of micritic matrix or among grains in higher-energy facies types, is blocky or drusy mosaic spar. In several MF types, it is preceded by circumgranular fibrous to bladed spar.

The facies association corresponds to restricted and open marine interior (facies zones 8 and 7) of a platform bordered by marginal sand shoals, or to the inner ramp setting (Flügel, 2004). This study does not give the final answer concerning the type of the platform due to the lack of seismic-scale profiles. However, the platform bordered by oolitic shoals and with a steep transition to the Slovenian Basin to the north may be a better model than the ramp model.

Acknowledgements

This study was financed by the Slovenian Research Agency (program number P1-0011). The technical staff of the Geological Survey of Slovenia is acknowledged for preparation of samples. Students P. Oprčkal and M. Jamnik assisted during field work. Reviewers Boštjan Rožič (Department for Geology, Faculty of Natural Sciences and Engineering, Ljubljana) and Adrijan Košir (Research Centre of the Slovenian Academy of Sciences and Arts) are acknowledged for discussions, useful comments in improvements to the manuscript. I am also most thankful to two anonymous researchers, who reviewed the very first version of the manuscript.

References

Azerêdo, A.C., Manuppella, G. & Ramalho, M.M. 2003: The Late Sinemurian carbonate platform and microfossils with Tethyan affinities of the Algarve Basin (south Portugal). Facies, 48: 49–60.

Bacelle, L. & Bosellini, A. 1965: Diagrammi per la stima visiva della composizione percentuale nelle rocce sedimentarie. Ann. Uni. Ferrara, N.S., Sez. IX: Sci. Geol. Paleontol., 1: 59–62.

Barattolo, F. & Romano, R. 2005: Shallow carbonate platform bioevents during the Upper Triassic-Lower Jurassic: an evolutive interpretation. Boll. Soc. Geol. It. (Ital. J. Geosci), 124: 123–142.

Blomeier, D.P.G. & Reijmer, J.J.G. 1999: Drowning of a Lower Jurassic carbonate platform: Jbel Bou Dahar, High Atlas, Morocco. Facies, 41: 81–110.

Bosence, D., Procter, E., Aurell, M., Bel Kahla, A., BouDagher-Fadel, M., Casaglia, F., Cirilli, S., Mehdie, M., Nieto, L., Rey, J., Scherreiks, R., Soussi, M. & Waltham, D. 2009: A dominant tectonic signal in high-frequency, peritidal carbonate cycles? A regional analysis of Liassic platforms from western Tethys. J. Sed. Res., 79: 389–415.

Brigaud, B., Vincent, B., Carpentier, C., Robin, C., Guillocheau, F., Yven, B. & Huret, E. 2014: Growth and demise of the Jurassic carbonate platform in the intracratonic Paris Basin (France): Interplay of climate change, eustasy and tectonics. Marine Petrol. Geol., 53: 3–29.

Bucković, D., Jelaska, V. & Cvetko Tešović, B. 2001: Facies variability in Lower Liassic carbonate successions of the western Dinarides (Croatia). Facies, 44: 151–162.

Buser, S. 1965: Stratigrafski razvoj jurskih skladov na južnem Primorskem, Notranjskem in zahodni Dolenjski (dissertation). University of Ljubljana, Faculty of Natural Sciences and Technology, Department for Mineralogy and Geology, Ljubljana: 101 p.

Buser, S. 1968: Basic Geological Map SFRY 1 : 100.000, The Ribnica Sheet, L 33-78. Zvezni geološki zavod Beograd.

Buser, S. 1989: Development of the Dinaric and the Julian carbonate platforms and of the intermediate Slovenian Basin (NW Yugoslavia). In: Carulli, G.B., Cucchi, F. & Radrizzani, C.P. (eds.): Evolution of the karstic carbonate platform: relation with other periadriatic carbonate platforms. Mem. Soc. Geol. Ital., 40 (1987): 313–320.

Buser, S. & Debeljak, I. 1996: Lower Jurassic beds with bivalves in South Slovenia. Geologija, 37–38: 23–62, doi:10.5474/geologija.1995.001.

Buser, S., Grad, K. & Pleničar, M. 1967: Basic Geological Map of SFRY 1 : 100.000, The Postojna Sheet, L 33-77. Zvezni geološki zavod, Beograd.

Buser, S., Kolar-Jurkovšek, T. & Jurkovšek, B. 2008: The Slovenian Basin during the Triassic in the light of conodont data. Boll. Soc. Geol. It. (Ital. J. Geosci.), 127: 257–263.

Caracuel, J.E., Giannetti, A. & Monaco, P. 2005: Multivariate analysis of taphonomic data in Lower Jurassic carbonate platform (northern Italy). C. R. Palevol, 4: 653–662.

Cobianchi, M. & Picotti, V. 2001: Sedimentary and biological response to sea-level and palaeoceanographic changes of a Lower-Middle Jurassic Tethyan platform margin (Southern Alps, Italy). Palaeogeogr., Palaeoclimatol., Palaeoecol., 169: 219–244.

Čadjenović, D., Kilibarda, Z. & Radulović, N. 2008: Late Triassic to Late Jurassic evolution of the Adriatic Carbonate Platform and Budva Basin, southern Montenegro. Sed. Geol., 204: 1–17.

Črne, A.E. & Goričan, Š. 2008: The Dinaric Carbonate Platform margin in the Early Jurassic: a comparison between successions in Slovenia and Montenegro. Boll. Soc. Geol. It. (Ital. J. Geosci.), 127: 389–405.

Debeljak, I. & Buser, S. 1997: Lithiotid bivalves in Slovenia and their mode of life. Geologija, 40: 11–64. doi:10.5474/geologija.1997.001.

Dozet, S. 1992: Litostratigrafske enote in značilne mikrofacije Kočevske jure. Min. Mettal. Quarterly, 39: 287–305.

Dozet, S. 1993: Lofer cyclothems from the Lower Liassic Krka limestone. Riv. Ital. Paleont. Strat., 99: 81–100.

Dozet, S. 1996: Foraminiferal and algal biostratigraphy of the Jurassic beds in southeastern Slovenia. Min. Mettal. Quarterly, 43: 3–10.

Dozet, S. 1999: Lower Jurassic dolomite-limestone succession with coal in the Kočevski Rog and correlation with neighbouring areas (southeastern Slovenia). Geologija, 41: 71–101, doi:10.5474/geologija.1998.004.

Dozet, S. 2009: Lower Jurassic carbonate succession between Predole and Mlačevo, Central Slovenia. RMZ – Materials and Geoenvironment, 56/2: 164–193

Dozet, S. & Strohmenger, C. 2000: Podbukovje Formation, central Slovenia. Geologija, 43/2: 197–212, doi:10.5474/geologija.2000.014.

Dragičević, I. & Velić, I. 2002: The northeastern margin of the Adriatic Carbonate Platform. Geol. Croat., 55: 185–232.

Dunham, R.J. 1962: Classification of carbonate rocks according to depositional texture. In: Ham W.E. (ed.): Classification of carbonate rocks. Tulsa, Oklahoma, AAPG Mem., 1: 108–121.

Embry, A.F. & Klovan, J.E. 1971: A Late Devonian reef tract on northeastern Banks Island, N.W.T. Bull. Can. Petrol. Geol., 19: 730–781.

Eren, M., Tasli, K. & Tol, N. 2002: Sedimentology of Liassic carbonates (Pirencik Tepe measured section) in the Aydincik (Içel) area, southern Turkey. J. Asian Earth Sci., 20: 791–801.

Flügel, E. 2004: Microfacies of carbonate rocks: Analysis, interpretation and application. Springer-Verlag, Berlin Heidelberg, New York: 984 p.

Fraser, N.M., Bottjer, D.J. & Fischer, A.G. 2004: Dissecting "lithiotis" bivalves: Implications for the Early Jurassic reef eclipse. Palaios, 19: 51–67.

Friedman, G. M. 2003: Classification of sediments and sedimentary rocks. In: Middleton, G. V. (ed.): Encyclopedia of sediments and sedimentary rocks. Springer: 127–135.

Fugagnoli, A. 2004: Trophic regimes of benthic foraminiferal assemblages in Lower Jurassic shallow water carbonates from northeastern Italy (Calcari Grigi, Trento Platform, Venetian Prealps). Palaeogeogr., Palaeoclimatol., Palaeoecol., 205: 111–130.

Fugagnoli, A. & Loriga Broglio, C. 1998: Revised biostratigraphy of Lower Jurassic shallow water carbonates from the Venetian Prealps (Calcari Grigi, Trento Platform, Northern Italy). Studi Trentini Sci. Natur. Acta Geol., 73: 35–73.

Gale, L. 2014: Lower Jurassic foraminiferal biostratigraphy of Podpeč Limestone (External Dinarides, Slovenia). Geologija, 57/2: 119-146, doi:10.5474/geologija.2014.011.

Galli, G. 1993: "Calcari Grigi" Formation, Jurassic, Venetian Alps. In: Galli, G. (ed.): Temporal and Spatial Patterns in Carbonate Platforms. Springer-Verlag, Berlin Heidelberg: 97–129.

Greene, S.E., Martindale, R.C., Ritterbush, K.A., Bottjer, D.J., Corsetti, F.A. & Berelson, W.M. 2012: Recognizing ocean acidification in deep time: An evaluation of the evidence for acidification across the Triassic-Jurassic boundary. Earth-Sci. Rev., 113: 72–93.

Hallam, A. 2001: A review of the broad pattern of Jurassic sea-level changes and their possible causes in the light of current knowledge. Palaeogeogr., Palaeoclimatol., Palaeoecol., 167: 23–37.

Hautmann, M., Benton, M. J. & Tomašových, A. 2008: Catastrophic ocean acidification at the Triassic-Jurassic boundary. N. Jb. Geol. Paläont. Abh., 249: 119–127.

Jamšek Rupnik, P., Popit, T., Jež, J. & Bavec, M. 2015: Field trip: Quaternary dynamics of the Ljubljana Basin. In: Quarternary Geology in Croatia and Slovenia, 4th scientific meeting, Zagreb, 25-26 March 2015. Croatian National INQUA Committee & Slovenian National INQUA Committee, Zagreb & Ljubljana.

Kastelic, V. & Carafa, M.M.C. 2012: Fault slip rates for the active External Dinarides thrust-and-fold belt. Tectonics, 31: TC3019.

Kastelic, V., Vrabec, M., Cunningham, D. & Gosar, A. 2008: Neo-Alpine structural evolution and present-day tectonic activity of the eastern Southern Alps: The case of the Ravne Fault, NW Slovenia. J. Struct. Geol., 30: 963–975.

Kramar, S., Bedjanič, M., Mirtič, B., Mladenović, A., Rožič, B., Skaberne, D., Gutman, M., Zupančič, N. & Cooper, B. 2015: Podpeč limestone: a heritage stone from Slovenia. Geol. Soc. London Spec. Publ., 407: 219–231.

Kramer, E. 1905: Das Laibacher Moor. Kleinmayr & Fed. Bamberg, Ljubljana: 205 p.

Lipold, M.V. 1858: Bericht über die geologische Aufnahme in Unter-Krain im Jahre 1857. Jb. Geol. R.-A., 9: 257–276.

Martinuš, M., Bucković, D. & Kukoć, D. 2012: Discontinuity surfaces recorded in shallow-

marine platform carbonates: an example from the Early Jurassic of the Velebit Mt. (Croatia). Facies, 58: 649–669, doi:10.1007/s10347-011-0288-7.

Masetti, D. 2002: Some remarks about facies and cyclicity in the Rotzo Member of the Calcari Grigi Formation (Trento Platform, Venetian Prealps, Middle Lias). Atti Ticinensi Sci. Terra, 43, 119–128.

Masetti, D., Claps, M., Giacometti, A., Lodi, P. & Pignatti, P. 1998: I Calcari Grigi della piattaforma di Trento (lias inferiore e medio, Prealpi Venete). Atti Tic. Sc. Terra, 40: 139–183.

Miler, M. & Pavšič, J. 2008: Triassic and Jurassic beds in Krim Mountain area (Slovenija). Geologija, 51/1: 87–99, doi:10.5474/geologija.2008.010.

Miler, M., Pavšič, J. & Dolenec, M. 2007: Determination of T/J boundary by $\delta^{13}C$ and $\delta^{18}O$ stable isotope analysis (Krim Mountain, Slovenia). RMZ – Materials and Geoenvironment, 54/2: 189–202.

Ogorelec, B. 2009: Spodnje jurske plasti v Preserju pri Borovnici. Geologija, 52/2: 193–204, doi:doi:10.5474/geologija.2009.019.

Ogorelec, B. & Rothe, P. 1993: Mikrofazies, Diagenese und Geochemie des Dachsteinkalkes und Hauptdolomits in Süd-West-Slowenien. Geologija, 35: 81–181.

Placer, L. 1999: Contribution to the macrotectonic subdivision of the border region between Southern Alps and External Dinarides. Geologija, 41: 223-255, doi:10.5474/geologija.1998.013.

Placer, L. 2008: Principles of the tectonic subdivision of Slovenia. Geologija, 51/2: 205-217, doi:10.5474/geologija.2008.021.

Pomoni-Papaioannou, F. & Kostopoulou, V. 2008: Microfacies and cycle stacking in Liassic peritidal carbonate platform strata, Gavrovo-Tripolitza platform, Peloponnesus, Greece. Facies, 54/3: 417–431, doi:10.1007/s10347-008-0142-8.

Radoičić, R. 1966: Microfacies du jurassiques des Dinarides externes de la Yugoslavie. Geologija, 9: 5–337.

Ramovš, A. 2000: Podpeč limestone, black and colorful Lesno Brdo limestone through time. Mineral, Ljubljana: 115 p.

Ruiz-Ortiz, P.A., Bosence, D.W.J., Rey, J., Nieto, L.M., Castro, J.M. & Molina, J.M. 2004: Tectonic control of facies architecture, sequence stratigraphy and drowning of a Liassic carbonate platform (Betic Cordillera, Southern Spain). Basin Res., 16: 235–257.

Sabatino, N., Vlahović, I., Jenkyns, H.C., Scopelliti, G., Neri, R., Prtoljan, B. & Velić, I. 2013: Carbon-isotope record and palaeoenvironmental changes during the early Toarcian oceanic anoxic event in shallow-marine carbonates of the Adriatic Carbonate Platform in Croatia. Geol. Mag., 150/6, 1085–1102 doi:10.1017/S0016756813000083.

Scheibner, C. & Reijmer, J.J.G. 1999: Facies patterns within a Lower Jurassic upper slope to inner platform transect (Jbel Bou Dahar, Morocco). Facies, 41: 55–80.

Strohmenger, C. & Dozet, S. 1991: Stratigraphy and geochemistry of Jurassic carbonate rocks from Suha krajina and Mala gora mountain (Southern Slovenija). Geologija, 33: 315–351, doi:10.5474/geologija.1990.008.

Šmuc, A. 2005: Jurassic and Cretaceous stratigraphy and sedimentary evolution of the Julian Alps, NW Slovenia. ZRC SAZU, Ljubljana 98 p.

Šribar, L. 1966: Jurassic sediments between the villages Zagradec and Randol in Krka Valley. Geologija, 9: 379–384.

Štukovnik, P., Dobnikar, M. & Žarnić, R. 2011: Podpeški apnenec v modelu prenove stebriščne lope centralnega stadiona v Ljubljani. Gradbeni vestnik, 60: 193–197.

Thierry, J. 2000: Late Sinemurian (193-191 Ma). In: Dercourt, J., Gaetani, M., Vrielynck, B., Barrier, E., Biju-Duval, B., Brunet, M.F., Cadet, J.P., Crasquin, S. & Sandulescu, M. (eds.): Peri-Tethys atlas, paleogeographical maps. CCGM/GGMW, Paris: map 7.

Tišljar, J., Vlahović, I., Velić, I. & Sokač, B. 2002: Carbonate platform megafacies of the Jurassic and Cretaceous deposits of the Karst Dinarides. Geol. Croat., 55: 139–170.

Tucker, M. E. 2001: Sedimentary petrology: an introduction to the origin of sedimentary rocks (3rd edition). Blackwell Science, Oxford and Northampton: 262 p.

Turnšek, D. & Košir, A. 2000: Early Jurassic corals from Krim Mountain, Slovenia. Razprave IV. Razreda SAZU, 41: 81–113.

Turnšek, D., Buser, S. & Debeljak, I. 2003: Liassic coral patch reef above the "Lithiotid limestone" on Trnovski gozd plateau, west Slovenia. Razprave IV. Razreda SAZU, 44: 285–331.

Velić, I. 2007: Stratigraphy and palaeobiogeography of Mesozoic benthic Foraminifera of the Karst Dinarides (SE Europe). Geol. Croat., 60: 1–113.

Verwer, K., Merino-Tomé, O., Kenter, J.A.M. & Della Porta, G. 2009: Evolution of a high-refief carbonate platform slope using 3D digital outcrop models: Lower Jurassic Djebel Bou Dahar, High Atlas, Morocco. J. Sed. Res., 79: 416–439, doi:10.2110/jsr.2009.045.

Vetters, H. 1933: Geologische Manuskriptkarte Radmannsdorf 1: 75.000. Geologische Bundesanstalt, Wien.

Vlahović, I., Tišljar, J., Velić, I. & Matičec, D. 2002: The Karst Dinarides are composed of relics of a single Mesozoic platform: Facts and consequences. Geol. Croat., 55: 171–183.

Vlahović, I., Tišljar, J., Velić, I. & Matičec, D. 2005: Evolution of the Adriatic Carbonate Platform: Palaeogeography, main events and depositional dynamics. Palaeogeogr., Palaeoclimatol., Palaeoecol., 220/3–4: 333–360, doi:10.1016/j.palaeo.2005.01.011

Vrabec, M. & Fodor, L. 2006: Late Cenozoic tectonics of Slovenia: structural styles at the Northeastern corner of the Adriatic microplate. In: Pinter, N., Grenerczy, G., Weber, J., Stein, S. & Medek, D. (eds.): The Adria microplate: GPS geodesy, tectonics and hazards. NATO Sci. Ser., IV, Earth Environ. Sci., 61: 151–168.

Wilmsen, M. & Neuweiler, F. 2008:. Sedimentology, 55/4: 773–807, doi: 10.1111/j.1365-3091.2007.00921.x.

GEOLOGIJA *58/2*, 139–154, Ljubljana 2015

http://dx.doi.org/10.5474/geologija.2015.011

The three-dimensional regional geological model of the Mura-Zala Basin, northeastern Slovenia

Tridimenzionalni regionalni geološki model Mursko-zalskega bazena, severovzhodna Slovenija

Dejan ŠRAM[1], Nina RMAN[2], Igor RIŽNAR[3] & Andrej LAPANJE[4]

[1,2,4] Geološki zavod Slovenije, Dimičeva ulica 14, SI–1000 Ljubljana,
e-mails: dejan.sram@geo-zs.si, nina.rman@geo-zs.si, andrej.lapanje@geo-zs.si
[3] G.E. Igor Rižnar s.p., e-mail: igor.riznar@telemach.net

Prejeto / Received 14. 9. 2015; Sprejeto / Accepted 1. 12. 2015; Objavljeno na spletu / Published online 30. 12. 2015

Key words: geological model, Haloze Formation, Špilje Formation, Lendava Formation, Mura Formation, Ptuj-Grad Formation, GeoMol, 3D-Explorer

Ključne besede: geološki model, Haloška formacija, Špiljska formacija, Lendavska formacija, Murska formacija, Ptujsko-grajska formacija, GeoMol, 3D-Explorer

Abstract

The Mura-Zala sedimentary Basin is a Neogene basin with many competing geopotentials, spanning parts of Slovenia, Austria, Croatia and Hungary. Here we present the 3D regional geological model of the Slovenian part of the Mura-Zala Basin, which was developed to integrate the latest information on the geological structure of NE Slovenia and to publish the model in an open-access mode for easier and faster assessment of geopotentials. This was achieved through the harmonisation of the legacy geological models, the reinterpretation of 145 borehole logs, the construction of the 3D numerical geological model in JewelSuite™, and delivering it into a 3D-Explorer environment. The model comprises nine lithostratigraphical units. The Pre-Neogene basement rocks are covered by the Haloze Formation; the Špilje Formation – Badenian and Sarmatian; the Lendava Formation – turbidites and slope; the Mura Formation – delta front and delta plain; and the alluvial Ptuj-Grad Formation. The model has two principal shortcomings, related to currently unavailable seismic reflection data faults were not implemented, and the Quaternary formations were not delimited. The model is useful for regional-scale studies and may reduce geological risks related to exploration in NE Slovenia. It will also support a better assessment of geopotentials and a more feasible approach to their development, and, eventually, will enable the harmonized management of our subsurface in 3D space. This can be achieved using the 3D-Explorer platform which enables the creation of arbitrary vertical cross-sections, horizontal slices and virtual boreholes.

Izvleček

Mursko-zalski sedimentacijski bazen je neogenski bazen s številnimi konkurenčnimi geopotenciali, ki se razširja v Sloveniji, Avstriji, Hrvaški in na Madžarskem. V članku predstavljamo 3D regionalni geološki model slovenskega dela Mursko-zalskega bazena. Razvit je za prikaz najnovejših informacij o geološki zgradbi SV Slovenije in objavo v prosto dostopni obliki, ki omogoča lažjo in hitrejšo oceno geopotencialov. To smo dosegli z uskladitvijo predhodnih geoloških modelov, reinterpretacijo 145 geofizikalnih popisov globokih vrtin, izdelavo 3D matematičnega modela s programom JewelSuite™ in njegovo implementacijo v orodju 3D-Explorer. Model prikazuje devet litostratigrafskih enot. Pred-neogenske kamnine v podlagi bazena so prekrite s Haloško formacijo, Špiljsko formacijo - sarmatij in badenij, Lendavsko formacijo - pobočje in turbiditi, Mursko formacijo - deltno čelo in ravnica ter aluvialno Ptujsko-grajsko formacijo. Model ima dve poglavitni slabosti, kot posledica nedostopnosti seizmičnih podatkov vanj niso vključeni prelomi in sedimenti kvartarne starosti niso razmejeni. Model je primeren za regionalne študije in zato lahko zniža geološko tveganje pri raziskavah v SV Sloveniji. S tem, ko podpira boljšo oceno geopotencialov in primernejši pristop k njihovem razvoju, bo sčasoma omogočil usklajeno upravljanje našega podpovršja v tridimenzionalnem prostoru. Raba 3D-Explorerja omogoča izdelavo poljubnih navpičnih in vodoravnih prerezov ter navideznih vrtin.

Introduction

The Pannonian Basin is a Tertiary sedimentary basin, which is considered to be a continental back-arc basin of the Carpathian orogeny (Jelen & Rifelj, 2005; Horváth et al., 2015). It is characterised by a major system of Neogene basins resting on a highly deformed and complexly faulted substrate of Mesozoic, Paleozoic, and Precambrian rocks of the Inner Carpathian foldbelt. Shared by several Central and Eastern European countries, the Pannonian Basin features a variety of vast and diverse geopotentials.

The Slovenian part of the Mura-Zala Basin (Fig. 1) is located on the western margin of the Pannonian Basin and continues on to Austria, Croatia and Hungary (Nádor et al., 2012).

In the past, the basin was called the Mura Depression (Vončina, 1966; Royden & Horváth, 1988; Mioč & Žnidarčič, 1989; Gosar, 1995) or the Mura Basin (Kralj & Kralj, 2000), and the Međimurje-Zala Basin (in Vrzel (2012) after Žižek (2006)).

The Mura-Zala basin is important for oil and gas production (e.g. Pleničar, 1954; Bader, 1976; Djurasek, 1988; Mioč & Žnidarčič, 1996; Lučić et al., 2001; Dolton, 2006; Kurevija & Vulin, 2011; Markič, 2013), for gas storage (e.g. Gosar, 2005), thermal water (e.g. Rman et al., 2012, 2015; Horváth et al., 2015), coal (e.g. Markič et al., 2011), CCS (e.g. Presečnik, 2008; Vangkilde-Pedersen et al., 2009), and its extensive groundwater reservoirs (e.g. Nosan, 1973; Žlebnik & Drobne, 1999; Kralj & Kralj, 2000; Rajver et al., 2012; Szőcs et al., 2013). New types of geopotentials, such as CO_2 and natural gas storage are competing with traditional uses, for example as a source of drinking and thermal water, and for oil and gas. Therefore, sustainable management of subsurface geopotentials requires an understanding of geology and geological structures, which can be facilitated by visualizing these reservoirs in 3D. Understanding 3D spatial relationships is a major challenge for spatial planning and licensing authorities, who need a clear picture of the subsurface on order to mitigate possible conflicts among the many users and countries involved.

Several geological studies provide a large public data repository as a web tool that is freely accessible online (see http://akvamarin.geo-zs.si/t-jam_boreholes/ or http://transenergy-eu.geologie.ac.at/). However, their value and attractiveness for stakeholders is rather poor due to the lack of an effective tool for visualising subsurface data in 3D.

The 3D regional geological model of the Slovenian part of the Mura-Zala Basin presented in this paper was developed by the Slovenian members of the project GeoMol (The GeoMol Team, 2015). The model aims to:

- publish available 3D spatial information on the geological structure of NE Slovenia,
- present the data using the latest lithostratigraphical characterisation of the Basin,
- enable open, faster and easier assessment of geopotentials.

This was achieved by reinterpretation and harmonisation of existing geological models, reinterpretation and digitalisation of log data, development of the 3D numerical geological model, and its implementation in the 3D-Explorer. This way, the opportunity to identify new areas for development of various geopotentials is freely available to everybody, without any special software.

Geological setting

The Mura-Zala Basin extends across most of north-eastern Slovenia (Fig. 1). Basin fill consists of Neogene sediments belonging to the Central Paratethys paleogeographic domain (Royden & Horváth, 1988). Regional stages in use for the Central Paratethys are therefore used to describe the formations in the model (Piller et al., 2007).

The lithostratigraphy of the Mura-Zala Basin was first interpreted for purposes of oil and gas research in the 1950s-1960s (Pleničar, 1954; Cigit, 1958; Vončina, 1966), which was followed by a geological mapping for the Basic Geological Map of Yugoslavia (Pleničar, 1968; Mioč & Žnidarčič, 1978, 1998; Aničić & Juriša, 1984; Žnidarčič & Mioč, 1987; Marković & Mioč, 1988). The determination of Miocene formations was based on lithological, biostratigraphical and geophysical markers (Naftaplin, 1966; Grandić et al., 1986; Turk, 1993; Mioč & Žnidarčič, 1996). Previously, earlier Miocene formations were also jointly named the Murska Sobota Formation (Fm.) while all Pontian to Quaternary sediments were named the Mura Fm. (Turk, 1993; Kralj & Kralj, 2000). The stratigraphy was upgraded during the latest regional reinterpretations based on a dynamic process approach and focusing on the evolution of sedimentary environments performed in several transnational projects, such as the AT-SLO project TRANSTHERMAL (Lapanje et al., 2007), the HU-SLO project T-JAM (Nádor et al., 2012), and the AT-HU-SK-SLO project TRANSENERGY (Rman & Lapanje, 2013), as well as separately (Lučić et al., 2001; Fodor et al., 2002, 2005; Jelen et al., 2006; Pavšič & Horvat, 2009). Currently, the most important publication on the regional lithostratigraphical settings is the Surface lithostratigraphic and tectonic structural map of the T-JAM project area, northeaster Slovenia, at 1:100,000 (Jelen & Rifelj, 2011), where the Neogene units are reinterpreted.

The Mura-Zala Basin was formed at the western margin of the continental rift that was active from the Late Ottnangian to the mid-Badenian (Márton et al., 2002; Jelen et al., 2006; Maros et al., 2012). An ENE – WSW to E – W oriented Ottnangian extension produced cascading subsidence along the dextral-transtensional Donat Fault zone in the south, and along the Raba extensional corridor (also left lateral transfer zone) in the north (Fig. 1). Along these fault zones, sub-basins were formed in half-grabens (Jelen & Rifelj, 2005; Jelen et al., 2006). The Mura-Zala Basin is characterized by two ENE – WSW trending sub-basins: the Haloze – Ljutomer – Budafa Sub-basin in the south along the Ljutomer and Donat Faults, and the Radgona – Vas Sub-basin in the north along the Rába Fault. A basement high named the Murska Sobota extensional block separates the two sub-basins. The northern and southern

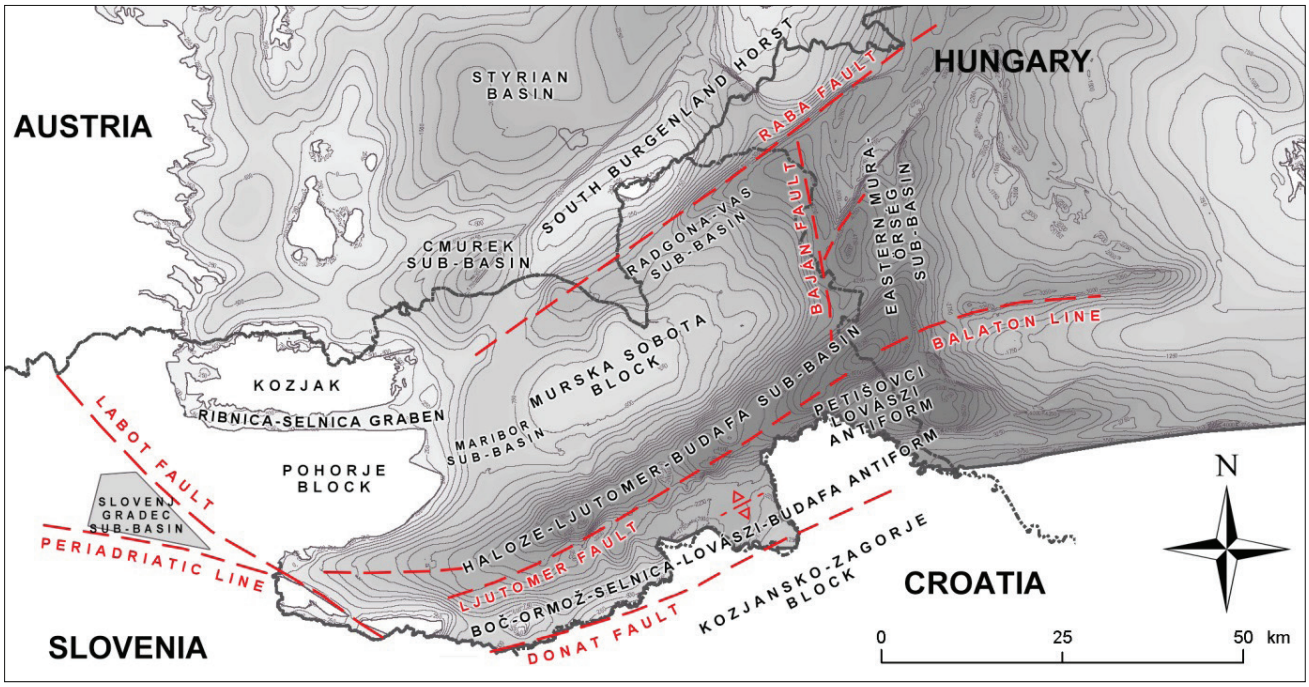

Fig. 1. Contour map of the pre-Neogene basement with major tectonic features (adapted from reports of Jelen et al., 2006, Maros et al., 2012). The extent of the Slovenj Gradec Sub-basin is only schematic and no information was available for Croatia.

margins of the Mura-Zala Basin are formed by the South Burgenland Horst and the Kozjansko – Zagorje tectonic block, respectively. The Pohorje and Murska Sobota extensional blocks formed along roughly N – S trending listric extensional faults between the Rába and Donat Fault zones. The Maribor Sub-basin formed above the faulted boundary between the two blocks. The Eastern Mura – Örseg Sub-basin subsided along the Bajan Fault running along the eastern side of the Murska Sobota block, roughly along the border between Slovenia and Hungary.

The lithostratigraphical description, sedimentary environmental and dynamic infill of the basin is summarised from Fodor et al. (2011), Jelen & Rifelj (2011) and Maros et al. (2012). The oldest Neogene sediments belong to the Early to mid-Miocene (Ottnangian to Early Badenian) Haloze Fm. The continental muddy breccias and conglomerates at the bottom of the sub-basins represent the initial phase of their filling, but higher up, the sediments soon turn into fine-grained deposits of marine character. The upper part of the Haloze Fm. includes also tuff and shallow marine deposits, e.g. Lithotamnian limestone, corresponding to a deposition in a short tectonic inversion and simultaneous sea level drop in the Early Badenian. These sediments have mostly low permeability.

The Špilje Fm. begins with the mid-Miocene (Badenian) transgression due to eustatic sea level rise and continuing the subsidence of the sub-basins. Shorelines shifted far inland and a connection between the Central and Mediterranean Paratethys was established. Poorly-permeable fine grained mud-rich turbidites deposited along the basin margins, and hemipelagic mud in the deepest parts of the sub-basins. Shallow marine deposition prevailed throughout the mid-Miocene (Badenian and Sarmatian) on the Murska Sobota extensional block, as well as to the south and north of the basin margins. Transgression was interrupted by the Late Badenian regression phase, which produced erosional surfaces in previously submerged areas. Coarse-grained clastic sediments of heterolithic facies were derived from the uplifted basement. Even limestones formed along the new shorelines that were established after regression. These shallow-water and coarse-grained deposits are generally highly permeable. After this short-lived regression, the deposition of low-permeability sediments continued and the western parts of the sub-basins were filled up by the end of the Sarmatian, by which time the connection with the rest of the Tethys was also severed.

In the Late Miocene (Pannonian), the area turned into a vast lake system. Rivers from the rising Eastern Alps continuously filled the still subsiding sub-basins with prograding deltas. Continuous subsidence and the Pannonian transgression led to the submergence of the Murska Sobota extensional block. Deposition of hemipelagic marl took place in the deepest parts of the sub-basins, and deltas prograded from the W and NW. The Lendava Fm. comprises turbidites fed from the prograding delta, which are overlain by fine-grained slope deposits. The sandy turbidites occur as isolated permeable bodies, whereas the fine-grained slope deposits represent a very low-permeability horizon covering the turbidites.

Well-permeable coarse-grained turbiditic sandstone and limestone of the Špilje and Lendava Fms. store significant quantities of oil and gas (Hasenhüttl et al., 2001) and oil-prone thermal water (Kralj & Kralj, 2000).

The deltaic sediments of the Mura Fm. are divided into delta front and delta plain facies. The delta front is represented by permeable tabular sand bodies deposited at the delta mouth, which are the most extensive and widely exploited geothermal aquifers in the region (Kralj, 2001; Kralj & Kralj, 2012; Rman et al., 2012; Rman, 2014). The delta plain sediments are mostly fine-grained silts with occurrences of coal (Markič et al., 2011). Permeable gravel lenses originating in distribution channels connect this part of the sequence with the delta front facies. The age of strata in the Mura Fm. generally decreases from W to E in the direction away from the former land surface.

In Pliocene, sediment deposition overwhelmed the subsidence, and delta plain sedimentation changed to an alluvial type of deposition, producing the Ptuj-Grad Fm. A phase of tectonic compression in Pliocene (Tomljenović & Csontos, 2001) induced inversion and folding that was restricted mainly to the Donat Fault zone. Alluvial sediments slowly covered the deltas and indicated a new organization of the drainage system in the Paratethyan domain. The Ptuj-Grad Fm. is quite permeable but does not contain extensive geothermal or freshwater aquifers (Žlebnik, 1978; Szőcs et al., 2013; Rman, 2014). The youngest sediments are mostly gravelly alluvial deposits of the Drava and Mura rivers. They are of Quaternary age and an important drinking water resource (Andjelov et al., 2006).

Methodology

Modelling procedure

Building a 3D geological model is a continuous process that includes several steps, depending on the type. Data pre-processing includes collecting, structuring and reinterpreting data. Maps and cross-sections are digitized and managed as vector data in GIS software where necessary. The final step is to integrate all this data into software for the 3D modelling process (Kaufmann & Martin, 2008). These steps are repeated each time new data is available. For a geological model, the process can be performed each time a new borehole is drilled, a new reflection seismic profile is made or a new geological map is published. In order to be able to update the existing model as quickly as possible, we have followed several methodological steps (Fig. 2).

We created a 3D model using several different software applications: MS Office Excel for the borehole database, AutoCAD (Internet) for constructing cross-sections, ArcMap (ESRI, 2014) for processing two dimensional data, and JewelSuite™ (Baker Hughes, 2014) for handling 3D models from previous studies and constructing the final three dimensional model. Building a model uses the data both ways, as a continuous exchange between software formats is necessary due to their reprocessing.

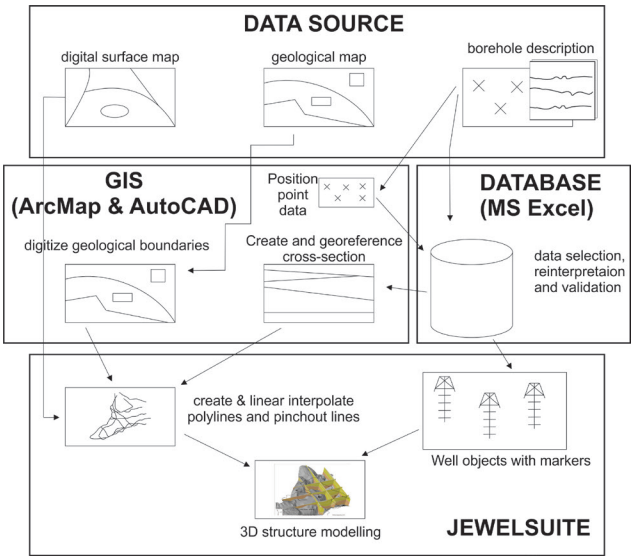

Fig. 2. Organigram of the methodology used to produce a 3D geological model (modified after Kaufmann & Martin, 2008).

Initially, we used mostly vector data (points, polylines and polygons) to create cross-sections. Some were derived from the raster data (by digitizing maps) but the raster data (digital surface map – CIAT, 2004) was also used. We collected four types of available source data:

- Published geological surface map (Mioč & Marković, 1998; Jelen & Rifelj, 2011),
- Models from previous studies of the area (Lapanje et al., 2007, Fodor et al., 2011, Maros et al., 2012, Rman, 2013),
- Digital surface map (CIAT, 2004) and
- Borehole lithological logs.

The information on boreholes was first collected and organized in an MS Excel database, and later harmonized and reinterpreted. Additionally, we created six interpretative cross-sections using AutoCAD: three in SW–NE and three in the NW–SE direction (Fig. 3). They are deliberately spatially equally distributed over the study area and intersect the most representative boreholes. These sections constituted the main input for the building of the 3D model, together with the 453 formation penetration points (FPP) from 145 reinterpreted borehole logs (see Table 3). Boreholes are very unevenly distributed over the model area, clustered in and around urban areas as well as in areas richer in oil and gas, and according to other geopotential probability, i.e. near Lendava, Gornja Radgona and Murska Sobota (Fig. 3).

Together with these cross-sections, the 3D models from previous studies were imported into the JewelSuite™ software. Based on all of the data, polylines in the three dimensional space were created. Additionally, boreholes (X, Y, Z, inclination and azimuth) and their formation penetration points were also imported. Using a combination of newly created polylines, the digitized surface geological map, and information on the horizontal extent of formations (from FPP),

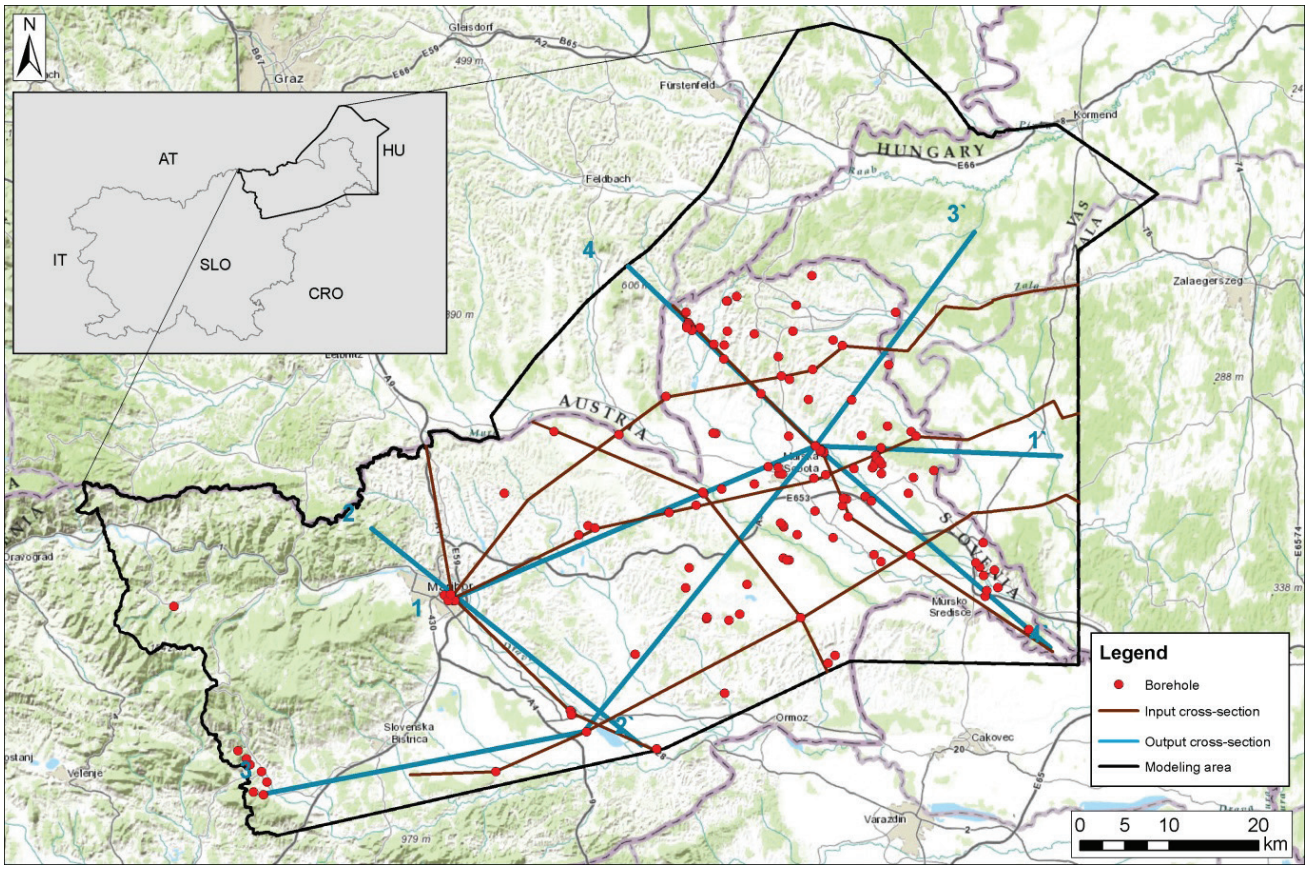

Fig. 3. Outline of the model area (black line) with locations of the input data: boreholes (red dots) and cross-sections (brown lines), as well as the cross-sections derived from the modelling (blue lines), which appear in Figure 5.

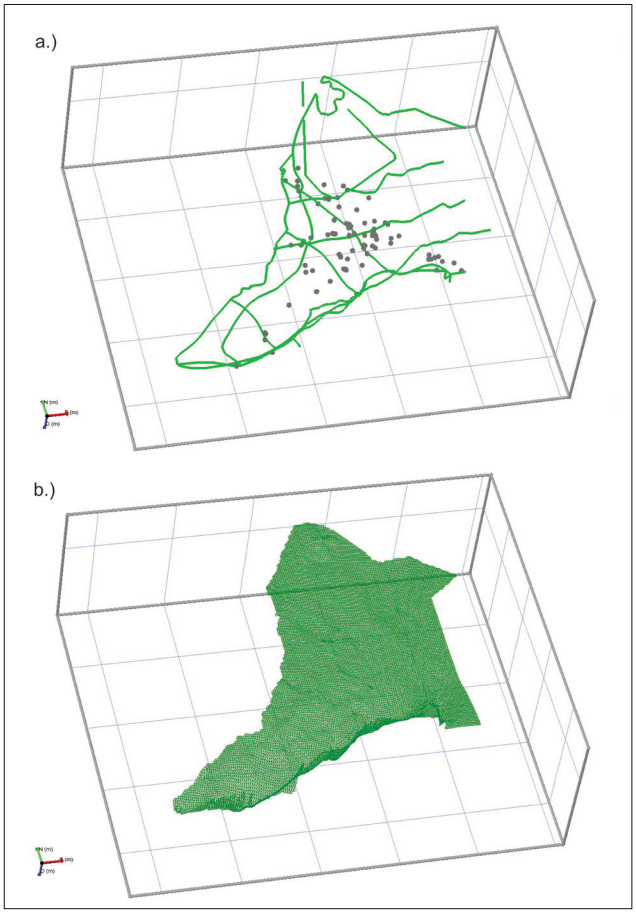

Fig. 4. Digitized polylines from cross-sections with FPP (a) and created trimesh from polylines (b) for one layer.

we created pinchout lines for all formations and defined their terminations (Fig. 4a). The pinchout lines were created using the JewelSuite™ and ArcMap simultaneously, being iteratively connected with the polylines, and determining the shape of the layers. These newly connected polylines were triangulated to a triangular mesh using a linear interpolation method (Fig. 4b).

Meshes of individual layers were additionally vertically fitted using the reinterpreted borehole data (FPP). The resulting model is a three dimensional trimesh layer model. Subsequently, the stratigraphic boundary surfaces were converted to regular gridded surfaces with a cell size of 500 × 500 m in order to have the possibility of using it with other software later (e.g. with FeFlow, ArcMap).

Extent and boundaries of the model

The 3D model covers NE Slovenia, with smaller parts entering Austria, Hungary and Croatia (Fig. 3). Geographically, the model is referenced in UTM 33 N projection using WGS84 datum. It extends 121 km in the E – W direction and 91 km in the N – S direction, over a total area of 5404 km^2. To the NW, the model is bounded by the state border between Slovenia and Austria, while it extends to the NE along the border of the TRANSENERGY pilot area (Fuks & Janža, 2013). Its eastern and southern boundaries

are controlled by the extent of the model from Rman (2013), which was constrained by the data available and the trace of the Ljutomer Fault. The western model boundary follows the groundwater bodies that close the Mura-Zala Basin.

Vertically, the model stretches from the Earth's surface down to the base of Neogene rocks. Enhanced digital surface data from the Shuttle Radar Topography Mission (CIAT, 2004) was used for the Earth surface. The base of Neogene rocks forms a basement surface of the Basin, whose geometry was adopted from earlier works (Fodor et al., 2011; Maros et al., 2012). Maximum elevation in the model is approximately 1500 m a.s.l. and the minimum approximately 6600 m b.s.l., being modelled north of Lendava.

Datasets and delineated units

Key stratigraphic units of the Mura-Zala Basin were reinterpreted using earlier geological models, existing mainly in 2D format: i) the pre-Neogene basement depth map (Lapanje et al., 2007), ii) the 1:100,000 Basic Geological Map of Yugoslavia and Slovenia, iii) the 1:100,000 Surface litostratigraphic and tectonic structural map of the T-JAM project area in northeastern Slovenia (Jelen & Rifelj, 2011), iv) the geological model of the T-JAM project (Fodor et al., 2011), v) the geological model of the TRANSENERGY project (Maros et al., 2012), and vi) the geological model of the PhD thesis of Rman (2013). A comparison of the defined formations is given in Table 1.

This new geological model of the Mura-Zala Basin comprises eight lithostratigraphical units, from pre-Quaternary deposits to the Haloze Fm. (Table 2).

Well logs from 145 boreholes (see locations in Fig. 3) were reinterpreted using lithological descriptions of cores and drilling chips, and available paleontological data to distinguish between sedimentary paleo-environments within the same formations that were not effectively separated in previous models. Since each formation was deposited in a distinct sedimentary paleo-environment, various sedimentological and hydrogeological characteristics can be used for classification instead of the very similar lithology of alternating mud (silt – clay), silt, and sand (Table 2). As clastic sediments prevail, spontaneous potential, resistivity and natural gamma-ray logs were used owing to their strong dependence on grain-size variation. Finally, as the architecture of the Quaternary sediments is currently under interpretation, they were not included in this geological model.

Due to time constrains the subdivision of the Špilje Fm. into Badenian and Sarmatian was performed on only 20 borehole logs used to create the six interpretative cross-sections. The division is based on the occurrence of Lithotamnian limestone.

The number of boreholes that reached different formation does not decrease with depth, from Ptuj-Grad Fm. to pre-Neogene basement rocks. This is because that not all formations occur over the entire study area, and therefore some boreholes in the western part of the model penetrate, for example, only the outcropping Špilje Fm., while others that should stratigraphically lie above it are not developed.

Table 1. Comparison of formation definitions with previous projects.

<table>
<tr><th rowspan="2">Formation</th><th rowspan="2">Subdivision</th><th rowspan="2">TRANS-THERMAL (Lapanje et al., 2007)</th><th rowspan="2">T-JAM (Fodor et al., 2011)</th><th colspan="2">TRANSENERGY</th><th rowspan="2">Rman (2013)</th></tr>
<tr><th>supraregional (Maros et al., 2012)</th><th>pilot area (Maros et al., 2012, Fuks et al. 2013)</th></tr>
<tr><td>Ptuj-Grad Fm.</td><td>/</td><td>yes</td><td>yes</td><td rowspan="3">not subdivided</td><td>yes</td><td>yes</td></tr>
<tr><td rowspan="2">Mura Fm.</td><td>delta plain facies</td><td rowspan="2">not subdivided</td><td>yes</td><td>yes</td><td>yes</td></tr>
<tr><td>delta front facies</td><td>yes</td><td>yes</td><td>yes</td></tr>
<tr><td rowspan="2">Lendava Fm.</td><td>slope facies</td><td rowspan="2">not subdivided</td><td>yes</td><td>yes</td><td>yes</td><td rowspan="5">not subdivided</td></tr>
<tr><td>turbidites</td><td>yes</td><td>yes</td><td>yes</td></tr>
<tr><td rowspan="2">Špilje Fm.</td><td>Sarmatian age</td><td rowspan="3">not subdivided</td><td rowspan="2">not subdivided</td><td>yes</td><td>yes</td></tr>
<tr><td>Badenian age</td><td>yes</td><td>yes</td></tr>
<tr><td>Haloze Fm.</td><td>/</td><td>yes</td><td>yes</td><td>yes</td></tr>
<tr><td>pre-Neogene rocks</td><td>/</td><td>yes</td><td>yes</td><td>yes</td><td>yes</td><td>yes</td></tr>
</table>

Table 2. Characteristics of separated formations in the 3D regional geological model as summarised from Maros et al. (2012). Note that Quaternary deposits were not distinguished.

Formation	Lithological description (after Jelen & Rifelj, 2011)	Distinguishing criteria of borehole logs	Average sand content	Sedimentary environment	Time period	Porosity
Ptuj-Grad Fm.	alternation of gravel, sandy, silty and clayey gravel, sand, gravely and silty sand, silt, sandy and silty clay, basaltic tuff, tuffite and basalt, isolated coal occurrences	specific lithology and paleontological determination, superposition	15%	alluvial plain	Latest Pannonian to Pliocene	10%
Mura Fm.	alternation of silty clay, clay, silt, gravely, sandy and clayey silt, sand, silty and gravely sand, sandy gravel and coal	specific lithology and paleontological determination, alternation of fining- and coarsening- upward sand bodies from geophysical borehole logs, coal occurrences	50%	delta plain	earliest Pannonian to Late Pontian	10%
	alternation of sand/ sandstone, silt, marl, clayey marl, clay, marly, sandy and silty clay, coal	specific lithology and paleontological determination, thick, coarsening-upward sand bodies from geophysical borehole logs, coal occurrences	70%	delta front		12-14%
Lendava Fm.	sandy silt, marly clay, occasional sand bodies	superposition and the presence of approx. 200 m thick uniform silt horizon without distinct stratification	5%	slope	Early Pontian	5%
	alternation of sand/ sandstone, silt, sandy, silty and clayey marl, clay	specific lithology and paleontological determination, sand bodies with occasional gravel, predominately non-graded from geophysical borehole logs	30% (turbidites 50%, silt 5%)	deep lacustrine turbiditic	Late Pannonian	7% (turbidites 10%, silt 5%)
Špilje Fm.	alternation of sand, sandstone, sandy and silty marlstone, silt, siltstone, marly and silty clay, conglomerate, locally sandy algal and oolitic limestone, dolomite, coal	specific lithology and paleontological determination	50%	Sarmatian shallow (and deep) marine, fluvial, terrestrial	Mid Badenian to Early Pannonian	7%
	alternation of silty and clayey marl, sandstone, locally algal limestone, conglomerate, dolomite, coal	specific lithology and paleontological determination	30%, shallow areas more permeable	Badenian shallow (and deep) marine	Early Badenian to Sarmatian	5%
Haloze Fm.	alternation of sandy and silty marl, sandstone, conglomerate, muddy breccia, oyster banks, tuff	specific lithology and paleontological determination	30%	shallow (and deep) marine, terrestrial	Karpatian to Early Badenian	5%
pre-Neogene rocks	Metamorphic and carbonate rocks, marl, sand/sandstone, conglomerate	/	/	metamorphic, marine, brackish, lacustrine	Paleozoic to Oligocene	/

As many as 453 formation penetration points were available from the 145 reinterpreted borehole logs (Table 3). Despite the fact that only 59 boreholes penetrated to the pre-Neogene basement rock, the total length of penetrated layers amounts to 156,436 m.

Lack of seismic sections and other data on the structural inventory of the area meant that the fault network could not be considered in this model. Publications imply that displacements along the faults affect mostly older Miocene sedimentary rocks and are estimated to measure a few tens of metres vertically, which is generally much less than laterally (Žlebnik, 1978; Gosar, 1995). The Ljutomer Fault (Fig. 1) is one of the most important faults in the investigated area. It is a large active strike-slip fault in a transpressive regime with a complex multiphase history (Mioč & Marković, 1998; Placer, 1999; Márton et al., 2002; Fodor et al., 2005; Placer, 2008). The Ptuj – Ljutomer – Budafa half-graben along it formed the Haloze – Ljutomer – Budafa Sub-basin by the Late Pontian. The Ptuj and Ljutomer parts remained a sub-basin and were renamed the Ptuj – Ljutomer Sub-basin, while the Haloze and Budafa parts were positively inverted to the Boč – Ormož – Selnica – Lovászi – Budafa antiform approximately in the Pliocene. The antiform consists of several anti- and synclines and was pushed on the Ptuj – Ljutomer Sub-basin (Sachsenhofer et al., 2001; Fodor et al., 2002; Jelen & Rifelj, 2006). The low-permeability layers of the Haloze, Špilje and Lendava Fms. were tilted into a subvertical position along the western part of the fault near Ptuj, therefore they form a lithological boundary which significantly restricts groundwater flow from south to north (Žlebnik, 1975, 1978; Jelen & Rifelj, 2006; Klasinc, 2013). This supports our decision to set the south boundary of the 3D model along the Ljutomer Fault trace. To the south-east of the model, we also included some area south of this fault, as the Neogene layers plunging eastward show some folding, but are not expected to form a hydraulic barrier for groundwater flow in the Mura and younger Fms.

Results and Discussion

Lithostratigraphical horizons

The pre-Neogene basement map and the Earth surface topography were used as input boundary constraints in the model. Between those two boundaries, eight Neogene lithostratigraphical boundaries were modelled. Thicknesses of formations is highly variable in space and can locally be far greater than the average thickness, depending largerly on the sedimentary and paleogeographical environment, as explained in Geological Settings.

The average thickness of modelled formations is 381 m, varying from 201 m for the Lendava Fm. - slope to 638 m for the Mura Fm. – delta plain (Table 3). The Lendava Fm. slope sediments do not exceed 650 m; while maximum thickness of the Ptuj-Grad Fm., the Mura Fm. – delta front, and the Lendava Fm. – turbidites vary from 952 to 1161 m (Table 3). Areas of maximum formation thickness do not coincide in space. For example, the Ptuj – Grad Fm. reaches its maximum thickness at the southern boundary of the model (in the Ptuj – Ljutomer Sub-basin) along the Ljutomer Fault (Fig. 5), whereas the Mura Fm. – delta front sediments are thickest in the SE part of the model near the SLO-HU border (Fig. 6).

The Mura Fm. – delta plain, the Špilje and the Haloze Fms. reach maximum thickness at 1533 to 2005 m (Table 3), but since they largely consist of low-permeability sediments this does not, unfortunately result in favourable geopotentials.

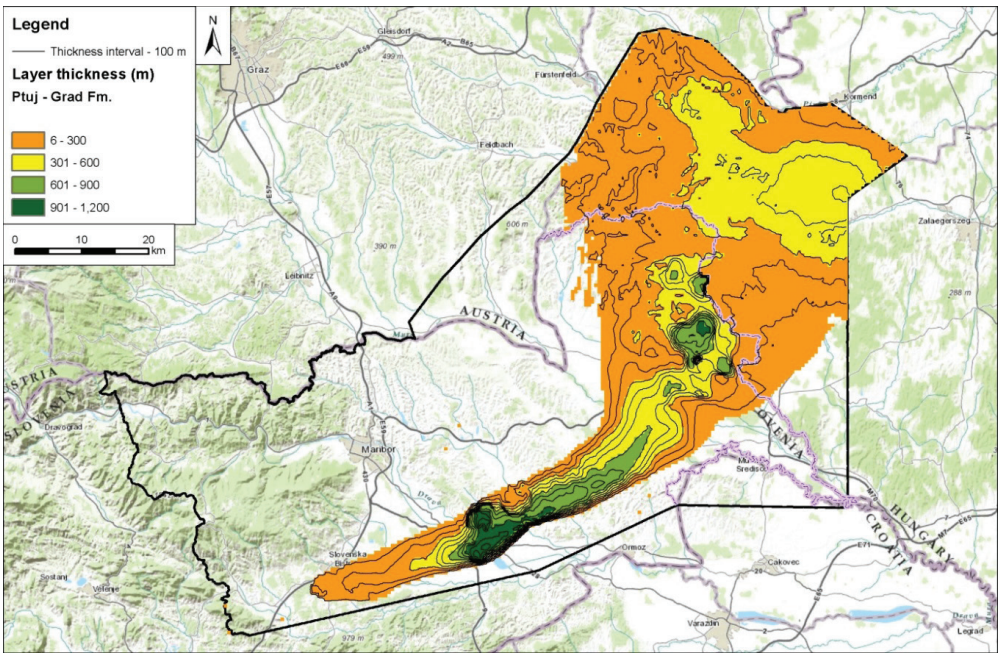

Fig. 5. Thickness of the modelled Ptuj-Grad Fm. alluvial sediments, which represent a moderately productive intergranular aquifer with fresh and lukewarm water.

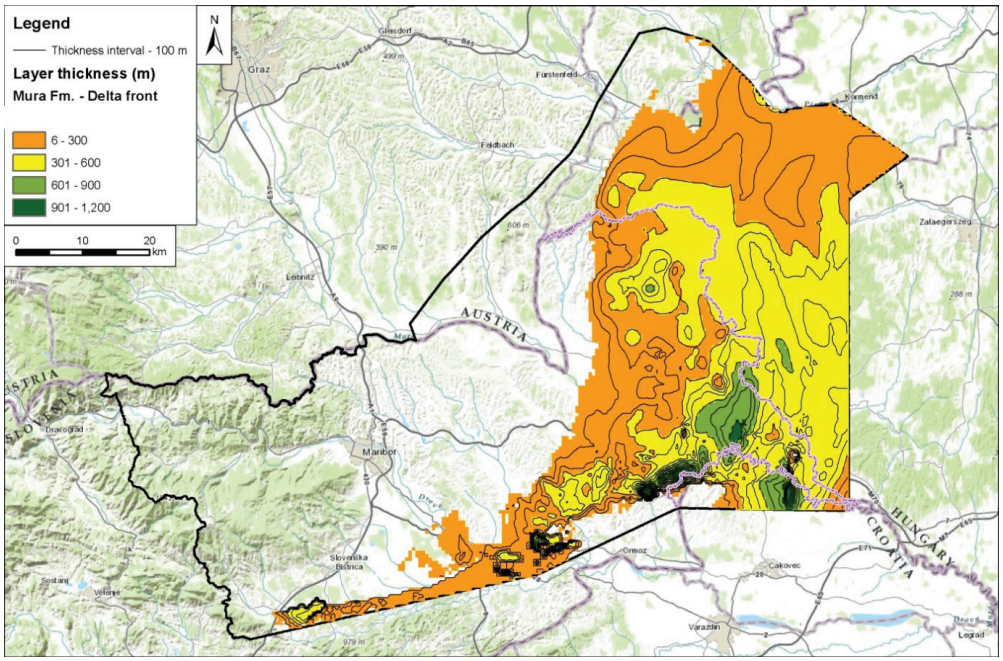

Fig. 6. Thickness of the modelled Mura Fm. – delta front sediments, which represent a highly productive intergranular geothermal aquifer.

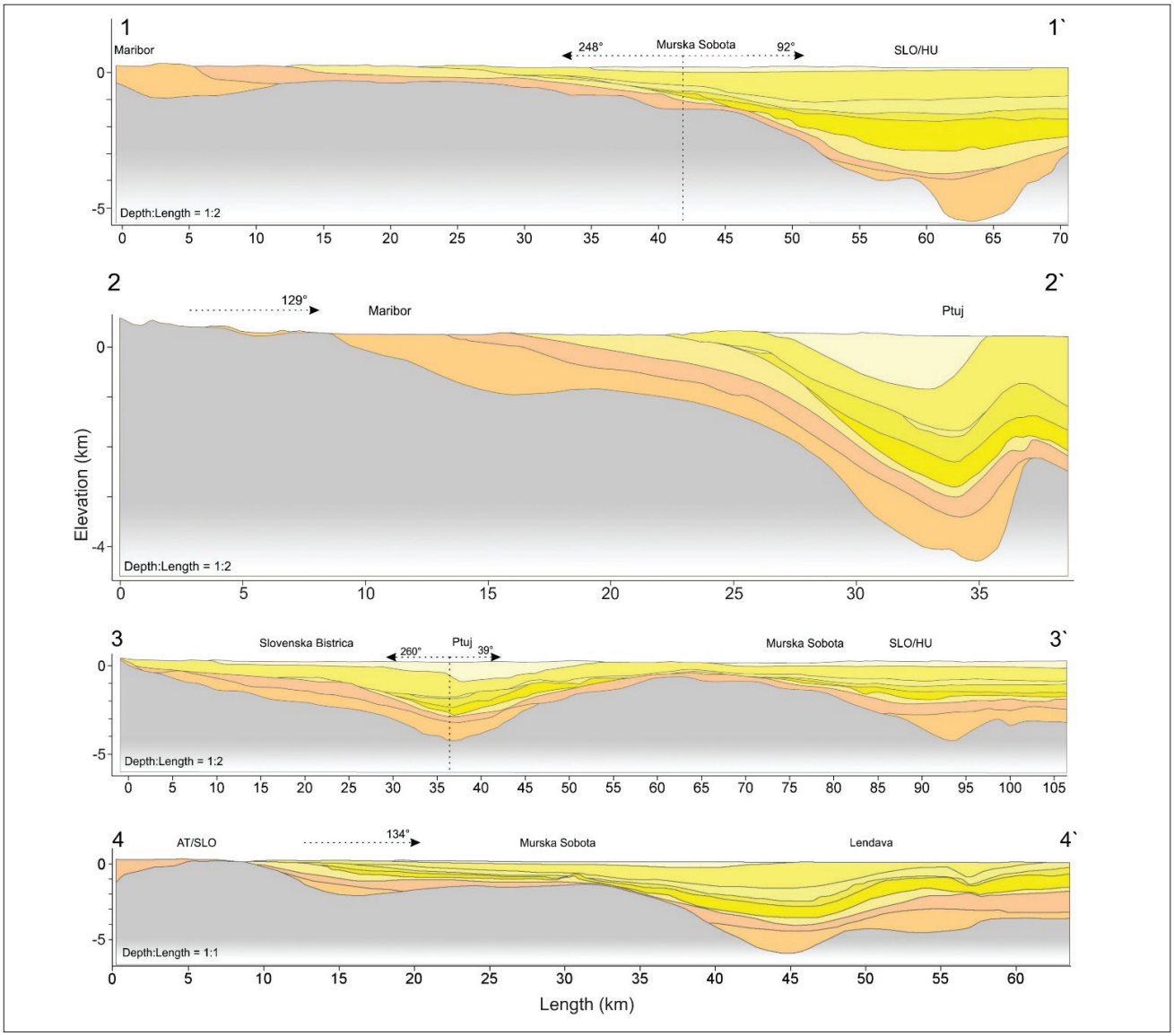

Fig. 7. Four sample cross-sections through the 3D regional geological model of the Mura-Zala Basin. For their position see Fig. 3, for a legend of geological units see Fig. 8. Note that the vertical scale in sections 1-1', 2-2' and 3-3' is 2 x vertically exaggerated. Arrows indicate the azimuth angle of the respective section.

2D visualization of the model

Four arbitrary cross-sections in various directions were made across the resulting regional geological model (Fig. 7). In order to gain a better spatial perspective of the entire modelled area, the model is also displayed in the form of a fence diagram (Fig. 8). While this visualization is useful in recognition and differentiation of spatial relationships in the model, it is still unsuitable for further application. Therefore, the 3D regional geological model was transferred to newly developed open-access GST 3D Explorer platform, as described in the following section.

3D visualization of the model

Transnational data exchange is very difficult in practice because it is complicated and constrained by diverse data policies, database systems and software solutions. In order to overcome this issue, the regional-scale 3D geological model of the Mura-Zala Basin has been converted for use in the 3D browser-analysis tool for visualisation and query, called the 3D-Explorer. This free online tool is based on a software development technology called GST (**G**eo Sciences in **S**pace and **T**ime) and is available through the web portal http://www.geomol.eu/3dexplorer. The aim of the project is to distribute open-source multi-dimensional geo-information from different sources as a joint and harmonised picture merged from different national repositories (The GeoMol Team, 2015). This tool interconnects the geological models that are maintained and continuously updated by the Geological Surveys with interested stakeholders, who are free to explore and query the subsurface at arbitrary depths and locations. Further technical details and instructions for use are described in the GeoMol project final report (The GeoMol Team, 2015, pages 158-165 and references therein).

The 3D-Explorer requires web a browser such as Firefox, Chrome, Opera or Safari. A public login without any username or password provides open access to the available 3D models. The input data can be dynamically visualised either as a set of stratigraphical surfaces (formation base and top horizons), point data, or volumes. A preferred spatial reference system with arbitrary coordinate transformation can be chosen. Topographic maps can be added to the visualization to facilitate orientation in space in addition to current coordinates, which are displayed at the cursor position. Exaggeration of the z-scale can be set to improve one's insight into the geometry of the 3D model (Fig. 9a). The slice-through feature enables fast creation of model cut-outs as a series of arbitrary vertical cross-sections and horizontal slices (Fig. 9b). Finally, a virtual borehole feature can generate information on depths of modelled units below any arbitrary point on the surface. All these visualizations can be exported for further use.

Quality of the model and open issues for further work

The 3D geological model is in a continuous stage of development. It was built according to a methodology that allows updating and improvements each time new data is available. The model was built with available data, hence its quality could not be verified by information from new/unused boreholes or cross-sections at this stage. Therefore, we challenge all interested parties to test and evaluate it with their own data, and provide us with feedback on possible improvements.

It became apparent that comparing the average and maximum thicknesses between borehole

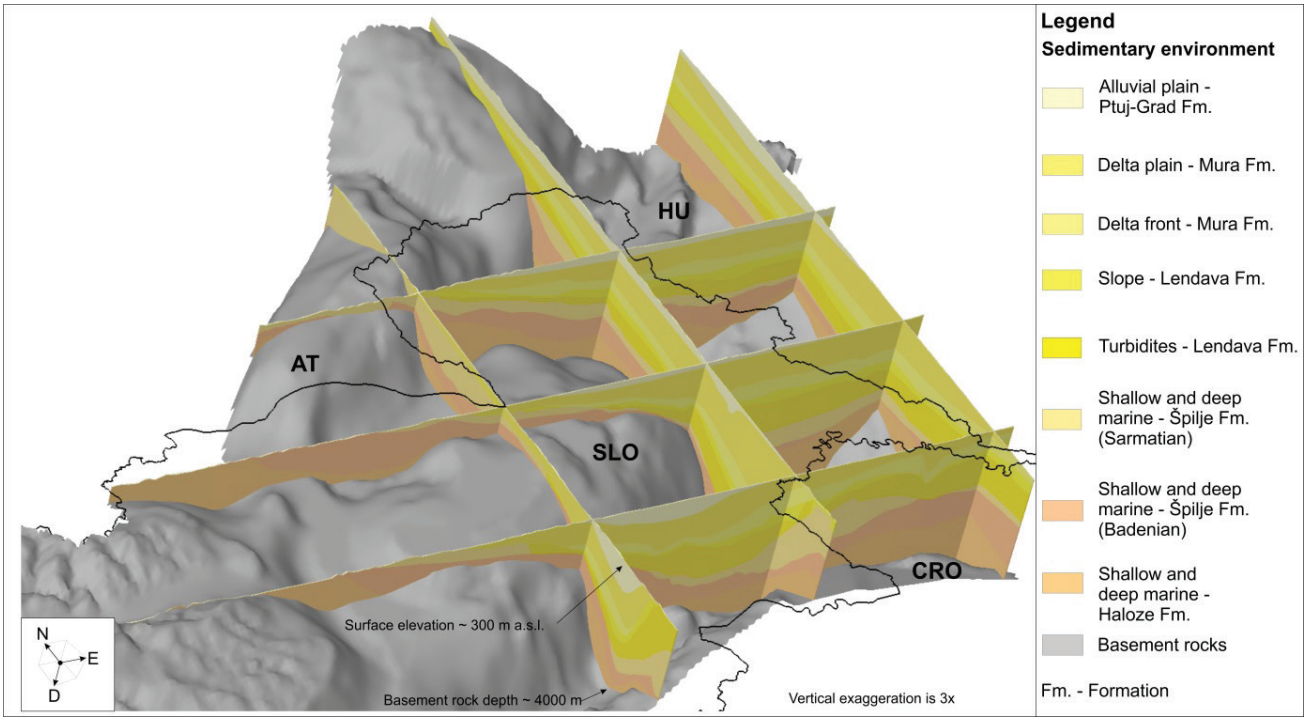

Fig. 8. Perpendicular fence diagram of the Mura-Zala Basin fill superimposed on the pre-Neogene basement. View from SW.

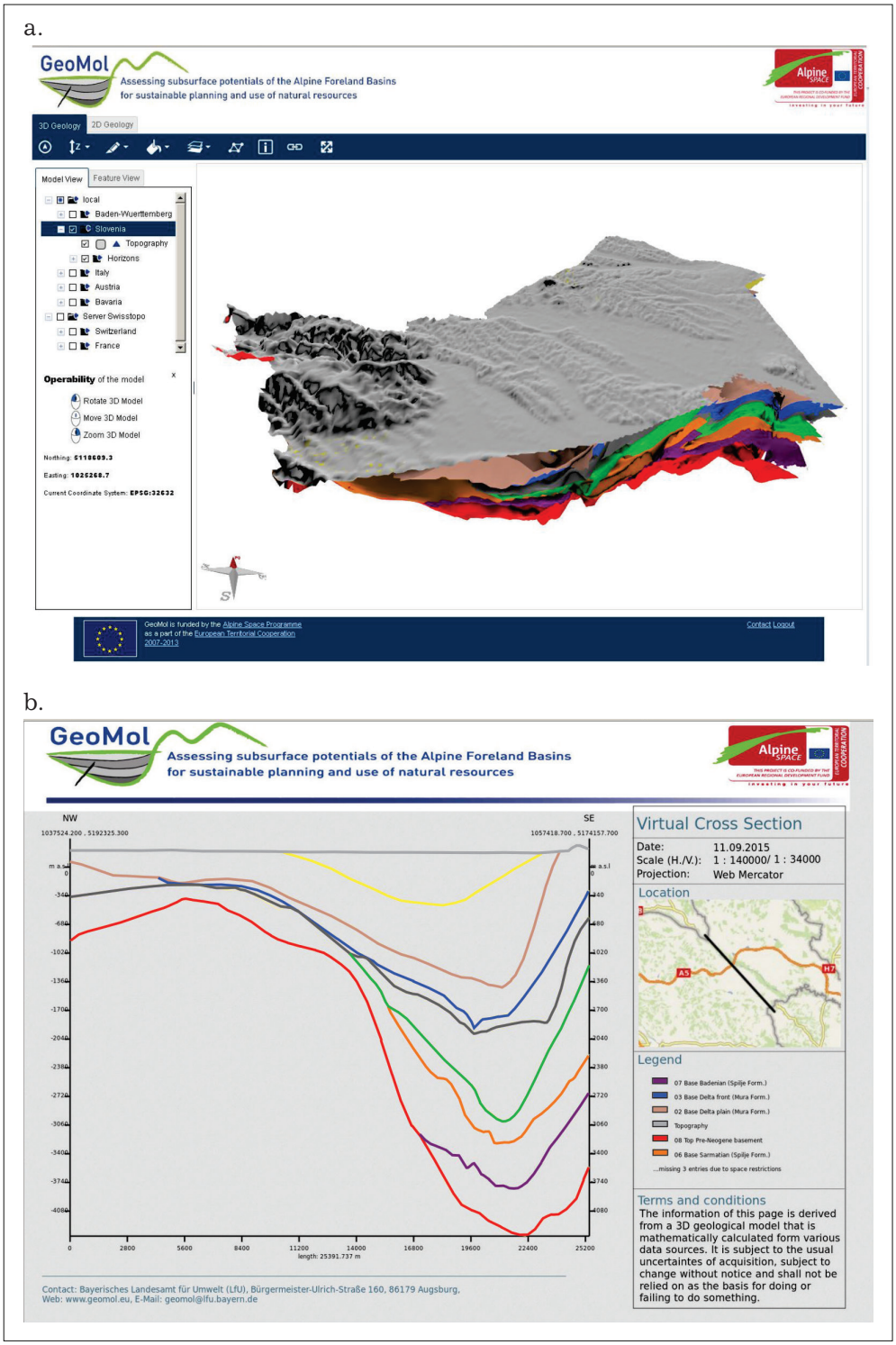

Fig. 9. Example of visualisation of the 3D geological model in the 3D-Explorer (a.) and arbitrary cross-section (b.).

logs and the model is not a straight forward process. The boreholes were available only for the Slovenian part of the model, but the model also includes parts of Austria, Hungary and Croatia (Fig. 3), which caused noticeable discrepancies between compared values. Across the state border the model was constructed based on data from previous models (see Methodology), and therefore exhibits a higher level of uncertainty compared to the central part of the model. Another issue arise in the Croatian territory, where the model was built based only on data from the surface geological maps (Mioč & Marković, 1998; Jelen & Rifelj, 2011).

We verified the Slovenian part of the model by comparing the modelled average and maximum formation thickness to data from borehole logs (Table 3). Discrepancies of maximum formation thickness range from 107 % to 232 %, for Lendava Fm. – turbidites and Haloze Fm., respectively. Surpluses of the rest, except for the Špilje Fm., are attributed to the fact that the boreholes do not penetrate the synclinal axis of the Ptuj-Grad Fm. in the Ptuj – Ljutomer Sub-basin (Figs. 1, 3, 5). The largest discrepancy occurs for the Haloze Fm., penetrated only by 25 boreholes. The surplus occurs in areas where no boreholes reach the Haloze Fm.

Table 3. Comparison of average and maximum formation thicknesses evaluated from borehole log information and the model, and the number of boreholes penetrating each formation.

Formation	Subdivision	No. of boreholes penetrating the formation	Borehole log		Model		Difference (%) (model/borehole log)	
			average	max	average	max	average	max
Ptuj – Grad Fm.	/	45	367	939	312	1161	85	124
Mura Fm.	delta plain	59	552	1240	638	2005	116	162
	delta front	68	262	541	273	952	104	176
Lendava Fm.	slope	65	155	482	201	650	130	135
	turbidites	55	412	1077	408	1150	99	107
Špilje Fm.	Sarmatian	77	485	1978	299	1820	/	/
	Badenian				517	1533		
Haloze Fm.	/	25	368	733	404	1700	110	232
pre-Neogene basement rocks	/	59	/	/	/	/	/	/

Comparison of average formation thicknesses ranges from 85 % to 130 % (Table 3). The largest discrepancy is observed for the Ptuj-Grad Fm. and Lendava Fm. – slope. We assume that the thicker Lendava Fm. - slope layer probably reduced the thickness of Ptuj-Grad Fm.

The major drawback with our model is that it currently does not include faults. Since many structural traps are fault-controlled, the absence of faults is a major shortcoming, for the assessment of oil and gas reservoirs or storage sites among others. Unfortunately, the Ljutomer Fault could not be introduced into the model: due to significantly different degrees of deformation along the fault (Fodor et al., 2002, Fig. 12), lack of quality seismic reflection data and other information along the fault, especially for the area south of the fault, made it impossible to interpret the geometry and offset of its stratigraphic horizons with a reasonable degree of accuracy. Therefore, the southern boundary of the model was assigned to follow its trace. However, in areas where density of borehole data is high enough, like in Lendava and the surroundings, our model reveals flexures and stair-like structures in the modelled stratigraphic surfaces that we interpret as resulting from offsets along the fault planes.

The quality of the modelled 3D lithostratigraphical boundaries can be assessed as very good along the six input cross-sections, in areas with high borehole density and in the vicinity of boreholes with information on formation penetration points. The model properly describes the regional geometry in the selected scale due to a reliable conceptual model, which is constructed based on previous studies of this area (see Methodology).

Several issues still remain: well-permeable shallow marine coarse-grained clastic rocks and limestone of the Špilje Fm., which may form important hydrocarbon or hydrogeothermal reservoirs, could not be better distinguished in the model due to a lack of seismic reflection data. The boundary between the Badenian and Sarmatian part of the Špilje Fm. is poorly constrained, with delineation based only on paleontological data and six interpretative cross-sections. The slope facies of the Lendava Fm. is very heterogeneous, which sometimes made it difficult to interpret its regional extent and separate it into two units – the turbidites and the slope. Moreover, where turbidites of the Lendava and Špilje Fms. are in direct contact – which is the case in deeper parts of the basin – they are difficult to differentiate. Consequently, the boundary between these formations is sometimes unreliable.

The Quaternary sediments were not modelled as a separate formation owing to two issues: their irrelevance for the evaluation of deep geopotentials, and because lithostratigraphical reinterpretation is still in process. Therefore, the current model needs to be combined with the latest open-access surface geological map of Jelen & Rifelj (2011) in order to identify areas where Quaternary sediments overlie the Neogene units. The cross-sections and virtual boreholes derived from the model must be treated with discretion in such areas.

Usability of the model

The presented 3D regional geological model is intended for use as a general overview of the geological setting of NE Slovenia. The key formations that hold out at least some perspective for various geopotentials are delineated in the entire area of the Slovenian part of the Mura-Zala Basin based on the overall average rock composition at a regional scale. Consequently, the model should not be used for detailed local studies. Potential users of the model are notified about this in a disclaimer that appears when accessing

the 3D-Explorer. Generally, the level of detail of the provided information is not suitable for any visualisation or query at a scale more detailed than 1 : 80,000.

The model is very useful for creating virtual boreholes and cross-sections at an arbitrary position in space, which enables quick preliminary testing whether a specific site of interest may have any geopotentials. Realistic assessments of investor expectations can be made quickly, e.g. whether they might find thermal water or not, and at what depth the aquifer is expected to occur. This should indirectly result in reduced geological risk, more feasible approaches to exploration, and lower financial investments. Similarly, this 3D model may serve as a source of input data for regional hydrogeological, geothermal, hydrogeochemical, etc. numerical models that enable the appraisal of volumes and capacities of reservoirs, simulation of regional groundwater flow, heat and mass flow, and similar.

The presented model currently exhibits a 3D layer shape. In the future, should be upgraded to a 3D solid model with assigned properties, such as porosity and hydraulic conductivity. That way the model will be far more usable and efficient, and speed up the evaluation of various geopotentials.

Conclusions

The presented 3D framework regional geological model of the Slovenian part of the Mura-Zala Basin represents a starting point for future developers, users and managers of our subsurface. This is the first 3D geological model in Slovenia that is published according to the principles of open-access, and incorporates the latest lithostratigraphical information about the area. In the long-term, the model will enable better assessment of geopotentials since better forecasting of subsurface geological structure facilitates faster and easier delineation of favourable areas for the exploitation of various commodities, like groundwater and raw materials, or for locating waste disposal sites. Therefore, focused and harmonized management can be achieved when various authorities begin to use the model to visualise 3D spatial distribution of the main lithostratigraphic units that hold various geopotentials.

Obtaining and interpreting the archived seismic reflection data is a key to any significant future improvement of the model. The incorporation of such will enable the inclusion of faults and individual high-permeability horizons, which will greatly improve the model's reliability. Another issue arises from the transboundary character of the Mura-Zala Basin (Nádor et al., 2012). The delineated units have been harmonised as much as possible with the Austrian and Hungarian geologists, but a sizeable gap in information appears along the border with Croatia. Continuation of geological structures and geopotentials to Croatia is undisputable (for example see Borović et al., in print), which is why new transboundary projects are desperately needed to harmonize the data at the triple-state junction of Slovenia, Croatia and Hungary.

We would like to invite all interested parties to test the model, available at http://www.geomol.eu/3dexplorer/, to evaluate it with their own data, and provide us with feedback on possible improvements.

Acknowledgements

The study within the project GeoMol was financially supported by the Alpine Space Programme 2007-2013 (2012-2015; project code 17-4-3-DE). N. Rman and D. Šram are members of the SI ARRS Programme P1-0020 Groundwaters and Geochemistry. The help of K. Koren and S. Mozetič is gratefully acknowledged, and the comments of two reviewers, dr. Drago Skaberne and assoc. prof. dr. Marko Vrabec, significantly improved the paper.

References

Andjelov, M., Gale, U., Kukar, N., Trišič, N. & Uhan, J. 2006: Ocena količinskega stanja podzemnih voda v Sloveniji = Groundwater quantitative status assessment in Slovenia (in Slovenian). Geologija, 49/2, 383–391, doi:10.5474/geologija.2006.027.

Aničić, B. & Juriša, M. 1984: Osnovna geološka karta SFRJ = Basic Geological Map of SFRJ 1:100.000 L 33-68 (List = Sheet Rogatec) (in Slovenian). Zvezni geološki institut Beograd.

Bader, A.A.M. 1976: O možnih zalogah nafte in plina v severovzhodni Sloveniji = Possible oil and gas resources in the northeastern Slovenia, BSc thesis (in Slovenian), University of Ljubljana, Faculty of Natural Science and Engineering, Ljubljana: 55 p.

Baker Hughes 2014: JewelSuite modelling manual. Delft: 953 p.

Borović, S., Marković, T. & Larva, O. in print: Protection of transboundary aquifers of Međimurje County (Croatia): status and prospects. International Journal of Environment and Health, http://www.inderscience.com/info/ingeneral/forthcoming.php?jcode=ijenvh.

CIAT 2004: Void-filled seamless SRTM data V1 90m. International Centre for Tropical Agriculture, http://srtm.csi.cgiar.org.

Cigit, K. 1958: O geoloških razmerah filovske naftne strukture = The geological settings of the Filovci oil structure (in Slovenian). Geologija, 4: 171–187.

Djurasek, S. 1988: Pregledna karta podloge tercijara sa otkrivenim naftnim i plinskim objektima = Overview map of the Tertiary basement with discovered oil and gas objects (in Serbo-Croatian). Nafta Lendava, GeoZS, Archive GeoZS.

Dolton, G.L. 2006: Pannonian Basin Province, Central Europe (Province 4808) - Petroleum Geology, Total Petroleum Systems, and Petroleum Resource Assessment. Bulletin 2204–B. Reston, Virginia, USGS.

Esri 2014: ArcGIS Desktop: Release 10. Redlands, CA: Environmental Systems Research Institute.

Fodor, L., Bada, G., Csillag, G., Horvath, E., Ruszkiczay-Rudiger, Z., Palotas, K., Sikhegyi, F., Timar, G., Cloetingh, S. & Horvat, F. 2005: An outline of neotectonic structures and morphotectonics of the western and central Pannonian Basin. Tectonophysics 410/1–4: 15–41, doi:10.1016/j.tecto.2005.06.008.

Fodor, L., Jelen, B., Márton, E., Rifelj, H., Kraljić, M., Kevrić, R., Márton, P., Koroknai, B. & Baldi-Beke, M. 2002: Miocene to Quaternary deformation, stratigraphy and paleogeography in northeastern Slovenia and Southwestern Hungary. Geologija, 45/1: 103–114, doi:10.5474/geologija.2002.009.

Fodor, L. Uhrin, A., Palotas, K., Selmeczi, I., Nador, A., Toth-Makk, A., Scharek, P., Rižnar, I. & Trajanova, M. 2011: Geological conceptual model within the frames of the T-JAM project. GeoZS, Ljubljana. MAFI, Budapest. http://www.t-jam.eu/domov/

Fuks, T. & Janža, M. 2013: Utilization potentials of the low-enthalpy geothermal aquifer of the Bad Radkersburg – Hodoš pilot area – based on 3D modelling results of the Transenergy project. Proceedings, European Geothermal Congress. Pisa, EGEC.

Fuks, T., Janža, M., Šram, D. & Lapanje, A. 2013: Report on Bad Radkersburg – Hodoš pilot area model, TRANSENERGY project. MFGI, Budapest. GeoZS, Ljubljana. GBA, Vienna, http://transenergy-eu.geologie.ac.at.

Gosar, A. 1995: Modeliranje refleksijskih seizmičnih podatkov za podzemno skladiščenje plina v strukturah Pečarovci in Dankovci-Murska depresija = Modelling of seismic reflection data for underground gas storage in the Pečarovci and Dankovci structures - Mura Depression (in Slovenian). Geologija, 37–38: 483–549, doi:10.5474/geologija.1995.019.

Gosar, A. 2005: Seismic reflection investigations for gas storage in aquifers (Mura Depression, NE Slovenia). Geologica Carpathica, 56: 285–294.

Grandić, S., Ogorelec, B., Mioč, P. & Košćec, J. 1986: Plan in program raziskav ležišč nafte in plina v S.R.Sloveniji za obdobje 1986-1990. Knjige 1-6 = Research plan and programe for oil and gas fields in Slovenia for period 1986-1970. Books 1-6 (in Slovenian). Ljubljana, Zagreb, INA Projekt Zagreb, GeoZS, Archive GeoZS.

Hasenhüttl, C., Kraljić, M., Sachsenhofer, R.F., Jelen, B. & Rieger, R. 2001: Source rocks and hydrocarbon generation in Slovenia (Mura Depression, Pannonian Basin). Marine and Petroleum Geology, 18/1: 115–132, doi:10.1016/S0264-8172(00)00046-5.

Horváth, F., Musitz, B., Balázs, A., Vegh, A., Uhrin A., Nador, A., Koroknai, B., Pap, N., Toth, T. & Worum, G. 2015: Evolution of the Pannonian basin and its geothermal resources. Geothermics, 53: 328–352, doi:10.1016/j.geothermics.2014.07.009.

Jelen, B. & Rifelj, H. 2005: Inner geodynamic control on the Late Paleogene and Neogene stratigraphy in Slovenia. Abstract book, 12th Congress R.C.M.N.S. Patterns in Processes in the Neogene of the Mediterraneian Region, Vienna, University of Vienna, Natural History Museum of Vienna: 116–118.

Jelen, B. & Rifelj, H. 2011: Površinska litostratigrafska in tektonska strukturna karta območja T-JAM projekta, severovzhodna Slovenija = Surface litostratigraphic and tectonic structural map of T-JAM project area, northeastern Slovenia 1: 100.000 (in Slovenian). GeoZS, Ljubljana, http://www.geo-zs.si/podrocje.aspx?id=489.

Jelen, B., Rifelj, H., Bavec, M. & Rajver, D. 2006: Opredelitev dosedanjega konceptualnega geološkega modela Murske depresije = Definition of current conceptual geological model of the Mura Depression (in Slovenian). Ljubljana, GeoZS, Archives GeoZS.

Kaufmann, O. & Martin, T. 2008: 3D geological modelling from boreholes, cross-sections and geological maps, application over former natural gas storages in coal mines. Computer and Geosciences, 35/1: 70–82, doi:10.1016/S0098-3004(08)00227-6.

Klasinc, M. 2013: Pliocenski vodonosnik Dravskega polja = Pliocene aquifer of the river Drava plain (in Slovenian). Bachelor Thesis. University of Ljubljana, Faculty of Natural Science and Engineering, Ljubljana: 85 p.

Kralj, P. 2001: Das Thermalwasser-System des Mur-Beckens in Nordost-Slowenien = Thermal water system in the Mura basin in the northeastern Slovenia, PhD thesis (in German). Aachen, RTWH Lehrstuhl für Ingenieurgeologie und Hydrogeologie: 57 p.

Kralj, P. & Kralj, Po. 2000: Thermal and mineral waters in north-eastern Slovenia. Environmental Geology, 39/5: 488–500, doi:10.1007/s002540050455.

Kralj, P. & Kralj, Po. 2012: Geothermal waters from composite clastic sedimentary reservoirs: geology, production, overexploitation, well cycling and leakage - A case study of the Mura basin (SW Pannonian basin). In: Yang, J. (ed.): Geothermal energy, technology and geology. Nova Science Publishers, 47–92.

Kurevija, T. & Vulin, D. 2011: High Enthalpy Geothermal Potential of the Deep Gas Fields in Central Drava Basin, Croatia. Water Resources Management, 25/12: 3041–3052, doi:10.1007/s11269-011-9789-y.

Lapanje, A., Bäk, R., Budkovič, T., Domberger, G., Götzl, G., Hribernik, K., Kumelj, Š., Letouzé-Zezula, G., Lipiarski, P., Poltnig, W. & Rajver, D. 2007: Geotermalni viri severne in severovzhodne Slovenije = Geothermal resources of the northern and north-eastern Slovenia (in Slovenian). RRA Koroška, GeoZS, Dravograd, Ljubljana: 126 p

Lučić, D., Saftić, B., Krizmanić, K., Prelgović, E., Britvić, V., Mesić, I. & Tadej, J. 2001: The Neogene evolution and hydrocarbon potential of the Pannonian Basin in Croatia. Marine and Petroleum Geology, 18/1: 133–147, doi:10.1016/S0264-8172(00)00038-6.

Markič, M. 2013: Zakaj nastopata zemeljski plin in nafta ravno na območju Lendave = Why do earth gas and oil occur in Lendava (in Slovenian). In: Senegačnik, A. (ed.): Mineralne surovine v letu 2013, GeoZS, Ljubljana: 122–138.

Markič, M., Turk, V., Kruk, B. & Šolar, S.V. 2011: Premog v Murski formaciji (pontij) med Lendavo in Murskim Središćem ter v širšem prostoru SV Slovenije = Coal in the Mura formation (Pontian) between Lendava and Mursko Središče, and in the wider area of NE Slovenia (in Slovenian). Geologija, 54/1: 97–120, doi:10.5474/geologija.2011.008.

Marković, S. & Mioč, P. 1988: Osnovna geološka karta SFRJ = Basic Geological Map of SFRJ 1:100.000 L 33-58 (List =Sheet Nađkaniža) (in Slovenian). Zvezni geološki zavod Beograd.

Maros, G. Jelen, B., Lapanje A., Rifelj, H., Rižnar, I. & Trajanova, M. 2012: Summary report of the geological models, TRANSENERGY project. MFGI, Budapest. GeoZS, Ljubljana. GBA, Vienna. ŠGÚDŠ, Bratislava, http://transenergy-eu.geologie.ac.at.

Márton, E., Fodor, L., Jelen, B., Márton, P., Rifelj, H. & Kevrić, R. 2002: Miocene to Quaternary deformation in NE Slovenia: complex paleomagnetic and structural study. Journal of Geodynamics, 34/5: 627–651, doi:10.1016/S0264-3707(02)00036-4.

Mioč, P. & Marković, S. 1998: Osnovna geološka karta Republike Slovenije in Republike Hrvaške = Basic Geological Map of R Slovenia and R Croatia 1:100.000 L 33-57 (List = Sheet Čakovec) (in Slovenian). GeoZS, IGI, Ljubljana, Zagreb: 84.

Mioč, P. & Žnidarčič, M. 1978: Osnovna geološka karta SFRJ = Basic Geological Map of SFRJ 1:100.000 L 33-55 (List = Sheet Slovenj Gradec) (in Slovenian). Zvezni geološki zavod, Beograd: 74 p.

Mioč, P. & Žnidarčič, M. 1989: Osnovna geološka karta SFRJ = Basic Geological Map of SFRJ 1:100.000 (Tolmač = Explanatory book Maribor and Leibnitz) (in Slovenian). Zvezni geološki zavod, Beograd: 60 p.

Mioč, P. & Žnidarčič, M. 1996: Geological characteristics of the oil fields in the Slovenian part of the Panonian Basin. Geologia Croatica, 49/2: 271–275.

Nádor, A., Lapanje, A., Tóth, G., Rman, N., Szocs, T., Prestor, J., Uhrin, A., Rajver, D., Fodor, L., Murati, J. & Szekely, E. 2012: Transboundary geothermal resources of the Mura – Zala basin: a need for joint thermal aquifer management. Geologija, 55/2: 209–224, doi:10.5474/geologija.2012.013.

Naftaplin, I. 1966: Litostratigrafske jedinice u terciarnom kompleksu Murske potoline = Lithostratigraphical units of the Tertiary complex in the Mura basin (in Serbo-Croatian). Zagreb, INA Naftaplin, Archive GeoZS.

Nosan, A. 1973: Termalni in mineralni vrelci v Sloveniji = Thermal and mineral springs in Slovenia (in Slovenian). Geologija, 16: 6–81.

Pavšič, J. & Horvat, A. 2009: Eocen, oligocen in miocen v osrednji in vzhodni Sloveniji = The Eocene, Oligocene and Miocene in Central and Eastern Slovenija. In: Pleničar, M., Ogorelec, B. & Novak, M. (eds.): Geologija Slovenije = The Geology of Slovenia., GeoZS, Ljubljana: 373–426.

Piller, W.E., Harzhauser, M. & Mandic, O. 2007: Miocene Central Paratethys stratigraphy – current status and future directions. Stratigraphy, 4/2: 151–168.

Placer, L. 1999: Prispevek k makrotektonski rajonizaciji mejnega ozemlja med Južnimi Alpami in Zunanjimi Dinaridi = Contribution to the macrotectonic subdivision of the border region between Southern Alps and External Dinarides. Geologija, 41: 223–225, doi:10.5474/geologija.1998.013.

Placer, L. 2008: Principles of the tectonic subdivision of Slovenia. Geologija, 51/2: 205–217, doi:10.5474/geologija.2008.021.

Pleničar, M. 1954: Obmurska naftna nahajališča = Oil fields of the Mura River area (in Slovenian). Geologija, 2: 36–93.

Pleničar, M. 1968: Osnovna geološka karta SFRJ = Basic Geological Map of SFRJ 1:100.000 L 33-45 (List = Sheet Goričko) (in Slovenian). Zvezni geološki zavod, Beograd.

Presečnik, M. 2008: Geološko skladiščenje CO_2 v vodonosnikih in ocena potenciala v Murski depresiji Geological storage of CO_2 in aquifers and assessment of its potential in Mura depression, BSc thesis (in Slovenian). University of Ljubljana: 111 p.

Rajver, D., Lapanje, A. & Rman, N. 2012: Možnosti proizvodnje elektrike iz geotermalne energije v Sloveniji v naslednjem desetletju = Possibilities for electricity production from geothermal energy in Slovenia in the next decade (in Slovenian). Geologija, 55/1: 117–140, doi:10.5474/geologija.2012.009.

Rman, N. 2013: Analysis of the extraction of thermal water from low enthalpy geothermal systems in sedimentary basin: a case study of the Mura-Zala sedimentary basin, PhD Thesis. University of Ljubljana, Ljubljana: 182 p.

Rman, N. 2014: Analysis of long-term thermal water abstraction and its impact on low-temperature intergranular geothermal aquifers in the Mura – Zala basin, NE Slovenia. Geothermics, 51: 214–227, doi:10.1016/j.geothermics.2014.01.011.

Rman, N. & Lapanje, A. 2013: Geothermal energy of the western margins of the Pannonian basin - Transboundary geothermal energy resources of Slovenia, Austria, Hungary and Slovakia. GeoZS, Ljubljana: 25 p.

Rman, N., Lapanje, A. & Rajver, D. 2012: Analiza uporabe termalne vode v severovzhodni Sloveniji = Analysis of thermal water utilization in the northeastern Slovenia (in Slovenian). Geologija, 55/2: 225–242, doi:10.5474/geologija.2012.014.

Rman, N., Gál, N., Marcin, D., Gal, N., Marcin, D., Weilbold, J., Schubert, G., Lapanje, A., Rajver, D., Benkova, K. & Nador, A. 2015: Potentials of transboundary thermal water resources in the western part of the Pannonian basin. Geothermics, 55: 88–98, doi:10.1016/j.geothermics.2015.01.013.

Royden, L.H. & Horváth, F. 1988: The Pannonian Basin, a study in basin evolution. Tulsa, Budapest, AAPG Memoir 45: 394.

Sachsenhofer, R.F., Jelen, B., Hasenhüttl, C., Dunkl, I. & Rainer, T. 2001: Thermal history of Tertiary basins in Slovenia (Alpine-Dinaride-Pannonian junction). Tectonophysics, 334: 77–99, doi:10.1016/S0040-1951(01)00057-9.

Szőcs, T., Rman, N., Süveges, M., Palcus, L., Toth, G. & Lapanje, A. 2013: The application of isotope and chemical analyses in managing transboundary groundwater resources. Applied Geochemistry - Special Issue, 32: 95-107, doi:10.1016/j.apgeochem.2012.10.006.

The GeoMol Team 2015: GeoMol - Assessing subsurface potentials of the Alpine Foreland Basins for sustainable planning and use of natural resources (project report). Augsburg, LfU. http://www.geomol.eu/report/index_html?lang=2

Tomljenović, B. & Csontos, L. 2001: Neogene – Quaternary structures in the border zone between Alps, Dinarides and Pannonian Basin (Hrvatsko zagorje and Karlovac basins, Croatia). International Journal of Earth Sciences, 903: 560–578, doi:10.1007/s005310000176.

Turk, V. 1993: Reinterpretacija kronostratigrafskih in litostratigrafskih odnosov v Murski udornini = Reinterpretation of chronostratigraphic and lithostratigraphic relations in the Mura Depression (in Slovenian). Rudarsko-metalurški zbornik, 40: 145–148.

Vangkilde-Pedersen, T., Kirk, K., Smith, N., Maurand, N., Wojcicki, A., Neele, F., Hendriks, C., Le Nindre., Y-M. & Anthonsen, K., L. 2009: Assessing European Capacity for Geological Storage of Carbon Dioxide, final report for project EU GeoCapacity. GEUS, BGS, IFP, TNO, BRGM, http://www.geology.cz/geocapacity/publications/D42%20GeoCapacity%20Final%20Report-red.pdf.

Vončina, Z. 1966: Strukturni i litofacijelni odnos Lendavske formacije u Mursko sobotskoj zoni = Structural and lithophacial relations of Lendava Formation in the Murska Sobota zone (in Serbo-Croatian). Zagreb, INA Naftaplin, Archive GeoZS: 37 p.

Vrzel, J. 2012: Hidrogeološka analiza odnosa med plitvim in globokim vodonosnikom na Radenskem območju = Hydrogeological analysis of relations between shallow and deep aquifers in the Radenci area, BSc thesis (in Slovenian). University of Ljubljana, Faculty of Natural Science and Engineering, Ljubljana: 124 p.

Žnidarčič, M. & Mioč, P. 1987: Osnovna geološka karta SFRJ = Basic Geological Map of SFRJ 1:100.000 L 33-56 and L 33-44 (Lista = Sheets Maribor and Leibnitz) (in Slovenian). Zvezni geološki zavod, Beograd.

Žižek, D. 2006: Dokumentacija o geoloških, hidrogeoloških, hidroloških, fizikalnih, fizikalno-kemijskih, kemijskih in mikrobioloških raziskavah ter tehničnih in tehnoloških pogojih izkoriščanja naravne mineralne vode Radenska Naturelle: Ekspertiza za priznavanje naravne mineralne vode = Documentation on geological, hydrogeological, hydrological, physical, physical-chemical, chemical and microbiological research and technical grounds on natural mineral water Radenska Naturelle exploitation: Expert opinion for recognition of natural mineral water (in Slovenian). Radenci, Archive Radenci d.d.

Žlebnik, L. 1975: Termalne in termomineralne vode v Prekmurju in Slovenskih goricah = Thermal and thermomineral waters in Prekmurje and Slovenske gorice (in Slovenian). Radenski vestnik, XIV: 25–35.

Žlebnik, L. 1978: Terciarni vodonosniki v Slovenskih goricah in na Goričkem = Tertiary aquifers in the Slovenske gorice and Goričko hills (in Slovenian). Geologija, 21: 311–324.

Žlebnik, L. & Drobne, F. 1999: Pliocenski vodonosniki - pomember vir neoporečne pitne vode za ptujsko-ormoško regijo = Pliocene aquifers - important quality drinking water source for Ptuj-Ormož region (in Slovenian). Geologija, 41: 339–354, doi:10.5474/geologija.1998.017.

Internet resource:

Internet: http://www.autodesk.com/products/autocad/overview (1.12.2015)

GEOLOGIJA *58/2*, 155–174, Ljubljana 2015

http://dx.doi.org/10.5474/geologija.2015.012

Conodont zonation of Lower Triassic strata in Slovenia

Konodontna conacija spodnjetriasnih plasti Slovenije

Tea KOLAR-JURKOVŠEK & Bogdan JURKOVŠEK

Geological Survey of Slovenia, Dimičeva ulica 14, SI–1000 Ljubljana, Slovenia;
email: tea.kolar@geo-zs.si, bogdan.jurkovsek@geo.zs.si

Prejeto / Received 8. 12. 2015; Sprejeto / Accepted 21. 12. 2015; Objavljeno na spletu / Published online 30. 12. 2015

Key words: conodont zonation, Lower Triassic, Southern Alps, Dinarides, Slovenia
Ključne besede: konodontna conacija, spodnji trias, Južne Alpe, Dinaridi, Slovenija

Abstract

The paper presents the results of a conodont study carried out in the Triassic strata in the area of the Slovenian part of the Southern Alps, External Dinarides and the Transition region between the External and Internal Dinarides. The following conodont zones have been distinguished: *Hindeodus praeparvus* Z., *H. parvus* Z., *Isarcicella lobata* Z., *I. staeschei – I. isarcica* Z., *H. postparvus* Z., *Hadrodontina aequabilis* Z., *Ha. anceps* Z., *Eurygnathodus costatus* Z., *Neospathodus planus* Z., *N. robustus* Z., *Platyvillosus corniger* Z., *Pl. regularis* Z., *Pachycladina obliqua* Z., *Foliella gardenae* Z., *Triassospathodus hungaricus* Z., *T. symmetricus* Z., *N. robustispinus - T. homeri* Z. and *T. triangularis* Z. The introduced conodont zonation spans from the Induan, including the Permian-Triassic boundary interval to the late Olenekian and is valid for the shallow shelf environments of western Tethys.

Izvleček

Predstavljeni so rezultati večletnih raziskav spodnjetriasnih plasti s konodonti na prostoru slovenskega dela Južnih Alp, Zunanjih Dinaridov in prehodnega območja med Zunanjimi in Notranjimi Dinaridi. V raziskanih profilih so bile ugotovljenje naslednje konodontne cone: *Hindeodus praeparvus, H. parvus, Isarcicella lobata, I. staeschei – I. isarcica, H. postparvus, Hadrodontina aequabilis, Ha. anceps, Eurygnathodus costatus, Neospathodus planus, N. robustus, Platyvillosus corniger, Pl. regularis, Pachycladina obliqua, Foliella gardenae, Triassospathodus hungaricus, T. symmetricus, N. robustispinus - T. homeri* in *T. triangularis*. Izdvojene konodontne cone obsegajo čas od spodnjega induana, vključno s permsko triasnim mejnim intervalom, do zgornjega olenekija. Vpeljana je konodontna conacija za okolja plitvega šelfa zahodne Tetide.

Introduction

Conodont research in Slovenia started back in the sixties of the last century, during the time of elaboration of the Basic Geologic Map of Yugoslavia 1 : 100,000. The first analysis of conodont samples were carried out by the Serbian paleontologist Smiljka Pantić who determined the fauna from Lower Triassic strata of the Polhograjsko hribovje Hills (Grad & Ferjančič, 1976). Despite a rapid development of Slovenian conodontology in the following period, Lower Triassic strata were considered for more than two decades being poorly perspective for conodonts. It was only in the eighties of the last century when the fauna of the Smithian *Parachirognathus* / *Furnishius* conodont zone was collected in a section near Idrija (Kolar-Jurkovšek, 1990). In the following decades an intensive conodont research of the lowermost Lower Triassic succession contributed to definition of the Permian-Triassic boundary (PTB) interval, first in Slovenia, and then in the broader area of the Dinarides of Croatia and Serbia (Kolar-Jurkovšek et al. 2011c, 2012; Aljinović et al., 2014; Sudar, 2007).

After the Permian-Triassic catastrophe, as often named the greatest mass extinction, the global biosphere was greatly impoverished and needed some time to be able to recover to the previous diversity, as at the end of the Permian 70 % of genera of terrestrial vertebrates and 85 to 96 % of marine invertebrate species that lived at the end of the Paleozoic became extinct (Benton, 2005). The first pulse of extinction was already between the Middle and Upper Permian, at about 260 million years ago and the second between the Permian and Triassic, at about 252 million years ago. For the second - the main pulse between the Permian and Triassic a pronounced increase in volcanic activity was especially fatal. In the PTB interval sedimentary rocks is documented a sudden drop in δC^{13} that is today by researchers mostly linked with the release of frozen gas hydrates on the seafloor (Berner, 2002). The climate changes caused a change in ocean currents and change of the pH of sea water that greatly increased aridity in the supercontinent inland. Some studies indicate long-term global deep anoxic event in the PTB interval. The

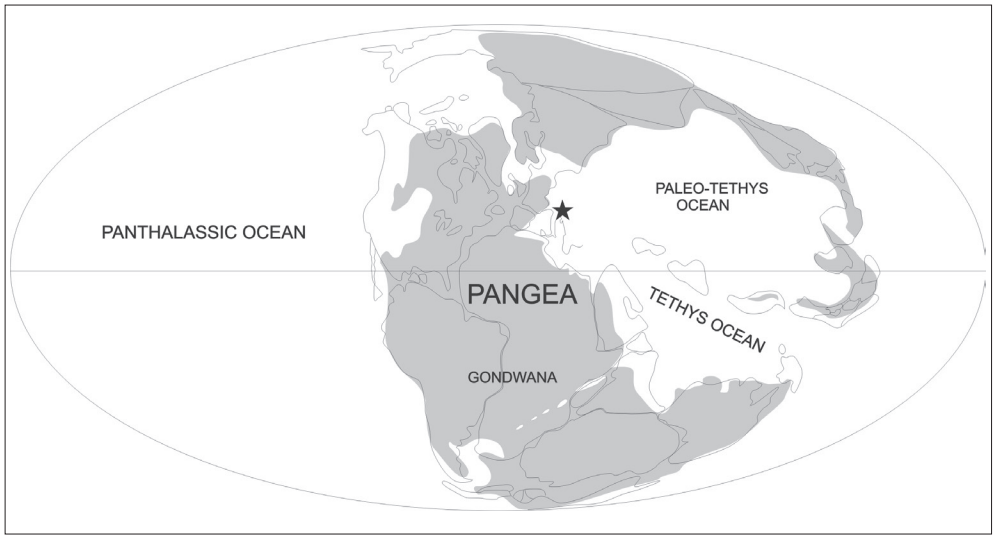

Fig. 1. Paleogeographic sketch of Earth in the Early Triassic. Star indicates the location of Early Triassic beds in Slovenia (modified from Scotese, 2001).

Panthalassa Ocean became fully stratified for almost 20 million years. Beginning, peak and the end of the oceanic stratification corresponds to the global biotic events from the decline in the number of species at the end of the Guadalupian, and extinction at the end of the Permian to the full recovery of life during the Anisian (Isozaki, 1997, 2009). Due to coincidence of timing of different triggers of the Permian-Triassic extinction, the biodiversity in the Mesozoic was significantly reduced for entire 25 million years.

In general, the Triassic Earth's crust was relatively stable until the Late Triassic, when disintegration was intensified caused by continental rifting. The Tethys Ocean, which has already begun to develop in the Permian south of the Paleotethys or south of the lands of Cimmeria, started to incise increasingly to the west during the Triassic and later already in the Jurassic it divided the Pangea into two halves, on Gondwana and Laurasia.

Review of conodont research in Lower Triassic strata in Slovenia

General geological setting

Slovenia is situated in the area of four major geotectonic units: the Dinarides, the Southern Alps, the Eastern Alps and the Pannonian Basin. Today's geological image of Slovenia is largely result of the collision of the Adriatic and European plates and accompanying tectonic processes, which persist even today. Paleozoic and Mesozoic structures are thus largely deformed, blurred or covered with sediments of the Pannonian Basin. All tectonic units of the Slovenian territory belong to the Adriatic lithosphere plate, which was originally connected to the African plate, and from the Mesozoic era onwards existed as a separate plate.

Paleozoic rocks of today's Slovenia were formed in the northern part of the former southern supercontinent Gondwana, mainly on its epicontinental shelf. More clearly their origin is

Fig. 2. Sketch of macrotectonic subdivision of the border region between the Southern Alps and External Dinarides in Slovenia showing Early Triassic sections with conodonts (modified and supplemented after Placer, 2008).

A – **Eastern Alps**: 1 – in general, 2 – Pluton of tonalite/granodiorite (Pohorje) and Periadriatic intrusive; **B – Southern Alps**: 3 – in general, 4 – Paleozoic, 5 – Slovenian Basin sediments; **C** – **External Dinarides**: 6 – in general, 7 – Paleozoic, 8 – Trnovo nappe, 9 – Paleozoic; **D** – **Transition area between External and Internal Dinarides**: 10 – in general; 11 – **Faults**: **PAL** – Periadriatic lineament, **IDF** – Idrija fault, **RVF** – Ravne and Sovodenj fault, **SAF** – Sava fault, **MRF** – Marija Reka fault; 12 – thrust and overthrust faults in Southern Alps; 13 – thrust and overthrust faults in Dinarides; 14 – tectonic slice; 15 – Induan conodonts; 16 – Olenekian conodonts.

Note: Tertiary and Quaternary, mainly molasse sediments of the Pannonian Basin, are not shown on the map.

Sections:

1 – Lukač near Žiri, Javorjev Dol
2 – Masore, Idrijca
3 –Vojsko
4 – Želin – Vrlejca
5 – Žiri surroundings
6 – Golob, Krkoč near Spodnja Idrija
7 – Tehovec near Medvode
8 – Horjul surroundings
9 – Šentjošt, Samotorca, Prevalc
10 – Iška
11 – Draga near Ig, Skopačnik near Želimlje
12 – Borštnik near Turjak
13 – Četež near Turjak
14 – Trojane
15 – Grmače near Šmartno
16 – Leskovica, Bogenšperk - Temnica
17 – Mišnica near Jurklošter
18 – Mokrice
19 – Studorski preval – Julian Alps
20 – Špica v sedlcih – Julian Alps
21 – Tržiška Bistrica
22 – Solčava surroundings

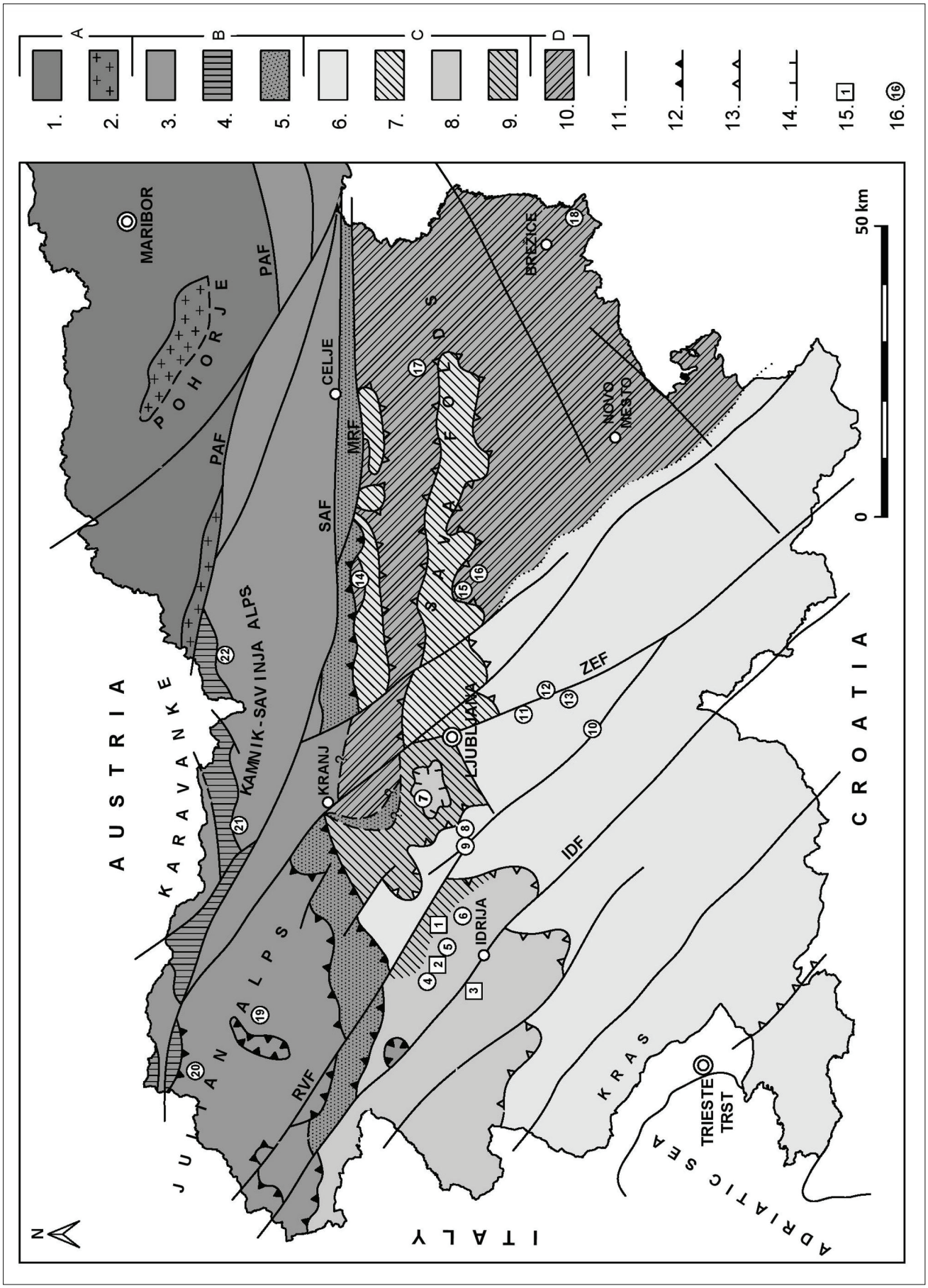
A
B
C
D
1.
2.
3.
4.
5.
6.
7.
8.
9.
10.
11.
12.
13.
14.
15. 1
16. 16
MARIBOR
POHORJE
PAF
CELJE
MRF
SAF
SAVA FOLDS
BREŽICE
NOVO MESTO
KRANJ
LJUBLJANA
ZEF
IDF
IDRIJA
KAMNIK-SAVINJA ALPS
KARAVANKE
JULIAN ALPS
RVF
KRAS
TRIESTE
TRST
AUSTRIA
ITALY
CROATIA
ADRIATIC SEA
50 km
0
N

recognized in the late Paleozoic, when most of the Earth's land masses were united in a supercontinent Pangea. From the east the Paleotethys Ocean incised in it, and at its southern end, however, the Tethys Ocean began to open (Fig. 1). Then an intensive intraoceanic carbonate platform gradually began to form in an autonomous Adriatic lithosphere plate. During the Permian and Lower Triassic there was still a unified sedimentation area, and its smaller part in Slovenia is called the Slovenian Carbonate Platform (Buser, 1989). During the Anisian and Ladinian the Slovenian Carbonate Platform began to disintegrate as a result of extensional tectonics on the edge of Eurasia, where the Meliata Ocean began to originate (Vrabec et al., 2009). All the activities were accompanied by strong volcanism. Until that time a uniform Slovenian Carbonate Platform disintegrated in the Adriatic-Dinaric Carbonate Platform in the south, and the Julian Carbonate Platform in the north, with an intermediate Slovenian Basin (Buser, 1989; Buser et al., 2007, 2008).

In today's geotectonic structure of Slovenia (Placer, 1999; Poljak, 2000) to the Southern Alps belong the sedimentary rocks that built large part of the Southern Karavanke, Julian Alps and the Kamnik-Savinja Alps. To the Transitional area between the External and Internal Dinarides belongs the area which extends from central Slovenia across the Sava Folds to the east and south-east to the Dolenjska and Gorjanci regions and continue further to Croatia. To the External Dinarides corresponds a greater part of southern and south-western Slovenia. To the Eastern Alps in Slovenia is ranked a territory of the Northern Karavanke situated north of the Periadriatic Lineament (Fig. 2).

Overview of the Early Triassic sections with conodonts

Lower Triassic marine sedimentary rocks in the area of the Southern and Eastern Alps, the External Dinarides and the Transitional area between the External and Internal Dinarides were sampled for conodont research. In all units the lithostratigraphic development of the Lower Triassic strata is more or less similar. Their lowest part containing conodonts of the PTB interval gave positive results only in the Idrija-Žiri area belonging to the External Dinarides. In the other units Olenekian conodonts were identified, whereas the conodont research of Lower Triassic strata in the Slovenian part of the Eastern Alps were negative.

Base of the Lower Triassic strata in all these geotectonic units is formed of limestone and dolomite of the Bellerophon Formation as a result of general marine transgression in a shallow shelf of west Paleotethys in the Late Pemian. For convenience, it is necessary to clarify the names of the Late Permian lithostratigraphic units, that were used in Slovenia. The first is the Karavanke Formation of the Southern Alps (Buser et al., 1989), which is represented mainly by dolomite development, and in its upper part there occur limestone and dolomite with characteristic Late Permian fossil association of the Bellerophon Formation (Skaberne et al., 2009). The second is the Žažar Formation of the External Dinarides, which was named by Ramovš (1958 a, b) and he distinguished twelve limestone levels with a brachiopod fauna of the Caucasus-Indoarmenian type. The name of the Žažar Formation was later taken up by some researchers (Grad & Ferjančič, 1976; Buser et al., 1989; Dolenec et al., 2004; Mlakar & Čar, 2009), although it is the lithological and biostratigraphic equivalent of the Bellerophon Formation of the Carnic Alps and the Dolomites in Austria and Italy (Farabegolli et al., 1986; Holser & Schönlaub, 1991).

Following a decision of the International Commission of the IUGS (Yin et al., 2001) to define the PTB based on the first appearance datum (FAD) of a globally spread conodont species *Hindeodus parvus* (Kozur & Pjatakova), there was also in Slovenia greatly increased interest to study the PTB interval. Researchers were particularly interested in the Idrija Žiri area in the western Alpine foothills. The geological structure of the area is relatively well known due to elaboration of the Basic Geological Map SFRY 1: 100,000, sheet Tolmin and Udine (Buser, 1986, 1987) and also due to extensive geological research of the Idrija mercury mine area (Mlakar, 1969; Placer, 1973, 1981; Mlakar & Čar, 2009; Čar, 2010). In sections in which the PTB is located entirely in the dolomite-evaporite strata, paleontological research did not reveal any results. However, in the sections in a limestone development, the boundary was often placed on the upper lithological boundary of the Bellerophon Formation (Grad & Ogorelec, 1980; Buser et al., 1989; Mlakar & Placer, 2000; Mlakar & Čar, 2009; Čar, 2010). There are two particularly interesting well-exposed sections in the limestone development near Idrija town (Masore and Idrijca sections), in which the PTB was defined on the basis of geochemical - isotopic studies (Dolenec & Ramovš, 1998; Dolenec & Ogorelec, 2001; Dolenec et al., 1999 a, 1999 b, 2001, 2004). The goal of an ongoing study of the two sections is to define the PTB based on biostratigraphic evidence.

In the Lukač section near Žiri in the External Dinarides, the PTB was for the first time defined in Slovenia according to an international criterion based on the finding of the conodont species *H. parvus* (Kolar-Jurkovšek & Jurkovšek, 2007). The section is similar to most other studied Permian-Lower Triassic sections in the Idrija-Žiri area of the Trnovo nappe, which is the highest thrust unit of the External Dinarides in this area. The obtained conodont faunas of the Lukač section enabled very fine biozonation due to rapid evolution of the genera *Hindeodus* and *Isarcicella* and for this reason the Lukač section represents a key section to define PTB interval strata in Slovenia that is taken also as a standard for conodont zonation for the whole Dinaric area (Kolar-Jurkovšek et al.,

2011a, 2011b, 2012). The Late Permian Bellerophon Formation is divided into two members, the lower Bellerophon Limestone and the Evaporite-dolomite Member of the rauchwacke type at the top of the formation (Kolar-Jurkovšek et al., 2011 b). On the dolomite there concordantly rest The transitional Beds of the Lukač Formation. A 3.3 m thick, shallow-water transitional interval consists of laminated mudstone, laminated micrite/biomicritne limestone and grainstone with parallel and cross-lamination. From the Transitional Beds a new species of foraminiferal species *Lingulonodosaria slovenica* Nestell et al. has been described (Nestell et al., 2011).

Above the Transitional Beds concordantly rest a 30 m of the Lower Triassic Streaky Limestone, which is composed of very thin strata of bioclastic limestone with minor siliciclastic component. Darker intermediate laminae give a »streaky« appearance to the limestone (Mlakar, 2002; Kolar-Jurkovšek & Jurkovšek, 2007), consisting mainly siliciclastic-clayey material that was reworked by organisms. Wavy and hummocky structure of the Streaky Limestone indicates a shallow subtidal environment with oscillations and storms.

In the upper part of the Lukač Formation than follows a 80 m strata of the Carbonate-clastic Member consisting of ooid grainstone, laminated silty micrite/biomicrite and calcareous siltstone. Deposition of the calcareous siltstone implies intensive terrigenous input in a very shallow depositional environment.

In the Lukač section six conodont zones have been identified, which can be well compared with biozonation of different sections in the Southern Alps, Meishan in China and some other sections in the world (Kolar-Jurkovšek et al., 2011 a). The upper Changhsingian (Late Permian) *Hindeodus praeparvus* Zone and the Induan (Early Triassic) *H. parvus, lsarcicella lobata, I. staeschei – I. isarcica, H. postparvus* and *Hadrodontina anceps* Zones have been distinguished. The first appearance datum of the species *Hindeodus parvus* in the Transitional Beds indicates systemic boundary between the Permian and Triassic (Kolar-Jurkovšek et al., 2006, 2011a, b).

Late Permian–Early Triassic succession of the Lukač section continues to the northwest and in a similar form it is exposed in a road cut of the Javorjev Dol area. Grad and Ogorelec (1980) set the the PTB in a dolomite, which corresponds to the Evaporite-dolomite Member of the Bellerophon Formation. Conodont fauna collected in the limestone of the Bellerophon Formation below the dolomite yields *H. praeparvus* Kozur and *H. latidentatus* (Kozur, Mostler & Rahimi-Yazd). However, the actual boundary with the Lower Triassic strata that outcrop along the road about 30 m in a direction to Sovodenj is covered and tectonized. In the Lower Triassic oolitic limestone strata *I. isarcica* (Huckriede) was collected.

In the Idrija-Žiri area three sections with the PTB are currently studied: the Masore, Idrijca and Vojsko sections. Conodont faunas were recovered from all three sections.

In the Masore section the limestone of the Bellerophon Formation attains a thickness of about 250 m. Its upper part is characterized by the fauna of the *H. praeparvus* Zone that has relatively wide range. The Bellerophon Limestone passes then through thin bedded, predominately microbialite limestone with stylolites into the Lower Triassic bedded limestone containing typical Induan conodont association with *I. isarcica*.

The same strata of the Permian-Triassic boundary as in the Masore section, occur 2 km laterally in the valley of the river Idrijca. There is visible only the highest part of the limestone of the Bellerophon Formation and the lowest microbialite part of the Lower Triassic strata (Kolar-Jurkovšek et al. 2015a; Aljinović et al. 2015). Also here were identified conodonts of the *H. praeparvus* Zone in the highest part of the Permian portion of the section, and the *I. isarcica - I. staeschei* Zone in the Lower Triassic microbialite part of the section.

The Vojsko section is situated on the eastern slope of the Vojsko plateau at an altitude of 770 m. According to Placer (1981) it belongs to the Kanomlja thrust slice, which lies directly below the Trnovo nappe, and the rocks are in the inverse position. Unlike the Masore section, where over 250 m thick succession of the Bellerophon Formation is exposed, in the section Vojsko only around 30 m of thickness is visible (Mlakar & Čar, 2009; Čar, 2010). In the highest part of the formation, about 2 m below the lithological boundary with light gray stromatolitic dolomite, there occur very rare and small sponge buildups (Sremac et al., submitted). The conodont fauna of this part is assigned to the *H. praeparvus* Zone.

Above the Bellerophon Formation lies medium gray thin bedded stromatolitic dolomite with clear lamination and stylolites that passes up to the medium bedded and slightly recrystallized dolomite and dolomitized limestone in which a conodont fauna of the *I. staeschei - I. isarcica* Zone was found. In the stratigraphically younger parts an increased content of limestone and clastic components is observed, initially in the form of olive green marl, then reddish brown calcarenite, siltstone and shale with lenses of oolitic limestone, followed by more than 100 m grained dolomite. The Lower Triassic sequence is ended by bedded dark gray limestone containing marl sheets, above which concordantly lies Anisian dolomite (Čar, 2010).

In addition to the study in a context of the previously described sections Lukač, Masore, Idrijca and Vojsko that include the PTB interval, interesting results of conodont study were obtained also in some other Lower Triassic

sections in the Idrija- Žiri area. It should be noted that the names of most Lower Triassic lithostratigraphic units in the External Dinarides have been traditionally based on the subdivision in the Dolomites and the Northern Calcareous Alps. Therefore also Slovenian geologists often divided the so-called Werfen Formation into lower »Seis Beds« (Seiser Schichten) and the upper »Campil Beds« (Campiler Schichten). Biostratigraphy of Lower Triassic strata was based mainly on macrofossills: ammonites, bivalves and gastropods, rarely on foraminifers, but conodont study was implemented only in a recent two decades. Precise litho-, bio- and chemostratigraphic study have demonstrated the lateral and vertical differences and similarities in litho- and biofacies of adjacent areas. Therefore, the »Seis« and »Campil« beds in the Slovenian part of the External Dinarides can no longer be regarded as chronostratigraphic equivalent of the facies of the Southern Alps (Aljinović et al., 2013 a, b). Distribution of Lower Triassic sediments in the External Dinarides clearly demonstrates temporal and lateral change of carbonate and siliciclastic sediments depending on various transgression-regression cycles on the extensive epeiric carbonate platform of west Tethys. Despite lithological variations between different Lower Triassic sedimentary areas in the External Dinarides in almost all sections their threefold division can be recognized into: the oldest part consisting of carbonates, the middle siliciclastic or mixed siliciclastic-carbonate part, and the third or the highest carbonate part (Buser 1969, 1974a; Aljinović et al., 2013a, b).

Already the first conodont study of the Lower Triassic strata of the Idrija-Žiri area in the nineties of the last century demonstrated that the greater part of the reddish »Seis« shales, siltstones and sandstones that contain also layers of oolitic limestone are not of the Induan but Olenekian in age. In the Želin-Vrlejca section a characteristic Smithian fauna with the following taxa: *Furnishius triserratus* Clark, *Hadrodontina* sp., *Pachycladina obliqua* Staesche and *Parachirognathus ethingtoni* Clark was documented and ranged to the *Parachirognathus/ Furnishius* Zone (Kolar-Jurkovšek, 1990).

The greater part of the Lower Triassic represented an extended recovery event following the Permian-Triassic mass extinction, as well as being marked by three minor crises (Stanley, 2009), which were reflected particularly in ammonites and conodonts during the late Griesbachian, late Smithian and late Spathian. The Smithian-Spathian boundary is indicated by a global warming (Galfetti et al., 2007; Sun et al., 2012), which is also indicated by a positive shift of $\delta^{13}C_{carb}$ (Richoz, 2006) as well as conodont size reduction (Chen et al., 2013).

A systematic sampling of five Lower Triassic sections in the Idrija-Žiri area of the Trnovo nappe has yielded the best Early Triassic conodont sequence in central and southern Europe. The recovered conodont faunas enabled us to distinguish nine conodont biozones spaning from the late Induan (Dienerian) to the Olenekian (Spathian) (Chen et al., 2015 a). In the five studied sections following conodont zones were determined: *Eurygnathodus costatus* Z., *Eurygnathodus hamadai* Z., *Foliella gardenae-Pachycladina obliqua* A.Z., *Neospathodus robustus* Z., *Platyvillosus corniger* Z., *Platyvillosus regularis* Z., *Triassospathodus hungaricus* Z., *Triassospathodus symmetricus* Z., and *Neospathodus robustispinus* Zones. The succession of the Lower Triassic zones is of particular value for stratigraphic correlation in central and southern Europe and it enables better correlation studies between the western and middle-eastern Tethys.

The sections in vicinity of Spodnja Idrija and Žiri could be regarding their position above the »Seis« beds traditionally compared with the »Campil« beds of the Dolomites, that in the highest part often contain Olenekian fauna with the ammonites of the genera *Tirolites* and *Dinarite*s, gastropods *Natiria* and *Turbo* and foraminifera *Meandrospira pusilla* (Ho). Since the development of Olenekian strata of the Žiri area significantly differs from the typical Campil Beds, the local beds are ranged to the new informal lithostratigraphical unit, the "Žiri Beds".

In the western part of the Alpine foothills the conodont study was directed to the Polhograjsko hribovje hills, which are situated west of Ljubljana between the Ljubljana moor in the south, Podlipščica to the west and to the north it is separated from the Škofja Loka hills by the Poljanska Sora River. All studies from different sections and outcrops have confirmed only the Olenekian age, whereas Induan strata have not been identified in this area.

In the Tehovec section, southwest of Medvode, a slightly marly biomicrite limestone lies on a thick bedded dark gray dolomite and with thin marlstone intercalations. In several beds also oolites are encountered. Among fossil molluscs there are represented *Natiria costata* (Münster) and *Costatoria costata* (Zenker) as well as rare badly preserved ammonites. Among the microfossils in the greater part of a 47 m section foraminifera *M. pusilla* occurs and the conodonts are represented by typical Lower Triassic shallow water elements *P. obliqua* and genera *Hadrodontina* and *Ellisonia* (Jurkovšek et al., 1999). Similar Lower Triassic successions are known from many other localities in the Polhograjsko hribovje Hills (Grad & Ogorelec, 1980; Ramovš, 1958b). These strata produced conodonts in the Horjul surroundings (Koreno, Samotorca, Prevalc and Šentjošt).

In the External Dinarides, Lower Triassic strata with conodonts were also found in several places of Notranjska and Dolenjska regions. Detail investigations have been done in the

sections on the southern and eastern outskirts of the Krimsko-mokrško hribovje hills. Buser (1969, 1974) roughly divided Early Triassic strata into three superposition packages. Below is bedded gray dolomite with claystone and siltstone intercallations, in the middle part is reddish shale and sandstone with intercalations of oolitic limestone, and in the upper part there is light gray dolomite with marl beds. In all sections conodonts were recovered only from the samples of the middle superposition package. The carbonate beds (sparitic limestone, calcarenite and oolite limestone), which are deposited between the reddish claystones, siltstones and fine grained sandstone in the Iška River gorge yield conodonts *Ellisonia* sp., *Foliella gardenae* (Staesche) *Hadrodontina* sp., *P. obliqua* and *P. ethingtoni*. The fauna is dominated by the elements of the conodont apparatus *P. obliqua* at different ontogenetic stages (Kolar-Jurkovšek & Jurkovšek, 1996). Similar conodont fauna was also found in Lower Triassic strata at Draga near Ig (Kolar-Jurkovšek & Jurkovšek, 1996), Četež near Turjak and Borštnik. The recovered conodont elements of these localities are comparable with the obtained Smithian faunas from the Želin-Vrlejca sections of the Idrija-Žiri area and near Tržič (Kolar-Jurkovšek, 1990, Kolar-Jurkovšek & Jurkovšek, 1995). From the middle superposition package of a variegated clastites containing oolitic limestone beds at Skopačnik near Želimlje (Dozet & Kolar-Jurkovšek, 2007) a Smithian species *F. gardenae* and *P. obliqua* are determined, whereas in the overlying dolomite strata which correspond to the upper carbonate superposition package the Spathian elements *T. homeri* (Bender) and *T.* ex gr. *triangularis* (Bender) were determined.

Similar lithological developments of Lower Triassic strata with conodonts as in the External Dinarides are also represented in the Transitional area between the External and Internal Dinarides, which extend from central Slovenia to the east on the territory of Croatia. The greater part of the Transitional area belongs to the Sava Folds, where in all of the investigated Lower Triassic strata conodonts were collected only in the middle mixed siliciclastic-carbonate part, which includes also oolitic limestone beds. Northwest of Trojane in the limestone between the reddish and olive grey clastites conodont species *Hadrodontina anceps* Staesche and *P. obliqua* have been found, in the Grmače section south of Litija *P. obliqua*, at Leskovica south of Bogenšperk and along the road between Bogenšperk and Temnica *P. obliqua* and *F. gardenae*. In the eastern Kozjansko region in the valley Mišnica north of Jurklošter the species *P. obliqua* was collected. All reported conodont elements indicate to a Smithian age of the sampled strata. A poorly preserved Early Triassic conodonts of the genera *Hadrodontina* and *Pachycladina* and some other non-identifiable fragments yield also some other test samples from the Sava Folds (Dobovica south of Podkum, Čebine north of Zagorje, etc.).

To the Transition region between the External and Internal Dinarides belongs also the Dolinski potok near Mokrice, which is located in the easternmost part of the Gorjanci - Žumberak Mt. near the Slovenian-Croatian border and it includes sedimentary rocks of the Smithian-Spathian interval (Kolar-Jurkovšek et al., submitted). The investigated part of the section is dominated by a thin bedded limestone with marl intercalations. Two limestone lithothypes are mainly represented: biomicrite/packstone and micritic limestone (mudstone). The following conodont zones have been distinguished: *Ha. aequabilis* Zone, *Platyvillosus corniger* Zone, *Pl. regularis* Zone and *Triassospathodus hungaricus* Zone. The same conodont zones were also discriminated in Lower Triassic sections of the Idrija-Žiri area (Kolar-Jurkovšek et al., 2015b; Chen et al., 2015 a) and they are particularly relevant for correlation of the equvalent strata of the adjacent as well as broader areas with significant sections of Asia and North America. The conodont material from this section has enabled the reconstruction of two conodont multielements: *T. hungaricus* (Kozur & Mostler) and *Pl. regularis* (Budurov & Pantić).

The conodont research in the Lower Triassic of the Slovenian part of the Southern Alps was carried out in the eastern part of the Julian Alps, the Southern Karavanke and Kamnik-Savinja Alps. For the Julian Alps, which comprise a large part of north-western Slovenia, is characterized by an overthrust structure. The largest is the Julian nappe (Placer, 2008) or the Julian Alps overthrust (Jurkovšek, 1987 a, b) which is formed of strata ranging from the Lower Triassic through the Cretaceous; its greater part is presented by the Upper Triassic shallow marine carbonates. Lower Triassic strata most frequently occur in discrete narrow bands or within smaller tectonic slices. Their footwall in this part of the Julian Alps is not visible, and in some places they are concordantly overlain by Anisian carbonate rocks.

At Studorski preval (Studor Pass), situated 4.5 km southeast of the peak of Mount Triglav (2864 m), the Lower Triassic strata are predominantly tectonized. In a tectonically undisturbed parts of the section microfacially two basic types occur: coarse tempestite sediment (microfacies A) and laminated or bioturbated calcareous mudstone and / or marl (microfacies B), pointing to a more distal parts of the ramp with storm influence. A similar formation also applies to the depositional environment of the Werfen Formation of the Southern Alps (Brandner et al., 2012). The Lower Triassic strata of Studorski preval are characterized by common gastropods *Natiria costata*, bivalves of the genera *Bakevellia, Avichlamys* and *Eumorphotis,* foraminifer fauna with the genera *Ammodiscus, Hoyenella* and *Glomospirella* corresponding the global »*Glomospira-Glomospirella*« foraminifer association. Ammonites in the microfacies B show that a connection to the open sea was unimpeded. The conodont fauna with *T. hungaricus* is typical of the lower Spathian

(Kolar-Jurkovšek et al., 2013). From Lower Triassic strata of the Studorski preval the first discovery of a fossil amphibian in Slovenia (Temnospondyl) was found, which most probably belongs to the group Capitosauridae (Lucas et al., 2008).

Similar Lower Triassic strata with gastropods *Natiria costata*, bivalves and very rare ammonites are tectonically squeezed in the area of Špica v Sedlcih located about 2 km northeast of the Vršič pass (Jurkovšek, 1987 a, b). In the limestone that corresponds to the microfacies B of Studorski preval some unidentifiable fragments of conodonts were found.

In a wider area of the Southern Karavanke on the dolomite of the Late Permian Bellerophon Formation there rest Lower Triassic strata that pass upward to the Anisian dolomite (Buser, 1980; Buser & Cajhen, 1978). Lower Triassic strata in the valley Tržiška Bistrica near Tržič belong to the South Karavanke overthrust that is in the south limited with the Sava fault, and in the north by the Košuta overthrust of the Southern Karavanke. The lower and upper boundaries of the investigated sequences are not exposed, but the strata can be roughly divided into two parts (Dolenec et al, 1981). For the lower part of the sequence are characterized numerous strata and lenses of reddish oolitic limestone that are interbedded with the shale sheets and limestone beds with detritic admixture. In the upper part there is interbedded darker limestone, sandstone, marlstone and dolomite. A total thickness of the Lower Triassic strata in the section is about 200 m, of which the two parts of the section of approximately the same thickness. Conodonts were collected in the oolitic and sparitic limestone of the lower part of the section (Kolar-Jurkovšek & Jurkovšek, 1995). The recovered conodonts *F. gardenae, Ha. anceps, P. obliqua* and *Pa. ethingtoni* suggest a Smithian age.

Lower Triassic strata of the South Karavanke overthrust built a great part of the Kamnik-Savinja Alps in the upper part of Savinja valley. In the area between the Logarska dolina, Solčava, Robanov kot and the northern slopes of Raduha these strata attain thickness up to 1000 m (Mioč, 1983; Mioč & Žnidarčič, 1983; Celarc, 2002, 2004; Žalohar & Celarc, 2010), but due to folding their thickness is only apparant. In the lowest part of the Lower Triassic strata there rests dolomite, which passes upwards into a carbonate-clastic succession of marlstone, siltstones, sandstone and marly limestone. Preliminary sampling of the limestones in the upper part of the stratigraphic sequences at several localities confirmed the presence of the Smithian conodont taxa *P. obliqua* and *Parachirognathus* sp., and the Spathian species *T. hungaricus*.

Conodont zonation

Altogether seventeen conodont zones can be distinguished in Lower Triassic strata of Slovenia (Fig. 3, 4). In this section these zones are described in ascending order, and in the beginning also a description of the latest Permian conodont Zone is added.

Hindeodus praeparvus Zone
(latest Changhsingian)

Lower limit: defined by the first occurrence (FO) of *Hindeodus praeparvus* Kozur. Upper limit: first appearance datum (FAD) of *H. parvus* (Kozur & Pjatakova). Associated taxa: *H. typicalis* Sweet, *H. latidentatus* (Kozur, Mostler & Rahimi-Yazd), *Hindeodus* sp., and *H.* cf. *pisai* Perri & Farabegoli.

Occurrence: Lukač (the upper part of the latest Permian Bellerophon Limestone Member of the Bellerophon Formation through the lowermost Transitional Beds - latest Permian); Javorjev Dol, Masore, Idrijca, Vojsko (latest Permian; Bellerophon Formation).

Remarks. In the Masore section the elements of *H. praeparvus* and *H. latidentatus* co-occur in the uppermost part of the Bellerophon Formation. Both taxa range also in the lowermost Triassic and based on their occurrence in absence of *H. parvus* these strata are attributed to the *H. praeparvus* Zone (Late Permian, latest Changhsingian). *H. praeparvus* was reported to range in the lowermost Triassic in the Dolomites (Perri & Farabegoli, 2003). Very rare elements of *Isarcicella* with a widely opened and thickened basal cavity are also present, of which some specimens are designated to *Isarcicella* cf. *prisca* Kozur, in the uppermost strata of the Bellerophon Formation. According to Perri (Perri & Farbegoli, 2003) the genus *Isarcicella* made its first appearance in the latest Permian and is marker to distinguish the Upper from the Lower *H. praeparvus* Zone in the Southern Alps. Thus the presence of isarcicellids in the upper part of the *H. praeparvus* Zone in the Masore section enables to divide this zone in the lower and upper part.

Hindeodus parvus Zone

Lower limit: first appearance datum of *H. parvus*. Upper limit: first appearance datum of *Isarcicella lobata* Perri & Farabegoli. Associated taxa: *H.* cf. *pisai* and *Hindeodus* sp.

Occurrence: Lukač (earliest Griesbachian; Transitional Beds of the Lukač Formation). Remarks: *H. parvus* first appearance datum is documented in the L1 sample of the Transitional Beds of the Lukač Formation, and its last appearance datum is in the *I. staeschei – I. isarcica* Zone (Streaky Limestone Member of the Lukač Formation). This conodont zone is characterized by scarce fauna of exclusive representation of hindeodids.

Isarcicella lobata Zone

Lower limit: first appearance datum of *I. lobata* Perri & Farabegoli. Upper limit: first appearance datum of *I. staeschei* Dai & Zhang and *I. isarcica* (Huckriede). Associated taxa: transitional form *H. praeparvus / H. parvus*, *H.* cf. *pisai, H.* cf. *eurypyge* Nicoll et al., *H. parvus, H. erectus* Kozur, *H. postparvus* (Kozur), *Hindeodus* sp., *I. turgida* (Kozur et al.), *I. lobata, I. inflata* Perri & Farabegoli, and *Isarcicella* sp.

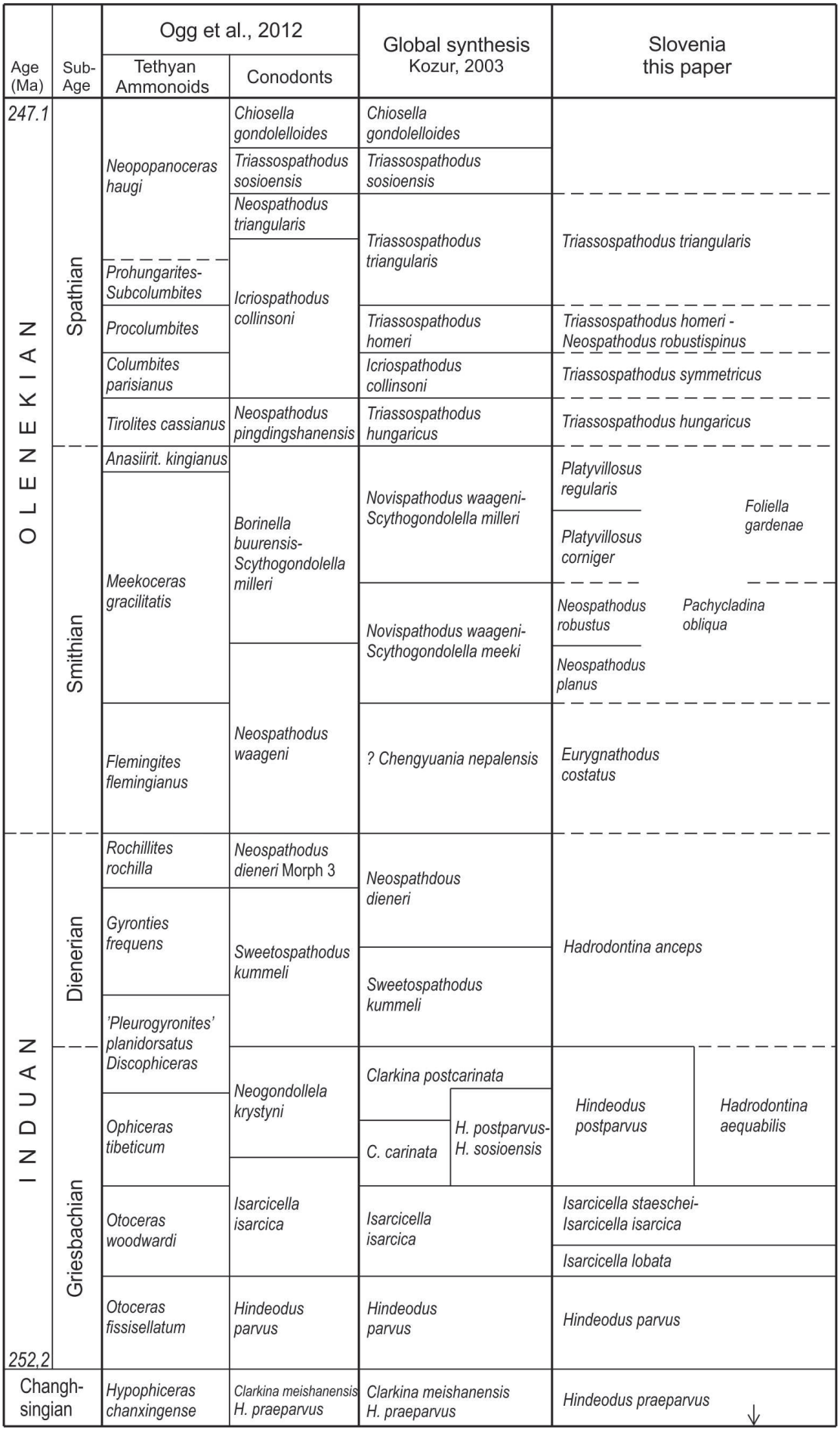

Fig. 3. Correlation of the Lower Triassic zones. Abbreviations: *C.* – *Clarkina, H.* – *Hindeodus*.

Occurence: Lukač (early Griesbachian; Transitional Beds of the Lukač Formation).

Remarks: *I. lobata* first appears in the Transitional Beds of the Lukač Formation. This zone is marked by the entry of several other taxa and it represents a recovery event. The entire stratigraphic range of the species *H. erectus* lies within this zone. Three other taxa (*H. postparvus, I. turgida, I. inflata)* have their entry (FAD) in this zone, whereas *H.* cf. *eurypyge* appears only in this zone.

***Isarcicella staeschei –Isarcicella isarcica* Zone**

Lower limit: first appearance datum of two isarcicellid taxa, *I. staeschei* and *I. isarcica*. Upper limit: last appearance datum of two isarcicellid taxa, *I. staeschei* and *I. isarcica* and the first appearance of *Hadrodontina* sp. *(Ha.* ex gr. *aequabilis)*. Associated taxa: *H. parvus, H. postparvus, Hindeodus* sp., *I. turgida, I. lobata, I. inflata,* and *Isarcicella* sp.

Occurrence: Lukač (Streaky Limestone Member of the Lukač Formation); Javorjev Dol, Masore, Idrijca, Vojsko ("Werfen Formation"); Griesbachian.

Remarks: This zone is marked by the entire stratigraphic range and co-occurrence of *I. staeschei* and *I. isarcica*. Five taxa (*H. postparvus, I. turgida, I. lobata, I. inflata,* and *Isarcicella* sp.) that appeared already in the previous zone continue with their presence in this zone. All associated taxa have the LAD within this zone, except *H. postparvus*. For the presence of numerous taxa the fauna of this zone is still part of the recovery event.

In the Lukač section the LAD of *I. staeschei* and *I. isarcica* coincides with the first occurrence of the genus *Hadrodontina* of which some elements can be identified as *Ha.* ex gr. *aequabilis*. In the Dolomites a successive appearance of some isarcicellid taxa is documented, i.e. *I. lobata - I. staeschei – I. isarcica* and moreover, the species *Ha. aequabilis* has a synchronous entry together with *I. staeschei.*

***Hindeodus postparvus* Zone**

Lower limit: first appearance datum of *H. postparvus* (Kozur) without the presence of *I. isarcica* and *I. staeschei*. Upper limit: last appearance datum of *H. postparvus*. Associated taxa: *Hadrodontina* sp., Ellisoniidae.

Occurrence: Lukač (latest Griesbachian; uppermost Streaky Limestone Member through the lowermost Carbonate-clastic Member of the Lukač section).

Remarks: This conodont zone in the Lukač section is marked by the highest portion of the stratigraphic range of *H. postparvus* without the presence of *I. isarcica* and *I. staeschei*. The discriminated *H. postparvus* Zone in the Lukač section is partly correlated with the *H. postparvus – H. sosioensis* Zone (Kozur, 2003).

***Hadrodontina aequabilis* Zone**

Lower limit: the first occurrence of *Hadrodontina aequabilis* Staesche. Upper limit: the first appearance datum of *Ha. anceps* Staesche. Associated taxa: *Hadrodontina* sp., Ellisoniidae.

Occurrence: Mokrice (late Griesbachian; "Werfen Formation").

Remarks: *Ha. aequabilis* was first described from the Dolomites (Staesche, 1964) and its multielement reconstruction was provided by Perri (1991). In the Mokrice section the *Ha. aequabilis* Zone has been distinguished where the marker taxon is present as a single species (Kolar-Jurkovšek et al., submitted). In the Dolomites, the *I. isarcica* Zone is succeeded by the succession of the zones based on euryhaline shallow water species: *Ha. aequabilis* Zone (latest Griesbachian - Dienerian), *Ha. anceps* Zone and *P. obliqua* Zone (Perri, 1991; Farbegoli & Perri, 2012).

Based on comparison with the Dolomites and regarding long range of *Ha. aequabilis* it is reasonable to conclude that the stratigraphic range of *H. postparvus* overlaps with the lower portion of the stratigraphic range of *Ha. aequabilis*. The later species has been reported also from Japan (Igo, 1996) and South Primorye in Russian Far East (Bondarenko et al., 2015).

***Hadrodontina anceps* Zone**

Lower limit: first occurrence of *Ha. anceps* Staesche. Upper limit: first occurrence of *P. obliqua*. Associated taxa: *Hadrodontina* sp., Ellisoniidae.

Occurrence: Lukač (Dienerian; middle and upper part of the Carbonate-clastic Member of the Lukač Formation).

Remarks: *Ha. anceps* was first described from the Dolomites (Staesche, 1964). The *Ha. anceps* multielement was first reconstructed by Perri & Andraghetti (1987). This zone is well correlated with the *Ha. anceps* Zone of the Dolomites where it is based on the position between the *Ha. aequabilis* Zone and followed by *P. obliqua* Zone (Perri,1991).

***Eurygnathodus costatus* Zone**

Lower limit: the first occurrence of *Eurygnathodus costatus* Staesche. Upper limit: the last occurrence of *E. costatus*. Associated taxon: *Eurygnathodus hamadai* (Koike).

Occurence: Golob (latest Dienerian and early Smithian; "Werfen Formation").

Remarks: *E. costatus* has been first described from the Dolomites, Italy (Staesche, 1964). In the Dinaric area and it has been later reported to occur in western Serbia (Budurov & Pantić, 1973), Croatia (Aljinović et al., 2006) and in Bosnia and Herzegovina. The species has been well documented from many sections in Asia (Chen et al., 2015a).

The GSSP of the Olenekian Stage has not been defined yet, but two proposals based on the FO of *Novispathodus waageni* have been put forward (Krystyn et al., 2007; Zhao et al., 2008). Both candidate sections, the Spiti of India and Chaohu in Anhui Province in China, are

characterized by presence of *E. costatus* that has short stratigraphic range. *E. costatus* has been reported to occur already in the latest Induan in some sections in Asia (Zhang, 1990; Igo, 2009, Chen et al. 2015b).

It is worthy to mention here that *Nv. waageni* has not been collected in the European sections and therefore *E. costatus* it is currently taken as an important marker around this boundary. The hitherto obtained data from Slovenia and other locations in the Dinarides unabled us to document its entire stratigraphic range and to define its precise stratigraphic position. The preliminary C-isotope data suggests, that the Induan-Olenekian boundary probably lies within the Golob section (Chen et al., 2015a) that means within the range of this taxon. Therefore in the Figure 3 the boundaries of this zone are presented with dashed lines.

Pachycladina obliqua Zone

Lower limit: the first occurrence of *P. obliqua*. Upper limit: the last occurrence of *P. obliqua*. Associated taxa: *Ha. anceps, Hadrodontina* sp., *Ellisonia* sp.

Occurence: Tehovec, Horjul and Žiri surroundings, Trojane, Grmače, Mišnica, Dobovica, Čebine (Smithian; "Werfen Formation").

Remarks: *P. obliqua* was first reported from the Dolomites, Italy by Staesche (1964) and also its multielement was first reconstructed from there (Perri & Andraghetti, 1987). The value for stratigraphy of *P. obliqua* in the Dolomites was first emphasized and was later confirmed also for the Dinarides (Perri, 1991; Kolar-Jurkovšek & Jurkovšek, 1995, 1996; Jelaska et al., 2003; Aljinović et al., 2011).

P. obliqua is the most frequent Early Triassic element reported from the entire Dinaric area, including Slovenia (Jurkovšek et al., 1999, Kolar-Jurkovšek & Jurkovšek, 2001; Dozet & Kolar-Jurkovšek, 2007), Croatia (Jelaska et al., 2003; Aljinović et al., 2006), Bosnia and Herzegovina (Aljinović et al., 2011), Serbia (Sudar, 1987). The exact stratigraphic range of *P. obliqua* in Slovenia has not yet been defined, but in the Dolomites it ranges from the Smithian to the lower Spathian (Perri & Andraghetti, 1987).

The fauna with dominating species *P. obliqua* and joined by *Hadrodontina* was assigned to the Smithian *P. obliqua* Zone and correlated to the *P. obliqua* Zone in the Dolomites as well as to the Lower Smithian Zone 7 (*Parachirognathus-Furnishius* Zone) of Sweet et al. (1971).

This species has been reported also from South China (Wang & Cao, 1981; Yang et al., 1986; Yan et al., 2013) and North America (Beyers & Orchard, 1991).

Foliella gardenae Zone

Lower limit: the first occurrence of *F. gardenae* (Staesche). Upper limit: the last occurence of *F. gardenae*. Associated taxa: *Ellisonia* sp., *Hadrodontina* sp., *P. obliqua, Furnishius triserratus* Clark, *Parachirognathus ethingtoni* Clark.

Occurrence: Iška, Draga, Skopačnik, Četež, Borštnik, Leskovica, Bogenšperk – Temnica, Želin-Vrlejca, Žiri and Solčava surroundings, Tržič, (late Smithian and earliest Spathian; "Werfen Formation").

Remarks: *F. gardenae* was originally reported from north Italy where it co-occurs with *P. obliqua,* however, in the upper portion of its stratigraphic range only (Staesche, 1964). This species has been later reported from the Dinaric area: Serbia (Budurov & Pantić, 1973; Sudar et al. 2014), Slovenia (Kolar-Jurkovšek, 1990 a; Kolar-Jurkovšek & Jurkovšek, 1995), Croatia (Aljinović et al., 2006). A limited geographic distribution of this species suggests it was ecologically restricted. It is possible that its occurrence is confined to the environment of the epeiric ramp conditions (Aljinović et al., 2013 a).

In western Serbia, the *F. gardenae* Zone is distinguished above the *E. costatus* Zone (Budurov & Pantić, 1974). It is worthwhile to mention that the two taxa have short stratigraphic ranges and according to the presented data, there is an intermediate interval without any evidence of conodont occurrences. Similar distribution revealing occurrence of *E. costatus* in the older strata and *F. gardenae* in the younger strata are supported by the situation in the Dolomites (Staesche, 1964).

Neospathodus planus Zone

Lower limit: the first occurrence of *Neospathodus planus*. Upper limit: the first occurrence of *N. robustus* Koike. Associated taxon: *Neospathodus* sp.

Occurrence: Žiri surroundings (Smithian; "Žiri Beds").

Remarks: This zone is distinguished based on a new species defined from Slovenia (Chen et al., 2015 a). The specimens of the namebearer of this zone are associated with other neospathodid elements determined as *Neospathodus* sp.

This zone can be roughly correlated to the lower protion of the *P. obliqua* Zone. It can be also correlated with the *Novispathodus waageni waageni* and *Discretella discreta* Zones which are reported from South China (Chen et al., 2013, 2015 b; Yan et al., 2013).

Neospathodus robustus Zone

Lower limit: the first occurrence of *N. robustus*. upper limit: the last occurrence of *N. robustus*. Associated taxon: *Neospathodus* sp.

Occurrence: Žiri surroundings (Smithian; "Žiri Beds").

Remarks: *N. robustus* was first reported from western Malaysia, and the first entry of this species is documented approximately 10 m higher (*ca.* 10m) than the LOs of *E. costatus* and *Nv.* cf. *waageni* (Koike, 1982). The reports on occurence of *N. robustus* are very rare.

In the Žiri area the lower *N. planus* and the succeeding *N. robustus* Zones are followed by the level with the *Platvyllosus* elements. Based on obtained data from Slovenia we may conclude that the *N. planus* and the *N. robustus* Zones can be correlated to the *P. obliqua* Zone.

***Platyvillosus corniger* Zone**

Lower limit: the first occurence of *Platyvillosus corniger*. Upper limit: the first occurrence *Pl. regularis* (Budurov & Pantić).

Occurrence: Žiri surroundings ("Žiri Beds"), Mokrice ("Werfen Formation"); Smithian.

Remarks: This zone is marked by the occurrence of a single species, the zonal namebearer. The *P. corniger* Zone can be together with the following *Pl. regularis* Zone roughly correlated with the *F. gardenae* Zone (see the remarks of the following zone).

***Platyvillosus regularis* Zone**

Lower limit: the first occurrence of *Pl. regularis*. Upper limit: the first occurrence *Triassospathodus hungaricus* (Kozur & Mostler).

Occurrence: Žiri surroundings ("Žiri Beds"), Mokrice ("Werfen Formation"); Smithian.

Remarks: This zone is marked by the occurrence of a single species, the zonal namebearer. The *Pl. regularis* has been reported from Serbia for the first time (Budurov & Pantić, 1973) and was assigned to the Ladinian genus *Pseudofurnishius* (e.g., Budurov & Pantić 1973). However taxonomic revision and new discoveries indicate that it should be assigned to genus *Platyvillosus* (Chen et al., 2015a, c).

Both *Platyvillosus* taxa have been collected in two sections in Slovenia, Žiri and Mokrice sections. The older strata in both sections are marked with the fauna of *Pl. corniger* that are followed by the strata with the fauna of *Pl. regularis*. Also in the first description of *Pl. regularis* there is no information about the composition of the fauna that enables us to speculate that the species in the type locality was collected as a monofauna. The absence of any accompaning fauna suggests to stressful conditions controlled by ecollogical factors that renders their comparison difficult.

In both Slovenian sections the *Pl. corniger* and the *Pl. regularis* Zones lie below the *T. hungaricus* Zone, similar as the *F. gardenae* Zone. Therefore it is reasonable to conclude that the faunas with *Platyvillosus* and *Foliella* are contemporaneous in Slovenia.

***Triassospathodus hungaricus* Zone**

Lower limit: the first occurrence of *T. hungaricus*. Upper limit: the first occurrence of *T. symmetricus* Orchard.

Occurrence: Studorski preval (Werfen Formation), Žiri surroundings ("Žiri Beds"), Mokrice, Solčava surroundings ("Werfen Formation"); Spathian.

Remarks: *T. hungaricus* was originally reported from Hungary from the strata with the ammonoid *Tirolites* (Kozur & Mostler, 1970).

In the Dinarides *T. hungaricus* has been just recently collected from Slovenia, as well as from Bosnia and Herzegovina (Kolar-Jurkovšek et al., 2013, 2014). The species has been also reported from the Sichuan Province, China (Tian et al., 1983). Some specimens determined as "*N.*" cf. *hungaricus* have been collected in Nevada (North America) (Lucas & Orchard, 2007).

Tirolites is widely accepted by stratigraphers as a marker for the Smithian-Spathian boundary (e.g., Kozur, 2003). According to Kozur (2003) the *T. hungaricus* Zone is presented as the first conodont zone of the Spathian. In the shallow western Tethys, *T. hungaricus* Zone lies in the lower Spathian, where *Icriospathodus collinsoni* (Solien) is missing (Kolar-Jurkovšek et al., 2013). The present zone can be roughly correlated with the lowermost Spathian *Pl. asperatus* Zone of the Great Basin, USA (Clark et al., 1979).

In the Mokrice section *T. hungaricus* occurs as the only species of this zone and it ranges up to the lowermost portion of the following zone characterized by the presence of *Neostrachanognathus tahoensis* Koike (Kolar-Jurkovšek et al., submitted).

***Triassospathodus symmetricus* Zone**

Lower limit: the first occurrence of *T. symmetricus*. Upper limit: the first occurrence of *Neospathodus robustispinus* Zhao & Orchard. Occurrence: Žiri surroundings (Spathian, "Žiri Beds").

Remarks: *T. symmetricus* was first reported from Oman and North America and it is accompanied by *Ic. collinsoni* and *T. homeri* (Mosher, 1968; Orchard, 1995). In the Slovenian section no accomapanied species were collected. *T. symmetricus* has also been reported from Italy (Perri, 1986), Greece (Dürkoop et al., 1986), North America (Mosher, 1973) and many sections in Asia (see Chen et al., 2015a, b).

This zone can be correlated with the *T. symmetricus* Zone of North Vietnam and the *Ic. collinsoni* zone of Jiarong, South China, as both zones lie immediately above the *Nv. pingdingshanensis* Zone (Chen et al., 2013, 2015b; Maekawa & Komatsu, 2014).

***Neospathodus robustispinus – Triassospathodus homeri* Zone**

Lower limit: the FO of *N. robustispinus* and/or the FAD of *T. homeri* (Bender). Upper limit: the LO of *N. robustispinus* and/or LAD *T. homeri*. Accompanied taxa: *T. symmetricus, N.* ex gr. *robustispinus*.

Occurrence: Žiri surroundings ("Žiri Beds"), Skopačnik (Werfen Formation); Spathian.

Remarks: *N. robustispinus* was first reported from Chaohu, Anhui province (South China), and it occurs in the lower Spathian ammonoid *Columbites-Tirolites* Zone (Zhao et al., 2008). *T. homeri* (Bender) was first described from Greece (Bender, 1970) and a worldwide distribution of the species is well documented (Orchard, 1995).

In the Slovenian section *N. robustispinus* is documented higher than the FO of *T. symmetricus*. The stratigraphic position of this zone can be roughly correlated to *T. homeri* Zone that is just below the *T. triangularis* Zone according to (Kozur, 2003). The *N. robustispinus - T. homeri* Zone in Slovenia probably correlates with the *T. homeri* Zone in South China (Chen et al., 2013, 2015b).

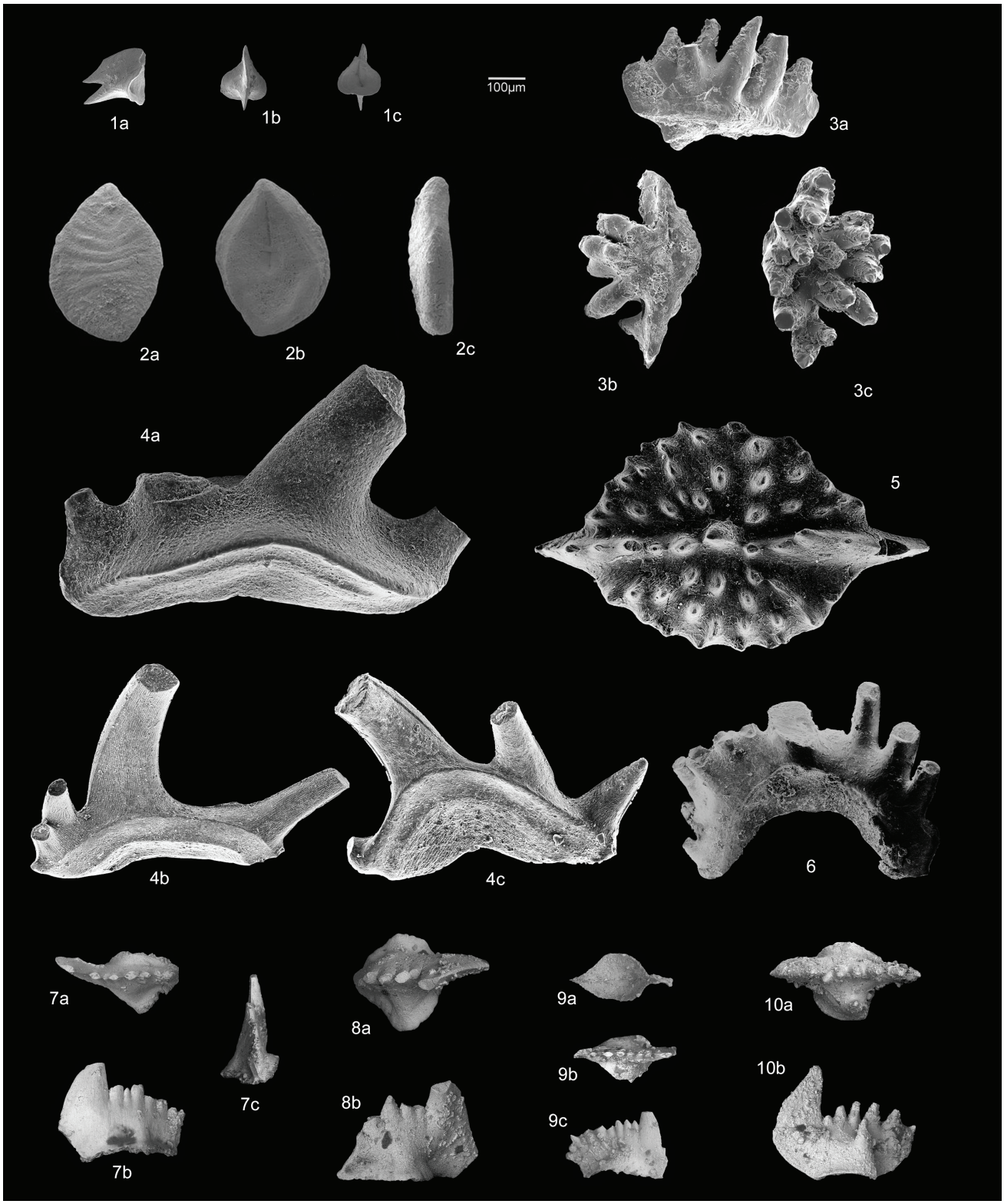

Fig. 4. Conodonts from the Lower Triassic of Slovenia.
1 a–c *Triassospathodus hungaricus* (Kozur & Mostler). Spathian, *Triassospathodus hungaricus* Zone. Mokrice, sample R1/3.
2 a–c *Eurygnathodus costatus* Staesche. Latest Dienerian – early Smithian, *Eurygnathodus costatus* Zone. Golob, sample 44/8.
3 a– c *Platyvillosus regularis* (Budurov & Pantić). Smithian, *Platyvillosus regularis* Zone. Žiri surroundings, sample 28/17.
4 a –c *Pachycladina obliqua* Staesche. Late Smithian – earliest Spathian, *Foliella gardenae* Zone. Iška, samples IŠ1, IŠ2.
5 – *Foliella gardenae* (Staesche). Late Smithian – earliest Spathian, *Foliella gardenae* Zone. Tržič, sample 66.
6 – *Hadrodontina anceps* Staesche. Late Smithian – earliest Spathian, *Foliella gardenae* Zone. Tržič, sample 59.
7 a –c *Hindeodus parvus* (Kozur & Pjatakova). Griesbachian, *Hindeodus parvus* Zone. Lukač, sample L1.
8 a– b *Isarcicella lobata* Perri & Farabegoli. Griesbachian, *Isarcicella lobata* Zone. Lukač, sample T.
9 a–c *Hindeodus postparvus* Kozur. Griesbachian, *Hindeodus postparvus* Zone. Lukač, sample 41.
10 a – b *Isarcicella staeschei* Dai & Zhang. Griesbachian, *Isarcicella isarcia* – *Isarcicella staeschei* Zone. Lukač, sample V.
All species are presented by the Pa element, except fig. 4 – *P. obliqua* is presented by the Pa, Sc, M elements in ascending order.

***Triassospathodus triangularis* Zone**

Lower limit: the FAD of *T. triangularis* (Bender). Upper limit: the LAD of *T. triangularis*.

Accompanied taxa: *T.* ex gr. *triangularis*. Occurrence: Skopačnik (Werfen Formation); Spathian.

Remarks: *T. triangularis* was first reported from Greece by Bender (1970) and it has been documented also from the Dolomites (Staesche, 1964; Perri & Andraghetti, 1987). The species has widespread distribution and has been extensively reported from many sections of the world (see Orchard, 1995; Chen et al., 2013, 2015b).

The marker taxon of the zone was collected also in a few sections south of Ljubljana, however, its entire range has not been well defined. Nevertheles, this zone can be compared to the *T. triangularis* Zone (Kozur, 2003).

Discussion and conclusions

The PTB interval in Slovenia is characterized by the genera *Hindeodus* and *Isarcicella* and the absence of gondolellids is obvious. Therefore, a conodont zonation for shallow facies of the Meishan section in China introduced by Wang (1996) and later refined for the Dolomites in Italy (Perri & Farabegoli, 2003) was applied. The Lukač section represents a key section to define the PTB interval strata in Slovenia as well as in the wider Dinarid area (Kolar-Jurkovšek et al., 2011a, 2012).

Certain levels of the Lower Triassic succession in Slovenia are marked by shallow water and euryhaline genera. Due to the absence of worldwide biozonal markers, a stratigraphic use of some taxa (i.e. *Hadrodontina aequabilis, Ha. anceps, Pachycladina obliqua*) was first recognized in the Dolomites, Italy (Perri, 1991) and was later applied also in the Dinarides (Jelaska et al., 2003). Therefore the use of euryhaline genera is important regional biostratigraphic tool in western Tethys.

Certain Olenekian faunas in Slovenia show very low diversity and many collected faunas are characterized by the presence of a single species, for example *Eurygnathodus costatus, E. hamadai, Platyvillosus corniger*, *Pl. regularis* and *Triassospathodus hungaricus*. The two *Platyvillosus* taxa have been hitherto reported only from the Dinarides. Stratigraphically important taxa for example: *Neospathodus dieneri, Novispathodus waageni*, *Icriospathodus collinsoni*, *Nv. pingdingshanensis* have not been documented to occur in Slovenia or the Dinarides.

For some time it was believed that the genus *Eurygnathodus* Staesche is a junior synonym of *Platyvillosus* Clark, Sincavage & Stone (e.g., Kozur & Mostler, 1973). Therefore there was certain misunderstanding in recognition of some Olenekian genera. In the Treatise of Invertebrate Paleontology (Clark et al., 1981), in the volume of the genus *Platyvillosus* as a synonym is regarded *Eurygnathodus* as well as ? *Foliella* Budurov & Pantić. The three genera have markedly different morphology and they are regarded as separate genera (e.g., Orchard, 2007; Chen et al., 2015a). The genus *Platyvillosus* was first described from North America and the type species is *Pl. asperatus* Clark, Sincavage & Stone. The relationship among all known occurrences of *Platyvillosus* representatives from Europe and North America is not clear.

In Slovenia, *Eurygnathodus* and *Platyvillosus* do not co-occur and this is in accordance with the data from Serbia (Budurov & Pantić, 1974). However, their relation is not yet solved. The P_1 element of *Platyvillosus* is demonstrated by the transitional forms from a neospathodid type ancestor as already suggested by Orchard (2007) and Chen et al. (2015a).

In Slovenia, the genera *Foliella* and *Platyvillosus* also do not co-occur and the recovered material does not reveal their relationship. *Foliella gardenae* has been documented only in Europe, however, the accompanied *Pachycladina* with an extensive geographical distribution enables worldwide comparison of the fauna.

Platyvillosus taxa have also limited geographic occurrence outside Slovenia. Of the two recognized species, only *Pl. regularis* has been known to occur in Serbia (Budurov & Pantić, 1973). Their occurrence outside the Dinarides has not yet been reported.

The two neospathodid taxa, *Neospathodus planus* and *N. robustus* occur in a level with obvious absence of *Novispathodus waageni*.

Certain recovered conodont faunas from Slovenia markedly differ from the contemporaneous conodont faunas of North America and Asia. A limited geographic distribution of some genera confined to the European sections suggests they were ecologically restricted and probably adapted to shallow water environments.

Triassospathodus hungaricus has been lately reported from few sections in the Dinarides where it occurs as single conodont species. Outside the area this species has been reported to occur in the Sichuan Province of South China (Tian et al., 1983) and moreover, Lucas & Orchard (2007) reported elements morphologically close or identical to "*Neospathodus*" cf. *hungaricus* from Nevada.

Representatives of the *T. symmetricus-homeri-triangularis* lineage are well documented and quite common worldwide.

Acknowledgements

The authors wish to thank to Milan N. Sudar (Belgrade, Serbia) for communications on the conodont part. Constructive and thoughtful review by Chen Yanlong (Graz Austria) is acknowledged. We are indebted to Galina P. Nestell and Merlynd Nestell (Arlington, Texas) for editing the manuscript. Facilities and technical staff of the Geological Survey of Slovenia

are gratefully acknowledged. The investigation was financially supported by the Slovenian Research Agency (programme number P1-0011and project number J1-6665). This is a contribution to the IGCP 572 »Recovery of ecosystems after the Permian-Triassic mass extinction« and IGCP 630 »Permian-Triassic climatic and environmental extremes and biotic response«.

References

Aljinović, D., Horacek, M., Krystyn, L., Richoz, S., Kolar-Jurkovšek, T. & Smirčić, D. 2013: Duje. Early Triassic epeiric ramp setting in the Dinarides (Croatia). In: World Summit on P-Tr Mass Extinction & Extreme Climate Change, June 13-15, 2013, Wuhan, China. Chen, Z.Q., Yang, H. & Luo, G. (eds.). Abstracts. Wuhan: State Key Laboratory of Biogeology and Environmental Geology, China University of Geosciences, 3–4.

Aljinović, D., Kolar-Jurkovšek, T. & Jurkovšek, B. 2006: The Lower Triassic shallow marine succession in Gorski Kotar region (External Dinarides, Croatia): Lithofacies and conodont dating. Rivista Italiana di Paleontologia e Stratigrafia, 112/1: 35 – 53.

Aljinović, D., Kolar-Jurkovšek, T., Jurkovšek, B. & Hrvatović, H. 2011: Conodont dating of the Lower Triassic sedimentary rocks in the external Dinarides (Croatia and Bosnia and Herzegovina). Rivista Italiana di Paleontologia e Stratigrafia, 117/1, 135–148.

Aljinović, D., Smirčić, D., Horacek, M., Richoz, S., Krystyn, L., Kolar-Jurkovšek, T. & Jurkovšek, B. 2014: Evolution of the Early Triassic marine depositional environment in the Croatian Dinarides. In: European Geosciences Union, General Assembly 2014, Vienna, Austria, 27 April-02 May 2014, (Geophysical research abstracts, ISSN 1607-7962, vol. 16). München: European Geosciences Union, http://meetingorganizer.copernicus.org/EGU2014/EGU2014-10284.pdf.

Aljinović, D., Smirčić, D., Kolar-Jurkovšek, T. & Jurkovšek, B. 2013: Karakteristike taložnog okoliša naslaga donjeg trijasa Dinarida. In: Babajić, E. (ed.): 5. savjetovanje geologa Bosne i Hercegovine, Pale, 24. - 25. 10. 2013. Zbornik sažetaka, (Zbornik radova Udruženja/udruge geologa Bosne i Hercegovine, ISSN 1840-4073). Sarajevo: Udruženje, Udruga geologa Bosne i Hercegovine, 3–4.

Bender, H. 1970: Zur Gliederung der Mediterranen Trias II. Die Conodontechronologie der Mediterranen Trias. Ann Geol. Pays Hell., 19: 465–540.

Benton, M. J. 2005: When life nearly died: The greatest mass extinction of all time. Thames & Hudson: 336 p.

Beyers, J.M. & Orchard, M.J. 1991: Upper Permian and Triassic conodont faunas from the type area of Cache Creek complex, south-central British Columbia, Canada. Geological Survey of Canada Bulletin 417, 269 – 297.

Berner, R.A. 2002: Examination of hypotheses for the Permo-Triassic boundary extinction by carbon cycle modeling. Proc. Nat. Acad. Sci. USA. 99/7, 4172–4177.

Bondarenko, L.G., Zakharov, Yu.D., Guravskaya, G.I & Safronov, P.P. 2015: Lower Triassic Zonation of Southern Primorye. Article 2. First Conodont Findings in *Churkites* cf. *syaskoi* Beds at the Western Coast of the Ussuri Gulf. Russian Journal of Pacific Geology, 9/3: 203–214.

Brandner, R., Horacek, M. & Keim, L. 2012: Permian-Triassic-Boundary and Lower Triassic in the Dolomites, Southern Alps (Italy). Field trip guide 29th IAS meeting of Sedimentology Schladming/Austria. Journal of Alpine Geology, 54: 379–404.

Budurov, K. & Pantić, S. 1973: Conodonten aus den Campiler Schichten von Brassina (Westserbien). II. Systematischer Tail. Bulletin of the Geological Institute-Series Paleontology, 22, 49–64.

Budurov, K. & Pantić, S. 1974: Die Conodonten der Campiler Schichten von Brassina (Westserbien). I. Stratigraphie und Conodonten-Zonen. Bulletin of the Geological Institute-Series Paleontology, 23: 49–64.

Buser, S. 1969: Osnovna geološka karta SFRJ 1 : 100.000. List Ribnica = Geological Map of SFRY 1: 100,000. Sheet Ribnica. Zvezni geološki zavod, Beograd.

Buser, S. 1974: Osnovna geološka karta SFRJ 1 : 100.000. Tolmač lista Ribnica = Geological Map of SFRY 1: 100,000. Explanatory Notes to the Sheet Ribnica. Zvezni geološki zavod, Beograd: 60 p.

Buser, S. 1980: Osnovna geološka karta SFRJ 1 : 100.000. Tolmač lista Celovec-Klagenfurt = Geological Map of SFRY 1: 100.000. Explanatory Notes to the Sheet Celovec- Klagenfurt. Zvezni geološki zavod, Beograd: 62 p.

Buser, S. 1986: Osnovna geološka karta SFRJ 1 : 100.000, Tolmač lista Tolmin in Videm = Geological Map of SFRY 1: 100,000. Explanatory Notes to the Sheet Tolmin and Videm. Zvezni geološki zavod, Beograd: 103 p.

Buser, S. 1987: Osnovna geološka karta SFRJ 1 : 100.000, List Tolmin in Videm = Geological Map of SFRY 1: 100,000. Sheet Tolmin and Videm. Zvezni geološki zavod, Beograd.

Buser, S. 1989: Developement of the Dinaric and the Julian Carbonate Platforms and of the intermediate Slovenian Basin (NW Yugoslavia). Mem. Soc. Geol. It., 34 (1986): 313–320.

Buser, S. & Cajhen, J. 1978: Osnovna geološka karta SFRJ 100.000. List Celovec (Klagenfurt) = Geological Map of SFRJ 1: 100.000. Sheet Celovec - Klagenfurt. Zvezni geološki zavod, Beograd.

Buser, S., Grad, K., Ogorelec, B., Ramovš, A. & Šribar, L. 1989: Stratigraphical, paleontological and sedimentological characteristics of Upper Permian beds in Slovenia (NW Yugoslavia). Mem. Soc. Geol. It., 34 (1986): 195–210.

Buser, S., Kolar-Jurkovšek, T. & Jurkovšek, B. 2007: Triasni konodonti Slovenskega bazena = Triassic conodonts of the Slovenian Basin. Geologija, 50/1, 19-28, doi:10.5474/geologija.2007.002.

Buser, S., Kolar-Jurkovšek, T. & Jurkovšek, B. 2008: The Slovenian Basin during the Triassic in the Light of Conodont Data. Boll. Soc. geol. It. (Ital. J. Geosci.), 127/2: 257–263.

Celarc, B. 2002: Tektonski stik med paleozojskimi in triasnimi kamninami pod Podolševo = Tectonic contact between Paleozoic and Triassic rocks south of Podolševa (Slovenia). Geologija, 45/2: 341–346, doi:10.5474/geologija.2002.030.

Celarc, B. 2004: Geološka zgradba severovzhodnega dela Kamniško-Savinjskih Alp = Geologic structure of Northeastern part of Kamnik-Savinja Alps. Disertacija. Univerza v Ljubljani, NTF – oddelek za Geologijo, Ljubljana: 137 p.

Chen, Y.L., Kolar-Jurkovšek, T., Jurkovšek, B., Aljinović, D. & Richoz, S. 2015a: Early Triassic conodonts and carbonate carbon isotope record of the Idrija-Žiri area, Slovenia. Paleogeography, Paleoclimatology, Paleoecology, doi:10.1016/j.palaeo.2015.12.013.

Chen, Y.L., Jiang, H.S., Lai, X.L., Yan, C.B., Richoz, S., Liu, X.D. & Wang, L.N., 2015b: Early Triassic conodonts of Jiarong, Nanpanjiang Basin, southern Guizhou Province, South China. Journal of Asian Earth Sciences, 105: 104–121.

Chen, Y.L., Krystyn L., Orchard, M.J., Lai X.L., & Richoz S. 2015c: A review of the evolution, biostratigraphy, provincialism and diversity of Middle and early Late Triassic conodonts. Papers in Palaeontology, doi:10.1002/spp2.1038.

Chen, Y.L., Twitchett, R.J., Jiang, H.S., Laai, X.L., Yan, C.B., Sun, Y.D., Liu, X.D. & Wang, L.N. 2013: Size variation of conodonts during Smithian-Spathian (Early Triassic) global warming event. Geology, 41/8: 823–826.

Chen, Y., Twitchett, R.J., Jiang, H.S., Laai, X.L., Yan, C.B., Sun, Y.D., Liu, X.D. & Wang, L.N., 2013: Size variation of conodonts during Smithian-Spathian (Early Triassic) global warming event. Geology, 41/8 823–826.

Clark, D.L., Paull, R.K., Sollen, M.A. & Morgan, W.A. 1979: Triassic Conodont Biostratigraphy in the Great Basin. Brigham Young University Geology Studies, 36/3: 179–183.

Clark, D.L., Sweet., W.C., Bergström, S.M., Klapper, G., Austin, R.L., Rhodes, F.H.T., Müller, K.J., Ziegler, W., Lindström, M., Miller., J.F. & Harris, A.G. 1981: Treatise on Invertebrate Paleontology. Part W Miscellanea. Supplement 2 Conodonta. The Geologic Society of America, Inc. and The University of Kansas, 202 pp., Boulder, Colorado, and Lawrence, Kansas,

Čar, J. 2010: Geološka zgradba idrijsko-cerkljanskega hribovja – Tolmač h Geološki karti idrijsko-cerkljanskega hribovja med Stopnikom in Rovtami 1:25.000 = Geological structure of the Idrija – Cerkno hills – Explanatory Book to the Geological map of the Idrija – Cerkno hills between Stopnik and Rovte 1:25,000. Geološki zavod Slovenije, Ljubljana: 127 p.

Dolenec, T., Lojen, S. & Dolenec, M. 1999a: The Permian-Triassic boundary in the Idrijca Valley (Western Slovenia): isotopic fractionation between carbonate and organic carbon at the P/Tr transition. Geologija, 42: 165–170, doi:10.5474/geologija.1999.011.

Dolenec, T., Lojen, S. & Ramovš, A. 2001: The Permian–Triassic boundary in Western Slovenia (Idrijca Valley section) magnetostratigraphy, stabile isotopes and elemental variations. Chem. Geol., 175: 175–190.

Dolenec, M. & Ogorelec, B. 2001: Organic carbon isotope variability across the P/Tr boundary in the Idrijca valley section (Slovenia): A high resolution study = Variabilnost izotopske sestave organskega ogljika na permsko-triasni meji v dolini Idrijce: detajlna študija. Geologija, 44/2: 331–340, doi:10.5474/geologija.2001.025.

Dolenec, T., Ogorelec, B., Dolenec, M. & Lojen, S. 2004: Carbon isotope variability and sedimentology of the Upper Permian carbonate rocks and changes across the Permian-Triassic boundary in the Masore section (Western Slovenia). Facies, 50: 287–299.

Dolenec, T., Ogorelec, B., Lojen, S. & Buser, S. 1999b: Meja perm-trias v Masorah pri Idriji = Permian-Triassic boundary in the Idrijca Valley: Masore section. RMZ, Materiali in geookolje, 46/3: 449–452.

Dolenec, T., Ogorelec, B. & Pezdič, J. 1981: Zgornjepermske in skitske plasti pri Tržiču =Upper Permian and Scythian beds in the Tržič area. Geologija, 24/2: 217–238.

Dolenec, T. & Ramovš, A. 1998: Isotopic changes at the Permian-Triassic boundary in the Idrijca Valley (W Slovenia). RMZ, Materiali in geookolje, 45/3-4: 405–411.

Dozet, S. & Kolar-Jurkovšek, T. 2007: Spodnjetriasne plasti na južnovzhodnem obrobju Ljubljanske kotline, osrednja Slovenija = Lower Triassic beds in the southern borderland of the Ljubljana depression, central Slovenia. RMZ, Materiali in geookolje, 54/3: 361–386.

Dürkoop, A., Richter, D.K. & Stritzke, R. 1986: Facies, Age and Correlation of Triassic Red Limestones (»Hallstatt Type«) from Epidavros, Adhami and Hydra (Greece). Facies, 14: 105–150.

Farabegoli, E., Levanti, D. & Perri, M.C. 1986: The Bellerophon Formation in the southwestern Carnia. The boundary Bellerophon-Werfen Formation. In: Italian IGCP 203 Group (eds.), Permian-Triassic Boundary in the South-Alpine Segment of the Western Tethys. Excursion Guidebook, SGI and IGCP 203 Meeting, 4-12, July 1986, Pavia, 69–75.

Farabegoli, E., & Perri, M.C., 2012: Millenial Physical Events and the End-Permian Mass Mortality in the Western Palaeothethys: Timing and Primary Causes. In: Talent, J.A. (ed.): International Year of Planet Earth, 719 – 758, Springer Science + Business Media B.V.

Galfetti, T., Hochuli, P.A., Brayard, A., Bucher, H., Weissert, H. & Vigran, J.O. 2007: Smithian-Spathian boundary event: Evidence for global climatic change in the wake of the end-Permian biotic crisis. Geology, 35/4: 291–294, doi:10.1130/G23117A.1

Grad, K. & Ferjančič, L. 1976: Osnovna geološka karta SFRJ 1:100.000. Tolmač lista Kranj = Basic Geological Map of SFRY 1:100,000. Explanatory notes on the Sheet Kranj. Zvezni Geološki zavod, Beograd: 70 p.

Grad, K. & Ogorelec, B. 1980: Zgornjepermske, skitske in anizične kamnine na Žirovskem ozemlju = Upper Permian, Scythian and Anisian rocks in the Žiri area. Geologija, 23/2: 189–220.

Holser, W.T. & Schönlaub, H.P. (eds.) 1991: The Permian-Triassic boundary in the Carnic Alps of Austria (Gartenkofel region). Abh. Geol. Bundesanst: 451 - 232.

Igo, H. 1996: Silurian to Triassic conodont biostratigraphy in Japan. Acta Micropalaeontologica Sinica, 13: 143–160.

Igo, H. 2009: Conodont succession. In: Shigeta, Y., Zakharov, Y., Maeda, H., Popov, A.M. (eds.): The Lower Triassic system in the Abrek Bay Area, South Primorye, Russia. National Museum of Nature and Science, Tokyo: 218 p.

Isozaki, Y. 1997: Permo-Triassic boundary superanoxia and stratified superocean: records from lost deep sea. Science, 276: 235–238.

Isozaki, Y. 2009: Illawarra Reversal: The fingerprint of superplume that triggered Pangean breakup and the end-Guadalupian (Permian) mass extinction. Gondwana Research, 15: 421–432.

Jelaska, V., Kolar-Jurkovšek, T., Jurkovšek, B. & Gušić, L. 2003: Triassic beds in the basement of the Adriatic-Dinaric carbonate platform of Mt. Svilaja (Croatia) = Triasne plasti v podlagi Jadransko-dinarske karbonatne platforme na planini Svilaja (Hrvaška). Geologija, 46/2: 225–230, doi:10.5474/geologija.2003.019.

Jurkovšek, B., 1987a: Osnovna geološka karta SFRJ 1 : 100.000. List Beljak in Ponteba = Geological Map of SFRJ 1: 100.000. Sheet Beljak in Pontebba. Zvezni geološki zavod, Beograd.

Jurkovšek, B. 1987b: Osnovna geološka karta SFRJ 1 : 100.000. Tolmač lista Beljak in Ponteba = Geological Map of SFRJ 1: 100.000. Explanatory Notes to the Sheet Beljak in Pontebba. Zvezni geološki zavod, Beograd: 58 p.

Jurkovšek, B., Ogorelec, B. & Kolar-Jurkovšek, T. 1999: Lower Triassic beds from Tehovec = Polhov Gradec Hills, Slovenia. Geologija, 41: 29 – 40, doi:10.5474/geologija.1998.002.

Koike, T. 1982: Triassic Conodont Biostratigraphy in Kedah West Malaysia. In: Kobayashi, T., Toriyama, R. & Hashimoto, W. (eds.): Geology and Paleontology of Southeast Asia, 23: 9–51.

Kolar-Jurkovšek, T. 1990: Smithian (Lower Triassic) conodonts from Slovenia, NW Yugoslavia. N. Jb. Geol. Paläont. Mh., 9: 536–546.

Kolar-Jurkovšek, T., Aljinović, D., Nestell, G.P.& Jurkovšek, B. 2013: New paleontological and lithological evidence at the Permian - Triassic boundary in Slovenia (NW Dinarides). In: Chen, Z.Q., Yang, H. & Luo, G. (eds.): World Summit on P-Tr Mass Extinction & Extreme Climate Change, June 13-15, 2013, Wuhan, China. Abstracts. Wuhan: State Key Laboratory of Biogeology and Environmental Geology, China University of Geosciences, 40.

Kolar-Jurkovšek, T., Chen, Y., Jurkovšek, B. & Richoz, S. & Aljinović, D. 2015b: An Early Triassic conodont sequence from Slovenia (Mokrice and Idrija-Žiri areas). In: Nurgaliev, D.K. (ed.):18th International Congress on the Carboniferous and Permian, August 11-15, 2015, Kazan, Russia. Abstracts volume. Kazan University Press, Kazan: 96.

Kolar-Jurkovšek, T., Chen, Y., Jurkovšek, B., Poljak, M., Aljinović, D & Richoz, S.: Conodonts biostratigraphy of the Smithian-Spathian (Olenekian, Early Triassic) in Mokrice, western Slovenia and reconstruction of some conodont apparatuses. (submitted).

Kolar-Jurkovšek, T. & Jurkovšek, B. 1995: Lower Triassic conodont fauna from Tržič (Karavanke Mts.. Slovenia). Eclogae geol. Helv., 88/3: 789–801.

Kolar-Jurkovšek T. & Jurkovšek, B. 1996: Contribution to the knowledge of the Lower Triassic conodont fauna in Slovenia. Razprave IV. Razreda Sazu, XXXVII 1: 3–21.

Kolar-Jurkovšek, T. & Jurkovšek, B. 2001: Conodont researches in the Lower Triassic strata of Slovenia. Geol. Zbor., Povzetki referatov, 15. Posvetovanje slovenskih geologov 16: 46–47.

Kolar-Jurkovšek, T. & Jurkovšek, B. 2007: First record of *Hindeodus-Isarcicella* population in Lower Triassic of Slovenia. Paleogeography, Paleoclimatology, Paleoecology, 252: 72–81, doi:10.1016/j.palaeo.2006.11.036

Kolar-Jurkovšek, T., Jurkovšek, B. & Aljinović, D. 2006: *Hindeodus parvus* v plasteh P/T intervala pri Žireh. In: Režun, B. et al. (eds.): Zbornik povzetkov, 2. Slov. geol. kongres Idrija, 47.

Kolar-Jurkovšek, T., Jurkovšek, B. & Aljinović, D. 2011a: Conodont biostratigraphy and lithostratigraphy across the Permian-Triassic boundary at the Lukač section in western Slovenia. Rivista Italiana di Paleontologia e Stratigrafia, 117/1: 115–133.

Kolar-Jurkovšek, T., Jurkovšek, B., Aljinović, D. & Nestel, G.P. 2011b: Stratigraphy of Upper Permian and Lower Triassic Strata of Žiri Area (Slovenia) = Stratigrafija zgornjepermskih in spodnjetriasnih plasti Žirovskega ozemlja. Geologija, 54/2, 193–204, doi:10.5474/geologija.2011.015.

Kolar-Jurkovšek, T., Jurkovšek, B., Aljinović, D. & Nestell, G.P. 2011c: Biostratigrafska določitev permsko-triasne meje v profilu Lukač. In: Rožič, B. (ed.).: 20. posvetovanje slovenskih geologov = 20th Meeting of Slovenian Geologists, Ljubljana, november 2011. Razprave, poročila = Treatises, reports, (Geološki zbornik, ISSN 0352-3802, 21). Ljubljana: Univerza v Ljubljani, Naravoslovnotehniška fakulteta, Oddelek za geologijo, 56–59.

Kolar-Jurkovšek, T., Jurkovšek, B., Aljinović, D. & Nestell, G.P. 2012: Lukač section - a key for a definition of the Permian - Triassic boundary in the Dinarides. In: IGCP 572 Closing Conference, 30 May - 7 June 2012, Eger, Hungary. Abstract volume & field guide - Bükk Mountains. Eger, 21–22.

Kolar-Jurkovšek, T., Jurkovšek, B., Aljinović, D. Nestell, G.P. & Smirčić, D. 2015a: Microbial deposits in the Permian-Triassic boundary interval of the Slovenian Dinarides. In: Nurgaliev, D.K. (ed.): 18th International Congress on the Carboniferous and Permian, August 11-15, 2015, Kazan, Russia. Abstracts volume. Kazan: Kazan University Press, 95.

Kolar-Jurkovšek, T., Jurkovšek, B., Nestell, G.P., & Aljinović, D. 2013: Permian - Triassic boundary interval in Slovenia: new micropaleontological data. In: Albanesi, G.L. & Ortega, G. (eds.): Conodonts from the Andes : proceedings of the 3rd International Conodont Symposium & Regional Field Meeting of the IGCP project 591, [Buenos Aires, 2013], (Publicación especial, ISSN 0328-347X, no. 13). Buenos Aires: Asociación Paleontológica Argentina, 143.

Kolar-Jurkovšek, T., Jurkovšek, B., Vuks, V.J., Hrvatović, H., Aljinović, D., Šarić, Ć. & Skopljak, F. 2014: The Lower Triassic platy limestone in the Jajce area (Bosnia and Herzegovina). Geologija, 57/2, 95–104, doi:10.5474/geologija.2014.009.

Kolar-Jurkovšek, T., Vuks, J. V., Aljinović, D., Hautmann, M., Kaim, A. & Jurkovšek, B. 2013: Olenekian (Early Triassic) fossil assemblage from Eastern Julian Alps (Slovenia). Ann. Soc. Geol. Polon., 83: 213–227.

Kozur, H. 2003: Integrated ammonoid, conodont and radiolarian zonation of the Triassic. Hallesches Jahrb. Geowiss., B 25: 49–79.

Kozur, H. & Mostler, H. 1970: Neue Conodonten aus der Trias. Ber. Nat.-Med. Ver., 58: 429–464.

Krystyn, L., Richoz, S. & Bhargava, N.O. 2007: The Induan- Olenekian Boundary (IOB) in Mud – an update of the candidate GSSP section M04. Albertiana, 36: 33–49.

Lucas, S. G., Kolar-Jurkovšek, B. & Jurkovšek, B. 2008: First record of fossil amphibian in Slovenia (Lower Triassic, Olenekian). Rivista Italiana di Paleontologiae Stratigrafia, 114/1: 323–326.

Lucas, S.G. & Orchard, M.J. 2007: Triassic lithostratigraphy and biostratigraphy north of Currie, Elko County, Nevada. Bulletin, New Mexico Museum of Natural History and Science, 40: 119–126.

Maekawa T. Komatsu, T. 2014. Conodont Succession. In: Shigeta Y., Komatsu T., Maekawa, T. & Tran, H.D., (eds.): Olenekian (Early Triassic) stratigraphy and fossil assemblages in Northeastern Vietnam. National Museum of Nature and Science Monographs (Tokyo, Japan), 45: 51–54.

Mioč, P. 1983: Osnovna geološka karta SFRJ 1 : 100.000. Tolmač lista Ravne = Geological Map of SFRY 1: 100.000. Explanatory Notes to the Sheet Ravne. Zvezni geološki zavod,Beograd: 69 p.

Mioč, P. & Žnidarčič, M. 1983: Osnovna geološka karta SFRJ 1 : 100.000. List Ravne = Geological Map of SFRY 1: 100.000. Sheet Ravne. Zvezni geološki zavod, Beograd.

Mlakar, I. 1969: Krovna zgradba idrijsko-žirovskega ozemlja = Nappe Structure of the Idrija – Žiri Region. Geologija, 12: 5–72.

Mlakar, I. 2002: O nastanku hidrografske mreže in nekaterih kraških pojavih na Idrijskem = On the origin of the hydrographic net and some karst phenomena in the Idrija region. Acta carsologica, 31/2: 9–60.

Mlakar, I. & Čar, J. 2009: Geološka karta idrijsko-cerkljanskega hribovja med Stopnikom in Rovtami 1:25.000 = Geological structure of the Idrija – Cerkno hills between Stopnik and Rovte 1:25,000. Geološki zavod Slovenije, Ljubljana.

Mlakar, I. & Placer, L. 2000: Geološka zgradba Žirovskega vrha in okolice = Geological structure of the Žirovski vrh and surrounding). In: Florjančič, A.P. (ed.): Rudnik urana Žirovski vrh (The Uranium mine Žirovski vrh). Doneski 1: 34–45, Didakta, Radovljica.

Mosher, L.C. 1968: Triassic Conodonts from Western North America and Europe and Their Correlation. Journal of Paleontology, 42/4: 895–946.

Mosher, L.C. 1973: Triassic conodonts from British Columbia and the Northern Arctic Islands. Bulletin - Geological Survey of Canada 222: 141–192.

Nestell, G.P.,Kolar-Jurkovšek, T., Jurkovšek, B. & Aljinović, D. 2011: Foraminifera from the Permian-Triassic transition in Western Slovenia. Micropaleontology, 57/3: 197–222.

Ogg, J.G. 2012: Triassic. In: Gradstein, F.M., Ogg, J.G., Schmitz, M.D. & Ogg., G.M. (eds.): The Geologic Time Scale 2012, Elsevier B.V, 2: 681–730.

Orchard, M.J. 1995. Taxonomy and Correlation of Lower Triassic (Spathian) Segminate Conodonts from Oman and Revision of Some Species of *Neospathodus*. Journal of Paleontology, 69/1: 110–122.

Orchard, M.J. 2007: Conodont diversity and evolution through the latest Permian and Early Triassic upheavals. Palaeogeography, Palaeoclimatology, Palaeoecology, 252/1-2: 93–117, doi:10.1016/j.palaeo.2006.11.037.

Perri, M.C. 1991: Conodont biostratigraphy of the Werfen Formation (Lower Triassic), Southern Alps, Italy. Bollettino della Societa Paleontologica Italiana, 30/1: 23–46.

Perri, M.C. & Andraghetti, M. 1987: Permian-Triassic boundary and Early Triassic conodonts from the southern Apls, Italy. Riv. It. Paleont. Strat., 93/3: 291–328.

Perri, M.C. & Farabegoli, E. 2003: Conodonts across the Permian-Triassic boundary in the Southern Alps. Cour. Forsch. Inst. Senckenberg, 254: 281–313.

Placer, L. 1973: Rekonstrukcija krovne zgradbe idrijsko žirovskega ozemlja = Reconstruction of the Nappe Structure of the Idrija-Žiri Region. Geologija, 16: 317–334.

Placer, L. 1981: Geološka zgradba jugozahodne Slovenije = Geologic structure of southwestern Slovenia. Geologija, 24/1: 27–60.

Placer, L. 1999: Contribution to the macrotectonic subdivision of the border region between Southern Alps and External Dinarides = Prispevek k makrotektonski rajonizaciji mejnega ozemlja med Južnimi Alpami in Zunanjimi Dinaridi. Geologija, 41 (1998): 223–255, doi:10.5474/geologija.1998.013.

Placer, L. 2008: Principles of the tectonic subdivision of Slovenia. Geologija, 51/2: 205–217, doi:10.5474/geologija.2008.021.

Poljak, M. 2000: Strukturno-tektonska karta Slovenije 1:250.000, izdelana po podatkih OGK SFRJ 1:100.000 = Structural-Tectonic Map of Slovenia 1:250,000. Geološki zavod Slovenije, Ljubljana.

Ramovš, A. 1958a: Razvoj zgornjega perma v loških in polhograjskih hribih = Die Entwicklung des Oberperms in Bergland von Škofja Loka und Polhov Gradec. Razpr. 4. Razr. SAZU, 8: 451–622.

Ramovš, A. 1958b: O faciesih v zgornjem wordu in zgornjem permu v Sloveniji. Geologija 4: 188–190.

Richoz, S. 2006: Stratigraphie et variations isotopiques du carbone dans le Permien supérieur et le Trias inférieur de la Néotéthys (Turquie, Oman et Iran). Memoirs de Géologie (Lausanne) 46: 1–251.

Scotese, C.R. 2001: Atlas of Earth History. Paleogeography, PALEOMAP Project, Arlington, Texas, 1: 52 p.

Skaberne, D., Ramovš, A. & Ogorelec, B. 2009: Srednji in zgornji perm = Middle and Upper Pewrmian. In: Pleničar, M., Ogorelec, B. & Novak, M. (eds.): Geologija Slovenije = Geology of Slovenia, 137–154.

Sremac, J., Jurkovšek, B., Aljinović, D. & Kolar-Jurkovšek, T. 2015: Fossils and microfacies of Bellerophon Formation of the Vojsko Plateau = Fosili i mikrofacijes formacije Bellerophon zaravni Vojsko. V: 100-ta obljetnica rođenja akademkinje Vande Kochansky-Devidé: knjiga sažetaka = 100th birth anniversary of Vanda Kochansky-Devidé, full member of Academy: abstracts. Zagreb: Hrvatska akademija znanosti i umjetnosti, 78–79.

Sremac, J., Jurkovšek, B., Aljinović, D. & Kolar-Jurkovšek, T.: Fossils and mikrofacies of Bellerophon Formation from the Vojsko Plateau. (submitted)

Staesche, U. 1964: Conodonten aus dem Skyth von Südtirol. N. Jb. Geol. Paläont. Abh., 119: 247–306.

Stanley, S.M. 2009: Evidence from ammonoids and conodonts for multiple Early Triassic mass extinctions. PNAS, 106/36: 15226–15267.

Sudar, M. 1986: Trassic microfossils and biostratigraphy of the Inner Dinarides between Gučevo and Ljubišnja Mts., Yugoslavia. Geol. an. Balk. poluos., 50: 151–394 (in Serbian, English summary).

Sudar, M.N., Chen, Y.L., Kolar-Jurkovšek, T., Jurkovšek, B., Jovanović, D. & Forel, M.B. 2014: Lower Triassic (Olenekian) microfauna from Jadar Block (Gučevo Mt., NW Serbia). Annales Geologiques de Peninsule Balkanique, 75: 1–15. doi:10.2298/GABP1475001S.

Sudar, M., Jovanović, D., & Kolar-Jurkovšek,T., 2007: Late Permian conodonts from Jadar Block (Vardar Zone, northwestern Serbia). Geologica Carpathica, 58/ 2: 145–152.

Sun, Y.D., Joachimski, M.M., Wignall, P.B., Yan, C.B., Chen, Y.L., Jiang, H.S., Wang, N.L. & Lai, X.L. 2012: Lethally Hot Temperatures during Early Triassic Greenhouse. Science, 338: 366–370.

Sweet, W.C., Mosher, L.C., Clark, D.L., Collinson, J.W. & Hasenmueller, W.A. 1971: Conodont Biostratigraphy of the Triassic. In: Sweet, W.C. & Bergström, S.M., (eds.): Symposium on conodont Biostratigraphy, Geological Society of America, Memoir, 127: 441–465.

Tian, C.R., Dai, J. & Tian, S.G. 1983: Triassic Conodonts. In: Chengdu Institute of Geology and Mineral Resources (eds.), Paleontological Atlas of Southwest China, Volume of microfossils. Geological Publishing House, Beijing, 345–398, pls. 79–100.

Vrabec, M., Šmuc, A., Pleničar, M., Buser, S. 2009: Geološki razvoj Slovenije - povzetek = Geological evolution of Slovenia - an overview. In: Pleničar, M., Ogorelec, B. & Novak, M. (eds.): Geologija Slovenije = Geology of Slovenia. Geološki zavod Slovenije, Ljubljana, 23–40.

Wang, Z.H. & Cao, Y.Y. 1981: Early Triassic conodonts from Lichuan, Western Hubei. Acta Micropalaeontologica Sinica, 20/4: 363–375.

Wang, C.Y. 1986: Conodont evolutionary lineage and zonation for the Latest Permian and the Earliest Triassic. Permophiles, 29: 30–37.

Yan, C.B., Wang, L.N., Jiang, H.S., Wignall, P.B., Sun, Y.D., Chen, Y.L. & Ali, X.L. 2013: Uppermost Permian to Lower Triassic conodont at Bianyang Section, Guizhou province, South China. Palaios, 28: 509–522.

Yin, H., Zhang, K., Tong, J., Yang, Z. & Wu, S. 2001: The Global Stratotype Section and Point (GSSP) of the Permian-Triassic Boundary. Episodes, 24: 102–114.

Zhang, S.X. 1990. On the lower Triassic conodont sequence of western Guangxi. Journal of Graduate School, China Univeristy of Geosciences, 4/2: 1–15

Zhao, L.S., Tong, J.N., Zhang, S.X. & Sun, Z.M., 2008: An Update of Conodonts in the Induan-Olenekian Boundary Strata at West Pingdingshan Section, Chaohu, Anhui Province. Journal of China University of Geosciences, 19/3, 207–216,

Žalohar, J. & Celarc, B. 2010: Spodnjetriasne plasti v slovenskih Alpah =Lower Triassic beds in the Slovenian Alps. Scopolia, Suppl., 5: 54–55.

GEOLOGIJA *58/2*, 175–182, Ljubljana 2015

http://dx.doi.org/10.5474/geologija.2015.013

Hidrogeologija na prehodnem območju med Prekmurskim poljem in Goričkim (SV Slovenija)

Hydrogeology of the transition area between Prekmursko polje and Goričko (NE Slovenia)

Katja KOREN[1], Mihael BRENČIČ[2,1] & Andrej LAPANJE[1]

[1]Geološki zavod Slovenije, Dimičeva ulica 14, SI–1000 Ljubljana;
e-mail: katja.koren@geo-zs.si, andrej.lapanje@geo-zs.si
[2]Univerza v Ljubljani, NTF, Oddelek za geologijo, Aškerčeva cesta 12, SI–1000 Ljubljana;
e-mail: mihael.brencic@ntf.uni-lj.si

Prejeto / Received 6. 11. 2015; Sprejeto / Accepted 15. 12. 2015; Objavljeno na spletu / Published online 30. 12. 2015

Ključne besede: hidrogeološko kartiranje, vodnjak, merjenje gladine podzemne vode, karta gladin podzemne vode, napajanje podzemne vode

Key words: hydrogeological mapping, dug well, groundwater level measurements, groundwater table contour map, groundwater recharge

Izvleček

Na prehodnem območju med gričevnatim Goričkim in uravnanim Prekmurskim poljem je bilo aprila 2014 izvedeno podrobno hidrogeološko kartiranje, v okviru katerega so bili registrirani pojavi podzemne in površinske vode. Opravljene so bile meritve gladine, temperature, elektroprevodnosti in pH vrednosti podzemne vode izbranih vodnjakov. Na podlagi teh podatkov je bila izrisana karta gladin podzemne vode in določene smeri njenega toka. Na območju Goričkega podzemna voda teče od severa proti jugu, na stiku med Goričkim in Prekmurskim poljem se smer toka zaradi spremembe reliefa in hidrogeoloških karakteristik sedimentov, spremeni proti jugovzhodu, kar se odraža v povijanju hidroizohips. Tok podzemne vode v osrednjem delu Prekmurskega polja je vzporeden toku reke Mure, to je v smeri od severozahoda proti jugovzhodu. Meritve terenskih fizikalno–kemijskih parametrov so pokazale, da se pH vrednost in temperatura podzemne vode na Goričkem in Prekmurskem polju ne razlikujeta. Vrednosti elektroprevodnosti so na Prekmurskem polju nekoliko višje kot na Goričkem.

Abstract

In April 2014 a detailed hydrogeological mapping was performed in the transition area between the hilly Goričko in the north and the flatland of Prekmursko polje in the south (NE Slovenia). The occurrence of groundwater and surface water phenomena were registered and groundwater levels determined in a number of dug wells. Some basic physico-chemical parameters of water, i.e. temperature, electrical conductivity and pH were measured. Groundwater level map of the area was drawn and groundwater flow directions determined. In the Goričko area, groundwater flows from north to south, while in Prekmursko polje groundwater flow is parallel to the flow of the Mura River, i.e. NW-SE. In the transition area between Goričko and Prekmursko polje groundwater countor lines bend substantialy indicating a change in the relief as well as change of the hydrogeological characteristic of sediments. The groundwater pH and temperatures in Goričko and Prekmursko polje, are simillar. However, the electrical conductivity of groundwater in Prekmursko polje is higher than in Goričko.

Uvod

Goričko je hribovito območje v severovzhodni Sloveniji, s povprečno nadmorsko višino približno 300 m, ki se na severu in zahodu nadaljuje v Avstrijo ter na vzhodu na Madžarsko, na jugu pa postopoma prehaja v ravnino Prekmurskega polja. Geomorfološko stik med njima predstavlja pas, sestavljen iz sistema nizkih pleistocenskih teras, ki jih je ustvarila reka Mura z akumulacijo in erozijo (Gams, 1959). Na območju teras so odloženi prodi, peščeni prodi, glinasti prodi in prodnati peski (Jelen & Rifelj, 2011), katerih prepustnost se v smeri proti Prekmurskemu polju povečuje. Pas se razteza od Cankove na zahodu do Žitkovcev na vzhodu, njegova površina pa je ocenjena na približno 180 km² (sl. 1). Prekmursko polje in Goričko se razlikujeta tako po hidrogeoloških, litoloških kot tudi po tektonskih razmerah.

Iz arhivskih kart gladin podzemne vode Kralj (1979) izhaja, da je na stiku med Goričkim in Prekmurskim poljem drugačna smer toka kot na osrednjem delu Prekmurskega polja in da se podzemna voda na severnem obrobju Prekmurskega polja napaja z Goričkega.

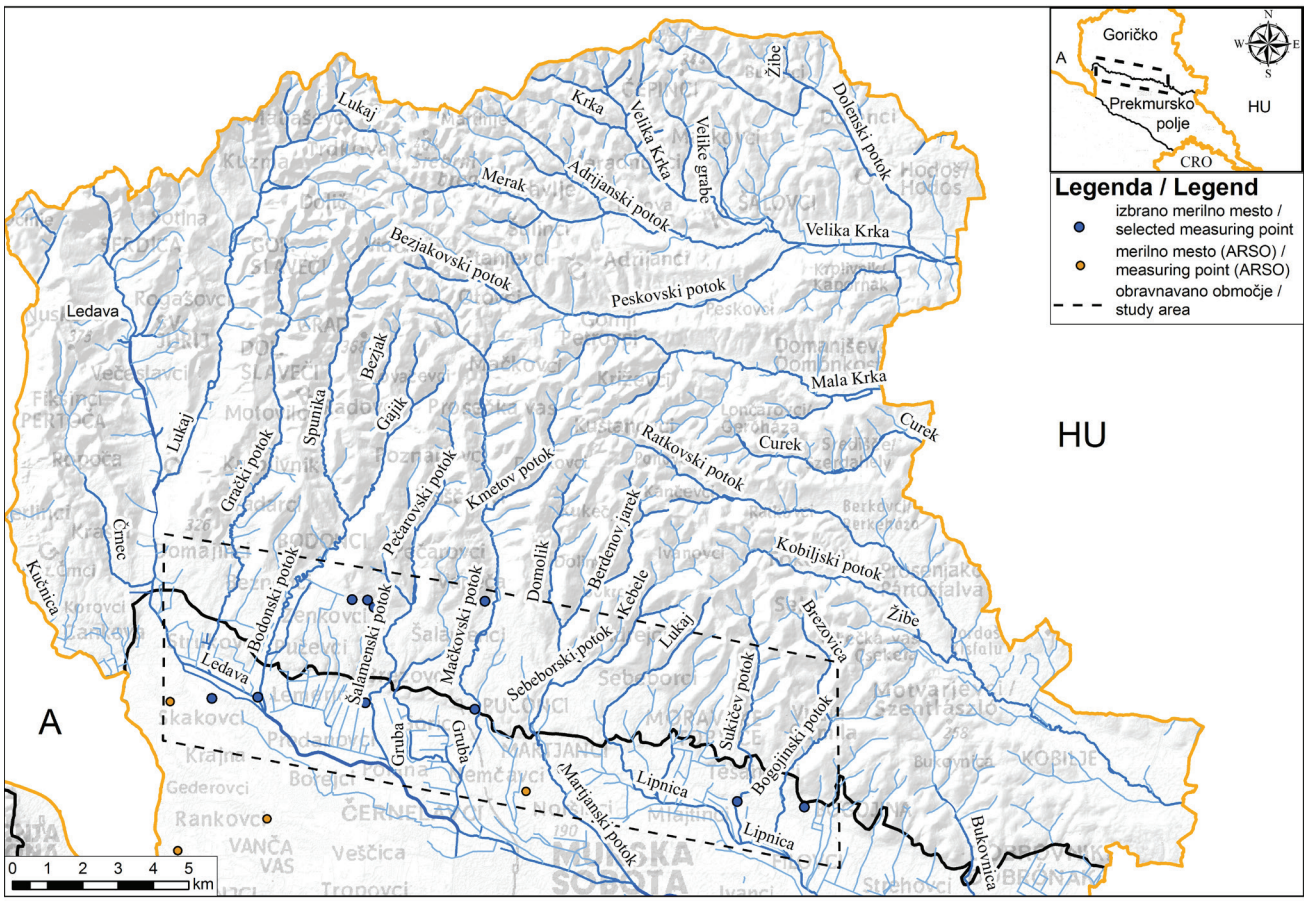

Sl. 1. Položaj potokov na Goričkem
Fig. 1. Streams in the area of Goričko

Vodotoki na zahodu Goričkega tečejo proti jugu in se na osrednjem delu Prekmurskega polja izlijejo v reko Ledavo. Na severovzhodnem delu Goričkega, tečejo proti jugovzhodu in vzhodu, v isti smeri kot Mala in Velika Krka. Ti reki tečeta proti vzhodu na Madžarsko kjer se združita v Krko (madž. Kerka), ki se na državni meji med Slovenijo in Madžarsko izlije v reko Muro. Na zahodnem Goričkem, ob Ledavi, so potoki daljši kot v vzhodnem delu. V Ledavo so v smeri od zahoda proti vzhodu izlivajo: Bodonski, Pečarovski, Beznovski, Mačkovski, Sebeborski, Martjanski, Krnski, Bogojinski, Sukičev, Andrejski in Dolinski potok, Lipnica, Lukaj, Črnec, Dobel in Bezjak (sl. 1). Stalni pretok je prisoten le v Bodonskem, Mačkovskem in Martjanskem potoku, drugi pa predvsem v poletnih mesecih, presahnejo (Ciglar, 1975).

Ledava je z 71 km dolžine najdaljša reka na Goričkem. Izvira v bližini Gleichenberga, v Avstriji, nato teče po Goričkem od severa proti jugu. Pri Topolovcih seka pleistocensko teraso ter teče v smeri proti jugovzhodu, po ravnini vse do državne meje z Madžarsko, kjer se izliva v Muro (sl. 1). Je njen glavni pritok v Sloveniji, ki ima zaradi prevlade slabše prepustnih tal, zelo gostoto drenažno mrežo. Tudi drugi potoki na Goričkem imajo razvejane drenažne mreže, na prehodu v ravninski del, kjer so tla bolj prepustna kot na Goričkem, začnejo zaradi majhnega naklona površine vijugato. V povirnem delu so struge ožje in globlje.

Goričko je pomembno tudi z vidika pojavljanja mineralne vode, predvsem na območju Nuskove (Žlebnik, 1974), ki pa se trenutno še ne uporablja v komercialne namene. Prekmursko polje je glede teh virov bogatejše, na območju Petanjcev se nahaja mineralna voda, na območju Renkovcev, Moravskih Toplic in Lendave pa termalna voda. Na območju Prekmurskega polja, zlasti na širšem območju Petišovcev, so v preteklosti potekale intenzivne raziskave nafte in plina, kjer so bila odkrita ekonomsko pomembna naftna polja (Pleničar, 1954).

Namen članka je podati hidrogeološke razmere na stičnem območju med hribovitim Goričkim in ravninskim Prekmurskim poljem. Razpoložljivi podatki (Novak, 1966; Kralj, 1979) nakazujejo, da se del podzemne vode na severnem območju Prekmurskega polja napaja z Goričkega, in da stik med tema dvema pokrajinskima enotama predstavlja območje hidrogeološkega prehoda, kjer se v smeri od severa proti jugu spremenijo hidrogeološke razmere in s tem tudi smer toka podzemne vode. S hidrogeološkim kartiranjem smo želeli potrditi domnevi o obstoju prehodnega območja in o smeri napajanja na severni meji Prekmurskega polja.

Predhodne raziskave na obravnavanem območju

V preteklosti so se geološke raziskave izvajale lokalno, predvsem z namenom opredelitve geomehanskih pogojev za gradnjo manjših objektov

(Novak, 1966; Ciglar & Filipič, 1987). To je razlog za šibko poznavanje geologije Goričkega v celoti, v primerjavi z južno ležečim Prekmurskim poljem. Rezultati večine opravljenih raziskav na območju Goričkega niso bili objavljeni in so na razpolago le v obliki delovnih poročil, predvsem v arhivu Geološkega zavoda Slovenije.

Območje severnega dela Prekmurskega polja je hidrogeološko raziskal Kralj (1979) in rezultate strnil v diplomskem delu. Novak (1966) je raziskoval lokalne hidrogeološke razmere na območju Puconcev in izdelal hidrogeološko karto, ki prikazuje gladino podzemne vode na Prekmurskem polju in na stiku z Goričkim na sami lokaciji. V zadnjem obdobju večina raziskav zajema hidrogeološko interpretacijo monitoringa gladin podzemne vode na odlagališču Puconci. Hidrogeološko opredelitev območja odlagališča je podal Drobne (1989), podrobnejšo karakterizacijo pa Brenčič (2003). Raziskave morebitnih nahajališč kremenovega proda in peska (Ciglar & Filipič, 1987) so potekale predvsem na območju vasi Bodonci, Kuštanovci, Korovci in Puconci. Za ekonomsko primerno nahajališče se je izkazalo le nahajališče v Puconcih. V občini Puconci, pa so bile na območju Doline opravljene tudi inženirsko geološke raziskave (Čarman, 2014). Na območju Nuskove je bilo izvrtanih nekaj vrtin za določitev količin mineralne vode ter opredelitev vodonosnih plasti (Žlebnik, 1974), na območju celotnega Pomurja pa je bilo v zadnjih letih izvedenih tudi veliko raziskav geotermalnih virov (Rman et al., 2012). Izvedene so bile tudi petrografske raziskave (Kralj, 1999) v okolici Grada na Goričkem, v katerih je bil podrobneje raziskan apofilit iz zgornjepliocenskih vulkanoklastov. Geokemične raziskave zgornjepliocenskih meljastih in peščenih sedimentov iz vrtine Mt-7 (Kralj, 2003) so potekale na območju Moravskih toplic. Rezultate geofizikalnih raziskav izvedenih za potrebe skladiščenja plina v strukturah Pečarovci in Dankovci je opisal Gosar (1996).

Hidrogeološki opis območja

Goričko gradijo slabše prepustni, heterogeni sedimenti, predvsem gline in melji, ki se izmenjujejo z dobro prepustnimi peski in prodi (Ciglar, 1975). Glede na to sklepamo, da je infiltracija padavin na Goričkem zaradi slabše prepustnih krovnih plasti, nižja kot na Prekmurskem polju. Slednje je zgrajeno pretežno iz dobro prepustnih prodov in peskov, slabše prepustne plasti sedimentov pa se v glavnem pojavljajo v lečah oziroma v podlagi kvartarnega vodonosnika.

Površje Goričkega prekrivajo predvsem sedimenti Špiljske, Murske in Ptujsko-grajske formacije (Jelen & Rifelj, 2011) neogenske starosti. Med Kučnico in Ledavo prevladujejo sedimenti Špiljske formacije, ki so se odlagali v plitvomorskem okolju, območje ob Ledavi (na Goričkem) prekrivajo sedimenti Murske formacije, odloženi na deltni ravnici in deltnem čelu, na njih pa so v osrednjem in vzhodnem delu Goričkega odloženi sedimenti aluvialne ravnice Ptujsko-Grajske formacije. Vrhove grebenov na vzhodnem Goričkem prekrivajo slabo sortirani rečni prodi, z lečami glin in peskov (Ciglar & Filipič, 1987; Beguš et al., 2002) domnevno pliocenske ali pleistocenske starosti (Jelen & Rifelj, 2011).

V holocenu so manjši potoki in hudourniki z območja Goričkega nanašali sedimente v smeri proti jugu (Pleničar, 1970). Tako so v strugah potokov na Goričkem in na severnem robu Prekmurskega polja odloženi prodi, peski, melji in peščene gline (Jelen & Rifelj, 2011). Površje na območju Goričkega se znižuje v smeri od severa proti jugu (sl. 1).

Podzemna voda na Goričkem se nahaja v srednje izdatnih kvartarnih in pliocenskih medzrnskih vodonosnikih, ki jih gradijo prodne, peščene in meljne plasti ter vmesne, tanjše slabo do zelo slabo prepustne plasti. Zaradi tega so pogosti lokalni polzaprti vodonosniki, nekatere med njimi lahko opredelimo tudi kot viseče vodonosnike (Prestor et al., 2006).

Predkvartarna podlaga na obravnavanem delu Prekmurskega polja tone v smeri od severozahoda proti jugovzhodu. Predstavljajo jo predvsem zelo slabo prepustni pliocenski sedimenti (glina, melj in lapor), med njimi pa prevladuje glinena komponenta (meljna glina, peščena glina, laporasta glina).

Visoko izdaten kvartarni medzrnski vodonosnik na območju Prekmurskega polja vsebuje pomembne količine podzemne vode za oskrbo prebivalstva s pitno vodo (Mali & Hötzl, 1990). V nekaterih primerih kemijsko stanje te podzemne vode ni primerno za pitno vodo, predvsem zaradi prisotnosti nitrata in pesticidov (Mihorko & Gacin, 2014).

Na stiku med Goričkim in Prekmurskim poljem se sedimenti razlikujejo po poroznosti in prepustnosti. Za kvartarni medzrnski vodonosnik sta značilni visoka prepustnost in izdatnost, s koeficientom prepustnosti med $1{,}0 \cdot 10^{-3}$ in $5{,}0 \cdot 10^{-3}$ m/s, poroznostjo od 0,15 do 0,35 in gradientom podzemne vode od 0,001 do 0,002 (Brenčič, 2009).

Na območju Puconcev, na meji med Goričkim in Prekmurskim poljem, se nahajajo izmenjujoče plasti heterogenih pliocenskih in pleistocenskih sedimentov, ki imajo različno prepustnost ter se lečasto prepletajo. Zato pride do razlike v smeri hidravličnega gradienta (Brenčič, 2006). Koeficient prepustnosti je v razponu med $1{,}4 \cdot 10^{-6}$ in $1{,}3 \cdot 10^{-4}$ m/s (Brenčič 2008; Bokan, ustna informacija).

Metode

Hidrogeološko kartiranje

Hidrogeološke razmere smo opredelili s podrobnim kartiranjem območja južnega roba Goričkega in severnega roba Prekmurskega polja. Kartiranje smo izvedli v aprilu 2014.

Pregledali smo vse dostopne hišne vodnjake na obrobju Goričkega v naseljih Strukovci, Puževci, Brezovci, Puconci, Martjanci, Tešanovci, Bogojina, Sebeborci, Vaneča, Bodonci in Šalamenci (sl. 1). Tovrstne objekte za monitoring uporabljamo večinoma v primerih, ko na razpolago ni primernejših objektov za odvzem vzorcev podzemne vode. Pri takšnih objektih je potrebno računati z možnostjo točkovnega onesnaženja z bližnjih površin, še posebej v vodnjakih na kmečkih dvoriščih (Prestor et al., 2006). Pri tem je potrebno poudariti, da v več primerih lastniki niso dovolili dostopa do vodnjakov, zaradi česar je gostota opravljenih meritev na nekaterih območjih majhna. Pri interpretaciji smo upoštevali tudi podatke o meritvah gladin podzemne vode na merilnih mestih s katerimi upravlja Agencija RS za okolje (sl. 2).

Vsi preiskani vodnjaki so bili izkopani ročno in okrepljeni s cevmi premera 1 m ali več. Prav tako so vsi zaščiteni pred neposrednim vdorom padavinske vode s pokrovom ali s streho. Najgloblji vodnjak se nahaja v Šalamencih in je globok 36 m. Večina vodnjakov se za lastno oskrbo s pitno vodo ne uporablja več, ker so hiše priklopljene na javni vodovodni sistem. Večinoma lastniki vodo iz vodnjakov uporabljajo le občasno za zalivanje vrtov.

Enkratne meritve gladin podzemne vode in fizikalno–kemijskih parametrov podzemne vode so potekale 25. aprila 2014. V dneh pred opravljenimi meritvami je rahlo deževalo, prav tako na dan meritev. Poleg gladin podzemne vode so bili v vodnjakih izmerjena še elektroprevodnost, temperatura in pH vrednost (tabela 1). Fizikalno–kemijski parametri so bili merjeni z merilnikom pH/Cond 340i proizvajalca WTW. Natančnost pri meritvah elektroprevodnosti znaša ±0,5%, pri pH vrednosti ±0,03 in pri temperaturi ±0,1°C.

Izris hidroizohips

Pri izrisu karte gladin podzemne vode sta bili uporabljeni dve interpolacijski metodi. Hidroizohipse so bile izrisane s triangulacijo z linearno interpolacijo in s pomočjo navadnega krigiranja, ki je bilo uporabljeno kot kontrolna metoda (Yang et al., 2004). Izris je bil na podlagi strokovne ocene tudi ročno korigiran. Podatki gladin podzemne vode so grafično predstavljeni in izdelani s pomočjo programa ArcGIS (ESRI, 2014).

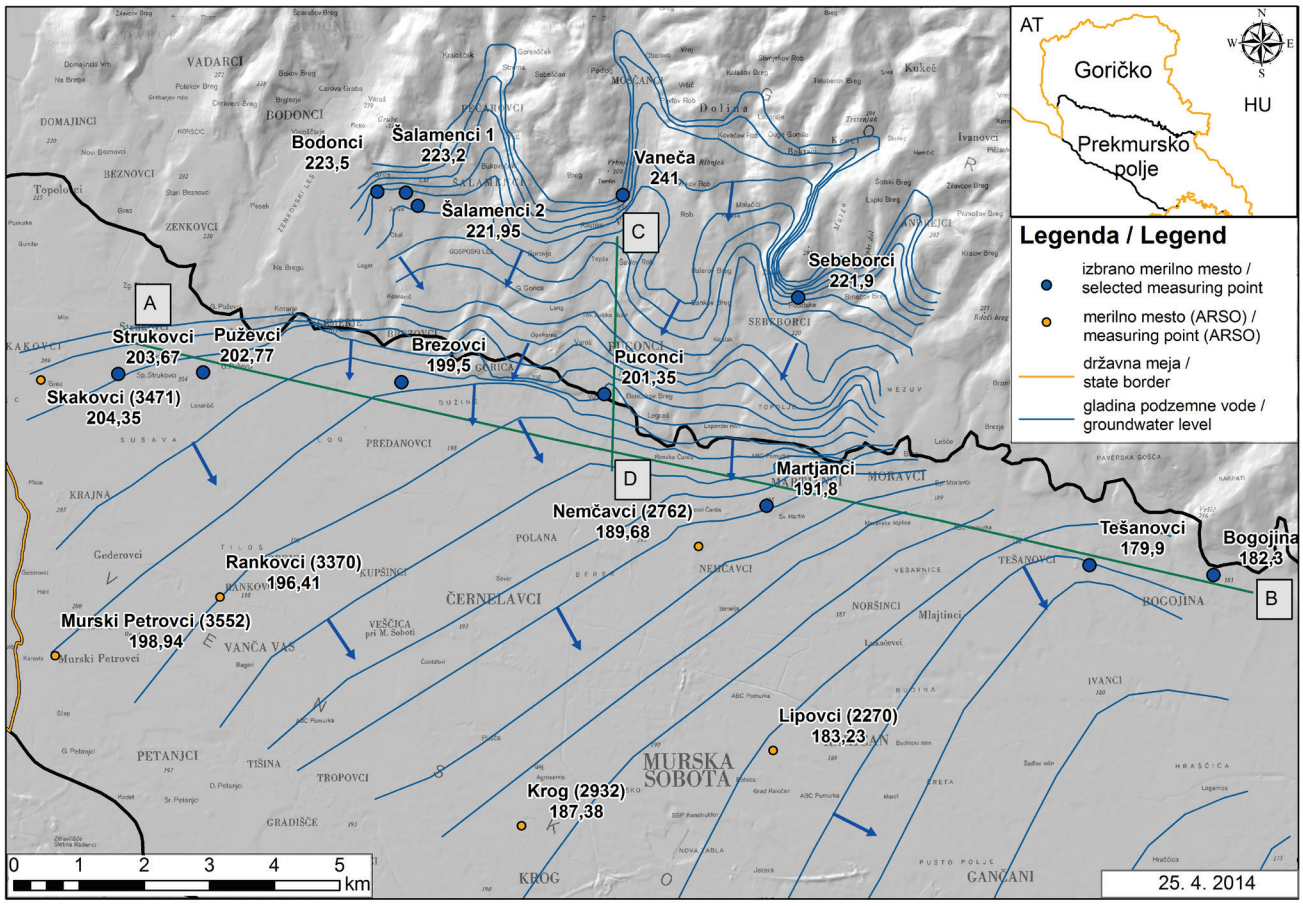

Sl. 2. Karta gladin podzemne vode z dne 25. 4. 2014 z lokacijami kartiranih vodnjakov in vrisanimi hidrogeološkimi profili.
Fig. 2. Groundwater table countour map on the day of 25. 4. 2015 with dug wells and hydrogeological profiles.

Ker pa podatki izmerjenih gladin niso bili zadostni, saj je mreža merilnih mest bila preredka, smo pri izrisu karte gladin podzemne vode na obravnavanem območju, upoštevali tudi opazovalna mesta Agencije RS za okolje ter morfologijo površja na območjih, kjer tečejo potoki. Zaradi pomanjkanja podatkov o gladinah podzemne vode smo predpostavili, da so potoki v stiku s podzemno vodo, in da njihove pretočne višine predstavljajo gladino podzemne vode na stiku potoka in vodonosnika.

Koordinate lokacij individualnih vodnjakov so določene s pomočjo Atlasa okolja (Internet 1), na podlagi najbližjih hišnih številk in lokacij vodnjakov na pripadajočih parcelah. Kote ustij vodnjakov, so določene na podlagi seštevka kote terena, ki izhaja iz digitalnega modela reliefa (DMV 5) podanega v Atlasu okolja (MOP-GURS, 2011) in na terenu izmerjene višine ustij vodnjakov.

Rezultati in interpretacija

Na podlagi podrobnega hidrogeološkega kartiranja in meritev gladin podzemne vode v vodnjakih smo določili obliko gladine podzemne vode na prehodnem območju med Goričkim in Prekmurskim poljem (sl. 2) ter izrisali dva reprezentativna profila poteka podzemne vode (sl. 3, 4).

V vodnjakih na severnem robu Prekmurskega polja se podzemna voda nahaja plitvo pod površjem, plitveje od 5 m. Najvišja gladina podzemne vode na stičnem območju, ki reliefno pripada Prekmurskemu polju, je bila izmerjena v Puževcih (203,04 m.n.v.) in najnižja v Bogojini (182,70 m.n.v.). Gradienti gladine podzemne vode se gibljejo v razponu od 0,0010 do 0,0015. Podzemna voda ima enotno smer toka, od severozahoda proti jugovzhodu.

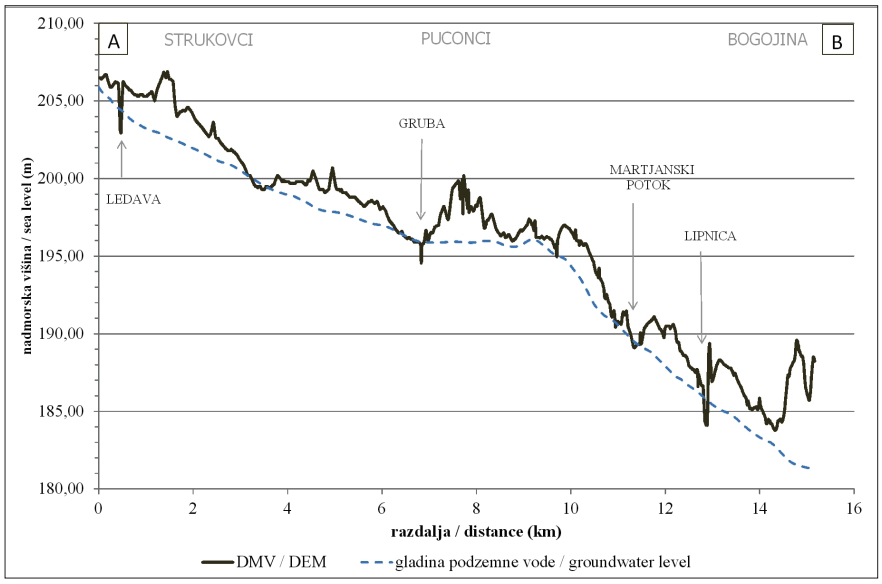

Sl. 3. Interpretiran hidrogeološki profil A – B na Prekmurskem polju (glej sl. 2).
Fig. 3. Hydrogeological profile A – B in Prekmursko polje (see Fig. 2).

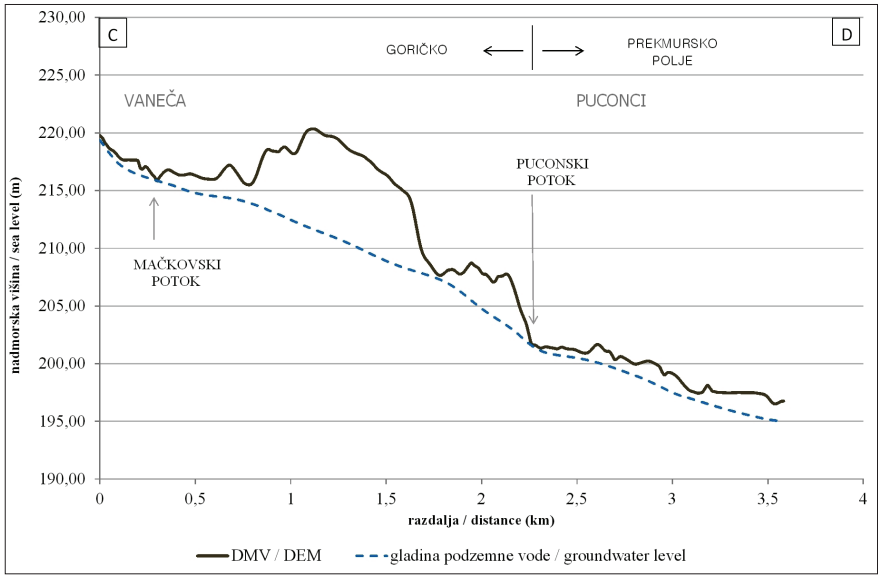

Sl. 4. Interpretiran hidrogeološki profil C – D na prehodu z Goričkega na Prekmursko polje (glej sl. 2).
Fig. 4. Hydrogeological profile C – D in transition area from Goričko to Prekmursko polje (see Fig. 2).

Podzemna voda na južnem obrobju Goričkega je kot pričakovano, globlja. Izjema je vodnjak v Vaneči, kjer je bila gladina podzemne vode izmerjena na globini 0,5 m (241,90 m.n.v.). V tem primeru gre najverjetneje za viseči vodonosnik, vezan na plast gline, katere pojavljanje je v tem predelu pogosto (Ciglar, 1975; Brenčič, 2006). V ostalih vodnjakih se podzemna voda nahaja na globini med 8 in 24 m.

Prevladujoča smer toka podzemne vode na južnih obronkih Goričkega je vezana na smeri vodotokov, ki tečejo v smeri od SSV proti JJZ, ter na oblikovanost reliefa, ki pada v enaki smeri. Dodaten vpliv na obliko gladine podzemne vode na južnih obronkih Goričkega imajo tudi sedimenti, v katerih se izmenjujejo drobnozrnati (gline in melji) in debelejši (pesek in prod) sedimenti. Zaradi tega smo območje opredelili kot slabše prepustno od Prekmurskega polja. Posledica tega so višji gradienti gladin podzemne vode na južnem robu Goričkega. Vrednosti gradientov se gibljejo na intervalu od 0,011 do 0,013. Vzpetine med površinskimi vodotoki predstavljajo razvodnice, kjer se podzemna voda razteka na vzhod in zahod, lokalno tok podzemne vode praviloma sledi pobočjem. Izrazita razvodnica je tako prisotna med Bodonskim potokom in Šalamenskim potokom ter med Puconskim potokom in Sebeborskim potokom. V vzhodnem delu obravnavanega območja lahko glede na podatke iz zahodnega dela obravnavanega območja, interpretiramo smer toka podzemne vode v smeri severa proti jugu.

Na prehodu z Goričkega v Prekmursko polje se smer toka podzemne vode spremeni, tok se iz smeri SSE-JJZ obrne v smeri SZ-JV. Tako korenita sprememba smeri in gradientov gladine na stičnem območju, ki se gibljejo okoli 0,01 nakazujejo, da je prepustnost sedimentov relativno nizka. Od tod izhaja, da je bilančno gledano prispevek napajanja podzemne vode iz območja Goričkega na območje Prekmurskega polja relativno majhen.

Na dan meritev fizikalno–kemijskih parametrov podzemne vode, je znašala povprečna temperatura zraka na meteorološki postaji Murska Sobota

Tabela 1. Fizikalno–kemijski parametri podzemne vode in njena gladina izmerjena 25. 4. 2014.
Table 1. Groundwater's physicochemical parameters and groundwater level, measured 25. 4. 2014.

	Lokacija / Location	GKX	GKY	Kota ustja (m.n.v.) / Well construction elevation (m.a.s.l.)	Globina do podzemne vode / Groundwater depht (m)	Kota gladine podzemne vode (m.n.v.) / Groundwater elevation (m.a.s.l.)	Globina vodnjaka / Well depth (m)	pH	Elektroprevodnost / Electrical conductivity (µS/cm)	Temperatura vode / Water temperature (°C)
Južni rob Goričkega / Southern edge of Goričko	Bodonci	176821	585466	240,25	16,75	223,50	20	6,8	282	13,8
	Šalamenci 1	176809	585906	247,10	23,90	223,20	36	7,1	422	14,0
	Šalamenci 2	176607	586087	235,65	13,70	221,95	17	7,0	1492	13,0
	Vaneča	176773	589237	242,40	1,40	241,00	4	7,0	201	13,7
	Sebeborci	175197	591929	230,20	8,30	221,90	17	7,1	441	13,7
Severni rob Prekmurskega polja / North edge of Prekmursko polje	Strukovci	174023	581487	205,32	1,65	203,67	6	7,3	785	13,3
	Puževci	174050	582791	206,37	3,60	202,77	7	7,4	1516	13,7
	Brezovci	173899	585838	201,70	2,20	199,50	7	7,1	534	13,2
	Puconci	173714	588952	204,00	2,65	201,35	5	7,2	454	13,6
	Martjanci	172001	591441	194,60	2,80	191,80	6	7,3	331	13,1
	Tešanovci	171091	596401	184,50	4,60	179,90	6	7,1	496	12,5
	Bogojina	170940	598307	184,50	2,20	182,30	4	6,7	852	13,2
Merilna mesta ARSO / Sampling location ARSO	Skakovci	173930	580300	206,10	1,75	204,35	/	/	/	/
	Nemčavci	171380	590400	193,43	3,75	189,68	/	/	/	/
	Murski Petrovci	169700	580520	201,79	2,85	198,94	/	/	/	/
	Rankovci	170600	583050	198,29	1,59	196,70	/	/	/	/
	Krog	167090	587680	189,99	2,61	187,38	/	/	/	/
	Lipovci	165060	594540	180,89	2,26	178,63	/	/	/	/

– Rakičan 14,2 °C (Internet 3). Terenske meritve fizikalno–kemijskih parametrov so pokazale, da se vode zelo razlikujejo (Tabela 1). Najvišje vrednosti elektroprevodnosti so bile izmerjene v vodnjaku Puževci (1516 µS/cm), sledi mu vodnjak Šalamenci 2 (1492 µS/cm). Dokaj visoke vrednosti elektroprevodnosti so prisotne tudi v nekaterih drugih vodnjakih (Bogojina in Strukovci) in kažejo na onesnaženje, katerega izvor sta najverjetneje kmetovanje in pridelava ohišnice. Povprečna temperatura in pH vrednost podzemne vode, znašata 13,4 °C in 7,1.

Sklep

Na podlagi hidrogeološkega kartiranja smo na območju prehoda med Goričkim in Prekmurskim poljem izdelali podrobno karto gladin podzemne vode. S pomočjo te kartesmo potrdili hipotezo, da se podzemna voda severnega dela Prekmurskega polja napaja z Goričkega. Glede na prostorsko porazdelitev gladine podzemne vode ocenjujemo, da je bilančni prispevek tega dotoka relativno majhen. Zaradi vertikalnega in horizontalnega izmenjavanja sedimentov različne zrnavosti in s tem prepustnosti, se pojavljajo različne hidrodinamsko pogojene vodonosne strukture, od odprtih do polzaprtih vodonosnikov. Kakšno je medsebojno hidravlično razmerje podzemne vode v njih še ni znano. V zvezi s hidrogeološkimi razmerami na obravnavanem območju ostaja vrsta vprašanj še odprtih.

Do nadaljnjega ostaja odprto tudi vprašanje, ali površinski vodotoki vodonosnikom predstavljajo hidravlično mejo in v kakšni meri napajajo podzemno vodo. V prispevku smo takšno vlogo vodotokov le predpostavili, ker je bila gostota opravljenih meritev gladin podzemne vode v prostoru premajhna, da bi omogočila zanesljiv izris gladin podzemne vode.

Navkljub analizi vseh razpoložljivih podatkov, brez dopolnilnih raziskav, ki bodo vključevale vrtanje dodatnih opazovalnih vrtin ter geofizikalne raziskave, podrobnejše interpretacije hidrogeoloških razmer na obravnavanem območju, ni mogoče podati. K razjasnitvi vprašanj in izračunu vodne bilance bi veliko prispeval tudi matematični model toka podzemne vode, katerega zanesljivost je pogojena z dobrim 3D geološkim modelom in nizom podatkov za njegovo umerjanje.

Zahvala

Zahvaljujemo se Aleksandru Bokanu iz podjetja Geovrtina, d.o.o. za posredovane podatke in sodelavcu Dejanu Šramu, za pomoč pri obdelavi podatkov v programu ArcGIS. Prispevek je bil deloma pripravljen v okviru aktivnosti programske skupine »Podzemne vode in geokemija« P-0020, ki jo financira Javna agencija za raziskovalno dejavnost RS. Hvala tudi dr. Nini Rman za natančen pregled članka ter konstruktivne predloge za izboljšanje članka.

Literatura

Beguš, T., Sotlar, K., Hoblaj, R. & Brenčič, M.: Geološka spremljava izgradnje predora Stanjevci. Geologija, 45/2: 305–310, doi:10.5474/geologija.2002.024.

Brenčič, M. 2003: Hidrogeološko poročilo za potrebe izdelave obratovalnega monitoringa na odlagališču Puconci (neobjavljeno poročilo). Ljubljana, Arhiv GeoZS: 5 str.

Brenčič, M. 2006: Hidrogeološka interpretacija monitoringa gladin podzemne vode na odlagališču Puconci za leto 2005 (neobjavljeno poročilo). Ljubljana, GeoZS: 14 str.

Brenčič, M. 2008: Hidrogeološko poročilo za potrebe izvajanja monitoringa podzemne vode na območju sortirnice odpadkov CERO Puconci (neobjavljeno poročilo). Ljubljana, Arhiv GeoZS: 27 str.

Brenčič, M. 2009: Podzemna voda. V: Pleničar, M., Ogorelec, B. & Novak, M. (ured.): Geologija Slovenije, 543–552.

Ciglar, K. 1975: Poročilo o geoloških raziskavah kremenovega proda in peska Puconci 1974 (neobjavljeno poročilo). Ljubljana, Arhiv GeoZS: 272 str.

Ciglar, K. & Filipič, Š. 1987: Kremenov pesek in prod Puconci. Geologija, 30: 333–342.

Čarman, M. 2014: Bočno razširjanje kot posebna oblika gibanja tal na območju Doline v občini Puconci. Geologija, 57/1, 63–70, doi:10.5474/geologija.2014.007.

Drobne, F. 1989: Tehnološko-ekološki projekt za ureditev sanitarnega deponiranja komunalnih odpadov pri Puconcih (neobjavljeno poročilo). Geološka in hidrogeološka presoja. Ljubljana, Arhiv GeoZS: 2 str.

ESRI 2014: ArcGIS Desktop: Release 10. Redlands, CA: Environmental Systems Research Institute.

Gams, I. 1959: Geomorfologija in izraba tal v Pomurju. Geološki zbornik, 5: 205–251.

Gosar, A. 1996: Modeliranje refleksijskih seizmičnih podatkov za podzemno skladiščenje plina v strukturah Pečarovci in Dankovci - Murska depresija. Geologija, 37/38 (1994/95): 483–549, doi:10.5474/geologija.1995.019.

Jelen, B. & Rifelj, H. 2011: Površinska litostratigrafska in tektonska strukturna karta območja T-JAM projekta, Severovzhodna Slovenija., GeoZS, http://www.geo-zs.si/UserFiles/677/Image/Karte_nasl/15062012_dmv.pdf

Kralj, P. 1979: Hidrogeolgija severnega dela Murskega polja. Diplomska naloga, Univerza v Ljubljani, VTO Montanistika, Odsek za geologijo, Ljubljana: 61 str.

Kralj, Po. 1999: Apofilit iz zgornjepliocenskih vulkanoklastitov Grada v severovzhodni Sloveniji. Geologija, 42: 151–158, doi:10.5474/geologija.1999.009.

Kralj, Po. 2003: Geochemistry of Upper Pliocene silty and sandy sediments from the well Mt-7, Moravci Spa, North-Eastern. Geologija, 46/1: 117–122, doi:10.5474/geologija.2003.011.

Mali, N. & Hötzl, M. 1990: Hidrogeološke in hidrogeokemične raziskave podtalnice na območju SOB Lendava med reko Muro in Ledavo (neobjavljeno poročilo). Ljubljana, Arhiv GeoZS, 10 str.

Mihorko, P. & Gacin, M. 2014: Ocena kemijskega stanja podzemnih voda v Sloveniji v letu 2013. Ljubljana, ARSO.

MOP – GURS, 2011: Digitalni model višine 5 × 5 m. Ljubljana.

Novak, D. 1966: Hidrogeološke razmere v območju nahajališča kremenovega peska v Puconcih (neobjavljeno poročilo). Ljubljana, Arhiv GeoZS, 9 str.

Pleničar, M. 1954: Obmurska naftna nahajališča. Geologija, 2: 36–93.

Pleničar, M. 1970: Osnovna geološka karta SFRJ 1:100.000. Tolmač za list Goričko in Leibnitz (L 33-45) Beograd: Zvezni geološki zavod, Beograd: 52 str.

Prestor, J., Urbanc, J., Janža, M., Meglič, P., Šinigoj, J., Hribernik, K., Komac, M., Strojan, M., Bizjak, M., Feguš, B., Brenčič, M., Krivic, M., Kumelj, Š., Požar, M., Hötzl, M., Sušnik, A., Benčina, D., Kranjc, M. & Gacin, M. 2006: Nacionalna baza hidrogeoloških podatkov za opredelitev teles podzemne vode Republike Slovenije (neobjavljeno poročilo). Geološki zavod Slovenije, 27 zvezkov. http://prenit.geo-zs.si/IstraHidro/images/Povezave/3-Metodologija.pdf

Rman, N., Lapanje, A. & Rajver, D. 2012: Analiza uporabe termalne vode v severovzhodni Sloveniji. Geologija, 55/2: 225-242, doi: doi:10.5474/geologija.2012.014

Yang, C., Kao, S., Lee, F. & Hung, P. 2004: Twelve Different Interpolation Methods: A Case Study of Surfer 8.0. International archives of photogrammetry remote sensing and spatial information sciences, 35/2: 778–785.

Žlebnik, L. 1974: Hidrogeološke razmere v Nuskovi na Goričkem. Geologija, 17: 477–491.

Internetni viri:

Internet 1: Atlas okolja. http://gis.arso.gov.si/ (4. 11. 2015)

Internet 2: http://vode.arso.gov.si/hidarhiv/pod_arhiv_tab.php (26. 4. 2014)

Internet 3: http://meteo.arso.gov.si/ (26. 4. 2014)

GEOLOGIJA *58/2*, 183–194, Ljubljana 2015

http://dx.doi.org/10.5474/geologija.2015.014

Assessment of nitrate transport in the unsaturated (coarse gravel) zone by means of tracing experiment (Selniška dobrava, Slovenia)

Ocena transporta nitrata v nezasičeni coni prodnega vodonosnika s sledilnim poskusom (Selniška dobrava, Slovenija)

Nina MALI & Anja KOROŠA

Geological Survey of Slovenia, Dimičeva ul. 14, SI–1000 Ljubljana, Slovenia;
e-mail: anja.korosa@geo-zs.si

Prejeto / Received 9. 11. 2015; Sprejeto / Accepted 17. 12. 2015; Objavljeno na spletu / Published online 30. 12. 2015

Key words: nitrate transport, unsaturated zone, lysimeter, coarse gravel aquifer, tracing experiment
Ključne besede: transport nitrata, nezasičena cona, lizimeter, prodnati vodonosnik, sledilni poskus

Abstract

Nitrate pollution in groundwater, originating mainly from agricultural activities, remains a worldwide issue. This is also pertinent to Slovenia, where nitrate leaching from agricultural areas is one of the major groundwater resource management problems. The contamination spread in the aquifer is directly related to the hydraulic properties of the upper, unsaturated and the lower, saturated zone. The article presents study of water and nitrate pollution transport in the unsaturated zone in a field laboratory – lysimeter in Selniška dobrava. Water and nitrate transport parameters were estimated by a combined tracing experiment with deuterated water and $Ca(NO_3)_2$. Deuterium was used as a conservative tracer of water movement, and $Ca(NO_3)_2$ was used as a nitrate tracer in the unsaturated zone. The δ^2H and nitrate concentrations in the unsaturated zone water were measured monthly during the period from April 2006 to July 2007. All together 36 samplings were performed. The fastest and dominant flow velocities were calculated based on injection time, the first tracer appearance time, and the time of highest concentration. Mean flow velocity and vertical dispersion were estimated by an analytical best-fit method using the one-dimensional convection–dispersion model. The results were used to estimate the nitrate transport parameters in the coarse gravel aquifer Selniška dobrava. They can be used also for nitrate transport estimations in other aquifers with similar hydrogeological characteristics and can serve as a base for determining the measures for nitrate reduction in groundwater.

Izvleček

Onesnaženje podzemne vode z nitratom, ki izvira predvsem iz kmetijske dejavnosti, še vedno ostaja v svetu velik problem. To velja tudi za Slovenijo, kjer je spiranje nitrata iz kmetijskih površin eden glavnih problemov pri upravljanju z viri podzemne vode. Širjenje onesnaženja v vodonosniku je neposredno povezano s hidravličnimi lastnostmi zgornje nezasičene in spodnje nasičene cone. Članek predstavlja študijo prenosa vode in onesnaženja z nitratom v nezasičeni coni v terenskem laboratoriju - lizimetru v Selniški dobravi. Prenos vode in nitrata smo ocenili s kombiniranim sledilnim poskusom z uporabo devterijeve vode in $Ca(NO_3)_2$. Devterijevo vodo smo uporabili kot konzervativno sledilo, $Ca(NO_3)_2$ pa smo uporabili kot sledilo nitrata. V vodi nezasičene cone smo mesečno merili δ^2H in koncentracije nitrata v obdobju od aprila 2006 do julija 2007. Opravili smo 36 vzorčenj. Najhitrejše in dominantne hitrosti toka smo izračunali na podlagi časa injiciranja, prvega pojava sledila in časa pojava najvišjih koncentracij. Povprečno hitrost toka in vertikalno disperzijo smo ocenili z analitično metodo, z uporabo enodimenzionalnega konvekcijsko-disperznega modela. Rezultate smo uporabili za oceno parametrov transporta nitrata v vodonosniku s podobnimi lastnostmi, visoko prepustnem vodonosniku Selniška dobrava. Rezultati raziskave se lahko uporabijo za oceno transporta nitrata tudi na drugih vodonosnikih s podobnimi hidrogeološkimi pogoji in lahko služijo kot osnova za določitev ukrepov za zmanjšanje pojavov nitratov v podzemni vodi.

Introduction

It is well known that groundwater contamination from agricultural nonpoint sources is one of the major pollution problems (Lockhart et al., 2013; Wang et al., 2013; Lopez et al., 2015), often occurring as the result of anthropogenic activities, lack of management, and over-exploitation of groundwater resources (Pisciotta et al., 2015). Excess nitrogen from agricultural fertilizers and manure poses a significant environmental issue (Kronvang et al., 2009; Refsgaard et al, 2015), pertaining also to Slovenia, where nitrate leaching from agricultural areas is one of the major groundwater resource management problems. In the last few decades in Slovenia, nitrate concentrations in granular

aquifers on same places have increased, mainly as a consequence of the agricultural application of manure and fertilizers (EARS, 2014). The excessive use of chemicals and fertilizers increases the risk of groundwater pollution. Thus, the prevention of contamination is the primary strategy of water quality management (Ceplecha et al., 2004).

The prevention, control and combat of groundwater pollution are addressed in various European Union (EU) and national legislative acts (Pisciotta et al., 2015). The EU Water Framework Directive (EC, 2000), WFD, and its daughter Directive on the Protection of groundwater against Pollution (EC, 2006), GWD, establish criteria for the characterization of groundwater status (quality and quantity). Regarding nitrates, GWD sets the quality standard for assessing groundwater chemical status at 50 mg/l. Moreover, the Nitrates Directive (EEC, 1991) is an integral part of the WFD and it was drawn up with the specific purpose to reduce water pollution caused by nitrates from agricultural sources, and to prevent further pollution from nitrates. EU members are required to identify waters affected by nitrate pollution and designate nitrate vulnerable zones. Slovenia acknowledged this directive with a national regulation The Water Act (Official Gazette, 67/2002, 110/2002, 2/2004, 41/2004, 57/2008, 57/2012), and the Regulation on the protection of waters against pollution caused by nitrates from agricultural sources (Official Gazette, 113/09, 5/13, 22/15).

Nitrogen is a widely used plant nutrient, which is essential for the growth and development of a healthy crop. Excessive application of nitrogen fertilizers can lead to significant nitrate leaching out of the root zone, because plant uptake and microbial immobilization cannot remove the entire nitrate from the solution (Pratt & Adriano, 1973). Nitrate is not actively absorbed by roots and has a high potential to move downwards. So the amount of nitrate lost is dependent on the quantity of nitrate available to be leached. Other factors affecting nitrate leaching are the precipitation-intense rainfall events or surplus of water provided by irrigation, evapotranspiration, drainage, soil texture, soil porosity, occurrence of preferential flow paths, etc. (Wu et al., 1997; Cameria et al., 2003).

Since nitrate is soluble, it has high mobility and is thus easily leached from the unsaturated zone (Vinod et al., 2015). So, the spread of contamination in the aquifer is directly related to the hydraulic properties of the upper unsaturated and lower saturated zone (Seiler & Zojer, 2001). In order to solve this problem it is very important to determine the hydraulic properties of materials in the unsaturated zone and pollutant transport through the unsaturated zone. The unsaturated zone largely controls groundwater recharge by retaining precipitation, while at the same time providing preferential flow paths for infiltration (Kerziminska et al., 2014). The determination of unsaturated zone properties is an important point to be tackled for an advanced understanding of hydrological systems. The residence time of water and its distribution within the aquifer may help to define the vulnerability of the groundwater system (Schwientek et al., 2009). Furthermore, it presents the time span provided for attenuation processes (dispersion, diffusion, and sorption). Therefore, it is crucial for scientific studies and for water resources management to know the transport characteristics and velocities within the investigated system (Schwientek et al., 2009).

Nitrate transport was studied with tracer experiments using a lysimeter facility in the Selniška dobrava aquifer, which lies in the north-east of Slovenia. The aim of this study was to describe the nitrate transport processes in a high-permeable coarse gravel unsaturated zone by means of a tracing experiment. The lysimeter was designed on the basis of previous hydrogeological investigations in the area (Mali et al., 2007). A combined tracing experiment was performed using both deuterated water and calcium nitrate as fertilizer. Conservative tracers are necessary to obtain groundwater transport properties. Deuterated water is known as a very useful tracer for this purpose (Becker & Coplen, 2001; Mali et al., 2007) due to its conservative behavior. Moreover, deuterated water is easy to handle, simple to analyse, non-toxic, and has a reasonable price. Compared to other groundwater tracers, deuterium shows the highest degree of conservativeness (Leis & Benischke, 2004), therefore it was chosen to study water movement.

The EU WFD (EC, 2000) requires an additional reduction of nitrate load, which will be very costly for the agricultural sector. To improve the groundwater quality status of groundwater bodies at risk, measures must be taken. For this purpose, it is necessary to determine the mass balance of nitrogen from the application to their occurrence in groundwater. The objective of this study was to determine the nitrate transport properties and velocity through the unsaturated zone of a gravel aquifer Selniška dobrava with a tracing experiment. One of the aims is to specify parameters of nitrate transport in coarse gravel unsaturated zone which will be used to model nitrate transport in other aquifers with similar hydrogeological characteristics such as for example Dravsko polje, which was declared as a water body at risk due to the presence of nitrate.

Material and methods

Lysimeter area description

The lysimeter is located in the area of the principal aquifer of Selniška dobrava, in the north-east of Slovenia (Fig. 1) (X = 5154641, Y = 5536401 according to Gauss–Krüger). The main aquifer Selniška dobrava can be classified as an intergranular aquifer of high permeability (Mali

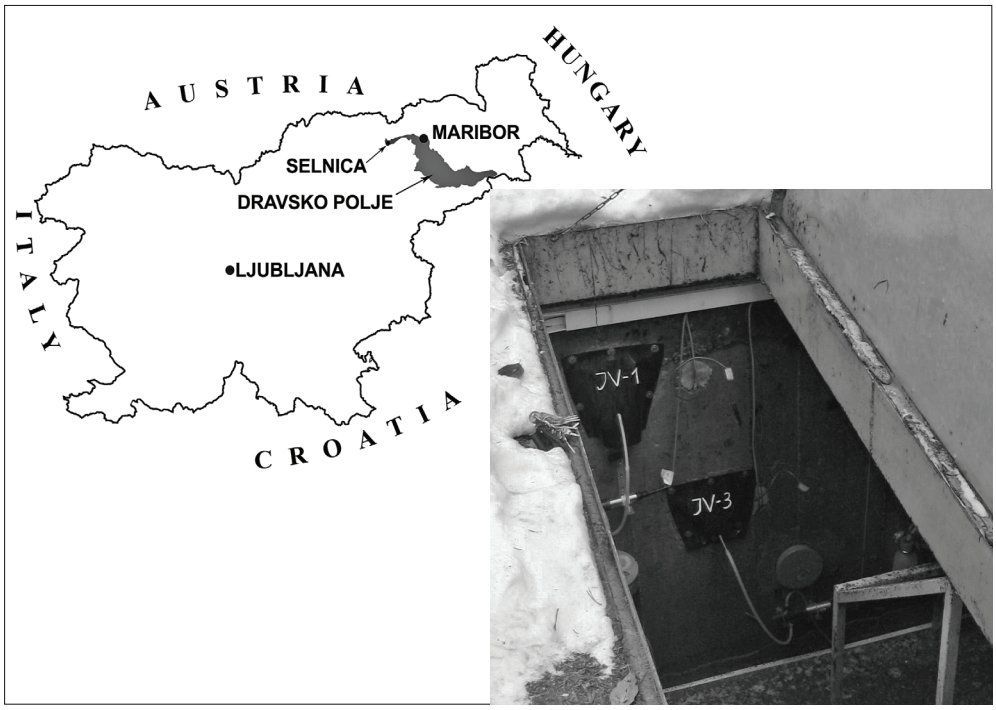

Fig. 1. Study area location
Sl. 1. Območje raziskav

et al., 2005; Mali, 2006). The thickest coarse gravel deposit is estimated at about 50 m. Thickness of unsaturated zone is specified from 25 to 37 m on the average. Thickness of the saturated layer along the aquifer is estimated at 7-14 m, and even more in the deepest sections (Mali et al., 2005; Mali, 2006). The hydraulic conductivity of the coarse gravel aquifer is estimated to be 5×10^{-3} m/s (Mali & Janža, 2005). The area has a moderate continental climate of central Slovenia with a typical continental precipitation regime and an average annual rainfall between 1200 and 1300 mm. The average annual air temperature lies between 8 and 12 °C (Mali & Janža, 2005).

The larger area of the lysimeter location is covered by mixed forest. The soil at this location was defined as distric cambisol (Gosar, 2000). The hydraulic conductivity of the soil was estimated at 1.5-4.5 × 10^{-5} m/s by double ring infiltrometer method (Mali, 2006). The gravel at lysimeter location consists of metamorphic rock and carbonates (limestone, marble-sandstone, marble and agglutinated carbonate gravel). In places, the gravel is incrusted by calcite. Based on granulometric analyses the hydraulic conductivity of the coarse gravel was estimated at 2.9×10^{-3}–6.9×10^{-2} m/s (Mali, 2006).

Experimental set-up

The lysimeter site is designed as a field laboratory (Fig. 2). Dimensions are 2 m × 2 m, 5 m deep, with walls 0.2 m thick. There are 10 sampling and measuring points at different depths (from JV-1 to JV-10) with approximately equal distances by depth. For groundwater sampling in the unsaturated zone drainage samplers connected to a water sampling system were installed (Mali, 2006). A detailed description of the lysimeter is in previously published papers (Mali et al. 2007; Mali & Urbanc, 2009).

Deuterium and nitrate tracing experiment

The tracing experiment was performed in 20th of April 2006 after a period of intensive snow melting. Water and nitrate transport processes were assessed by a combined tracing experiment with deuterated water and calcium nitrate ($Ca(NO_3)_2$). Deuterium was used as a conservative tracer of water movement, and $Ca(NO_3)_2$ was used as a tracer of nitrate in an unsaturated zone. Before tracer injection, irrigation with groundwater was performed to reach good field capacity. 1.2 kg of $Ca(NO_3)_2$ and 1000 ml of D_2O (70%) were dissolved in 50 l of pumped groundwater in barrel and injected by sprinkler irrigation. After injection the tracer was again splashed by irrigated groundwater. The area of irrigation was 9.5 m^2. The distribution of the artificial rainfall was controlled by 10 precipitation measuring points. The average amount of irrigated water was 50 mm.

Sampling and analytical methods

The δ^2H values and nitrate concentrations in the unsaturated zone water were measured monthly during the period from April 2006 to July 2007. During the first period, samples were collected at 14-day intervals, and then the sampling period was extended to one month. All together 36 samplings were performed.

Measurements for δ^2H were carried out in the laboratory of Joanneum Research Forschungsgesellschaft mbH, Institute of Water Resources Management, Hydrogeology and Geophysics, and chemical analyses of samples for nitrate were carried out in laboratory of Water Supply Company Vodovod-Kanalizacija from Ljubljana.

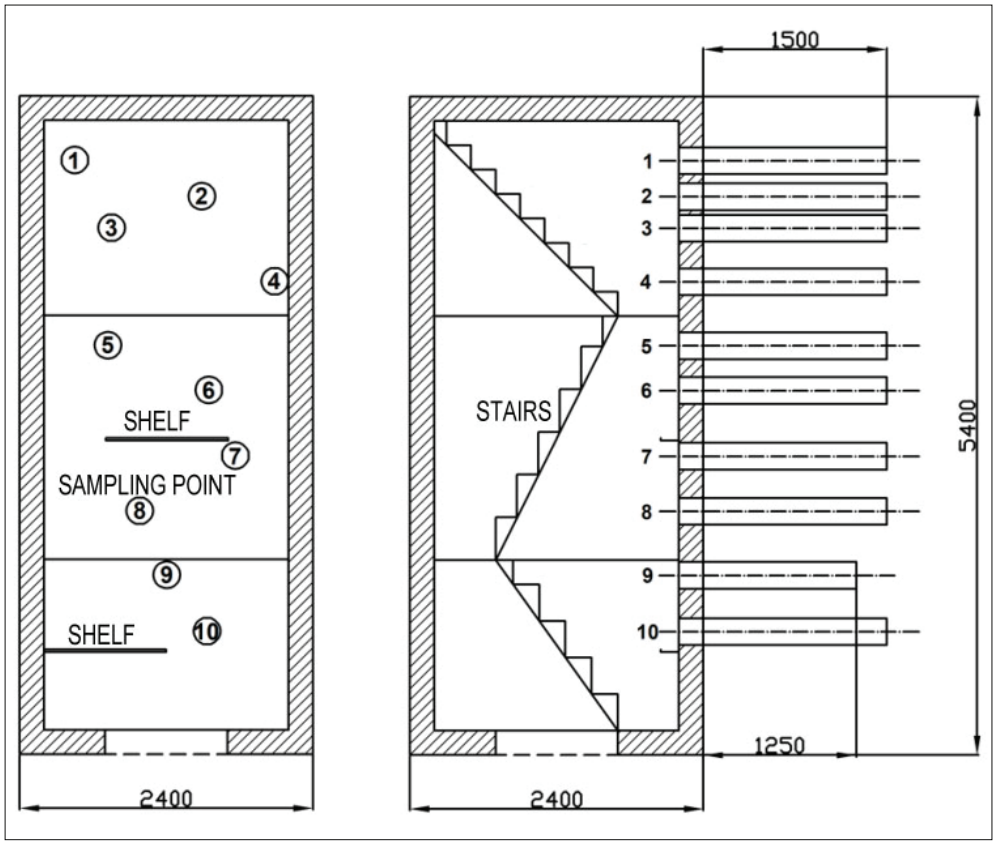

Fig. 2. Lysimeter cross-section
Sl. 2. Prerez lizimetra

Deuterium was measured in continuous flow mode by chromium reduction using a ceramic reactor slightly modified from Morrison et al. (2001). A high temperature oven (HEKAtech, Germany) was fitted with a EuroAS 300 liquid auto sampler (EuroVector, Italy). The elemental analyzer (EA) was configured with a Cr packed reactor held isothermally at 1050 °C. Water samples contained in 2 ml capacity septa-sealed vials were placed on the carousel of the liquid auto sampler which was fitted with a 10µl injection syringe (SGE Europe). A sequence of one wash cycle of 3.5 µl volume was carried out for each sample prior to injection into the Cr reactor. Water samples were injected into a septa-sealed injector port. The resulting water vapour was flushed into the reactor by the carrier helium gas via a 1-mm-i.d. stainless steel probe extending into the ceramic reactor tube (Al_2O_3). A sample size of 1.4 µl of water was used for the analysis. Water injected into the reactor was reduced by Cr, resulting in the quantitative conversion to hydrogen gas according to Eq 1.

$$2Cr_{(s)} + 3H_2O_{(l)} = Cr_2O_{3(s)} + 3H_{2(g)} \quad (1)$$

The H_2 generated in the Cr reactor was carried in the He stream through the GC column to an open split sampling capillary and into the source of a Finnigan DELTA^{plus} continuous flow stable isotope ratio mass spectrometer.

Nitrate analyses were performed in an ISO 17025 accredited laboratory by ion chromatography according to ISO 14911:1998 standard. The apparatus was ion chromatograph Metrohm MIC-3, Switzerland, controlled by IC Net 2.3 SR4 software. Calibrations were made by Merck CertiPUR reference materials, Germany. QC control samples were purchased from Fluka, Switzerland. All necessary dilutions were made with ultra-pure water from the system Easypure LF, Barnstead/Thermolyne International, USA. The working range was from 2.2 mg/L to 110 mg/L (as NO_3^-). Nitrate in the analysis is expressed as NO_3-N concentrations. For evaluation of breakthrough curves NO_3-N concentrations were used.

Evaluation and interpretation of tracing tests

Based on the injection time, the first tracer appearance time, the time of highest concentration and the distance between the top of the lysimeter and the observation point, the fastest flow velocity and dominant flow velocity were calculated.

For the evaluation of breakthrough curves from a tracing test we used a best-fit method of the computer program TRACI'95 (1998). TRACI'95 was used to estimate the mean flow velocity and vertical dispersion. For analytical solution, the one-dimensional convection–dispersion model with standardizing values for single porosity was chosen.

$$C_{fN}(x,t) = \frac{C_f(x,t)}{C_N(x,t)} = \sqrt{\left(\frac{t_N}{t}\right)^3} \exp\left[\frac{1-\frac{t_N}{t}}{4t_N t_0}\left(P_D - \frac{t_N t}{P_D}\right)\right] \quad (2)$$

with boundary conditions:

$$C_f(0,t) = \frac{M}{Q}\,\delta(t)$$

$$C_f(\infty,t) = 0$$

$$C_f(x,t) = 0$$

Where C_f is the tracer concentration in water, C_N normalized concentration, t_0 mean transit time, t time variable, t_N time after injection when normalized concentration was observed, x is the distance between the injection and the observation point, P_D is a dispersion parameter, M is the mass of injected tracer and Q is the volumetric flow rate.

In the case of the multiple peak phenomena in breakthrough curves the Multi-Peak-Modus model was used.

Dispersion parameter P_D is related to the dispersion coefficient by:

$$P_D = \frac{D}{v.x} \tag{3}$$

where D is in this case the vertical dispersion coefficient and v the mean flow velocity.

Because the basis of the analytical best-fit model is the concentration of tracer (mg/m^3), the ‰ δ^2H values of results had to be converted. The mg/l concentrations of ^{2}H were calculated from the slightly modified equation published by Becker and Coplen (2001), taking into account the influence of water density (Mali et al., 2007).

$$Deuterium_{conc} = 34.721\left[\frac{1000 + \delta D_{VSMOW}}{1000}\right] \tag{4}$$

Results and discussion

Fig. 3 present breakthrough curves of both tracers with the precipitation amount for the entire sampling period. Both tracers were detected at all ten sampling points. The tracers occurred shortly after injection, within one day at almost all points. At some points the highest values were detected immediately after tracer injection (JV-1, JV-3, JV-4), and they are most likely a consequence of intensive irrigation at the time of injection or contamination. These values are not taken into account in further processing. At the first sampling point JV-1 that was the only peak of breakthrough curve, since which the values only decreased (Fig. 3). Therefore, this point is not included in further processing for determining transport parameters.

The precipitation data shows that several periods with heavy precipitation occurred during the tracing experiment (end of May 2006, in the middle of August and September 2006, and in February 2007). All these events were well identified in breakthrough curves of both tracers. Diagrams show that the high amount and intensity of precipitation (heavy rain events) are reflected in some measuring points (JV-5, JV-6, JV-7, JV-9) and have effect on δ^2H values and nitrate concentrations (Fig. 3), but not equally in all sampling points.

On the basis of tracing experiment results for both tracers the fastest and dominant flow velocities were calculated (Table 1, Table 3). Based on tracing experiment results, estimations of the mean flow velocity and vertical dispersion (Table 1, Table 3) were made by analytical best-fit method, using a one-dimensional convection-dispersion model with standardising values for single porosity. At some sampling points more breakthrough curve peaks were detected. In these cases, for the evaluation of tracing experiment results the Multi-Peak-Modus model was used (JV-3, JV-5, JV-6, JV-9, and JV-10) (Fig. 4, Fig. 5).

Deuterium

The highest values of deuterium among all sampling points occurred in JV-1 (4670‰) immediately after injection. If we do not take into account the value of the first day, the maximum value detected in JV-1 was 1305‰ and in JV-3 1139‰. As in JV-3, the highest values in JV-2 (212‰), JV-4 (659‰) and JV-5 (509‰) were observed at the end of May, but in a different order of magnitude. In this period the highest concentrations were also observed in sampling points JV-9 (284‰) and JV-10 (175‰) at the bottom of the lysimeter. In both sampling points more peaks in the deuterium breakthrough curves were recorded in August 2006 and February 2007. The maximum value in JV-6 (159‰) was detected in September 2007, while in JV-8 at the end of November 2007. Finally, there was a maximum value at sample site JV-7 in February 2007, when the peaks in JV-9 and JV-10 were last registered. Different hydrogeological conditions at specific points result in a various occurrence and height of peaks at a certain time.

The fastest flow velocity (Table 1) increases with depth from 0.19 to 0.493 m/day. Due to the breakthrough of tracer at the time of irrigation, the fastest flow velocity was not calculated for JV-1, JV-2 and JV-3. Because of the different depth position of the sampling points and because of the detection of tracer at the same sampling time it seems that velocity increases with depth. Irrespective of this, it is important for the estimation of the fastest flow velocity to assess the probability of fastest pollution effect on the aquifer through the unsaturated zone.

The dominant flow velocity is related to the time of the highest concentration (Käss, 1998). The graph of precipitation and δ^2H values shows

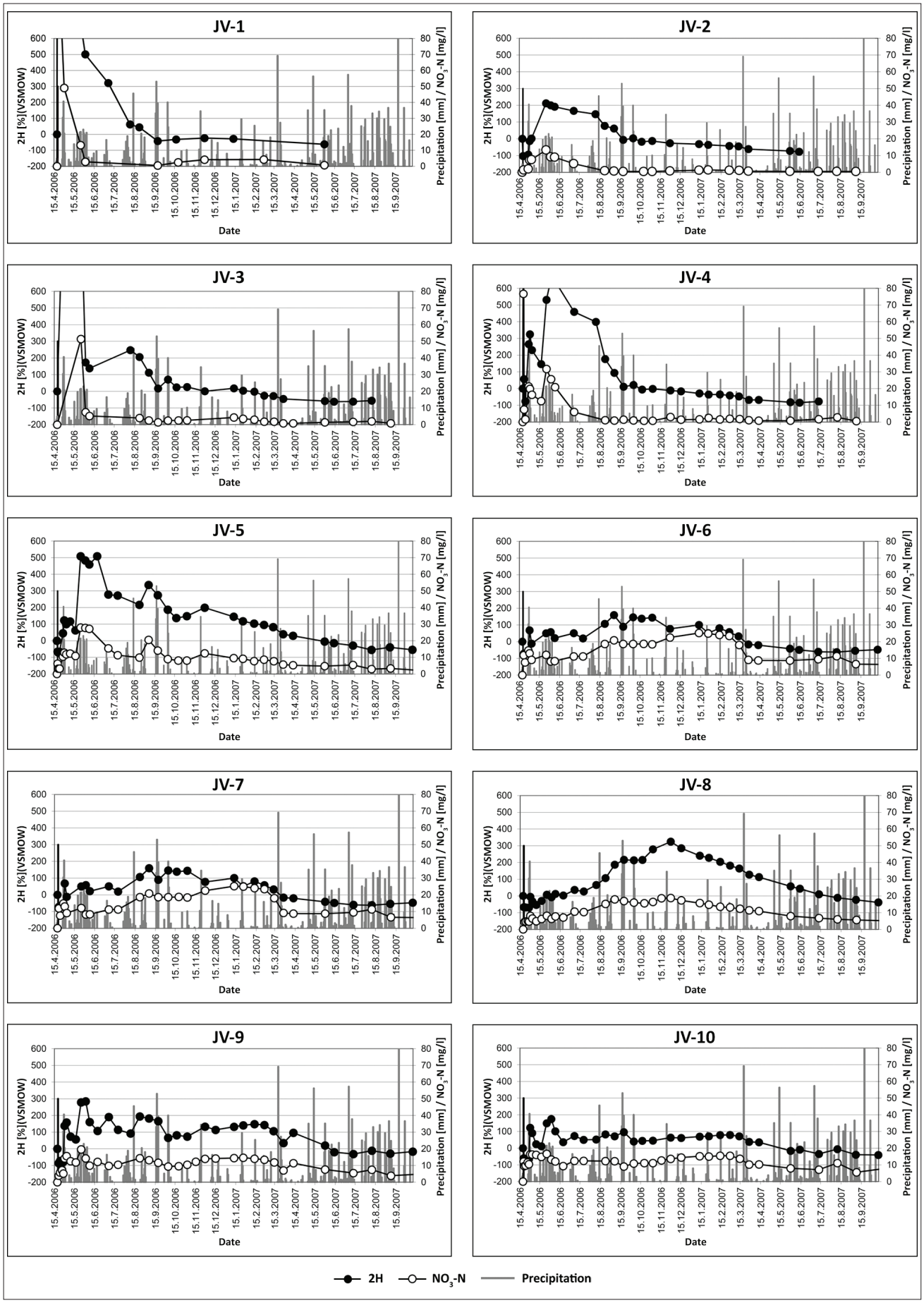

Fig. 3. Deuterium (‰) and nitrate (mg/l) breakthrough curves and precipitations (mm) during the tracing experiment.
Sl. 3. Devterijeve (‰) in nitratne (mg/l) krivulje pojavljanja sledila ter količina padavin (mm) v času sledilnega poskusa.

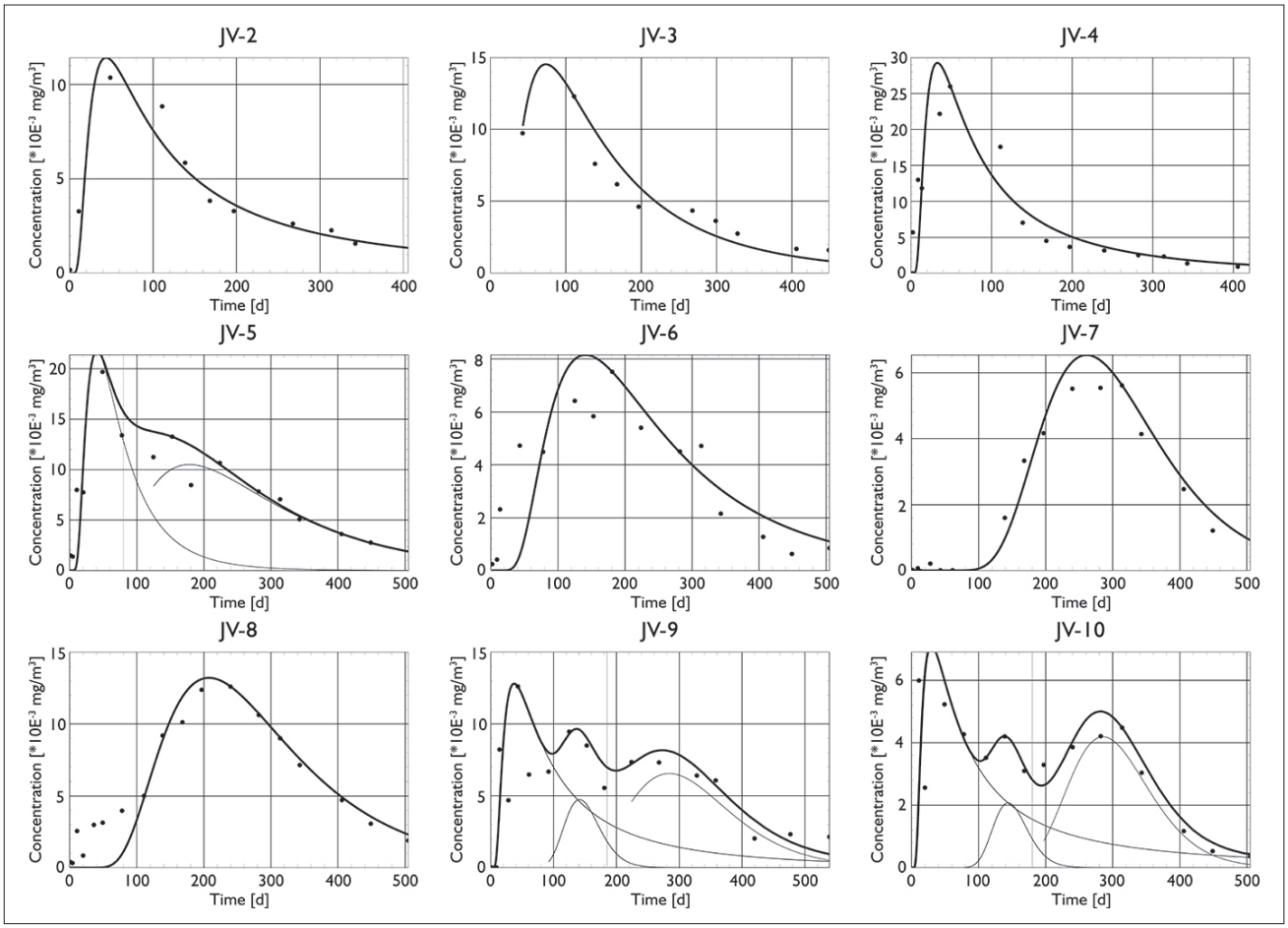

Fig. 4. Best fit curves for deuterium concentrations (10^{-3} mg/m^3).
Sl. 4. Modelirane krivulje koncentracij devterija (10^{-3} mg/m^3).

that also the occurrence of the highest δ^2H values coincides with the stronger precipitation event. The lowest values of dominant velocity occurred in JV-3 and JV-7 (0.010 m/d). JV-8 has a dominant flow velocity of 0.015 m/day, and JV-6 of 0.017 m/day, whereas at other sampling points dominant flow velocities range from 0.023 to 0.036 m/day (Table 1).

The best evaluation of the matrix water flow is the mean flow velocity (Table 1). In Fig. 4 the modeled best fit curves for estimation of deuterium mean flow velocity are presented. Through the entire lysimeter, mean flow velocities based on δ^2H values were estimated between 0.002 and 0.029 m/day. In the upper part of the lysimeter the estimated mean flow velocities were lower compared to the lower part. To a depth of 1.08 m they were in the range from 0.002 m/d (JV-2) to 0.006 m/d (JV-3). From the depth of 1.5 m (JV-4) to the bottom of the lysimeter, the calculated mean flow velocities were higher, between 0.007-0.029 m/d. The average value of the mean flow velocity is estimated at 0.012 m/d and corresponds to the previously published results (Mali, 2006).

The volume of discharge water in the drain systems was measured as the water volume in the water collector. During the winter, because of snow cover and frozen soil, there were no conditions for water flow in the unsaturated zone. So there was no outflow water from JV-1 up to including sampling point JV-7. However, from cumulative values of outflow water volume (Table 2) we can evaluate the discharge dynamics. From the initial injection to 12.7.2007 the outflow volume of the water at the deepest sampling point was 395l. The next most productive drain was JV-8 (167l). The deepest sampling drains discharge more groundwater from the unsaturated zone (JV-10, JV-9, and JV-8) than the upper sampling points (JV-1, JV-2, and JV-3) because of wider recharge area. In the gravel deposits deeper than 3m (JV-8, JV-9 and JV-10) vertical water flow exists all the time so we assume the field capacity was constantly high. Other points are affected more by dry conditions during periods of low precipitation and ground frost.

Tracer recovery was estimated based on outflow water volume and ^{2}H concentrations. Table 2 shows the quantities, percentages of recovered and injected deuterium tracer by the sampling points. Until the end of July 2007, 5101 mg of ^{2}H in the outflow water represents 3.64 % of the total injected tracer. The highest amounts of deuterium occurred at JV-10, JV-9, and JV-8 (1612 mg, 986 mg, and 874 mg), which accounts for 32 %, 19 %, and 17 % of the entire recovered tracer and 0.6-1.1 % of the total injected tracer. In the

Table 1. Fastest, dominant (dom.) and mean flow velocities (m/s) of deuterium tracer.
Tabela 1. Najhitrejša, dominantna (dom.) in srednja hitrost toka (m/s) devterijevega sledila.

		JV-2	JV-3	JV-4	JV-5	JV-6	JV-7	JV-8	JV-9	JV-10
Distance	m	0.820	1.080	1.580	2.040	2.41	2.95	3.4	3.93	4.390
Fastest f.	m/d	-	-	0.190	0.255	0.241	0.295	0.34	0.393	0.439
Dom. f.	m/d	0.023	0.010	0.036	0.034	0.017	0.01	0.015	0.032	0.029
Mean f.-1	m/d	0.002	0.006	0.010	0.025	0.009	0.01	0.012	0.021	0.015
Mean f.-2	m/d	-	-	-	0.007	-	-	-	0.026	0.029
Mean f.-3	m/d	-	-	-	-	-	-	-	0.012	0.014
Dispersion-1	m^2/s	0.003	0.002	0.011	0.013	0.005	0.002	0.005	0.066	0.108
Dispersion-2	m^2/s	-	-	-	0.002	-	-	-	0.002	0.097
Dispersion-3	m^2/s	-	-	-	-	-	-	-	0.002	0.001

Table 2. Cumulative outflow water volume (l) and recovery amount (%) of deuterium tracer.
Tabela 2. Skupni iztok vode (l) in delež (%) povrnjenega devterijevega sledila.

		JV-1	JV-2	JV-3	JV-4	JV-5	JV-6	JV-7	JV-8	JV-9	JV-10	Cumulative
outflow water volume	l	7.61	26.39	28.91	95.22	53.36	82.79	80.76	167.10	153.93	395.09	
amount of recovery tracer	mg	64.83	91.58	105.56	371.62	509.09	306.65	178.34	874.28	986.78	1612.64	5101.37
% of recovery tracer amount	%	1.27	1.80	2.07	7.29	9.98	6.01	3.50	17.14	19.34	31.60	100.00
% of whole amount of tracer	%	0.05	0.07	0.08	0.27	0.36	0.22	0.13	0.62	0.70	1.15	3.64

remaining sampling points tracer recovery values were between 64 mg and 509 mg accounting for 1.2–10 % of the total recovered tracer and 0.04–0.4 % of the initial amount of tracer injected.

Nitrate

Like deuterium, also nitrate was detected at all sampling points. From the breakthrough curves it appears that the nitrate behaves slightly differently from deuterium. Fig. 3 indicates that the nitrate breakthrough curves have several peaks. This is explained by the dependence on rainfall and vegetation activity which affects the nitrate content in the unsaturated zone. Even in zero sampling, different background concentrations of nitrate were detected. At lower sampling points, background concentrations reach also 12–19 mg/l (NO_3-N). Thus, in the diagrams the natural fluctuation of nitrate can be followed as a tracer. Like for deuterium, the highest concentration of nitrate was detected at JV-1 (134.4 mg/l NO_3-N) on the first day, and after that the concentrations fall. The next high concentration was recorded at JV-3 (51.4 mg/l NO_3-N) at the end of May. At that time the highest nitrate concentrations were reached also at sampling points JV-2 (13.3 mg/l NO_3-N), JV-4 (31.7 mg/l NO_3-N), and JV-5 (27.9 mg/l NO_3-N). At sample sites JV-9 (19.7 mg/l NO_3-N) and JV-10 (16.6 mg/l NO_3-N) the first peak appears at that time. The next two peaks followed at these sites in August 2006 and in February 2007. Nitrate concentrations at that time were 14.4–14.7 mg/l NO_3-N at JV-9, and 12.4–15.5 mg/l NO_3-N at JV-10. At sampling point JV-6 nitrate concentrations reach the first peak (20.8 mg/l NO_3-N) at the same time as deuterium reaches its maximum in September 2006. The next peak was documented in the end of January 2007 (25.2 mg/l NO_3-N). At sampling site JV-7 a completely different behavior of breakthrough curve was detected. In the first period we perceive a lower curve due to the higher background concentrations of nitrate. Elevated levels as a result of the tracer injection occurred until the end of 2006 and increase to the maximal recorded concentration of nitrate at JV-7 (28.1 mg/l NO_3-N) in April 2007.

Table 3 gives the estimates of water flow velocity obtained from the nitrate tracing data. Because the nitrate tracer appears immediately after injection because of contamination, we do not give the maximum velocity for JV-2 and JV-3. The evaluation for the fastest flow velocity of nitrate is the same as in deuterium at sampling points JV-4 (0.190 m/d) and JV-5 (0.255 m/d) (Table 3). At points JV-6 to JV-10 the estimation of nitrate flow velocity is slightly higher than in case of deuterium (0.301– 0.549 m/d).

The lowest dominant velocity of nitrate is determined at sampling points JV-6 and JV-7 (0.009 m/day) (Table 3). The highest dominant flow velocity, 0.036 m/day, is found at JV-4. Dominant velocities for other sampling points vary from 0.015 to 0.032 m/day (Table 2).

In Table 3 mean flow velocities for all recognized peaks of nitrate breakthrough curves are given. The mean flow velocities based on nitrate concentration breakthrough curves were estimated by analytical best-fit method (Fig. 5). For JV-2, JV-3, JV-5, JV-6, JV-9, and JV-10 the Multi-Peak-Modus model was used. Up to the depth of 1.08 m (JV-2, JV-3) the mean flow velocities are estimated at 0.003–0.019 m/d, on average 0.011 m/d. In JV-4 the mean flow velocity is 0.016 m/s. From sampling point JV-5 to JV-8 the mean flow velocities range between 0.008–0.12 m/d, on average 0.010 m/d. The highest mean flow velocities were calculated in the lower part of the lysimeter at JV-9 and JV-10. Tracer is moving between 0.014–0.197 m/d. Not considering

Table 3. Fastest, dominant (dom.) and mean flow velocities (m/s) of nitrate.
Tabela 3.Najhitrejša, dominantna (dom.) in srednja hitrost (m/s) toka nitrata.

		JV-2	JV-3	JV-4	JV-5	JV-6	JV-7	JV-8	JV-9	JV-10
Distance	m	0.82	1.08	1.58	2.04	2.41	2.95	3.4	3.93	4.39
Fastest f.	m/d	-	-	0.19	0.255	0.301	0.369	0.425	0.491	0.549
Dom. f.	m/d	0.02	0.026	0.036	0.032	0.009	0.009	0.015	0.028	0.023
Mean f.-1	m/d	0.019	0.019	0.016	0.01	0.011	0.008	0.012	0.117	0.197
Mean f.-2	m/d	0.003	0.004	-	0.01	0.009	-	-	0.03	0.015
Mean f.-3	m/d	-	-	-	-	-	-	-	0.014	
Dispersion-1	m^2/s	0.003	0.003	0.024	0.016	0.003	0.000	0.006	0.019	0.051
Dispersion-2	m^2/s	0	0	-	0.016	0	-	-	0.005	0.001
Dispersion-3	m^2/s	-	-	-	-	-	-	-	0.001	-

Table 4. Cumulative outflow water volume (l) and recovery amount (%) of nitrate tracer.
Tabela 4. Skupni iztok vode (l) in delež (%) povrnjenega nitratnega sledila.

		JV-1	JV-2	JV-3	JV-4	JV-5	JV-6	JV-7	JV-8	JV-9	JV-10	Cumulative
outflow water volume	l	7.61	26.39	28.91	95.22	53.36	82.79	80.76	167.10	153.93	395.09	
amount of recovery tracer	mg	46.87	59.61	102.19	503.40	607.87	360.45	289.05	965.45	725.18	1144.20	4804.27
% of recovery tracer amount	%	0.98	1.25	2.13	10.48	12.65	7.50	6.02	20.10	15.09	23.82	100.00
% of whole amount of tracer	%	0.02	0.03	0.05	0.25	0.30	0.18	0.14	0.47	0.35	0.56	2.35

the highest estimated mean flow velocities at JV-9 and JV-10, the average mean flow velocity is estimated at 0.013 m/d. We anticipate that these unrealistically high concentrations of first peak occurred due to high background concentrations.

Tracer recovery was estimated based on the outflow water volume and nitrate concentrations. Table 4 shows the quantities, percentages of recovered and injected tracer by the sampling points. Until the end of the tracing experiment (July 2007) 4804 mg of NO_3-N drained through the sampling system in the lysimeter, which is 2.35 % of the total injected tracer. The highest amounts of recovered nitrate were recorded at JV-8 and JV-10, 1144 mg and 965 mg NO_3-N, which accounts for 24 % and 20 % of the entire recovered tracer and 0.47-0.56 % of the total injewcted tracer. In the remaining sampling points tracer recovery concentrations were between 47 mg and 725 mg NO_3-N accounting for 0.98-15.09 % of the total recovered tracer and 0.02-0.35 % of the initial amount of tracer injected.

Discussion

A comparison of the deuterium and nitrate breakthrough curves shows that the results of deuterium and nitrate tracers give a similar distribution (Fig. 3). At sampling points JV-1, JV-5, JV-8, JV-9 and JV-10 breakthrough curves of deuterium and nitrate tracer have the same shape at the same time. A maximum concentration of nitrate at sampling points JV-4 and JV-5 coincides with the first higher increase in deuterium values during a period of high precipitation.

From the calculations of the fastest and dominant velocities for both tracers (Table 1 and Table 3), we can see that the results are comparable. The fastest average flow of nitrate in the unsaturated zone is estimated at 0.369 (0.019-0.549) m/day, and of deuterium 0.308 (0.019-0.439) m/day. An estimate of the strongest impact of pollution can be made on the basis of the dominant flow, which is calculated on the basis of the occurrence of the highest tracer concentrations. The dominant flow in the unsaturated zone for nitrate is estimated at 0.022 (0.009-0.036) m/day, and for deuterium at 0.023 (0.01-0.036) m/day. The highest values of the dominant flow were assessed in the middle of the lysimeter at sampling sites JV-4 and JV-5, where the highest concentrations were achieved between 40 and 50 days from the beginning of the experiment. At the bottom of the lysimeter the highest concentrations occurred between 230 and 313 days.

The long-term impact of pollution is estimated on the basis of the mean flow velocity (Käss, 1998). This is the velocity which determines the transfer of most of the tracer. The mean flow velocity calculations of both tracers show some differences (Table 1, Table 3). In breakthrough curves of nitrate several peaks could be recognized (Fig. 5), while the deuterium breakthrough curves are more homogeneous, with one peak (Fig. 4). The phenomenon is the consequence of the presence of nitrate in the natural environment of the lysimeter. The content of nitrate in the soil and in the unsaturated zone is linked to the vegetation activity in relation to the use of nitrogen in various stages of plant growth. Background levels of nitrate have an impact on an indicated nitrate concentration during the tracer experiment. As a result, the calculated mean flow velocities of nitrate are slightly higher than of deuterium. Given the fact that deuterium is the ideal tracer, according to the results of individual peaks analysis and taking into account background nitrate concentrations, it can be concluded that the retention times of both tracers are comparable. The estimation of

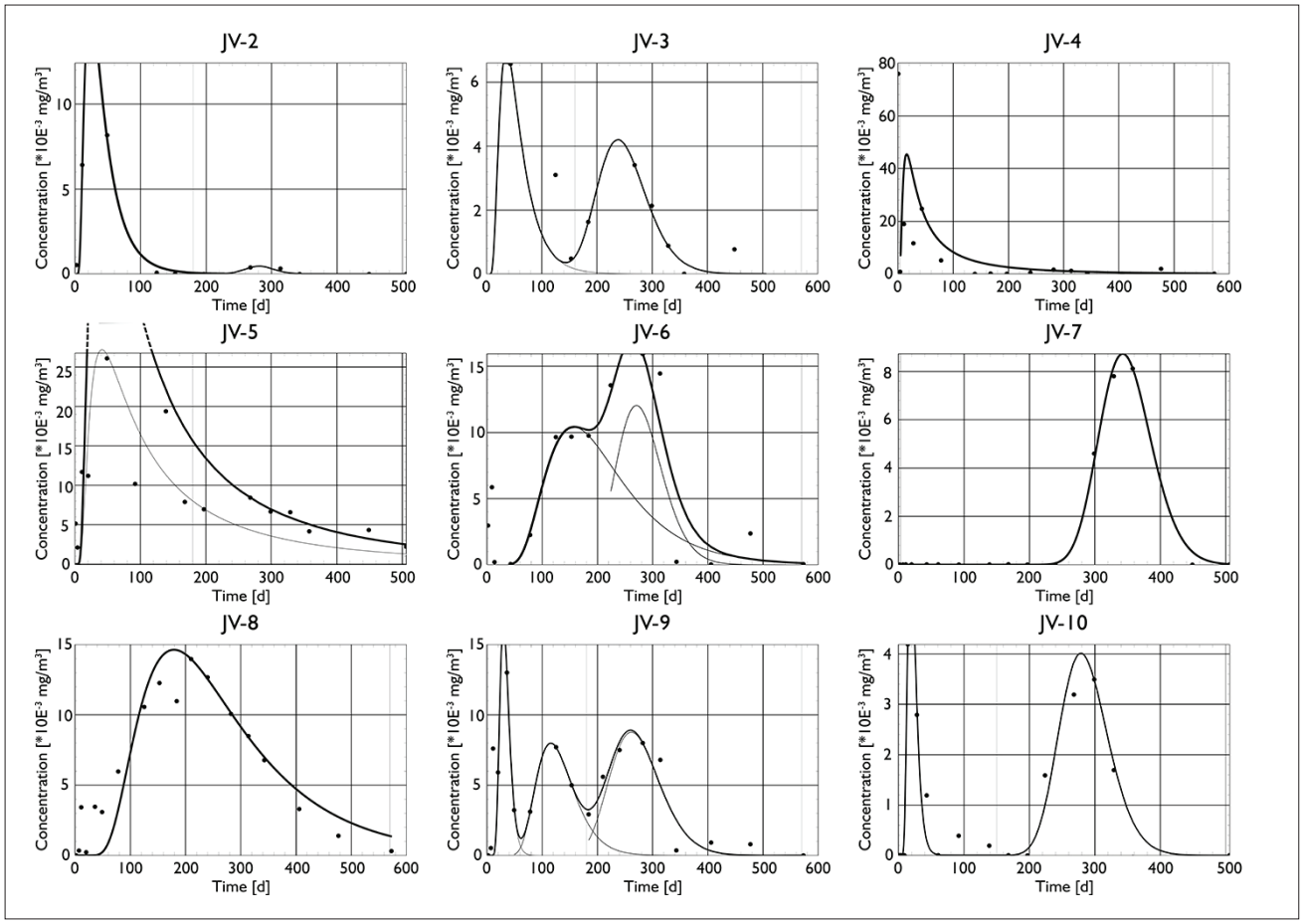

Fig. 5. Best fit curves for nitrate concentrations (10^{-3} mg/m^3)
Sl. 5. Modelirane krivulje koncentracij nitrata (10^{-3} mg/m^3)

the mean flow velocity for nitrate in coarse gravel unsaturated zone (the hydraulic conductivity 2.9×10^{-3}–6.9×10^{-2} m/s) is 0.0013 m/d.

The nitrate flow velocity in the unsaturated zone is important for assessing the impact of nitrogen excess from agriculture on groundwater. The problem is exceeded threshold nitrate concentrations at some places. The results of tracing experiment will be used in further modeling of nitrate transport in order to identify measures to improve groundwater quality status. Based on our results, some conclusions about transport of nitrate in Selniška dobrava can be made. The thickness of the unsaturated zone on lysimeter location reaches 27.5 m. If it is assumed that the ground water level is 27.5, average first speed of nitrate is 0.369 m/d the first contamination can reach the water in 74 days. Based on the average dominant flow velocity (0.022 m/d) the percolation time is 3.42 years. When the estimated mean flow velocity is 0.013 m/d, the time of pollution arrival is estimated at 5.80 years.

Conclusions

The aim of the tracing experiment in a lysimeter was to determine the characteristics of nitrate transport in the unsaturated zone. The results revealed that nitrate travels with almost the same dynamics as deuterium, which is used as a conservative tracer. The differences in results between individual points show local differences in the structure of the unsaturated zone, which affects different flow properties. Some differences between the two tracers' breakthrough curves were recognized. At the same sampling sites the nitrate breakthrough curves have more peaks. The phenomenon is the consequence of the presence of nitrate in the natural environment of the lysimeter. The content of nitrate in the soil and in the unsaturated zone is linked to the vegetation activity in relation to the use of nitrogen in various stages of plant growth. Background levels of nitrate have an impact on an indicated nitrate concentration during the tracer experiment.

Based on the results of the tracer experiment, the characteristics of nitrate flow dynamics through the coarse gravel unsaturated zone with a hydraulic conductivity in the range of 2.9×10^{-3} - 6.9×10^{-2} m/s were estimated. The evaluation for the fastest flow velocity of nitrate is 0.190–0.549 m/d, on average 0.369 m/d. The dominant flow of nitrate in the unsaturated zone is estimated at 0.022 (0.009–0.036) m/day. Calculations of the fastest and dominant velocities for both tracers are comparable, while the calculated mean flow velocities of nitrate are slightly higher than those of deuterium. Given the fact that

deuterium is the ideal tracer, according to the results of individual peaks analysis and taking into account background nitrate concentrations, it can be concluded that the retention times of both tracers are comparable. The estimation of the mean flow velocity for nitrate in our case is 0.013 m/d.

The purpose of determining the movement of nitrate through the unsaturated zone is also to assess the impact of nitrate pollution from agriculture on groundwater. If we assume an average thickness of the coarse gravel unsaturated zone at 27.5 m with a conductivity of about 5×10^{-3} m/s, as is the case in Selniški dobrava, we come to the following assessment of nitrate pollution movement:

- At an average fastest flow of 0.369 m/d, pollution reaches the groundwater level in 74 days.
- With the thickness of the unsaturated zone and the dominant velocity of 0.022 m/d, the percolation time is estimated at 3.42 years.
- The mean flow velocity in the matrix flow was estimated at 0.013 m/d. The mean residence time is estimated at 5.80 years.

The tracing experiment has again proved to be a very useful tool to assess the behavior of nitrate as the selected pollutant in the unsaturated zone. On the basis of the determined range of nitrate flow properties, the estimation of pollution influence on aquifer and groundwater measures can be provided. The results of tracing experiment will be used in further modelling of nitrate transport in order to identify measures for groundwater quality status improvement.

Acknowledgements

The study presented in the paper was carried out within the Research Programme Groundwater and geochemistry (P1-0020) and PhD work of A. Koroša financed by the Slovenian Research Agency (ARRS). Special thanks go to Primož Auersperger from Water Supply Company Vodovod-Kanalizacija for great help and suggestions and Albrecht Leis from JOANNEUM RESEARCH Forschungsgesellschaft mbH, Resources - Institute for Water, Energy and Sustainability.

Literature

Becker, M. W. & Coplen, T. B. 2001: Use of deuterated water as a conservative artificial groundwater tracer. Hydrogeological Journal, 9/5: 512–516, doi:10.1007/s100400100157.

Cameria, M.R., Fernando, R.M. & Pereira, L.S. 2003: Monitoring water and NO3-N in irrigated maize fields in the Sorraia watershed. Agricultural Water Management, 60: 199–216.

Ceplecha, Z.L.,Waskom, R.M., Bauder, T.A., Sharkoff, J.L. & Khosla, R. 2004: Vulnerability assessments of Colorado ground water to nitrate contamination. Water Air Soil Pollut, 159: 373–394, doi:10.1023/B:WATE.0000049188.73506.c9.

EARS (Environmental Agency of the Republic of Slovenia) 2014: Poročilo o kakovosti podzemne vode v Sloveniji v letu 20013. Ljubljana: 14-20 p.

EC 2000: Water Framework Directive 2000/60/EC. European Commission.

EC 2006: Groundwater Daughter Directive 2006/118/EC. European Commission.

EEC1991: Council Directive concerning the protection of waters against pollution caused by nitrates from agricultural sources 91/676/EEC. European Commission.

Gosar, M. 2000: Poročilo o preiskavi talnega profila PS-5 pri Selnici ob Dravi. Ljubljana, Geološki zavod Slovenije Report: 6 p.

Käss, W. 1998: Tracing techniques in Geohydrology. Rotterdam, A.A. Balkema: 581 p.

Kronvang, B., Borgvang, S.A. & Barkved, L. J. 2009: Towards European harmonised procedures for quantification of nutrient losses from diffuse sources — the EUROHARP project. Journal of Environtal Monitoring,11: 503–5, doi:10.1039/b902869m.

Krzeminska, D. M., Bogaard, T. A., Debieche, T.-H., Cervi, F., Marc, V. & Malet, J.-P. 2014: Field investigation of preferential fissure flow paths with hydrochemical analysis of small-scale sprinkling experiments. Earth Surf. Dynam. 2: 181–195, doi:10.5194/esurf-2-181-2014.

Leis, A. & Benischke, R. 2004: Comparison of different stable hydrogen isotope-ratio measurement techniques for tracer studies with deuterated water in the unsaturated zone in groundwater. Paper presented at the 7th Workshop of European Society for Isotope Research (ESIR), Berichte des Institutes für Erdwissenschaften Karl-Franzes-UniversitäGraz, Seggauberg, 27 June – 1 July 2004.

Lockhart, K.M., King, A.M. & Harter, T. 2013: Identifying sources of groundwater nitrate contamination in a 2 large alluvial groundwater basin with highly diversified intensive agricultural production. Journal of Contaminant Hydrology, 151: 140–154, doi:10.1016/j.jconhyd.2013.05.008.

Lopez, B., Baran, N. & Bourgine, B. 2015: An innovative procedure to assess multi-scale temporal trends in groundwater quality: Example of the nitrate in the Seine–Normandy basin, France. Journal of Hydrology, 522: 1–10, doi:10.1016/j.jhydrol.2014.12.002.

Mali, N., Janža, M., Rikanovič, R., Marinko, M., Herič, J., Levičnik, L. & Mozetič, S. 2005: Raziskave Selniške Dobrave - Raziskovalna dela z določitvijo lokacij vodnjakov in ogroženosti vodnega vira na Selniški Dobravi. GeoZS, Ljubljana: 16 p.

Mali, N. & Janža, M. 2005: Ocena ranljivosti vodonosnika s SINTACS modelom v GIS okolju. Geologija, 48/1: 127–140, doi:10.5474/geologija.2005.012.

Mali, N. 2006: Characterization of transport processes in the unsaturated zone of a gravel aquifer by natural and artificial tracers. Ph.D. thesis. University of Nova Gorica, Nova Gorica: 96 p.

Mali, N., Urbanc, J. & Leis, A. 2007: Tracing of water movement through the unsaturated zone of a coarse gravel aquifer by means of dye and deuterated water. Enviromental Geology, 51/8: 1401–1412, doi: 10.1007/s00254-006-0437-4.

Mali, N. & Urbanc, J. 2009: Isotope oxygen-18 as natural tracer of water movement in a coarse gravel unsaturated zone. Water, air and soil pollution, 203/1: 291–303, doi:10.1007/s11270-009-0012-1.

Morrison, J., Brockwell, T., Merren, T., Fourel, F. & Philips, A.M. 2001: On-line high-precision stable hydrogen isotopic analyses on nanoliter water samples. Analytical Chemistry, 73, 3570–3575.

Pisciotta, A., Cusimano, G. & Favara, R. 2015. Groundwater nitrate risk assessment using ntrinsic vulnerability methods: A comparative study of environmental impact by intensive farming in the Mediterranean region of Sicily, Italy. Journal of Geochemical Exploration, 156: 89–100, doi:10.1016/j.gexplo.2015.05.002.

Pratt P.F. & Adriano D.C. 1973: Nitrate concentrations in the unsaturated zone beneath irrigated fields in southern California. Soil Science Society of America Journal, 37: 321–322.

Refsgaard, J. C., Auken, E., Bamberg, C. A., Christensen, B. S. B., Clausen, T., Dalgaard, E., Effersø, F., Ernstsen, V., Gertz, F., Hansen, A. L., He, X., Jacobsen, B. H., Høgh Jensen, K., Jørgensen, F., Flindt Jørgensen, L., Koch, J., Nilsson, B., Petersen, C., De Schepper, G., Schamper, C., Sørensen, K. I., Therrien, R., Thirup, C., Viezzoli, A. 2014: Nitrate reduction in geologically heterogeneous catchments - A framework for assessing the scale of predictive capability of hydrological models. Science of the Total Environment, 468–469: 1278–1288, doi:10.1016/j.scitotenv.2013.07.042.

Schwientek, M., Maloszewski, P., Einsiedl, F. 2009: Effect of the unsaturated zone thickness on the distribution of water mean transit times in a porous aquifer. Journal of Hydrology, 373: 516–526, doi:10.1016/j.jhydrol.2009.05.015.

Seiler, K.P. & Zoejer, H. 2001: Role of tracers in the unsaturated zone. In: Tracers in the Unsaturated Zone (Investigations 1996-2001). ATH (ed.): Beiträge zur Hydrogeologie, 52: 11–15.

TRACI'95: 1998. Computer program. In: Kass, W (ed.): Tracing techniques in Geohydrology. A.A. Balkema, Rotterdam.

Official Gazette: Waters Act (ZV-1). No. 67/2002, 110/2002, 2/2004, 41/2004, 57/2008, 57/2012.

Official Gazette: Regulation on the protection of waters against pollution caused by nitrates from agricultural sources. No. 113/09, 5/13, 22/15, Ljubljana.

Urbanc, J., Krivic, J., Mali, N., Ferjan Stanič, T., Koroša, A., Šram, D., Mezga, K., Bizjak, M., Medić, M., Bole, Z., Lojen, S., Pintar, M., Udovč, A., Glavan, M., Kacjan-Maršić, N., Jamšek, A., Valentar, V., Zadravec, D., Pušenjak, M. & Klemenčič Kosi, S. 2014: Možnosti kmetovanja na vodovarstvenih območjih: zaključno poročilo projekta. Geološki zavod Slovenije; Univerza v Ljubljani, Biotehniška fakulteta; Institut Jožef Stefan; Kmetijsko gozdarski zavod; Ljubljana: 65.

Vinod, P. N, Chandramouli, P. N. & Koch, M. 2015: Estimation of Nitrate Leaching in Groundwater in an Agriculturally Used Area in the State Karnataka, India, Using Existing Model and GIS. Aquatic Procedia, 4: 1047 – 1053, doi:10.1016/j.aqpro.2015.02.132

Wang, L., Butcher, A. S., Stuart, M. E., Goddy, D.C. & Bloomfield, J.P. 2013: The nitrate time bomb: a numerical way to investigate nitrate storage and lag time in the unsaturated zone. Environmental Geochemistry and Health, 35: 667–681.

Wu, J.J., Bernardo, D.J., Mapp, H.P., Geleta, S., Teague, M.L., Watkins, K.B., Sabbagh, R.L., Elliott, R.L. & Stone, J.F. 1997: An evolution of nitrogen runoff and leaching potential in the high plains. Journal of Soil and Water Conservation, 52: 73–80.

Žlebnik, L. 1982: Hydrogeology of the Drava field. Geologija, 25/1: 151–164.

GEOLOGIJA *58/2*, 195-200, Ljubljana 2015

http://dx.doi.org/10.5474/geologija.2015.015

Nov primerek ribe *Protriacanthus gortanii* D'Erasmo, 1946 (Protriacanthidae, Tetraodontiformes) iz zgornjekrednih plasti pri Komnu (Slovenija)

New specimen of *Protriacanthus gortanii* D'Erasmo, 1946 (Protriacanthidae, Tetraodontiformes) from the Upper Cretaceous beds near Komen (Slovenia)

Matija KRIŽNAR

Prirodoslovni muzej Slovenije, Prešernova 20, SI–1001 Ljubljana; mkriznar@pms-lj.si

Prejeto / Received 29. 9. 2015; Sprejeto / Accepted 5.11. 2015; Objavljeno na spletu / Published online 30. 12. 2015

Ključne besede: *Protriacanthus*, Tetraodontiformes, kredne ribe, Komenski apnenec, Komen, Slovenija
Key words: *Protriacanthus*, Tetraodontiformes, Cretaceous fishes, Komen Limestone, Komen, Slovenia

Izvleček

Okolica Komna na Tržaško-komenski planoti je že dve stoletji znano najdišče krednih vretenčarjev. Med njimi prevladujejo ribe kostnice, ki so posebej pogoste v Komenskem apnencu Povirske formacije. Iz ploščastih apnencev prihaja nova najdba primerka majhne ribe *Protriacanthus gortanii*, ki je bila prvič opisana ravno iz teh plasti. Riba ima značilno morfologijo z močnimi bodicami plavutnic na hrbtni in trebušni strani. Najdba predstavlja verjetno že deveti raziskani primerek iz stratigrafsko dobro opredeljenega najdišča na Tržaško-komenski planoti.

Abstract

Surroundings of Komen on Trieste-Komen Plateau are known more than two centuries as Cretaceous vertebrates site. Most frequent finds are of teleostei fishes in Komen Limestone within the Povir Formation. From platy and laminated limestone a new specimen of *Protriacanthus gortanii* is described. The new specimen has a characteristic morphology with strong dorsal and pelvic fin spines. The new find of *Protriacanthus gortanii* is probably the ninth specimen discovered so far, but it is only one with a well established stratigraphic position.

Uvod

Kredne ribe iz okolice Komna so znane že od prve polovice 19. stoletja, o čemer pričajo nekateri zapisi v takratnih časopisih (Calligaris et al., 1994; Križnar, 2013). Kredne vretenčarje (predvsem ribe in morske plazilce) iz okolice Komna so raziskovali zlasti Heckel (1850), Steindachner (1860), Kner (1867), Bassani (1882), Gorjanović-Kramberger (1895) in D'Erasmo (1946). V zadnjih desetletjih so kredno ribjo favno proučevali in omenjali tudi Calligaris (1992), Cavin s sodelavci (2000) in Križnar (2014).

Združbe fosilnih rib in drugih fosilov Tržaško-komenske planote se pojavljajo v različno starih plasteh, čeprav so si nekateri faciesi litološko zelo podobni (Cavin et al., 2000; Jurkovšek et al., 2013). V Komenskem apnencu Povirske formacije so ostanki rib ponekod pogosti. Iz teh ploščastih in bituminoznih apnencev z roženci izhaja tudi novi ostanek *Protriacanthus gortanii*.

Komenski apnenec (Povirska Formacija) in paleontološka vsebina

Med kamninami Povirske formacije se pojavljajo tudi različno debeli vložki Komenskega apnenca (Jurkovšek et al., 2013; Palci et al., 2008), ki ga predstavljajo predvsem ploščasti apnenci z roženci (sl. 1). Starost Komenskega apnenca je cenomanijska (Jurkovšek et al., 2013). Med mikrofosili se v Povirski formaciji pojavlja biostratigrafsko pomembna *Broeckina* (*Pastrikella*) *balcanica* Cherchi, Radoičić & Schroeder. Predvsem so iz Komenskega apnenca znane fosilne ribe *Belonostomus lesinaensis* Bassani, *Chirocentrites coroninii* Heckel, *Chirocentrites microdon* Heckel, *Sauroramphus freyeri* Heckel, *Coelodus saturnus* Heckel, nekatere druge pikdontne ribe ter mnoge druge (Calligaris, 1992; Cavin et al., 2000). Pregled ribje favne iz Komenskega apnenca so prikazali tudi Palci s sodelavci (2008), kjer prikazujejo okoli trideset rodov, ki se pojavljajo v najdiščih okoli Komna. Poleg ostankov vretenčarjev se v ploščastih apnencih Povirske formacije pojavljajo tudi rastlinski ostanki (Jurkovšek et al., 2013) in redkejši fosili nevretenčarjev, tudi morske zvezde (Križnar et al., 2008). Cenomanijsko starost Povirske formacije opredeljuje tudi pojavljanje školjk *Chondrodonta joannae* (Choffat) (Jurkovšek et al, 2013).

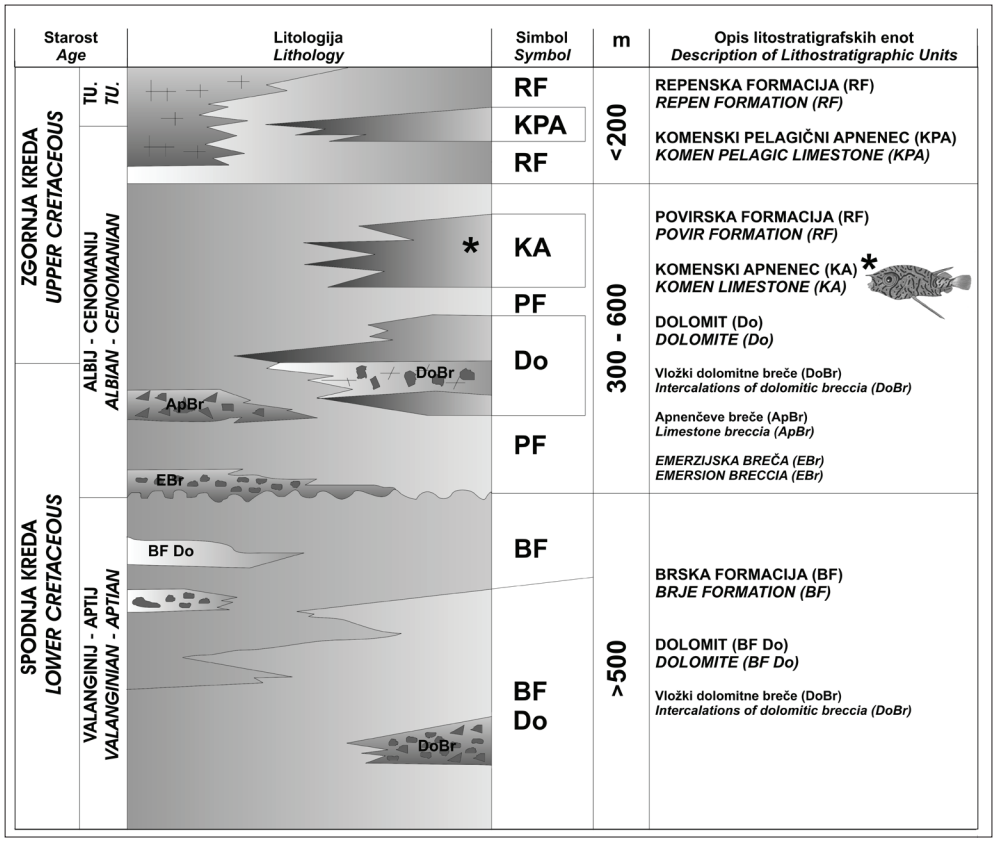

Sl. 1. Geološki stolpec z litostratigrafskimi enotami Repenske, Povirske in Brske formacije iz okolice Komna. (prirejeno po Jurkovšek et al., 2013). Stratigrafski položaj primerka *Protriacanthus gortanii* je označen z zvezdico.

Fig. 1. Geological column with lithostratigraphic units of Repen, Povir and Brje Formations (after Jurkovšek et al., 2013). Stratigrafic position of the specimen *Protriacanthus gortanii* is marked with asterisk.

Paleontološki del

Sistematika po: Tyler & Sorbini, 1996

Classis Actinopterygii Klein, 1885
Ordo Tetraodontiformes Berg, 1940
Superfamilia Plectocretacicoidea Tyler & Sorbini, 1996
Familia Protriacanthidae Tyler & Sorbini, 1996

Genus *Protriacanthus* D'Erasmo, 1946

Za ribe rodu *Protriacanthus* je značilna ena močna in druga šibkejša hrbtna (dorzalna) bodica. Še daljše so bodice na trebušni plavutnici. Rod *Protriacanthus* je poznan le iz najdišč v okolici Komna. D'Erasmo (1946) je nov rod opisal na osnovi enega primerka (sl. 2). Dodatnih sedem primerkov rodu sta opisala Sorbini & Guidotti (1984) (sl. 2). Rod *Protriacanthus* sta Tyler & Sorbini (1996) pripisala novi družini Protriacanthidae in opravila tudi revizijo vrst iz te družine.

Protriacanthus gortanii D'Erasmo, 1946

(Tabla 1, a-e / Plate 1, a-e)

1946 *Protriacanthus gortanii* n. gen. et n. sp. – D'Erasmo, 116-117, fig. 31-33.
1984 *Protriacanthus gortanii* d'Erasmo, 1946 – Sorbini & Guidotti, 247-263, fig. 1-4.
1996 *Protriacanthus gortanii* d'Erasmo, 1946 – Tyler & Sorbini, 27-36, fig. 18-24.

Material: Primerek na kamniti plošč (tabela 1), ki je nekoliko poškodovan zaradi izpostavljenosti vremenskim vplivom. Ohranjen je velik del telesa z glavo. Primerek (brez evidenčne številke) je shranjen v zasebni paleontološki zbirki Damjana Jensterleta (Bled, Slovenija).

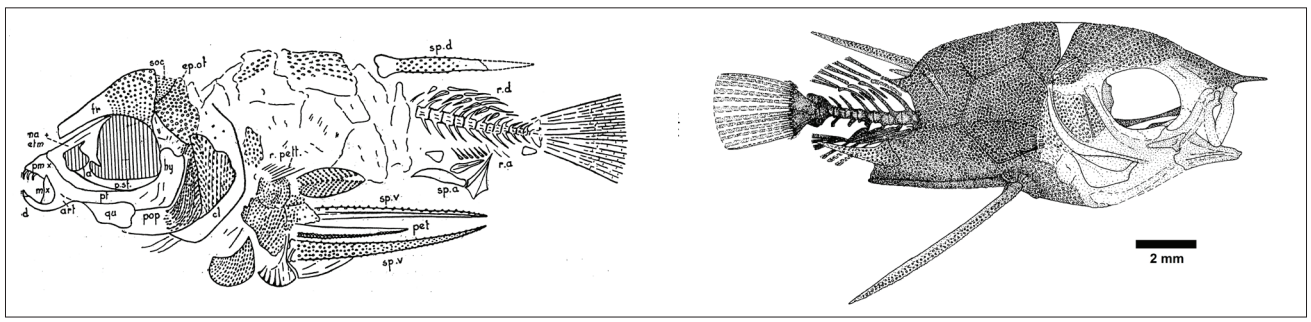

Sl. 2. *Protriacanthus gortanii* D'Erasmo, 1946. Levo: Risba holotipa (po D'Erasmo, 1946). Desno: Delna rekonstrukcija vrste (po Tyler & Sorbini, 1996)

Fig. 2. *Protriacanthus gortanii* D'Erasmo, 1946. Left: drawing of holotype specimen (from D'Erasmo, 1946). Right: Reconstruction of the species (from Tyler & Sorbini, 1996)

Tabela 1. Primerjava nekaterih dimenzij (kostnih elementov) pri primerkih *Protriacanthus gortanii*. [1]Dimenzije povzete po Tyler & Sorbini (1996, str. 35, Tab. 2).

Table 1. Comparison of dimensions (of some bones) of specimens *Protriacanthus gortanii*. [1]Measurements after Tyler & Sorbini (1996, p. 35, Tab. 2).

	Oznake primerkov / specimens	Dolžina telesa / Standard length (SL) mm	Višina telesa / Body depth mm	Dolžina trebušne plavuti / Pelvic-spine length mm	Dolžina 1. hrbtne bodice / 1st dorsal-spine length mm
1	holotip (IGPUB IFDC29)[1]	20,5	7,6	7,9	4,9
2	MCSNV T919[1]	18	6,9	7,3	4,4
3	MCSNV T916[1]	16	6	7,7	5,3
4	MCSNV T913[1]	14,5	6	6,8	3,9
5	MCSNV T915[1]	14	5,7		
6	MCSNV T914[1]	13	4,9	5,5	
7	MCSNV T918[1]	12	4,4	4,7	
8	**Nov primerek (v tem delu) New specimen (this work)**	13,2	5,3	5,2	2,35

Najdišče: Najdišče leži ob cesti med Komnom in Škrbino, zahodno od naselja Jablanec, približno 1,2 km severno od Komna. Ob cesti je večji vsek, kjer so razkriti ploščasti apnenci z redkimi vložki rožencev (sl. 3). Najdišče je zaščiteno kot naravna vrednota državnega pomena. Na najdišču, na površini kamnitih ploščic, so bili odkriti tudi drugi ostanki fosilnih rib iz družin Pycnodontidae (zobje) in Dercetidae (ostanki glave) ter najpogostejših ostankov redu Clupeiformes (verjetno iz rodu *Clupavus* Arambourg), ki še niso bili raziskani.

Opis primerka: Dolžina (SL) ohranjenega primerka je 13,2 mm, višina telesa je približno 5,3 mm. Na zgornjem delu je ohranjena prva bodica hrbtne plavuti. Dolžina bodice je 2,34 mm (tab. 1, sl. d). Telo primerka je v osrednjem delu telesa pokrito s ploščicami (okostenele luske). Glava je močno poškodovana oziroma je razločen le frontalni del (tab. 1, sl. a) in parafenoid pri očesni odprtini. Ostali znaki so nerazločni. V spodnjem delu primerka je ohranjena močna bodica (PS) trebušne plavuti (tab. 1, sl. e). Dolžina bodice trebušne plavutnice je 5,2 mm. Od vretenca (Ver) sta razločni le dve, verjetno PU4 in PU3 (po Tyler & Sorbini, 1996) in nerazločne kosti repne plavuti (tab. 1, sl. c).

Primerjava: Nekoliko slabša ohranjenost primerka še vedno dovoljuje primerjavo z ostalimi. Glede na ostale opisane primerke *Protriacanthus gortanii*, ki jih podajata Tyler & Sorbini v tabeli 2 (1996, str. 35) se primerek najbolje ujema s primerkom MCSNV T914. Sicer pa tudi razmerja (dolžina telesa, višina telesa, dolžina hrbtne bodice) pri ostalih primerkih sovpadajo (tabela 1).

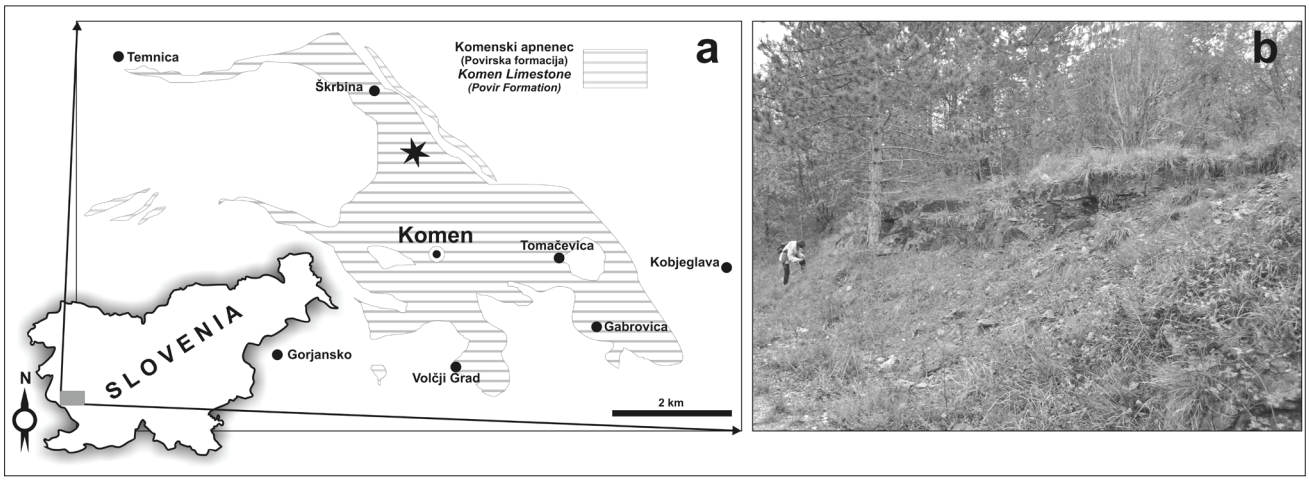

Sl. 3. Položaj najdišča (označen z zvezdico) in razširjenost Komenskega apnenca (a) (prirejeno po Jurkovšek et al., 2013). Najdišče ob cestnem useku med Komnom in Škrbino (b).

Fig. 3. Locality map showing the outcrop of Komen Limestone (a) (adapted from Jurkovšek et al., 2013), fossil site is marked with asterisk. Outcrop at locality on road Komen – Škrbina (b).

Geografska in stratigrafska razširjenost: Vrsta *Protriacanthus gortanii* je do sedaj poznana le iz najdišč na Krasu (Slovenija). D'Erasmo (1946) in Sorbini & Guidotti omenjajo kot najdišča primerkov le okolico Komna, brez natančnih lokacij. Tyler & Sorbini (1996), ki sta taksonomsko ponovno raziskala primerke stratigrafsko uvrščata primerke v zgornji cenomanij do spodnji turonij. Naš primerek izhaja iz Komenskega apnenca (Povirska formacija) zgornje cenomanijske starosti (Palci et al., 2008; Jurkovšek et al., 2013).

Zaključki

Iz Komenskega apnenca Povirske formacije je opisan še en primerek ribe *Protriacanthus gortanii*. Primerek je tudi edini z znano natančno stratigrafsko pozicijo, v primerjavi z ostalimi primerki (osem primerkov iz muzejskih zbirk), ki so jih predstavili D'Erasmo (1946), Sorbini & Guidotti (1984) in pri reviziji vrste tudi Tyler & Sorbini (1996). Naš primerek se morfološko dobro ujema s preostalimi primerki, kljub nekoliko slabši ohranjenosti. Vrsta *Protriacanthus gortanii* se verjetno pojavlja le v cenomanijskih plasteh v okolici Komna.

Zahvala

Zahvaljujem se dr. Jamesu C. Tyleru (National Museum of Natural History, Smithsonian Institution) za posredovanje nekaterih literarnih virov in opombe ob pregledu slikovnega gradiva. Zahvaljujem se tudi dr. Miloši Milerju (Geološki zavod Slovenije) za izdelavo in pomoč pri fotografiranju primerka pod elektronskim mikroskopom.

New specimen of *Protriacanthus gortanii* D'Erasmo, 1946 (Protriacanthidae, Tetraodontiformes) from the Upper Cretaceous beds near Komen (Slovenia)

Extended summary

From Upper Cretaceous beds near Komen on Trieste-Komen Plateau (Slovenia) a new specimen of *Protriacanthus gortanii* is described. The specimen (stored in a private collection of D. Jensterle, Bled) is the first with a documented stratigraphic position and it derives from the Komen Limestone within the Povir Formation (Upper Cenomanian age) (Fig. 1). Fossil site (outcrop) of the new specimen is the road cut between Komen and Škrbina village in platy and laminated limestone (Fig. 3). Some other fossil fishes from Pycnodontidae and Dercetidae family and additional numerous disarticulated specimens of Clupeiformes fishes (probable genus *Clupavus*) were collected from the same beds.

Preservation of the new specimen is moderately good (Pl. 1), with missing caudal-fin region. Specimen length (SL) is 13.2 mm, with body depth 5.3 mm. On head the frontal region bones and parasphenoid bone are disctinctive (jaws and rostral bones are absent). The carapace scale plates are preserved in the middle part of specimen. The first dorsal spine and pelvic spines are disctinctive. Only tree vertebrae are visible.

The new find of *Protriacanthus gortanii* is probable the ninth specimen discovered. This species is present only on the Trieste-Komen Plateau (Slovenia) and is stratigraphically limited to platy and laminated limestone of the Komen Limestone (Povir Formation).

TABLA 1 – PLATE 1

Protriacanthus gortanii, Komen – Škrbina, Komenski apnenec (Povirska formacija).
a – Primerek na kamnini. Merilo 5 mm.
b – risba primerka iz slike a. Merilo 5 mm.
c – vretenca na zadnjem delu primerka. Merilo 500 µm.*
d – prva bodica hrbtne plavuti. Merilo 500 µm.*
e – vrhnji del bodice trebušne plavuti. Merilo 500 µm.*

Okrajšave: DS – bodica hrbtne plavuti, F – frontalni del glave, PS – bodica trebušne plavuti, Ver – vretenca.
*Fotografije narejene na SEM JEOL JSM 6490LV, Geološki zavod Slovenije.

Protriacanthus gortanii, Komen – Škrbina, Komen Limestone (Povir Formation).
a – Specimen on matrix. Scale bar 5 mm.
b – Drawing of specimen from a. Scale bar 5 mm.
c – Vertebrae (Ver) on posterior part of specimen. Scale bar 500 µm.*
d – First dorsal spine. Scale bar 500 µm.*
e – Pelvic spine. Scale bar 500 µm.*

Abbreviations: DS – Dorsal spine, F – Frontal, PS – Pelvic spine, Ver – Vertebrae.
*Photo by JEOL JSM 6490LV scanning electron microscope (SEM), Geological Survey of Slovenia)

TABLA 1 – PLATE 1

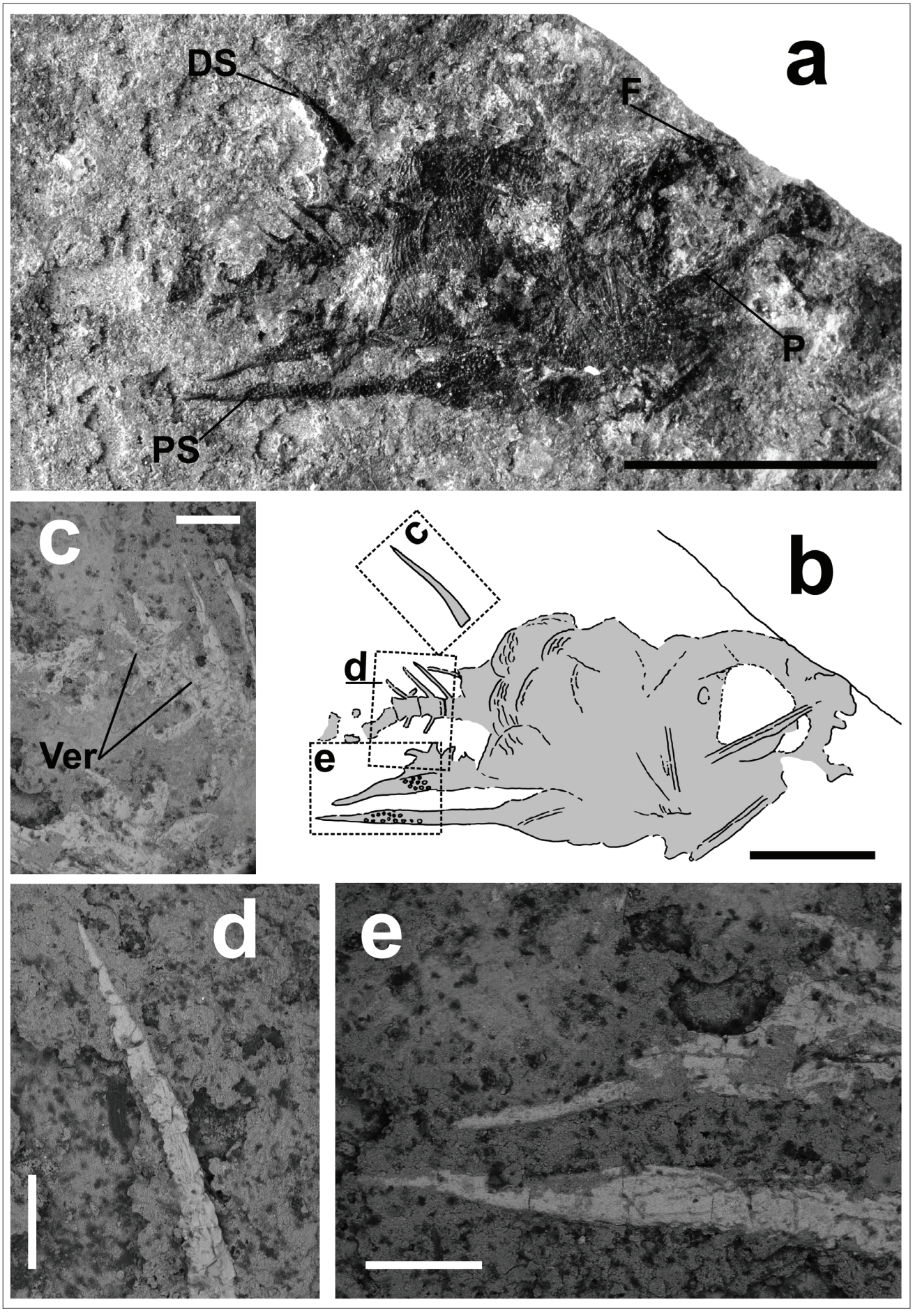

Literatura

Bassani, F. 1882: Descrizione dei Pesci fossili di Lesina accompagnata da appunti su alcune altre ittiofaune cretacee (Pietraroia, Voirons, Comen, Grodischtz, Crespano, Tolfa, Hakel, Sahel-Alma e Vestfalia). Denkschr. Akad. Wiss., Math.-naturw. Cl., 45/2: 195-288.

Calligaris, R. 1992: I pesci fossili dei calcari ittiolitici di Comen e di faciea a questa correlabili conservati nelle collezioni del Museo civico di Storia Naturale di Trieste. Atti Museo Civico di Storia Naturale di Trieste, 44: 57–111.

Calligaris, R. 1994: 95 milioni di anni fa: il periodo cretacico attraverso i fossili di Comeno ed altri reperti del Carso. Museo civico di Storia Naturale di Trieste: 1–24.

Cavin, L., Jurkovšek B. & Kolar-Jurkovšek, T. 2000: Stratigraphic succession of the Upper Cretaceous fish assembleges of Kras (Slovenia). Geologija, 43/2: 165–195, doi:10.5474/geologija.2000.013.

D'Erasmo, G. 1946: L'ittiofauna cretacea dei dintorni di Comeno, nel Carso triestino. Atti della Reale Accademia delle Scienze Fisiche, Matematiche e Naturali di Napoli, 2: 1–136.

Gorjanović-Kramberger, D. 1895: Fosilne ribe Komena, Mrzleka, Hvara i M. Libanona. Djela Jugosl. akad. znanosti i umjetnosti Zagreb, 16: 1–67.

Heckel, J.J. 1850: Beiträge zur Kenntniss der fossilen Fische Oesterreichs. Denkschriften der Kaiserlichen Akademie der Wissenshaften, Matematisch- Naturwissenschaftliche Klasse, 1: 201–242.

Jurkovšek, B., Cvetko Tešović, B. & Kolar Jurkovšek, T. 2013: Geologija Krasa = Geology of Kras. Geološki zavod Slovenije, Ljubljana: 205 p.

Kner, K. 1867: Neuer Beitrag zur Kenntniss der fossilen Fische von Comen bei Gorz. Sitzungsberichte der Kaiserlichen Akademie der Wissenschaften. Mathematisch-Naturwissenschaftliche Klasse, 56: 171–200.

Križnar, M. 2013: O prvih najdbah krednih rib na Krasu. Proteus, 75/5: 225–227.

Križnar, M. 2014: Kredne piknodontne ribe (†Pycnodontidae) Krasa – zgodovinski pregled in najdbe danes. In: Rožič, B., Verbovšek, T. & Vrabec, M. (eds.): 4. Slovenski geološki kongres, Povzetki in ekskurzije, Ankaran.

Križnar, M., Žalohar, J. & Hitij, T. 2008: Kredna morska zvezda iz okolice Komna. Proteus, 71/3: 131.

Palci, A., Jurkovšek, B., Kolar-Jurkovšek, T. & Caldwell, M.W. 2008: New palaeoenvironmental model for the Komen (Slovenia) Cenomanian (Upper Cretaceous) fossil lagerstätte. Cretaceous Research, 29/2: 316–328, doi:10.1016/j.cretres.2007.05.003.

Sorbini, L. & Guidotti, G. 1984: Nuovi dati sull'osteologia di *Protriacanthus gortanii* D'Erasmo. Reprint Boll. Mus. civ. St. nat. Verona, 11: 247–264.

Steindachner, F. 1860: Beiträge zur Kenntniss der fossilen Fische Österreichs. II. Über einen neuen Vomer-ähnlichen Fische von Comen am Karst. Sitzungber. Math.-natuwiss. Cl. K. Akad. Wiss., 38 (1859): 763–788.

Tyler, J.C. & Sorbini, L. 1996: New superfamily and three new families of tetraodontiform fishes from the Upper Cretaceous: the earliest and most morphologically primitive plectognaths. Smithsonian Contributions to Paleobiology, 82: 1–59.

GEOLOGIJA *58/2*, 201–212, Ljubljana 2015

http://dx.doi.org/10.5474/geologija.2015.016

Nove najdbe rakovice *Styrioplax exiguus* Glaessner, 1928 (Decapoda, Brachyura) v miocenskih plasteh okolice Maribora

New reports of crab *Styrioplax exiguus* Glaessner, 1928 (Decapoda, Brachyura) from Miocene beds near Maribor, Slovenia

Rok GAŠPARIČ[1,2] & Eva HALÁSOVÁ[3]

[1]Oertijdmuseum De Groene Poort, Bosscheweg 80, NL–5283 WB Boxtel, Nizozemska;
e-mail: rok.gasparic@gmail.com
[2]Ljubljanska cesta 4j, 1241 Kamnik, Slovenija; e-mail: rok.gasparic@gmail.com
[3]Department of Geology and Paleontology, Faculty of Natural Sciences, Comenius University,
Mlynska dolina G, 842 15 Bratislava, Slovaška; e-mail: halasova@fns.uniba.sk

Prejeto / Received 28. 9. 2015; Sprejeto / Accepted 30. 11. 2015; Objavljeno na spletu / Published online 30. 12. 2015

Ključne besede: deseteronožci, miocen, badenij, Centralna Paratetida, paleogeografija, paleoekologija, Slovenija
Key words: Decapoda, Miocene, Badenian, Central Paratethys, Palaeogeography, Palaeoecology, Slovenia

Izvleček

V članku predstavljamo nove najdbe rakovice *Styrioplax exiguus* Glaessner, 1928, ki dopolnjujejo naše poznavanje paleogeografske in stratigrafske razširjenosti te zanimive paratetidne vrste. Opisani so primerki s treh najdišč v miocenskih plasteh Slovenskih goric v neposredni bližini Maribora. S preiskavami fosilne kalcitne nanoflore smo določili srednjemiocensko starost plasti, ki so se odložile v globjemorskem okolju Centralne Paratetide.

Abstract

In this paper we report new specimens of an interesting Paratethyan decapod *Styrioplax exiguus* Glaessner, 1928, which extend the known palaeogeographic and stratigraphic distribution of the species. The described specimens originate from three different localities from Miocene beds in the Slovenske gorice, in the vicinity of Maribor. By analysing the fossil nannoplankton assemblages we were able to determine a Middle Miocene age of these deep water beds of the Central Paratethys.

Uvod

Najdb celih in določljivih ostankov fosilnih rakovic je na področju današnje Slovenije razmeroma malo. Največ tovrstnih fosilnih ostankov v Sloveniji najdemo v eocenskih plasteh Istre (Pavlovec & Pavšič, 1985; Mikuž, 2010a) in miocenskih plasteh okolice Kamnika in Zasavja (Križnar, 2006; Križnar & Preisinger, 2008; Mikuž, 2010b; Mikuž & Pavšič, 2003). Iz miocenskih plasti slovenskega dela Štajerskega bazena Paratetide imamo do sedaj podatke o redkih posameznih najdbah fosilnih rakovic (Glaessner, 1928; Mikuž, 2003), o bogati združbi fosilnih rakov deseteronožcev iz spodnjemiocenskih plasti nahajališča Činžat na severnem pobočju Pohorja pa sta poročala Gašparič in Hyžný. (2015).

Glaessner (1928) je iz nahajališč St. Egidij (Šentilj) in St. Leonard (Lenart) prvič opisal vrsto majhne rakovice *Microplax exiguus*. Posamezne primerke te vrste poznamo tudi iz globjemorskih spodnjemiocenskih (karpatijskih) plasti nahajališča Cerova - Lieskove na Slovaškem (Hyžný & Schlögl, 2011), preko 70 primerkov pa je bilo pred kratkim opisanih tudi iz miocenskih plasti karpatijske starosti na nahajališču Činžat na severnem pobočju Pohorja (Gašparič & Hyžný, 2015), ki so se prav tako usedale v globjemorskem okolju.

V pričujočem članku predstavljamo nove najdbe rakovic vrste *Styrioplax exiguus* Glaessner, 1928, z dveh še neopisanih najdišč (Meljski hrib in Malečnik) v okolici Maribora, in še nepredstavljen primerek (inv. št. LMJ 5749) iz Glaessnerjeve zbirke, ki je bil najden pri Jarenini v Slovenskih goricah, in ga hranijo v avstrijskem Univerzalnem muzeju Joanneum v Gradcu. Plasti z ostanki rakovic na najdiščih Meljski hrib in Malečnik smo vzorčili tudi za pregled kalcitne nanoflore.

Geološka zgradba okolice najdišč

Na površju Slovenskih goric izdanjajo predvsem miocenske, pliocenske in kvartarne kamnine (Žnidarčič & Mioč, 1989; Mikuž & Gašparič, 2014). Miocenske plasti v okolici omenjenih novih najdišč rakovic so sestavljene iz laporjev, sljudnatih meljevcev in redkih vmesnih plasti peščenjakov in konglomeratov (Žnidarčič & Mioč, 1989).

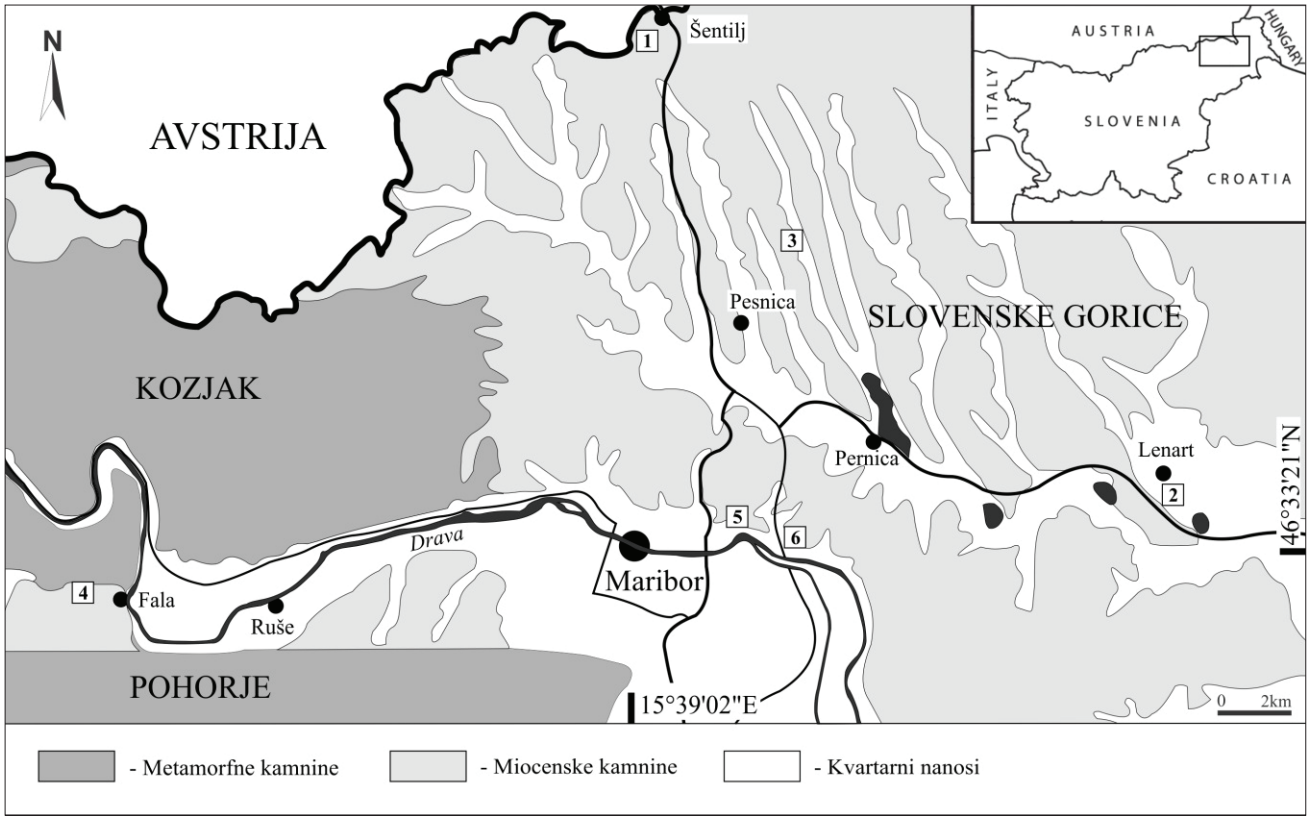

Sl. 1. Poenostavljena geološka skica (po Mioč & Žnidarčič, 1977; Žnidarčič & Mioč, 1989) in geografski položaj nahajališč rakovice *Styrioplax exiguus*. 1 – Šentilj, 2 – Lenart v Slovenskih goricah, 3 – Jarenina, 4 – Činžat na Pohorju, 5 – Meljski hrib, 6– Malečnik.

Fig. 1. Simplified geological sketch (after Mioč & Žnidarčič, 1977; Žnidarčič Mioč, 1989) and sites of fossil specimens of decapod *Styrioplax exiguus*. 1 – Šentilj, 2 – Lenart v Slovenskih goricah, 3 – Jarenina, 4 – Činžat na Pohorju, 5 – Meljski hrib, 6 – Malečnik.

Strukturno pripadajo Slovenske gorice Panonskemu bazenu (Placer, 1999), v ožjem smislu pa k tektonski enoti Slovenskih goric (Pavšič & Horvat, 2009). Miocenske plasti na obeh novih najdiščih so se odlagale v jugozahodnem delu Štajerskega bazena, ki je predstavljal del Centralne Paratetide. V spodnjem delu srednjega miocena (badenija) je Centralna Paratetida dosegla svoj največji obseg in se je povezovala preko t. i. slovenskega koridorja na jugozahodu z Mediteranom in preko Vzhodne Paratetide z Indijskim in Tihim oceanom (Rögl, 1999; Bartol, 2009).

Ekstenzijska tektonika, ki je povzročila lokalno pogrezanje manjših sedimentacijskih bazenov in transgresija morja v spodnjebadenijskem globalnem evstatičnem ciklu TB2.3 (Kovać et al., 2007) (sl. 2), pa sta omogočila nastanek globokih bazenov in močan dotok klastičnega materiala z bližjih kopnih predelov (Jelen in Rifelj, 2002).

Novi primerki rakovic so bili najdeni v sivih meljevcih Slovenskih goric, severovzhodno od Maribora, na najdiščih Meljski hrib (46°33'38''N, 15°40'33''E) in Malečnik (46°33'26''N, 15°42'05''E) (sl. 1).

Na širšem obravnavanem območju je Rijavec (1976, 1978) določila spodnjebadenijsko foraminiferno biocono *Praeorbulina-Orbulina saturalis*. Spodnjebadenijska foraminiferna favna je značilna za globokomorsko sedimentacijsko okolje, največja paleobatimetrija (globina okoli 1000 m) je korelirana s prej omenjeno transgresijo morja v ciklu TB2.3 (Rifelj & Jelen, 2001).

Paleontološki del

Sistematika povzeta po: Ng et al. (2008) in De Grave et al. (2009).

Infraorder BRACHYURA Linnaeus, 1758
Superfamily GONEPLACOIDEA MacLeay, 1838
Family CHASMOCARCINIDAE Serène, 1964
Subfamily CHASMOCARCININAE Serène, 1964

Genus *Styrioplax* Glaessner, 1969

***Styrioplax exiguus* (Glaessner, 1928)**
Sl. 4, 1–7

v*1928 *Microplax exiguus* Glaessner, 1928, Glaessner, 195, tabla 3, slike 14, 14a; tekst - slika 8.
1929 *Microplax exiguus* Glaessner; Glaessner, 258.
1969 *Styrioplax exiguus* (Glaessner); Glaessner, R527, slika 335/2.
2003 *Styrioplax exiguus* (Glaessner); Karasawa in Kato, 145.
2011 *Styrioplax exiguus* (Glaessner); Hyžný in Schlögl, 338, slike 12–15.
2015 *Styrioplax exiguus* (Glaessner); Gašparič in Hyžný, 149, slike 10–12.

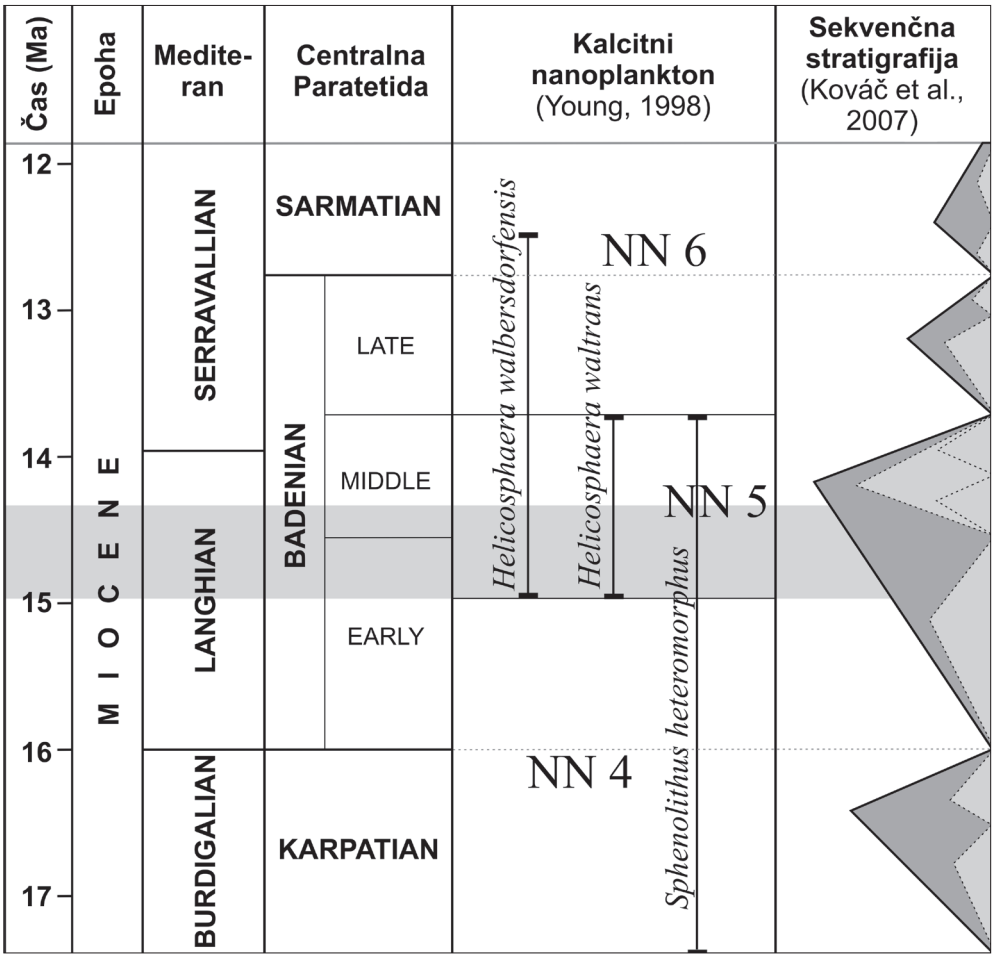

Sl. 2. Kronostratigrafska razdelitev miocena s prikazanimi stopnjami v Mediteranu in Centralni Paratetidi. Starost obravnavanih najdišč, določena na podlagi kalcitne nanoflore, je osenčena.

Fig. 2. Chronostratigraphic chart of Miocene, showing the Mediterranean and Central Paratethyan (regional) stages. The age of localities based on nanoplankton analysis is highlighted.

Material: Primerek RGA/SMNH 1676 iz najdišča Meljski hrib pri Mariboru predstavlja odtis trebušne strani rakovice, povezan s pripadajočimi okončinami. Dva primerka sta bila najdena tudi na nekaj kilometrov oddaljenem najdišču Malečnik: primerek RGA/SMNH 1135 predstavlja ostanek notranjega odtisa hrbtnega oklepa in del trebušne strani istega osebka, primerek RGA/SMNH 1136 / 1140 (odtis / jedro) pa sta polovici istega primerka, na katerem je ohranjen oklep z ostanki okončin. Vse tri primerke je našel avtor članka. Prikamnina je temnorjav sljudnat meljevec.

Fosilni ostanki so v drobnozrnatih meljastih in lapornatih plasteh obeh najdiščih dobro ohranjeni. Oklepi opisanih rakovic so povezani z okončinami in kažejo na minimalen transport po smrti ter na hitro stopnjo sedimentacije. Nekateri ostanki so delno razpadli, vendar ohranjeni skupaj. Pri primerku RGA/SMNH 1135 lahko opazimo obe polovici oklepa (hrbtno in trebušno) razprti in ločeni, vendar pa v tem primeru to ni posledica transporta, ampak značilen primer levitve rakovice.

Najdišče: Najdišče Meljski hrib je poznano po številnih fosilnih ostankih miocenske makrofavne in kosih fosilnega lesa, ki jih je moč najti v teh plasteh. Srednjemiocenske plasti se na severovzhodnem delu mesta Maribor ob malečniškem mostu strmo dvigajo nad reko Dravo in v profilu izdanjajo v višini okoli 100 m. Primerek rakovice je bil najden v spodnjem delu profila, kjer izdanjajo plasti meljevca, sive do temnorjave barve, v katerih so tudi leče peščenjakov. V teh plasteh so makrofosilni ostanki redki, zasledili smo le še redke ostanke škarij kalianasidnih rakov rovcev in pogoste bioturbacije. Višje na najdišču prehajajo v trše, svetlosive apnenčeve laporovce, v katerih so pogosti ostanki školjk (Mikuž & Gašparič, 2014), nekaj centimetrov veliki ostanki iregularnih morskih ježkov iz družine Shizasteridae in večji kosi okamenelega lesa. V najvišjem delu profila izdanjajo svetlo rjavi do rumeni apnenčevi laporovci, v katerih so pogosti ostanki kačjerepov (Mikuž & Gašparič, 2014).

Le 1500 m vzhodno od Meljskega hriba leži najdišče Malečnik, kjer so pri kmetijskih delih spomladi leta 2013 ob urejanju vinograda v bližini malečniške cerkve razkrili temno sive sljudnate meljevce, ki so litološko enaki kot bazalne plasti najdišča Meljski hrib. Na najdišču Malečnik, ki smo ga spomladi leta 2013 večkrat obiskali, so poleg dveh primerkov rakovice *Styrioplax exiguus* najdeni redki ostanki iregularnih morskih ježkov iz družine Shizasteridae.

Vsi fosilni ostanki so zaradi velikega kompakcijskega indeksa meljastih sedimentov zelo stisnjeni, vendar nedeformirani. Kalcitne lupine mehkužcev in kalcitno - hitinska povrhnjica skeleta deseteronožcev niso ohranjeni, vsi fosilni ostanki so ohranjeni le kot kamena jedra oz. odtisi v kamnini.

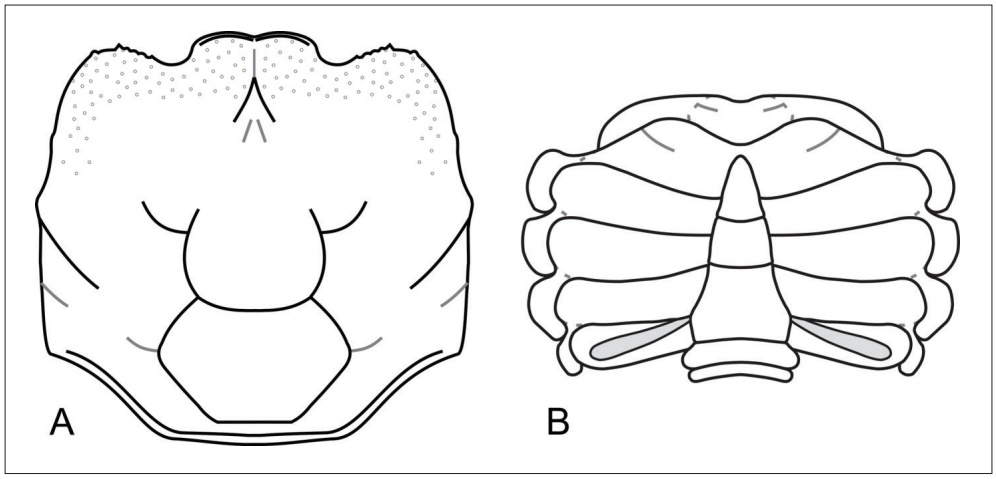

Sl. 3. *Styrioplax exiguus* (Glaessner, 1928), rekonstrukcija. A – hrbtna stran oklepa; B –trebušna stran oklepa samca (po Gašparič & Hyžný, 2015).

Fig. 3. *Styrioplax exiguus* (Glaessner, 1928), reconstruction. A – dorsal carapace; B – male venter (after Gašparič & Hyžný, 2015).

Tabela 1. Seznam znanih nahajališč rakovice *Styrioplax exiguus* in primerjava dimenzij največje širine in dolžine oklepa.

Table 1. List of known localities for *Styrioplax exiguus* specimens and comparison of maximum width and length of their dorsal carapace.

Vrsta / Taxon	Primerek / Specimen	Nahajališče / Locality	Avtorji /Authors	max. dolžina / length (mm)	max. širina / width (mm)
Styrioplax exiguus	LMJ 5453 (holotype)	Šentilj, Slovenija	Glaessner, 1928	5,6	6,1
Styrioplax exiguus	LMJ 5753	Lenart, Slovenija	Glaessner, 1928	5,5	6,9
Styrioplax exiguus	SNMZ 24868	Cerova Lieskove, Slovaška	Hyžný in Schlögl 2011	8,3	8,5
Styrioplax exiguus	SNMZ 35507	Cerova Lieskove, Slovaška	Hyžný in Schlögl 2011	6,5	8,0
Styrioplax exiguus	RGA/SMNH 0889	Činžat, Slovenija	Gašparič in Hyžný, 2015	9,1	9,4
Styrioplax exiguus	RGA/SMNH 1208	Činžat, Slovenija	Gašparič in Hyžný, 2015	5,5	6,2
Styrioplax exiguus	RGA/SMNH 1135	Malečnik, Slovenija	v tem članku	5,5	6,5
Styrioplax exiguus	RGA/SMNH 1140	Malečnik, Slovenija	v tem članku	7,3	8,4
Styrioplax exiguus	RGA/SMNH 1676	Meljski hrib, Slovenija	v tem članku	5,3	6,5
Styrioplax exiguus	LMJ 5749	Jarenina, Slovenija	v tem članku	8,4	8,5

Opis: Majhen oklep je ovalno-kvadratne oblike (sl. 3A) in skoraj enake dolžine kot širine (količnik širina/dolžina je okoli. 1,10) (tab. 1). Oklep je najširši v zadnjem delu, naprej se zoži. V preseku je oklep konveksne oblike in predvsem v zadnjem delu visoko dvignjen s strmim stranskim in zadnjim robom, proti sprednjemu robu pa je položnejši. Kljunec (ang. rostrum) je dvodelen, zaokrožen in obrobljen (sl. 4, 2–3). Pri odraslih osebkih je kljunec zraščen in dvojen, raven do konkaven, ter predeljen s plitvo brazdo, medtem ko je pri mlajših osebkih kljunec sestavljen iz dveh ločenih grebenov. Očesne jamice so plitve in ozke in se nadaljujejo s sinosoidnim sprednjim robom ter majhnim zaočesnim trnom, ki je razvit le pri odraslih osebkih. Sprednji stranski rob je zaobljen in konkaven (sl. 4, 5–6). Stranski rob je sinusoiden in se proti zadnjemu delu širi, v zadnjem delu na stranskem robu ima tudi opazen izrastek,

Sl. 4. *Styrioplax exiguus* (Glaessner, 1928)
1 – RGA/SMNH 1676, cel primerek s povezanimi hodilnimi okončinami (P) in kleščami (C);
2 – RGA/SMNH 1135, ločena hrbtni (d) in trebušni del oklepa (v) lev;
3 – RGA/SMNH 1135, notranji odtis hrbtnega dela oklepa;
4 – RGA/SMNH 1135, trebušni del oklepa samca, prsnica s sterniti (S) in zadek (A);
5 – RGA/SMNH 1140, hrbtni del oklepa z vidnimi sterniti (S);
6 – RGA/SMNH 1136, odtis hrbtnega dela oklepa primerka RGA/SMNH 1140;
7 – LMJ 5749, cel primerek iz Jarenine s povezanimi hodilnimi okončinami (P) in kleščami (C), hranjen v Univerzalnem muzeju Joanneum. Velikost vseh meril je 5 mm.

Fig. 4. *Styrioplax exiguus* (Glaessner, 1928)
1 – RGA/SMNH 1676, complete specimen with articulated pereiopods (P) and chelipeds (C);
2 – RGA/SMNH 1135, disassociated dorsal (d) and ventral carapace (v), exuvie;
3 – GA/SMNH 1135, internal cast of dorsal carapace;
4 – RGA/SMNH 1135, ventral carapace with sternum (S) exhibiting male abdomen (A);
5 – RGA/SMNH 1140, dorsal carapace showing exposed ventral sternites;
6 – RGA/SMNH 1136, cast of dorsal carapace of specimen RGA/SMNH 1140;
7 – LMJ 5749, complete specimen from Jarenina with articulated pereiopods (P) and chelipeds (C), deposited in Universalmuseum Joanneum. All scale bars are 5 mm.

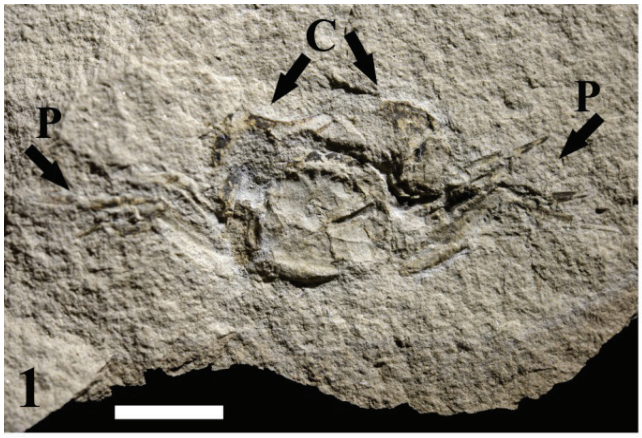
C
P
P
1

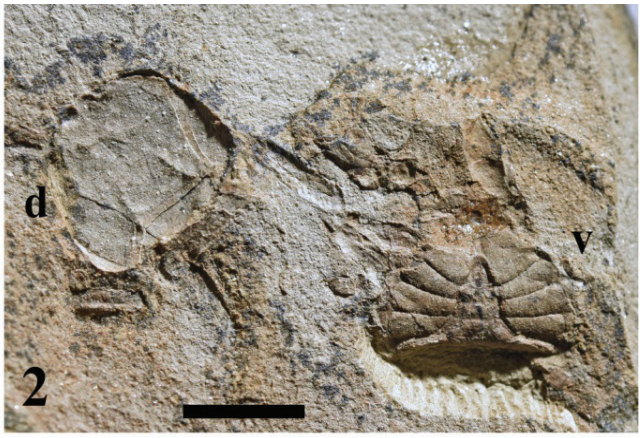
d
v
2

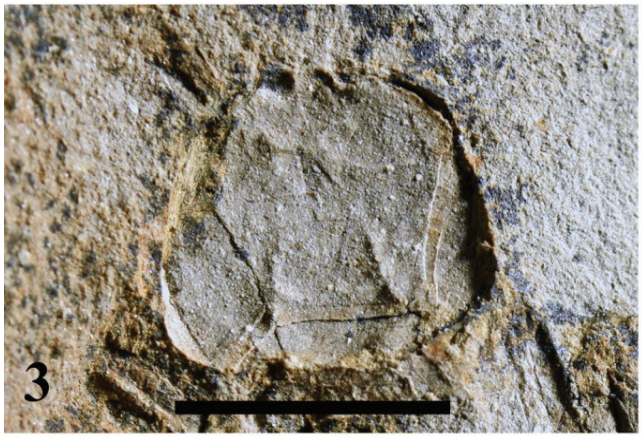
3


S
S
A
4


P
S
5


6


C
P
P
7

kjer se srednjepljučni greben seka s stranskim robom. Zadnji rob oklepa je raven, v sredini konkaven, obrobljen in na zadnjem stranskem robu tvori manjše konkavne zajede, v katerih ležijo zadnji par hodilnih okončin.

Hrbtna stran oklepa, ki je dobro ohranjena na primerku RGA/SMNH 1135 (sl. 4, 2–3) ter primerku RGA/SMNH 1140 (sl. 4, 5–6), je večinoma gladka in v sprednjem stranskem, pljučnem in želodčnem predelu posejana s posameznimi manjšimi bradavicami. Želodčni predel je jasno izražen in v zadnjem delu nabrekel, zadnji rob omejuje globoko zarezana in konkavna maternična (cervikalna) brazda, manj izrazita stranska robova pa se konvergentno ožita proti sprednjemu robu, kjer za kljunom tvorita poglobljen del. Srčni predel je ovalne do trapezoidne oblike in poleg želodčnega edini jasno opazen (primerek RGA/SMNH 1135). Srčni predel je v sredini dvignjen in s sinosoidno brazdo ločen od pljučnih predelov. Zgornjepljučni predel je širok in na zgornji strani omejen z nadaljevanjem maternične brazde, na spodnji pa s srednjepljučnim grebenom, ki poteka diagonalno od stranskega roba oklepa, kjer tvori zaobljen izrastek, proti srčnemu predelu. Srednje in spodnjepljučni predel sta slabše izražena in v opazovanih primerkih nista opazna.

Prsnica je lepo ohranjena na primerku RGA/SMNH 1135 (sl. 4, 4) in se proti zadnjemu delu razširi. Kontakti med posameznimi sterniti so konkavno oblikovani, sternita 1–2 sta zraščena, prav tako sta zraščena sternita 3–4, ostali sterniti pa so ločeni. Zadek lahko opazujemo na primerkih RGA/SMNH 1135 (sl. 4, 4) in RGA/SMNH 1676 (sl. 4, 1); v obeh primerih glede na ozko in koničasto obliko zadka ugotavljamo, da gre za moški osebek rakovice. Pri primerku RGA/SMNH 1140 (sl. 4, 5) lahko skozi delno odstranjen hrbtni del oklepa opazujemo posamezne sternite na prsnici, vendar spola ne moremo določiti. Moški zadek je ozek in trikotno koničast z ravnimi do rahlo konkavnimi stranicami, najširši v predelu tretjega somitnega segmenta (sl. 3B). Rep (ang. telson) je trikotne oblike, njegova dolžina je večja od širine.

Sl. 5. Kalcitna nanoflora.

1 – 5 *Helicosphaera waltrans* Theodoridis, 1984
6 *Helicosphaera walbersdorfensis* Müller, 1974
7 – 9 *Helicosphaera carteri* (Wallich, 1877) Kamptner, 1954
10 – 14 *Sphenolithus heteromorphus* Deflandre, 1953
15 *Calcidiscus premacintyrei* Theodoridis, 1984
16 *Umbilicosphaera rotula* (Kamptner, 1956) Varol, 1982
17 *Umbilicosphaera jafari* Müller, 1974
18 – 20 *Coccolithus miopelagicus* Bukry, 1971
21 – 22 *Coccolithus pelagicus* (Wallich, 1877) Schiller, 1930
23 *Pontosphaera multipora* (Kamptner, 1948) Roth, 1970
24 *Reticulofenestra pseudoumbilicus* (Gartner, 1967) Gartner, 1969
25 *R. haqii* Backman, 1978
26 *R. minuta* Roth, 1970
27 *Cyclicargolithus floridanus* (Roth & Hay, 1967) Bukry,1971
28 *Braarudosphaera bigelowii* (Gran et Braarud, 1935) Deflandre, 1947
29 *Discoaster variabilis* Martini & Bramlette, 1963
30 *Discoaster* spp.
Velikost vseh meril je 10 µm.

Fig. 5. Calcareous nannofossils.

1 – 5 *Helicosphaera waltrans* Theodoridis, 1984
6 *Helicosphaera walbersdorfensis* Müller, 1974
7 – 9 *Helicosphaera carteri* (Wallich, 1877) Kamptner, 1954
10 – 14 *Sphenolithus heteromorphus* Deflandre, 1953
15 *Calcidiscus premacintyrei* Theodoridis, 1984
16 *Umbilicosphaera rotula* (Kamptner, 1956) Varol, 1982
17 *Umbilicosphaera jafari* Müller, 1974
18 – 20 *Coccolithus miopelagicus* Bukry, 1971
21 – 22 *Coccolithus pelagicus* (Wallich, 1877) Schiller, 1930
23 *Pontosphaera multipora* (Kamptner, 1948) Roth, 1970
24 *Reticulofenestra pseudoumbilicus* (Gartner, 1967) Gartner, 1969
25 *R. haqii* Backman, 1978
26 *R. minuta* Roth, 1970
27 *Cyclicargolithus floridanus* (Roth & Hay, 1967) Bukry, 1971
28 *Braarudosphaera bigelowii* (Gran et Braarud, 1935) Deflandre, 1947
29 *Discoaster variabilis* Martini & Bramlette, 1963
30 *Discoaster* spp.
All scale bars are 10 µm

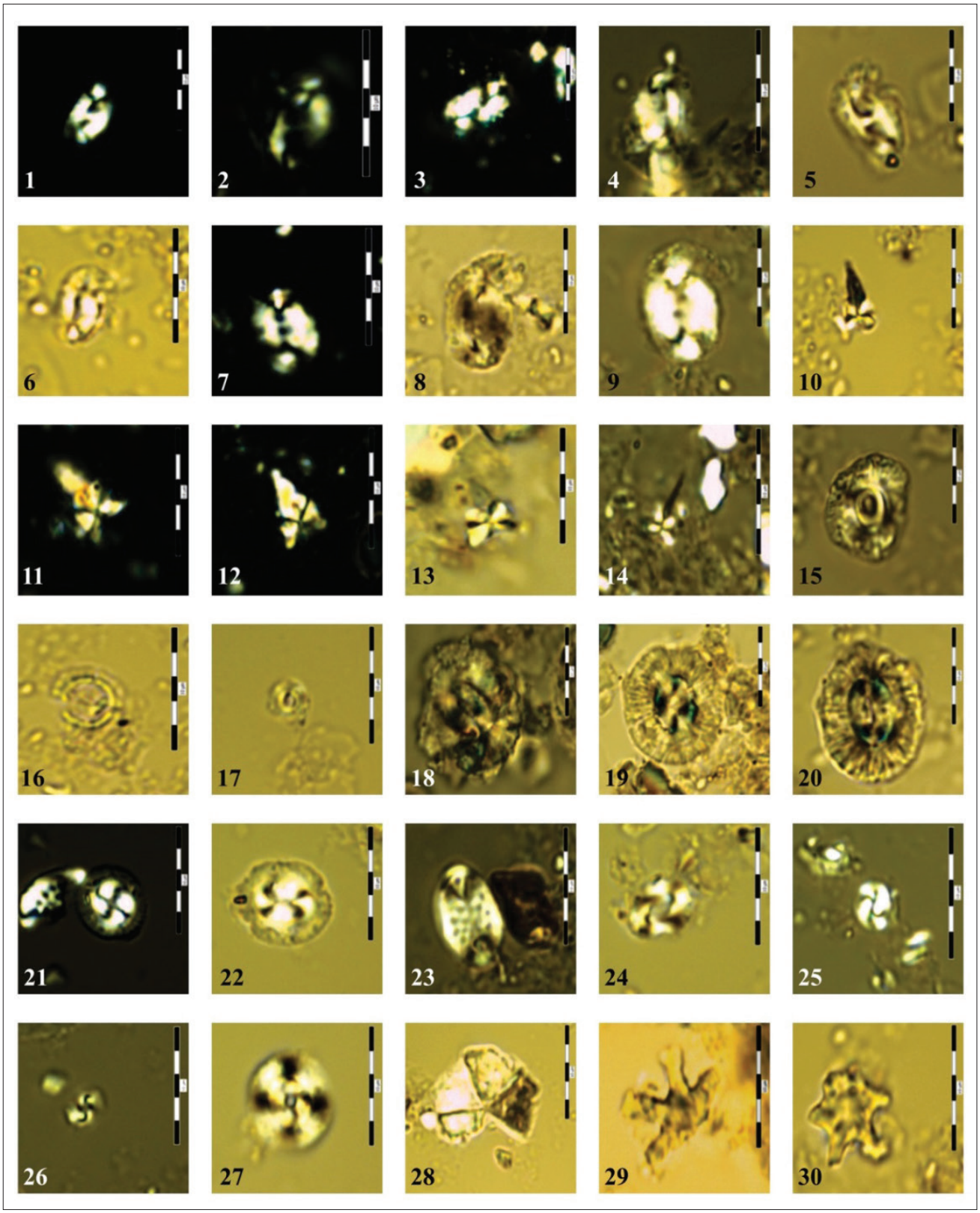
1
2
3
4
5
6
7
8
9
10
11
12
13
14
15
16
17
18
19
20
21
22
23
24
25
26
27
28
29
30

Somit 6 je skoraj kvadratne oblike in nekoliko širši kot dolg. Somiti 3–5 so zraščeni, pri primerku RGA/SMNH 1135 (sl. 4, 4) lahko opazimo tudi ostanek šiva med sicer negibljivima somitoma 3 in 4. Somita 1 in 2 v preiskovanem materialu nista ohranjena. Zanimiva je oblika sternita 8, ki je širok in v sredini prepognjen. Na njem leži pomožna kolčno-prsna plošča, ki varuje spolni kanal, v katerem pri moških osebkih leži penis.

Z oklepom povezane okončine so ohranjene le pri primerku iz Meljskega hriba (RGA/SMNH 1676) (sl. 4, 1). Hodilne okončine P2-P5 so tanke, dolge in neokleščene. Najdaljše so P4, medtem ko so P5 krajše in ležijo pod oklepom v posebej oblikovanih zajedah na spodnjem stranskem delu. Okončine so sploščene in ornamentirane s posameznimi manjšimi bradavicami. Zaključujejo se s koničastimi končnimi segmenti. Klešče so neenake, desne klešče nekoliko močnejše od levih, enostavne s tankimi prsti z zašiljenimi konicami in preprostimi zobmi na rezalni površini.

Primerjava: Posamezne lastnosti, ki rakovico *Styrioplax exiguus* uvrščajo med pripadnike družine Pilumnidae, sta opisala že Hyžný in Schlögl (2011), vendar sta menila, da najverjetneje pripada poddružini Rhizopinae; pred tem so to rakovico uvrščali v družino Goneplacidae (Glaessner, 1969). Pred kratkim opisan nov material (Gašparič & Hyžný, 2015) je razkril podrobnosti na prsnici moških primerkov, ki rakovico *Styrioplax exiguus* zanesljivo uvrščajo v družino Pilumnidae in podružino Chasmocarcininae, na kar sta sicer opozorila že Karasawa in Kato (2003).

Pripadniki poddružine Chasmocarcininae imajo trapezoidno obliko oklepa, dvojno oblikovan kljun, majhne očesne jamice s sinosoidnim sprednjim robom. Oklep je v predelu sprednjega roba približno enako širok kot zadaj, kljun in očesne jamice pa predstavljajo večji del sprednjega dela oklepa. V zadnjem stranskem delu imajo pripadniki te poddružine dobro razvite zajede za zadnji par hodilnih nog (Schweitzer & Feldmann, 2001). Za pripadnike Chasmocarcininae je značilno tudi, da so somiti 3–5 na zadku samcev zraščeni, hodilne noge pa so dolge in tanke (Feldmann et al., 2010). Vse naštete lastnosti lahko opazimo pri rodu *Styrioplax*, dodatno pa imajo primerki te rakovice razvito še pomožno kolčno-prsno ploščo na somitu 8 (Guinot et al., 2013).

Po opisanih morfoloških lastnostih bi rod *Styrioplax* lahko primerjali le s še danes živečim rodom *Chasmocarcinus* Rathbun, 1898, ki pa ima hrbtni oklep preprostejše morfologije z neizrazitimi osnovnimi hrbtnimi področji (želodčni in srčni predel, srednjepljučni greben), ki pa so pri rodu *Styrioplax* jasno opazni. Nekaj podobnosti v obliki in morfologiji oklepa lahko opazujemo s pripadniki rodu *Falconoplax* Van Straelen, 1933, ki pa imajo na sternitu 8 odprt spolni kanal in nimajo pomožne kolčno-prsne plošče. To pomembno morfološko lastnost si delijo pripadniki rodu *Styrioplax* in *Chasmocarcinus*.

Stratigrafska in paleogeografska razširjenost: Najdbe primerkov rodu *Styrioplax* so evidentirane iz spodnjemiocenskih (karpatskih) in srednjemiocenskih (badenijskih) plasti centralne Paratetide (Glaessner, 1928; Hyžný & Schlögl, 2011; Gašparič & Hyžný, 2015). Ostanki rakovic *Styrioplax exiguus* so pogosti v miocenskih plasteh severovzhodne Slovenije (Glaessner, 1928; Gašparič & Hyžný, 2015), kjer jih sedaj poznamo s šestih nahajališč (sl. 1), opisani pa so tudi iz miocenskih plasti karpatijske starosti na slovaškem nahajališču Cerova iz okolice Bratislave (Hyžný & Schlögl, 2011).

Do sedaj zbrani podatki kažejo na to, da je *Styrioplax exiguus* endemit na področju centralne Paratetide, fosilne ostanke te vrste pa najdemo izključno v finoklastičnih kamninah, ki so se odlagale v globjemorskih okoljih (Hyžný & Schlögl, 2011). Dejstvo, da fosilnih ostankov rakovice *Styrioplax exiguus* ne najdemo v miocenskih plasteh Mediterana potrjujejo teorijo, da je v srednjem miocenu anti-estuarijski morski režim preprečeval selitev organizmov iz področja Paratetide v takratni Mediteran (Harzhauser et al., 2007), po drugi strani pa organizmom iz Mediterana omogočal poselitev morskih območji Paratetide.

Kalcitni nanoplankton: Sl. 5, 1–30

V vzorcih iz obeh nahajališč je bilo pregledanih okoli 300 primerkov kalcitne nanoflore. Nanoplankton v pregledanih vzorcih je številčen, vendar je vrstna pestrost omejena le na nekaj značilnih taksonov. Nanofosili v vzorcih so različno dobro ohranjeni, od dobro ohranjenih primerkov do primerkov, pri katerih so opazne mehanske poškodbe in poškodbe nastale pri raztapljanju skeletov.

Opisano združbo definirajo pogosto pojavljanje ključne biostratigrafske vrste *Sphenolithus heteromorphus* Deflandre, 1953, skupaj s pogosto prisotnimi primerki vrste *Helicosphaera waltrans* Theodoridis, 1984 in redkimi primerki vrste *Helicosphaera walbersdorfensis* Müller, 1974. Opisano sopojavljanje omenjenih vrst je značilno za spodnjebadenijsko biocono NN5 (Martini, 1971). V pripravljenih vzorcih so pogosti tudi primerki vrst *Coccolithus pelagicus* (Wallich, 1877) Schiller, 1930, skupaj z velikimi primerki *Coccolithus miopelagicus* Bukry, 1971 in *Helicosphaera carteri* (Wallich, 1877) Kamptner, 1954. V analiziranih vzorcih se redko pojavljao še vrste *Calcidiscus premacintyrei* Theodoridis, 1984, *Pontosphaera multipora* (Kamptner, 1948) Roth, 1970, *Umbilicosphaera rotula* (Kamptner, 1956) Varol, 1982 in *U. jafari* Müller, 1974, *Reticulofenestra pseudoumbilicus* (Gartner, 1967) Gartner, 1969, *R. haqii* Backman, 1978 in *R. minuta* Roth, 1970, *Discoaster variabilis* Martini & Bramlette, 1963 ter *Thoracosphaera* sp.

Prisotni so tudi redki presedimentirani zgornjekredni nanofosili, npr. *Arkhangelskiella cymbiformis* Vekshina, 1959, in pogostejši presedimentirani peleocenski nanofosili, npr. *Discoaster lodoensis* Bramlette & Riedel, 1954 in *Reticulofenestra bisecta* (Hay, Mohler in Wade, 1966) Roth, 1970.

Stratigrafsko najpomembnejše je hkratno pojavljanje vrst *Sphenolithus heteromorphus* z *Helicosphaera waltrans* in odsotnost *H. ampliaperta* Bramlette and Wilcoxon, 1967, kar datira kamnine v spodnji del biocone NN5 (Martini, 1971) (sl. 2). Raziskana tafocenoza omogoča tudi korelacijo plasti z biocono NN5a (Grigorovič et al., 2001) oziroma z biohorizontom *Helicosphaera waltrans* (Švábenická, 2002; Ćorić & Švábenická, 2004). Pogostnost pojavljanja omenjene vrste v Paratetidi znotraj te biocone omenjajo tudi drugi avtorji (Grigorovič et al., 2001; Ćorić, 2003; Ćorić et al., 2007; Bartol, 2009). Tomanová Petrová in Švábenická (2007) povezujeta plasti iz horizonta *H. waltrans,* ki imajo bogato nanofloro, s transgresijo v spodnjebadenijskem globalnem evstatičnem ciklu TB2.3. Starost odloženih plasti na najdiščih Meljski hrib in Malečnik ocenjujemo na 14,91 do 14,36 milijonov let na podlagi zadnjega pogostega pojavljanja (LCO) vrste *Helicosphaera waltrans* (Abdul-Aziz et al., 2008) in zadnjega pojavljanja (LO) vrste *H. ampliaperta* (Lourens et al., 2004).

Sedimentacijsko okolje: Dosedanje najdbe rakovice *Styrioplax exiguus* so bile opisane iz globjemorskih sedimentacijskih okolij, kjer je na podlagi spremljajoče makrofavne in foraminifernih ter nanoplanktonskih združb določena paleobatimetrija med 125 in 250 m (Hyžný & Schlögl, 2011; Gašparič & Hyžný, 2015).

Poleg fosilnih ostankov deseteronožcev, globjemorsko sedimentacijsko potrjuje tudi foraminiferna favna (Rijavec, 1976; 1978) s pogosto makroskopsko opazno bentoško foraminifero *Bathysiphon taurinensis* Sacco, 1893, ki je značilna za globjemorska okolja (Saja et al., 2009).

Nizka vrstna raznolikost združbe fosilne kalcitne nanoflore s številčnimi helikosferami in redkimi diskoastri kaže na morsko okolje z normalno slanostjo in bližino kopnega (Ćorić & Švábenická, 2004). Prisotnost diskoastrov, pogosti primerki vrste *Coccolithus pelagicus* in številni majhni primerki retikulosferidnih vrst kažejo na dotok s hranili bogatih in hladnejših oceanskih vod (Ćorić& Rögl, 2004). Podobno velja za prisotnost vrste *Sphenolithus heteromorphus*, ki potrebuje s hranili še nekoliko bogatejše okolje kot diskoastri (Bartol & Pavšič, 2005). Zaradi prisotnosti presedimentiranih paleocenskih reliktov lahko sklepamo na bližino obale in z orogenetsko aktivnostjo povezano pogrezanje sedimentacijskega bazena.

Glede na navedeno ugotavljamo, da so se tudi plasti z najdbami rakovic *Styrioplax exiguus* na najdiščih Meljski hrib in Malečnik odlagale v globjemorskem okolju zgornjega batiala, v globini do 250 m. Nanoplanktonska združba kaže na globjemorsko priobalno okolje. Plasti so zapolnjevale enega izmed številnih sedimentacijskih bazenov, ki so se zaradi ekstenzijske tektonike hitro pogrezali, v to globjemorsko okolje pa je iz bližnjega kopnega dotekal drobnozrnat klastičen material.

Zaključki

Novo opisani primerki rakovice *Styrioplax exiguus* širijo poznavanje te zanimive vrste na našem ozemlju. Vrsta predstavlja endemitsko vrsto v miocenskih plasteh centralne Paratetide in velika večina do danes odkritih primerkov je najdena na področju severovhodne Slovenije. Vsi do sedaj najdeni primerki so opisani iz finoklastičnih globjemorskih sedimentov in potrjujejo teorijo, da je v srednjem miocenu anti-estuarijski morski režim preprečeval selitev organizmov iz področja Paratetide v takratni Mediteran.

Novi primerki in najdišča rakovice *Styrioplax exiguus* kažejo, da je bila to ena izmed najbolj razširjenih vrst deseteronožcev v miocenskih plasteh severovzhodne Slovenije. Posamezni primerki so najdeni tudi v podobnih miocenskih plasteh na Slovaškem in Madžarskem. S preko 80 pri nas najdenimi primerki je vrsta vsekakor pomemben del miocenske združbe deseteronožcev v Paratetidi.

Zahvale

Za fotografije primerkov shranjenih v graškem muzeju Joanneum se zahvaljujemo M. Hyžnýu (Univerza Comenius v Bratislavi, Fakulteta za naravoslovje, Oddelek za paleontologijo) ter A. Žibrat Gašparič (Univerza v Ljubljani, Filozofska fakulteta, Oddelek za arheologijo) za potrpežljivo lektoriranje. Del raziskav soavtorice Eve Halásove je podprt s strani Slovaške raziskovalne agencije s projektom št. APVV 0099-11.

Literatura

Abdul-Aziz, H., Di Stefano, A., Foresi, L. M., Hilgen, F. J., Iaccarino, S. M., Kuiper, K. F., Lirer, F., Salvatorini, G. & Turco, E. 2008: Integrated stratigraphy and 40Ar/39Ar chronology of early Middle Miocene sediments from DSDP Leg 42A, Site 372 (Western Mediterranean). Palaeogeography, Palaeoclimatology, Palaeoecology, 257/1–2: 123–138, doi:10.1016/j.palaeo.2007.09.013.

Backman, J. 1978: Late Miocene - Early Pliocene nannofossil biochronology and biogeography in the Vera Basin, SE Spain. Stockholm Contributions in Geology, 32: 93–114.

Bartol, M. & Pavšič, J. 2005: Badenian discoasters from the section in Lenart (Northeast Slovenia, Central Paratethys). Geologija, 48/2: 211–223, doi:10.5474/geologija.2005.018.

Bartol, M. 2009: Middle Miocene calcareous nannoplankton of NE Slovenia (western Central Paratethys). Založba ZRC/ZRC Publishing, Ljubljana: 136 p.

Bramlette, M. N. & Riedel, W. R. 1954: Stratigraphic value of discoasters and some other microfossils related to Recent coccolithophores. Journal of Paleontology, 28: 385–403.

Bukry, D. 1971: Cenozoic calcareous nannofossils from the Pacific Ocean. San Diego Society of Natural History Transactions, 16: 303–327.

Ćorić, S. 2003: Calcareous nannofossils biostratigraphy of the Mühlbach beds (Gaindorf Formation, Lower Badenian). Annalen des Naturhistorischen Museums in Wien, 104A: 15–21.

Ćorić, S. & Švábenická, L. 2004: Calcareous nannofossil biostratigraphy of the Grund Formation (Molasse Basin, Lower Austria). Geologica Carpathica, 55/2: 147–153.

Ćorić, S., Švábenická, L., Rögl, F. & Petrova, P. 2007: Stratigraphical position of *Helicosphaera waltrans* nannoplankton horizon (NN5, Lower Badenian). Joannea / Geologie und Paläontologie, 9: 17–19.

Deflandre, G. 1947: *Braarudosphaera* nov. gen., type d'une famille nouvelle de Coccolithophorides actuels a elements composites. Comptes Rendus (Hebdomadaires des Séances) de l'Académie des Sciences Paris, 225: 439–441.

Deflandre, G. 1953: Hétérogénéité intrinsèque et pluralité des éleménts dans les coccolithes actuels et fossiles. Comptes Rendus (Hebdomadaires des Séances) de l'Académie des Sciences Paris, 237: 1785–1787.

De Grave, S., Pentcheff, N. D., Ahyong, S. T., Chan, T. Y., Crandall, K. A., Dworschak, P. C., Felder, D. L., Feldmann, R. M., Fransen, C. H. J. M., Goulding, L.Y. D., Lemaitre, R., Low, M. E. Y., Martin, J. W., Ng, P. K. L., Schweitzer, C. E., Tan, S. H., Tshudy, D. & Wetzer, R. 2009: A classification of living and fossil genera of decapod crustaceans. The Raffles Bulletin of Zoology, Supplement, 21: 1–109.

Feldmann, R. M., Schweitzer, C. E. & Encinas, A. 2010: Neogene Decapod Crustacea from southern Chile. Annals of Carnegie Museum, 78/4: 337–366, doi:10.2992/007.078.0404.

Gartner, S. 1967: Calcareous nannofossils from Neogene of Trinidad, Jamaica, and Gulf of Mexico. Paleontological Contributions, University of Kansas, 29: 1–7.

Gartner, S. 1969: Correlation of Neogene planktonic foraminifera and calcareous nannofossil zones. Transactions of the Gulf Coast Association of Geological Societies, 19: 585–599.

Gašparič, R. & Hyžný, M. 2015: An early Miocene deep-water Decapod Crustacean Faunule from the slovenian part of the Styrian Basin and its palaeoenvironmental and palaeobiogeographical significance. Papers in Palaeontology, 1/2: 141–166, doi:10.1002/spp2.1006.

Glaessner, M. F. 1928: Die Dekapodenfauna des Österreichischen Jungtertiars. Jahrbuch der Geologischen Bundesanstalt, 78: 161–219.

Glaessner, M. F. 1929: Crustacea Decapoda. 1-464. In: Pompeckj, J. F. (ed.): Fossilium Catalogus I: Animalia, 41. W. Junk, Berlin.

Glaessner, M. F. 1969: Decapoda. In: Moore, R. C. (ed.): Treatise on Invertebrate Paleontology, Pt. R4. Geological Society of America & University of Kansas Press, 400–533.

Guinot, D., Tavares, M. & Castro, P. 2013: Significance of the sexual openings and supplementary structures on the phylogeny of brachyuran crabs (Crustacea, Decapoda, Brachyura), with new nomina for higher-ranked podotreme taxa. Zootaxa, 3665/1: 1–414, doi:10.11646/zootaxa.3665.1.1

Harzhauser, M., Kroh, A., Mandic, O., Piller, W. E., Göhlich, U., Reuter, M. & Berning, B. 2007: Biogeographic responses to geodynamics: A key study all around the Oligo–Miocene Tethyan Seaway. Zoologische Anzeiger: A Journal of Comparative Zoology, 26/4: 241–256, doi:10.1016/j.jcz.2007.05.001.

Hyžný, M. & Schlögl, J. 2011: An early Miocene deep-water decapod crustacean faunule from the Vienna basin (Western Carpathians, Slovakia). Palaeontology, 54/2: 323-349.

Jelen, B. & Rifelj, H. 2002: Stratigraphic structure of the B1 Tertiary tectonostratigraphic unit in Eastern Slovenia. Geologija, 45/1: 115-138, doi:10.5474/geologija.2002.010.

Kamptner, E. 1954: Untersuchungen über den Feinbau der Coccolithen. Anzeiger. Österreichische Akademie der Wissenschaften. Mathematische-Naturwissenschafliche Klasse. 87: 152–158.

Karasawa, H. & Kato, H. 2003: The family Goneplacidae MacLeay, 1838 (Crustacea: Decapoda: Brachyura): systematics, phylogeny, and fossil records. Paleontological Research, 7: 129–151, doi:10.2517/prpsj.7.129.

Kováč, M., Andreyeva-Grigorovich A., Bajraktarević Z., Brzobohatý R., Filipescu S., Fodor L., Harzhauser M., Oszczypko N., Pavelic D., Rögl F., Saftić B., Sliva L. & Studecka B. 2007: Badenian evolution of the Central Parathethys sea: paleogeography, climate and eustatic sea level changes. Geologica Carpathica, 58: 579–606

Križnar, M. 2006: Najdba ostankov rakovic rodu Marcophthalmus (Decapoda, Brachyura) iz miocenskih plasti Tuhinjske doline. Kamniški zbornik, 18: 309–314.

Križnar, M. & Preisinger, D. 2008: Rak Coeloma iz govške formacije Tunjiškega gričevja. Kamniški zbornik, 19: 335–338.

Linnaeus, C. 1758: Systema naturae per regna tria naturae, secundum classes, ordines, genera, species, cum characteribus, differentis, synonymis, Locis. Holmiae: Laur. Salvii: 824 p.

Lourens, L., Hilgen, F., Shackleton, N. J., Laskar, J. & Wilson, J. 2004: The Neogene period. In: Gradstein, F., Ogg, J. & Smith, A. (eds.): A Neogene time scale 2004. Cambridge University press, Cambridge, 409–440.

MacLeay, W. S. 1838: On the brachyurous decapod Crustacea brought from the Cape by Dr. Smith. 1862. In: Smith, A. (ed.): Illustrations of

the zoology of South Africa; consisting chiefly of figures and descriptions of the objects of natural history collected during an expedition into the interior of South Africa, in the years 1834, 1835, and 1836; fitted out by 'The Cape of Good Hope Association for Exploring Central Africa:' together with a summary of African zoology, and an inquiry into the geographical ranges of species in that quarter of the globe. Published under the authority of the Lords Commissioners of Her Majesty's Treasury, Invertebratae: 53–71.

Martini, E. 1971: Standard Tertiary and Quaternary Calcareous Nannoplankton Zonation.In: Farinacci, A. (ed.): Proceedings of the II Planktonic Conference. Edizioni Tecnoscienza, 2: 739–785.

Martini, E. & Bramlette, M. N. 1963: Calcareous nannoplankton from the experimental Mohole drilling. Journal of Paleontology, 37: 845–855.

Mikuž, V. 2003: Miocenske rakovice iz okolice Šentilja v Slovenskih Goricah = The Miocene crabs from vicinity Šentilj in Slovenske Gorice, Slovenia. Razprave IV. razreda SAZU, 44: 187–199.

Mikuž, V. 2010a: Ostanek eocenske rakovice iz kamnoloma Griža = The remain of eocene crab from Griža quarry, Slovenia. Folia biologica et geologica, 51/1: 21–26.

Mikuž, V. 2010b: Rakovice iz srednjemiocenskih plasti kamnolomov nad Trbovljami. Folia biologica et geologica, 51/1: 13–20.

Mikuž, V. & Gašparič, R. 2014: Nekaj redkih fosilov iz Slovenskih goric. Geologija, 57/2: 155-166, doi:10.5474/geologija.2014.013.

Mikuž, V. & Pavšič, J. 2003: »Kranjska rakovica« iz srednjemiocenskih – badenijskih skladov kamnoloma Lipovica nad Brišami. Geologija, 46/2: 245–250, doi:10.5474/geologija.2003.021.

Mioč, P. & Žnidarčič, M. 1977: Osnovna geološka karta SFRJ 1:100.000, List Slovenj Gradec, L33-55. Zvezni geološki zavod Beograd.

Müller, C. 1974: Nannoplankton aus dem Mittel-Miozän von Walbersdorf (Burgenland). Senckenbergiana lethaea, 55: 389–405.

Ng, P. K. L., Guinot, D. & Davie, P. J. F. 2008: Systema Brachyurorum Part I: An annotated checklist of extant Brachyuran Crabs of the World. The Raffles Bulletin of Zoology, 17: 1–286.

Pavlovec, R. & Pavšič, J. 1987: Biostratigrafija plasti z rakovicami v Istri = Biostratigraphy of beds with crabs from Istria. Geologija, 28/29, 55–68.

Pavšič, J. & Horvat, A. 2009: Eocene, Oligocene and Miocene in Central and Eastern Slovenia. In: Pleničar, M., Ogorelec, B. & Novak, M. (eds.): The Geology of Slovenia, Geološki zavod Slovenije, 373–426.

Placer, L. 1999: Prispevek k makrotektonski rajonizaciji mejnega ozemlja med Južnimi Alpami in Zunanjimi Dinaridi =Contribution to the macrotectonic subdivision of the border region between Southern Alps and External Dinarides. Geologija, 41, 223–255, doi:10.5474/geologija.1998.013.

Rathbun, M. J. 1898: The Brachyura of the biological expedition to the Florida Keys and the Bahamas in 1893. Bulletin from the Laboratories of Natural History of the State University of Iowa, 4/3: 294 p.

Rifelj, H. & Jelen, B. 2001: Do the Karpatian and Badenian microforaminiferal faunas of Slovenia reflect global climatic and tectonic changes? Geološki zbornik, 16: 34–41.

Rijavec, L. 1976: Biostratigrafija miocena v Slovenskih goricah = Biostratigraphy of Miocene Beds from Slovenske Gorice. Geologija, 19: 53–79.

Rijavec, L. 1978: Tortonska in sarmatska mikrofavna v zahodnem delu Slovenskih goric =. Tortonian and Sarmatian microfauna from the Western Slovenske Gorice hills. Geologija, 21/2: 209–238.

Roth, P. H. 1970: Oligocene calcareous nannoplankton biostratigraphy. Eclogae Geologicae Helvetiae, 63: 799–881.

Rögl, F. 1999: Mediterranean and Paratethys. Facts and hypotheses of an Oligocene to Miocene Paleogeography (short overview). Geologica Carpathica, 59: 339–349.

Sacco, F. 1893: Le genre Bathysiphon a l'etat fossile. Bulletin de la Société géologique de France, 21 p.

Saja, D. B., Pfefferkorn, H. W. & Phipps, S. P. 2009: Bathysiphon (Foraminiferida) at Pacheco Pass, California: a geopetal, paleocurrent, and paleobathymetric indicator in the Franciscan Complex. Palaios, 24: 181–191.

Schiller, J. 1930: Coccolithineae. In: Rabenhorst, L. (ed.): Kryptogamen-Flora von Deutschland, Österreich und der Schweiz. Akademische Verlagsgesellschaft, 89–267.

Schweitzer, C. E. & Feldmann, R., M. 2001: Differentiation of the fossil Hexapodidae Miers, 1886 (Decapoda: Brachyura) from similar forms. Journal of Paleontology, 75: 330–345.

Serène, R. 1964: Redescription du genre *Magasthesius* Rathbun et definition des Chasmocarcininae, nouvelle sous-famille des Goneplacidae (Decapoda, Brachyura). Crustaceana, 7: 175–187.

Švábenická, L. 2002: Calcareous nannofossils of the Upper Karpatian and Lower Badenian deposits in the Carpathian Foredeep, Moravia (Czech Republic). Geologica Carpathica, 53/3: 197–210.

Theodoridis, S. 1984: Calcareous nannofossil biostratigraphy of the Miocene and revision of the helicoliths and discoasters. Utrecht Micropaleontological Bulletin, 32: 1–271.

Tomanová Petrová, P. & Švábenická, L. 2007: Lower Badenian biostratigraphy and paleoecology: a case study from the Carpathian Foredeep (Czech Republic). Geol. Carpathica, 58/4: 333–352.

Van Straelen, V. 1933: Sur des Crustaces Decapodes Cenozoiques du Venezuela. Bulletin du Musee Royal d'Histoire Naturelle de Belgique, 9/10: 1–14.

Vekshina, V. N. 1959: Coccolithophoridae of the Maastrichtian deposits of the West Siberian lowlands. Siberian Science Research Institute of Geology Geophysics Mineralogy and Raw Materials, 2: 56–81.

Young, J. R. 1998: Neogene. In: Bown, P.R. (ed.): Calcareous Nannofossil Biostratigraphy. British Micropalaeontological Society Publications Series. Chapman & Hall, 225–265.

Žnidarčič, M. & Mioč, P. 1987: Osnovna geološka karta SFRJ 1:100.000, list Maribor in Leibnitz, L33-56, L33–44, Zvezni geološki zavod, Beograd.

GEOLOGIJA *58/2*, 213–220, Ljubljana 2015

http://dx.doi.org/10.5474/geologija.2015.017

Occurrence of Samarskite-Y in the Mineralized Umm Lassifa Pegmatite, Central Eastern Desert, Egypt

Mohamed Fahmy RASLAN

Nuclear Materials Authority, P.O. Box. 530, El Maadi, Cairo, Egypt e-mail: raslangains@hotmail.com

Prejeto / Received 5. 7. 2015; Sprejeto / Accepted 10. 12. 2015; Objavljeno na spletu / Published online 30. 12. 2015

Key words: Samarskite-Y, microprobe analysis, Umm Lassifa granitic pegmatite, Eastern Desert, Egypt.

Abstract

Samarskite-Y, with an average assay of about 43.23% Nb_2O_5 and 17.43% Y_2O_5 has been identified in the mineralized pegmatite bodies injected in Gabal Umm Lassifa monzogranite. The mineral is associated with columbite, zircon, monazite, cassiterite, ilmenite and rutile. The mineralogy and geochemistry of the studied samarskite variety were determined using microscopic examination and X-ray Diffraction (XRD) as well as quantitative analysis by both Field emission scanning electron microscope and electron microprobe analysis. Microscopic investigation revealed that the defined samarskite crystals are characteristically velvet-yellow brown to bloody red in color and having a characteristic pendent vitreous or resinous luster.

Analytical data confirmed the presence of samarskite-Y whose composition corresponding to empirical formula: $[(Y_{0.42}, REE_{0.44}, Th_{0.076}, Si_{0.05}, Ca_{0.007}, U_{0.07}, Fe_{0.077})\ \Sigma_{1.15}\ (Nb_{0.81}, Ta_{0.04}, Ti_{0.14})\ \Sigma_{0.86}\ O_4]$. Accordingly, the mineralized Umm Lassifa pegmatite can be considered as a promising target ore for its rare-metal mineralization that includes mainly Nb, Ta, Y, REE and Zr together with U and Th.

Introduction

Several studies worldwide have revealed the presence of granite-pegmatite-hosted rare-metal mineralization including Nb-Ta oxides and zircon (e.g., Matsubara et al., 1995; Hanson et al., 1999; Erict, 2005; William et al., 2006; Pal et al., 2007; Raslan et al., 2010). The Umm Lassifa area is located some 70 km to the southwest of El Qusier city at the Red Sea Coast, Central Eastern Desert of Egypt. It lies between longitudes 34° 12' and 34° 20' E and latitudes 25° 36' and 25° 38' N (Fig.1). Several workers studied the regional geology of the studied area (e.g., Amin & Mohamed, 1954; Kamal El-Din.; 1995, Khudier et al., 1995; Ali, 2001, Abdel Wahed et al., 2005).

The studied pegmatites present in the monzogranite of Umm Lassifa pluton are restricted to along the contact with granodiorite (Fig. 1). The monzogranite forms the main granitic mass of Umm Lassifa pluton. The studied pegmatites occur either as small pockets or as vein like bodies and usually of composite type. These pegmatite bodies are of variable size ranging between 1–3 m in width and 2–6 m in length (Fig.1). The mica pockets are common and restricted in association with feldspar.

Most occurrences of radioactive minerals of Egypt are in granites and associated pegmatites. Several Nb-Ta occurrences have been recorded in different localities of the Eastern Desert, namely, El Naga, Abu Khurg, Abu Dabbab, Noweibi, and Abu Rushied (Hussein, 1990; Raslan & Ali, 2011). It is interesting in this regard to mention that author identified Samarskite-Y, columbite and zircon from Ras Baroud granite –pegmatite in the Central Eastern Desert (Raslan et al., 2010) and in the stream sediments surrounding the Ras Baroud granitic pluton (Raslan, 2009). Moreover, ishikawaite (uranium-rich samarskite) with an average assay of approximately 50% Nb_2O_5 and 26% UO_2 has been identified for the first time in Egypt in the mineralized Abu Rushied gneissose granite (Raslan, 2008).

Abu Rushied gneissose granite (Raslan, 2008). In addition, Raslan and Ali (2011) identified ferrocolumbite, ishikawaite, uranopyrochlore, and fergusonite in the rare-metal pegmatites of Abu Rushied granitic gneisses. Accordingly, the aim of the present paper is to identify the mineralogical and geochemical characteristics of samarskite-Y variety in the studied area.

Methodology

To verify the objectives of this study, a representative sample of the mineralized Umm Lassifa pegmatite was collected. The sample was properly crushed, ground and sieved to size fractions between 0.800 mm – 0.063 mm before subjecting to heavy liquid separation using

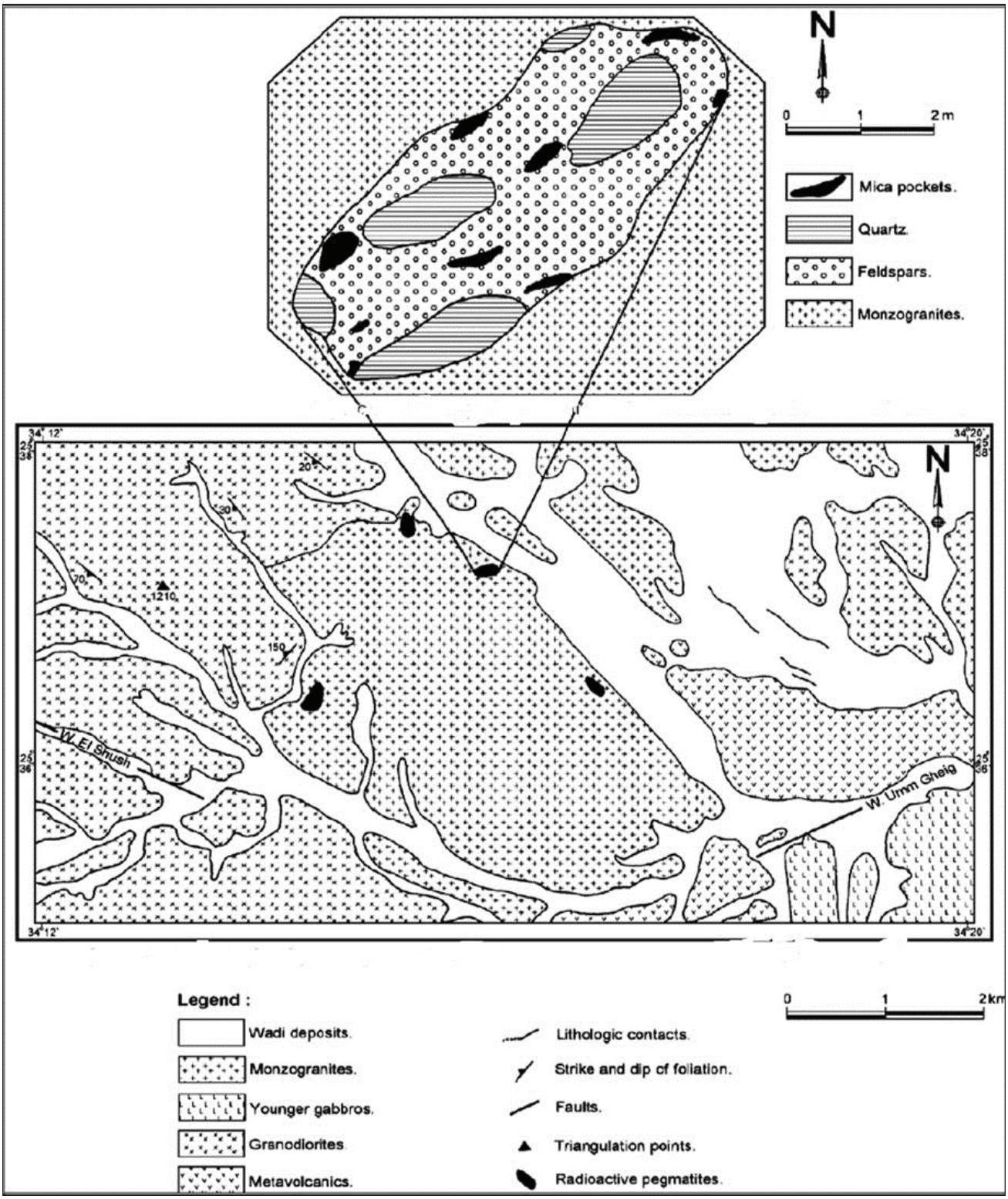

Fig.1. Geologic map of G. Umm Lassifa, Central Eastern Desert, Egypt and sketch showing the studied composite pegmatite pocket in the monzogranite of G. Umm Lassifa.

bromoform (specific gravity=2.85 gm/cm^3). From the obtained heavy fractions, pure mineral grains of samarskite variety were handpicked and investigated under the binocular microscope. Some of the picked mineral grains were subjected to X-ray Diffraction analysis using a Phillips X-ray diffractometer (Model PW-105018) with a scintillation counter (Model PW-25623/00) and Ni filter and an environmental scanning electron microscope (ESEM). This instrument includes Philips XL 30 energy-dispersive spectrometer (EDS) unit. The applied analytical conditions were an accelerating voltage of 30 kV with a beam diameter of 1–2 μm for a counting time of 60-120 s and a minimum detectable weight concentration ranging from 0.1 to 1 wt%. All these analyses were carried out at the laboratories of the Egyptian Nuclear Materials Authority (NMA).

In addition, the studied samples were analyzed using the field emission scanning electron microscope (JEOL 6335F) at the Particle Engineering Research Center (PERC), University of Florida, USA. This instrument is fitted with an Oxford Energy Dispersive X-ray spectrometer (EDS) for elemental analysis of micro areas, a backscattered electron detector that allows compositional imaging. The applied analytical conditions were an accelerating voltage of 0.5 – 30 kV, 1.5 nm (at 15 kV/5.0 nm (at 1.0 kV). The imagining modes were secondary electron imaging (SEI) and backscatter electron imaging (BEI). Lines scan of relative concentrations of multiple elements, and X-ray maps of relative concentrations of multiple elements were also performed.

Finally, thin, polished sections of some mineral grains were also analyzed using a JEOL Superprobe 733, at the Particle Engineering Research Center (PERC), University of Florida, USA, with an accelerating voltage of 15 kV and a beam size of approximately 1 µm. The used standards for analysis included niobium metal (for Nb), tantalum metal (for Ta), biotite (for Ti-Fe-Si), uranium metal (for U), monazite (for Th), fluorite (for Ca), and cubic zirconia (for Zr-Y).

Results and discussion

Microscopic investigation

Under the binocular microscope, the examined samarskite crystals were found to be distributed in almost all size fractions between 0.800 mm - 0.063 mm. The defined samarskite crystals are generally massive with a granular form and having a characteristic vitreous or resinous luster (Fig. 2). Also, the investigated mineral crystals are generally translucent, compact, metamict and hard. Under a polarizing microscope, the samarskite grains are mainly velvet-yellow brown to bloody red in colour (Figs.3 A,B,C and D). They occur as translucent grains that are 0.1– 0.5 mm in size (Fig.3). Separated samarskite grains are present as short prismatic to tabular crystals, exhibiting vitreous luster and conchoidal fractures. Samarskite grains commonly exhibit partial to complete alteration effects along micro cracks and grain boundaries as well as the metamictization effect (Fig.3). Altered varieties are darker brownish to opaque in thin sections and whitish grey in reflected light (Figs.3E and F).

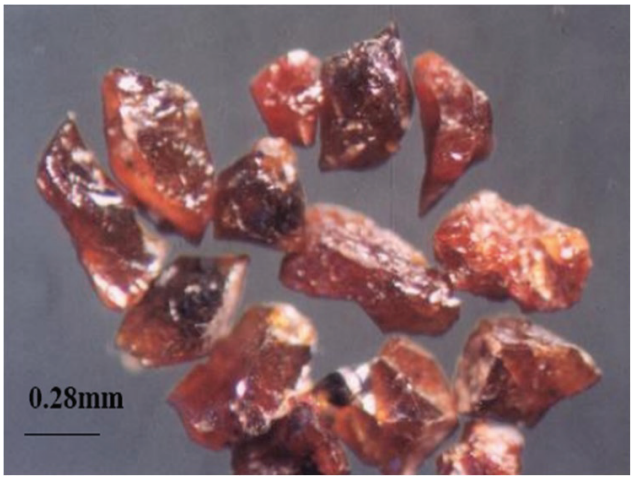

Fig. 2. Samarskite-Y crystals exhibiting massive granular shape with reddish brown colour, Binocular microscope

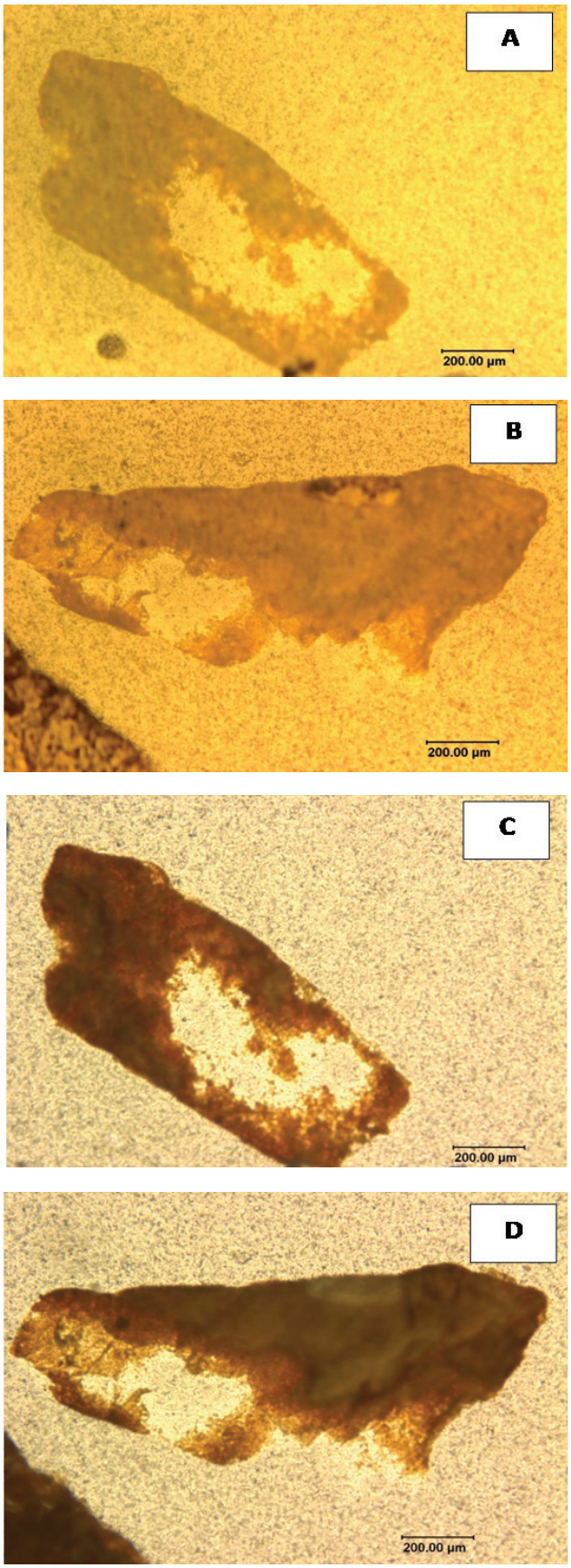

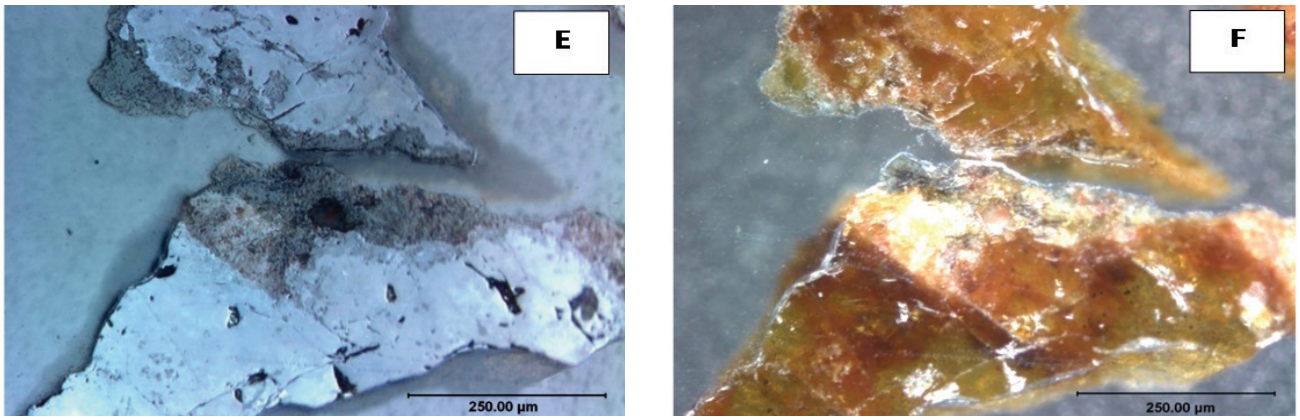

Fig. 3. Umm Lassifa samarskite-Y crystals in thin sections:

A–B: velvet-yellow brown to bloody red crystals exhibit partial to complete alteration effects along micro cracks and grain boundaries, Polarized light, PL. C–D: The same crystals as in previous photos between crossed Nichols, C.N. E–F: Altered crystals showing variation in colour between reflected light and crossed Nichols respectively.

X-ray Diffraction

Pure monomineralic sample from samarskite grains was prepared by hand picking and subjected to XRD analyses. The obtained XRD data for samarskite after annealing (heat treatment) are presented in (Fig. 4). The data conforms to the ASTM card index No. 2-0690 for samarskite.

Scanning electron microscope study

ESEM data of the studied samarskite grains (Figs. 5A and B) show that the mineral is enriched in Nb and Y whereas the contents of the other REEs are much lower such as Ce, Nd, Sm, Gd and Yb. Uranium and thorium are commonly present as minor elements. On the other hand, several samarskite grains have also been subjected to semi-quntitative analyses using a field emission scanning electron microscope coupled with EDS. The obtained EDS data (Figs. 5E and F) show Nb,Y and REE as the essential components and U and Th as minor elements, which confirmed the ESEM/EDS results. The distribution of uranium and thorium within the crystal is actually heterogeneous and their contents increase in the bright parts within the crystal and also with increasing Y. Scan- line elemental analyses along the crystals (Figs. 5C and D) and the elemental scan maps for some samarskite crystals reflect the predominant elements in the mineral such as Nb and Y (Fig. 6). The presence of Br and Rb indicated in Figs. 5e, f and Fig. 6 is probably a result of spectral overlap between Al Kα and Br Lα peaks, and between Rb Lα and Si Kα.

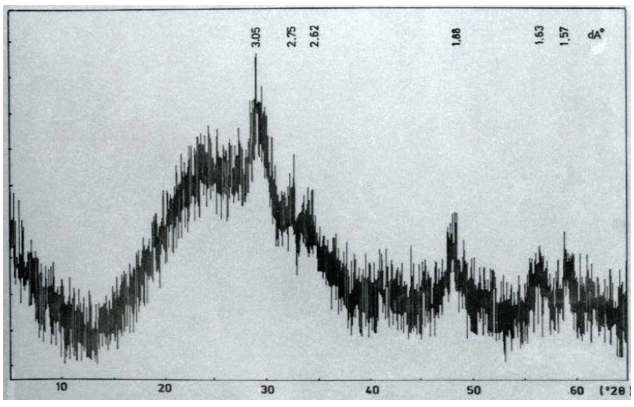

Fig. 4. XRD diffractogram for samarskite (ASTM card No. 2-0690).

Electron microprobe analyses

The obtained microprobe analyses (Table 1) of the investigated samarskite have resulted in the following average composition in wt%: Nb_2O_5, 43.23; Ta_2O_5, 3.66; TiO_2, 0.44; UO_2, 4.38; ThO_2, 4.65; Y_2O_3, 17.43; MnO, 0.32; CaO, 0.26; FeO, 2.30; $SiO_2$1.74 and total REE of 22.09 with an average sum of 100.50 wt%. Table 1 shows the chemical empirical formulae that is recalculated on the basis of 4 oxygen; viz, $[(Y_{0.35}, REE_{0.44}, Th_{0.07}, Si_{0.05}, Ca_{0.007}, U_{0.07}, Fe_{0.07}) \Sigma_{1.05} (Nb_{0.67}, Ta_{0.55}, Ti_{0.01}) \Sigma_{0.74} O_4]$. The microprobe analyses were plotted on a ternary diagram of Hanson et al., (1999) which shows the A-site occupancy of the samarskite group of minerals (Fig. 7). It was found that all the data points plot in the samarskite-Y field.

Samarskite belongs to a group of Nb-Ta mineral varieties that occur in granite pegmatite and have the general formula $A_m B_n O_{2(m+n)}$, where A represents Fe, Ca, REE,Y, U and Th whereas B represents Nb, Ta and Ti. According to Hanson et al., (1999), samarskite –group minerals should include only those that have Nb>Ta and Ti in the B-site. Additionally, this group of minerals contains at least three species based on A-site chemistry. If REE+Y are dominant, the name samarskite-(REE+Y) should be used with the dominant of these cations as a suffix. If U+Th is dominant, the mineral is properly named ishikawaite whereas if Ca is dominant, the mineral should be named calciosamarskite. However, the exact nature of these minerals cannot be determined due to inability to quantify the valence state of iron present and dominant at the A-site in these minerals. Ishikawaite and calciosamarskite are light rare-earth element (LREE) depleted and heavy rare-earth element (HREE) enriched with Y dominant. Recently, samarskite-Yb has been identified as a new species of the samarskite group (William et al, 2006). Nickel and Mandrino (1987) described samarskite-Y as a mineral with Y+REE dominant at A-site.

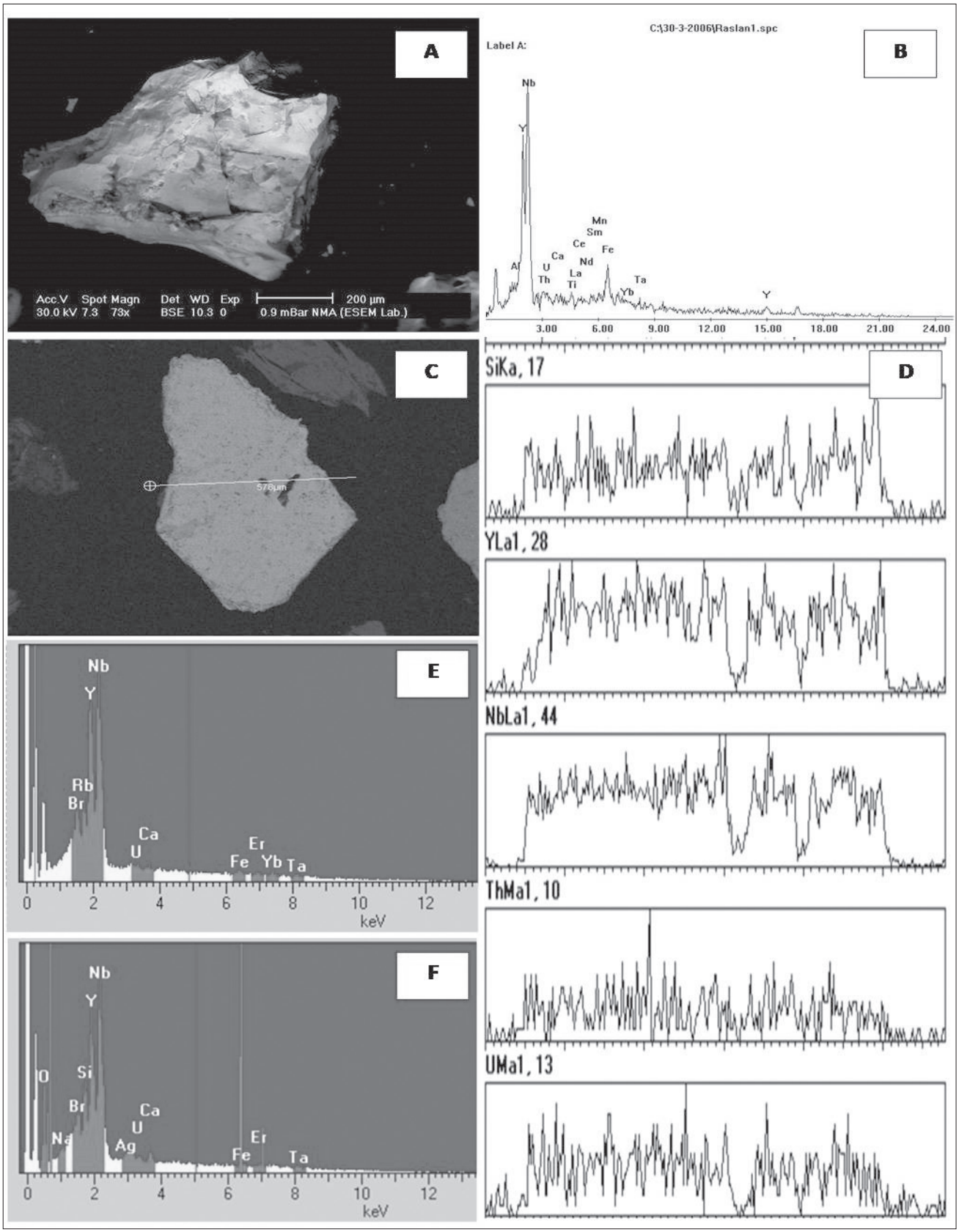

Fig. 5. SEM data of Umm Lassifa samarskite-Y. A–B: Backscattered electron image and corresponding EDX spectrum. C–D: BEI of a samarskite crystal with scan-line and its elemental scan-line analyses. E–F: EDX spectrum of samarskite-Y.

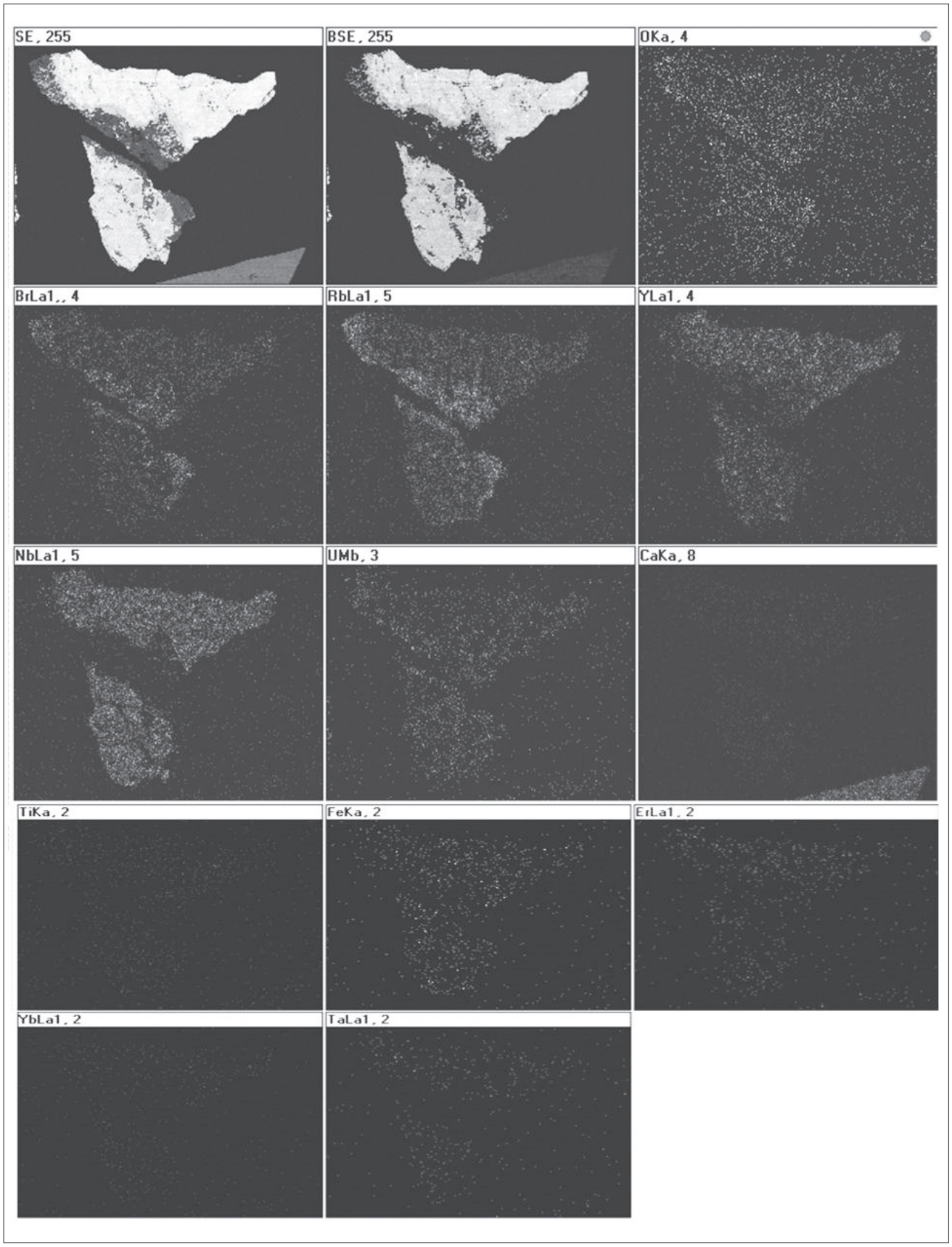

Fig. 6. Scan-maps showing the distribution of major and minor elements within samarskite-Y crystals.

From the obtained data, it is quite clear that the studied Nb-Ta mineral variety of Umm Lassifa pegmatite reflects the chemical composition of Y- and REE-rich samarskite species. The lines of evidence of the latter (samarskite-Y) can be summarized as follows:

1. The obtained EMPA data revealed that Nb_2O_5 is dominant in the investigated mineral where it attains content of 43.23 wt% in average. The sum of average content of Ta_2O_5 and TiO_2 attains 4.10 wt%, which is much lower than content of Nb_2O_5. The samarskite group comprises only those species in which the Nb content in B-site is higher than that of Ta and Ti. (Hanson et al., 1999).

2. The studied mineral actually falls within the compositional limits of both samarskite-Y and ishikawaite. Both samarskite-Y and ishikawaite have a dominant Nb in the B-site and the distinction between the two varieties must be based on the content of A-site occupancy.

3. In the studied Umm Lassifa samarskite species, the Y_2O_5 content ranges from 16.25 wt% to 18.87 wt% with an average of 17.43 wt% and the sum of REE ranges from 18.20 wt% to 24.19 wt% with an average of 22.09 wt%. Accordingly, the average Y+REE would attain up to 39.52% and samarskite-Y has been described as the mineral species in which Y+REE are the dominant components at the A-site (Nickel & Mandarino, 1987).

4. The studied samarskite species separated from Umm Lassifa pegmatite is characterized by the dominance of Y+REE in the A-site whereas Nb in the B-site is higher than both Ta+Ti. Therefore, the studied mineral species belongs to the compositional limits of samarskite-Y mineral species as specified in the literature.

Table 1. Selected EMPA analyses of samarskite-Y from Umm Lassifa pegmatite. Oxide contents are in wt%.

Oxides	Samarskite-Y				Average
	1	2	3	4	
TiO_2	*0.54*	*0.20*	*0.57*	*0.46*	0.44
Nb_2O_5	*46.42*	*43.54*	*42.24*	*40.70*	43.23
SiO_2	*0.72*	*0.65*	*2.99*	*2.61*	1.74
Ta_2O_5	*2.53*	*3.53*	*5.13*	*3.46*	3.66
MnO	*0.25*	*0.36*	*0.12*	*0.55*	0.32
UO_2	*2.60*	*4.01*	*6.60*	*4.32*	4.38
CaO	0.15	0.18	0.48	0.23	0.26
ThO_2	*4.72*	*3.80*	*6.36*	*3.71*	4.65
FeO•	*1.56*	*1.19*	*2.72*	*3.74*	2.30
Y_2O_5	*17.05*	*17.55*	*16.25*	*18.87*	17.43
∑REE	22.50	24.19	18.20	23.48	22.09
Total	99.04	99.20	101.66	102.13	100.50
Chemical formula of Samarskite-Y based on 4 oxygen					
Ti	0.017	0.006	0.018	0.014	0.014
Nb	0.87	0.83	0.80	0.75	0.81
Si	0.02	0.02	0.09	0.08	0.05
Ta	0.03	0.04	0.06	0.04	0.04
Mn	0.009	0.013	0.004	0.019	0.01
U	0.04	0.06	0.11	0.07	0.07
Ca	0.004	0.005	0.013	0.006	0.007
Th	0.07	0.067	0.11	0.06	0.076
Fe	0.05	0.04	0.09	0.13	0.077
Y	0.41	0.43	0.39	0.44	0.42
∑REE	0.45	0.48	0.36	0.46	0.44
Sum A	1.05	1.11	1.17	1.26	1.15
Sum B	0.917	0.876	0.878	0.804	0.86

FeO•= total iron as oxide

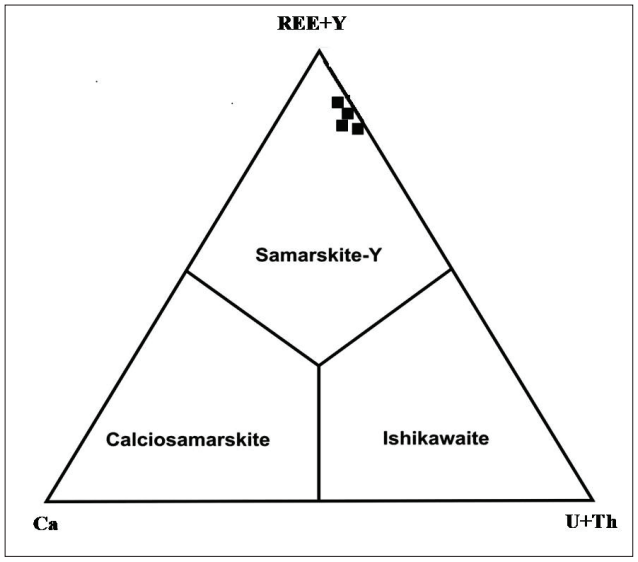

Fig. 7. Ternary diagram showing A-site occupancy of the samarskite group of minerals after Hanson et al. (1999). Umm Lassifa samarskite-Y is represented by closed squares.

Conclusions

Microscopic investigation, SEM, XRD and microprobe analyses confirm the presence of a samarskite-Y mineral species. The obtained microprobe analyses of the investigated samarskite have resulted in the following average in wt.%: Nb_2O_5, 43.23; Ta_2O_5, 3.66; TiO_2, 0.44; UO_2, 4.38; ThO_2, 4.65; Y_2O_3, 17.43; MnO, 0.32; CaO, 0.26; FeO, 2.30; $SiO_2$1.74 and total REE of 22.09 with an average sum of 100.50 %. Also, the microprobe analyses revealed the empirical formula: [($Y_{0.42}$, $REE_{0.44}$, $Th_{0.076}$, $Si_{0.05}$, $Ca_{0.007}$, $U_{0.07}$, $Fe_{0.077}$) $\Sigma_{1.15}$ ($Nb_{0.81}$, $Ta_{0.04}$, $Ti_{0.14}$) $\Sigma_{0.86}$ O_4]. The mineral is associated with columbite, zircon, monazite, cassiterite, ilmenite and rutile. The mineralized Umm Lassifa pegmatite can be considered as a promising target ore for its rare-metal mineralization that includes mainly Nb, Ta, Y, REE and Zr together with U and Th.

Acknowledgments

The performed analyses by field emission scanning electron microscope (JEOL 6335F) and a JEOL Superprobe 733 were carried out in the Material Science and Engineering Research Center. Major Analytical Instrumentation Center (MAIC) and Particle Engineering Research Center (PERC), University of Florida, USA.

References

Abdel Wahed, A.A., Raslan, M.F. & El Husseiny, M.O. 2005: Radioactive pegmatites of Umm Lassifa granitic pluton, Central Eastern Desert, Egypt: Mineralogical investigation, The 9th International Mining, Petroleum and Metallurgical Engineering Conference, February 21–4, 2005, Faculty of Engineering, Cairo University, Cairo: 12 p.

Ali, M.A. 2001: Geology, petrology and radioactivity of Gabal El-Sibai area, Central Eastern Desert, Egypt, Ph. D. Thesis, Cairo University: 300 p.

Amin, M.S. & Mohamed, I.H. 1954: Geology of Umm Lassifa district, Geol. Surv., Egypt: 13 p.

Erict, T.S. 2005. Identification and alteration trends of granitic- pegmatite-hosted (Y, REE, U, Th)-(Nb, Ta,Ti) oxide minerals: a statistical approach. Can. Mineral., 43/4: 1291–1303, doi:10.2113/gscanmin.43.4.1291.

Hanson, S. L., Simons, W. B., Falster, A. U., Foord, E. E. & Lichte, F. E. 1999: Proposed nomenclature for samarskite-group minerals: new data on ishikawaite and calciosamarskite". Mineralogical Magazine, 63: 27–63.

Hussein, A.A.1990: The mineral resources. In: Said, R. (ed.): Geology of Egypt. John Wiley and Sons Inc., Amsterdam: 744 p.

Kamal El- Din, G.M. 1995: Geochemistry and tectonic significant of the Pan-African El-Sibai window, Central Eastern Desert, Egypt, Ph.D. Thesis, Heidelberg Univ., Germany: 114 p.

Khudier, A.A., El-Gaby, S., Kamal El- Din, G.M., Asran, H.A. & Greiling, R.O. 1995: The Pre-Pan African deformed granite cycle of the Gabal El-Sibai swell, Eastern Desert, Egypt. J. Afr. Earth Sci., 21/3: 395–406.

Matsubara, S., Kato, A. & Matsuyama, F. 1995: Nb-Ta minerals in a lithium pegmatite from Myokenzen, Ibaraki Prefecture, Japan. Mineralogical Journal, 17: 338–345.

Nickel, E.H. & Mandarino, J.A. 1987: Procedures involving the IMA Commission on New Minerals and Mineral names, and guidelines on mineral nomenclature. Can. Mineral., 25: 353–377.

Pal, D.C., Mishra, B. & Bernhardt, H.J. 2007: Mineralogy and geochemistry of pegmatite hosted Sn-, Ta-Nb-, and Zr-Hf- bearing minerals from the southern part of the Bastar-Malkangiri pegmatite belt, Central India. Ore Geology Reviews, 30: 30–55.

Raslan, M. F. 2008: Occurrence of Ishikawaite (Uranium-rich Samarskite) in the Mineralized Abu Rushied Gneiss, Southeastern Desert, Egypt. International Geology Review Journal, 50: 1132–1140.

Raslan, M. F. 2009: Mineralogical and Minerallurgical characteristics of samarskite-Y, columbite and zircon from stream sediments of the Ras Baroud area, Central Eastern Desert, Egypt. The Scientific Papers of the institute of Mining of The Wroclaw University of Technology, Wroclaw, Poland, No.126, Mining and Geology, XII: 179-195.

Raslan, M. F. & Ali, M.A. 2011: Mineralogy and mineral chemistry of rare-metal pegmatites at Abu Rusheid granitic gneisses, South Eastern Desert, Egypt. Geologija, 54/2: 205–222, doi:10.5474/geologija.2011.016.

Raslan, M. F., El-Shall, H. E., Omar, S. A. & Daher, A. M. 2010: Mineralogy of polymetallic mineralized pegmatite of Ras Baroud granite, Central Eastern Desert, Egypt. Journal of Mineralogical and Petrological Sciences, 105/3: 123–134, doi: 10.2465/jmps.090201.

William, S.B., Hanson, S.L. & Falster, A.U. 2006: Samarskite-Yb: a new species of the samarskite group from the Little Pasty pegmatites, Jefferson County, Colorado, Can. Mineral., 44/5: 1119–1125, doi: 10.2113/gscanmin.44.5.1119.

GEOLOGIJA *58/2*, 221-232, Ljubljana 2015

http://dx.doi.org/10.5474/geologija.2015.018

Sarmatijski mehkužci iz najdišča Osek-1 v Slovenskih goricah

Sarmatian molluscs from site Osek-1 in Slovenske gorice, Slovenia

Vasja MIKUŽ[1] & Matija KRIŽNAR[2]

[1]Naravoslovnotehniška fakulteta, Oddelek za geologijo; Privoz 11, SI–1000 Ljubljana, Slovenija;
e-mail: vasja.mikuz@ntf.uni-lj.si
[2]Prirodoslovni muzej Slovenije, Prešernova 20, SI–1001 Ljubljana,
Slovenija; e-mail: mkriznar@pms-lj.si

Prejeto / Received 16. 10. 2015; Sprejeto / Accepted 1. 12. 2015; Objavljeno na spletu / Published online 30. 12. 2015

Ključne besede: mehkužci, srednji miocen, sarmatij, Centralna Paratetida, Spodnji Osek, Slovenske gorice
Key words: molluscs, Middle Miocene, Sarmatian, Central Paratethys, Spodnji Osek, Slovenske gorice, Slovenia

Izvleček

Obravnavani so srednjemiocenski - sarmatijski mehkužci iz najdišča Osek-1 v Slovenskih goricah blizu Spodnjega Oseka. Ugotovljeni so: polžja vrsta *Acteocina lajonkaireana* in štiri školjčne vrste *Musculus sarmaticus*, *Sarmatimactra eichwaldi*, *Ervilia dissita* in *Venerupis dissita*, ki določajo plastem v Oseku-1 spodnjesarmatijsko starost.

Abstract

This article is a contribution to the taxonomical investigation of Middle Miocene (Sarmatian) molluscs from section (fossil site) Osek-1 at Spodnji Osek (Slovenske gorice) in the Mura-Zala basin on western margin of Central Paratethys. One gastropod species *Acteocina lajonkaireana* and four bivalves *Musculus sarmaticus*, *Sarmatimactra eichwaldi*, *Ervilia dissita* and *Venerupis dissita* have been systematically described. The identified fauna is assigned to the Lower Sarmatian age.

Uvod

V marcu leta 1997 smo obiskali in pregledovali dve najdišči miocenskih mehkužcev pri Oseku. Pri Spodnjem Oseku smo vzorčili v sarmatijskih plasteh ter zbrali nekaj različnih oblik polžev in školjk. Najdišče z izdanki sarmatijskih plasti smo označili z Osek-1 (sl. 1a, b).

Iz najdišča Osek-1 smo v raziskave vključili tudi primerke, ki jih je našel Franci Golob s Ptuja. V letu 2003 jih je podaril Prirodoslovnemu muzeju Slovenije. V škatli s fosilnimi školjkami je bil listek z napisom: PMS – Inv. št. E. G. 12 (17 kosov različnih školjk v peščenem glinavcu, ponekod z rastlinskimi ostanki (miocen-sarmatij), Osek v Slovenskih goricah.

Geološke razmere okolice najdišča

Po podatkih Žnidarčič-a in Mioč-a (1988) ozemlje Slovenskih goric pripada k Panonskemu bazenu oziroma k tektonski enoti Slovenske gorice. Mioč in Žnidarčič (1989) iz okolice Oseka-1 omenjata brakične sarmatijske (M_3^1) peščene laporovce, pesek in prod. Starost je potrjena s foraminiferami, kakršnihkoli sarmatijskih mehkužcev ne omenjata. Iz neposredne bližine najdišča je znan tudi večji

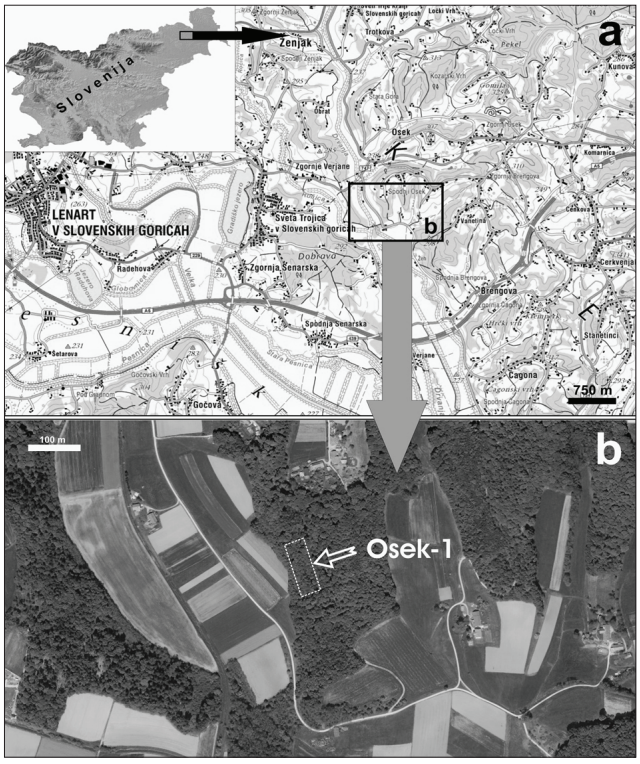

Sl. 1a, b. Geografski položaj najdišča Osek-1 v Spodnjem Oseku. Vir zemljevida: geopedia.si

Fig. 1a, b. Geographical position of fossil site Osek-1 at Spodnji Osek. Source of map: geopedia.si

podzemni kamnolom, kjer so izkoriščali debelejšo plast sarmatijskega ooidnega apnenca in peščenjaka (Planjšek in sod. 2002: 487). Po podatkih Pavšič-a in Horvat-a (2009: 410) sodi območje okrog Oseka v neogenski bazen Mura-Zala. V Štajerskem bazenu in bazenu Mura-Zala ležijo sarmatijske pretežno klastične kamnine zvezno na badenijskih skladih.

Paleontološki del

Sistematska razvrstitev polžev po: Wenz 1938; 1960, Golikov & Starobogatov 1975 in Bouchet & Rocroi 2005

Classis Gastropoda Cuvier, 1797
Cladus Cephalaspidea Fischer, 1883
Superfamilia Philinoidea Gray, 1850
Familia Cylichnidae H. Adams & A. Adams, 1854
Genus ***Acteocina*** Gray, 1847

Acteocina lajonkaireana (Basterot, 1825)
Tab. 1, sl. 1-5

1825 *Bullina Lajonkaireana*. Nob. – Basterot, 22, Pl. 1, Fig. 25
1840 *Bullina Lajonkaireana* Bast. – Grateloup, Bulléens, No. 2, Pl. 1, Figs. 45-46
1856 *Bulla Lajonkaireana* Bast. – Hörnes, 624, Taf. 50, Fig. 9c
1928 *Tornatina Lajonkaireana* Bast. – Friedberg, 542, Tabl. 35, Figs. 16a-16b
1954 *Acteocina lajonkaireana lajonkaireana* (Basterot) – Papp, 59, Taf. 10, Figs. 4a-4b, 5a-5b
1959 *Acteocina lajonkaireana lajonkaireana* (Basterot) – Boda, 628, táb. 32, figs. 6-7
1966 *Acteocina lajonkaireana* Basterot – Strausz, 472, Taf. 74, Fig. 25-26
1969 *Acteocina (Acteocina) lajonkaireana lajonkaireana* (Basterot, 1825) – Kojumdžieva, 117, Tabl. 39, Figs. 9a-9b, 10a-10b, 11a-11b, 14-15
1971 *Acteocina (Acteocina) lajonkaireana lajonkaireana* (Basterot) – Nicorici, 231, Pl. 7, Figs. 19-22
1995 *Acteocina lajonkaireana* (Basterot) – Zlinská & Fordinál, 75, Pl. 25, Fig. 4
2002 *Acteocina lajonkaireana* Basterot, 1825 – Harzhauser, 127, Taf. 11, Fig. 18
2002 *Acteocina lajonkaireana* (Basterot, 1825) – Harzhauser & Kowalke, 74, Pl. 13, Figs. 18-19
2003 *Acteocina lajonkaireana* (Basterot, 1825) – Harzhauser, 198, Tab. 1
2011 *Acteocina lajonkaireana* Bastretot, 1825 – Lukeneder et al., 772-773, Fig. 4. W
2013 *Acteocina lajonkaireana* (Basterot, 1825) – Hladilová & Fordinál, 39-40, Fig. 5. e
2013 *Acteocina lajonkaireana* (Basterot, 1825) – Tămaş et al., 78, Fig. 4h

Material in najdišče: Nekaj primerkov iz najdišča Osek-1, najdeni so v letu 1997. Izbrali smo pet primerkov (tabela 1). V najdišču so v sivorjavem, slabo vezanem in karbonatnem sljudnatem peščenjaku razmeroma pogostni.

Opis: Hišice so zelo majhne, visoke, ozke in sestoje iz 4 do 5 zavojev. Hišice so podobne olivam. Starejši zavoji so nizki, zadnji zavoj predstavlja 90% celotne hišice, ustje je dolgo in ozko. V spodnjem delu se ustje razširi in polkrožno zaključi. Pogostokrat so hišice brez starejših zavojev.

Tabela 1. Velikost primerkov vrste *Acteocina lajonkaireana* (Basterot).

Table 1. Size of *Acteocina lajonkaireana* (Basterot) specimens.

Primerki (Specimens)	Višina (Height) mm	Širina (Width) mm
I/1, T. 1, sl. 1	7,5	3
I/2, T. 1, sl. 2	7	2,5
H/1, T. 1, sl. 5	5	3
H/2, T. 1, sl. 3	6,5	3
H/3, T. 1, sl. 4	6	2,5

Pripombe: Rado (1963: 85, Fig. 5) je opisal ekološke značilnosti nekaterih miocenskih mehkužcev Romunije. Za vrsto *Acteocina lajonkaireana* piše, da pripada epifavni in da sodi med karnivore polže brakičnega okolja. Predstavniki te vrste naj bi živeli na globinah od 0 do 50m (Rado 1963: 86, Fig. 6).

Stratigrafska in geografska razširjenost: Basterot (1825: 22) opisano vrsto polža omenja iz miocenskih plasti južnozahodnega dela Francije. Grateloup (1840) jih omenja iz zgornjemiocenskih plasti Francije (Dax, Saint-Paul). Hörnes (1856: 626) jo opisuje iz brakičnih peščenih ceritijskih plasti Dunajske kotline. Fuchs (1875: 108) omenja iz okolice Sirakuze na Siciliji ooidni apnenec s sarmatijskimi mehkužci, med njimi tudi vrsto *Bulla lajonkaireana*. Friedberg (1928: 543) jih opisuje iz več najdišč sarmatijskih plasti na Poljskem. Papp (1954: 60) piše, da ta oblika polža nastopa v spodnjesarmatijskih plasteh avstrijskih najdišč in v ervilijskih in maktrinih plasteh zgornjega sarmatija. Nadalje še piše, da so njihove hišice majhne v starejših in večje v mlajših sarmatijskih plasteh. Boda (1959: 628-629) akteocine opisuje iz sarmatijskih plasti na Madžarskem. Rado (1963: 84) piše, da je vrsta *Acteocina lajonkaireana* najdena v Dunajski kotlini, na Madžarskem, v Romuniji in Ukrajini. Strausz (1966: 682) predstavlja primerek iz miocenskih plasti najdišča Várpalota na Madžarskem. Stancu in Andreescu (1968: 465) akteocine omenjajo iz tortonijskih skladov najdišč Delineşti in Rugi v Romuniji. Kojumdžieva (1969: 118) jih omenja iz spodnjega in srednjega sarmatija Bolgarije. Lubunescu in Pavnotescu (1970: 149) vrsto *Acteocina lajonkaireana* omenjajo iz sarmatijskih plasti Romunije, Moldavije, Pojske in Avstrije. Stancu in Popescu (1970: 177) jo omenjata iz tortonijskih plasti Romunije. Andreescu in Papaianopol (1970: Tabel. 1) akteocino navajajo iz spodnje in zgornjesarmatijskih plasti Romunije. Nicorici (1971: Pl. 7) jih predstavlja iz sarmatijskih najdišč Cioncu, Pîrîul in Vişinilor v Romuniji. Huică in sod. (1972: 356-357) jo omenjajo iz ervilijskih

in maktrinih plasti Romunije. Chinta (1973: 285) akteocine omenja iz spodnjesarmatijskih plasti Transilvanije v Romuniji. Zlinská in Fordinál (1995: 75) polžjo hišico vrste *Acteocina lajonkaireana* predstavljata iz spodnjesarmatijskih skladov Slovaške. Harzhauser (2002: 63-66, 127) vrsto *Acteocina lajonkaireana* opisuje iz karpatijskih skladov avstrijskih najdišč Teiritzberg pri kraju Stetten, Weinsteig in Kleinebersdorf. Harzhauser in Kowalke (2002: 74) jo opisujeta iz sarmatijskih plasti najdišča St. Margarethen na vzhodu Avstrije. Harzhauser (2003: 198) jo omenja iz karpatijskih skladov kotline Korneuburg v Avstriji. Lukeneder in sod. (2011: 772-773) jo predstavljajo iz plasti zgornje ervilijske cone najdišča Kettlasbrunn v Avstriji. Hladilová & Fordinál (2013: 40) jo predstavljata iz zgornjebadenijskih plasti najdišča Modra - Králová blizu Bratislave na Slovaškem. Tămaş s sod. (2013: 78) vrsto *Acteocina lajonkaireana* predstavljajo iz spodnjesarmatijskih plasti Romunije, nadalje še pišejo, da so jo našli tudi v Avstriji, Bolgariji, na Madžarskem in Slovaškem ter v Ukrajini.

Sistematska razvrstitev školjk po: Schultz 2001; 2003 in 2005

Ordo Mytiloida Férussac, 1822
Superfamilia Mytilacea Rafinesque, 1815
Familia Mytilidae Rafinesque, 1815
Subfamilia Crenellinae H. Adams & A. Adams, 1857
Genus ***Musculus*** Röding, 1798

Musculus sarmaticus (Gatujev, 1916)
Tab. 1, sl. 6-8

1954 *Musculus sarmaticus* (Gatuev). – Papp, 62, Taf. 1, Figs. 4, 5
1959 *Musculus sarmaticus* (Gatuev) – Boda, 589, Táb. 1, figs. 8-9; Táb. 2, figs. 1-3
1960 *Modiola sarmatica* Gat. – Vadász, 605, Táb. 59, Fig. 2
1969 *Musculus sarmaticus* (Gatuev, 1916) – Kojumdžieva, 56, Tabl. 20, Figs. 4a-4b, 5-6; Tabl. 21, Fig. 1
1970 *Musculus sarmaticus* (Gat.) – Andreescu & Papaianopol, Pl. 1, Fig. 3
1974 *Musculus (Musculus) sarmaticus* (Gatujev) – Papp, 357, Taf. 12, Figs. 4, 5
2001 *Musculus (Musculus) sarmaticus* (Gatujev, 1916) – Schultz, 109, Taf. 8, Figs. 16a-16b
2011 *Musculus sarmaticus* (Gatuev, 1916) – Lukeneder et al., 771, Fig. 3 A_1 - A_2

Material: Trije primerki iz PMS na sivem nekarbonatnem muljevcu (tabela 2). Največja (12/1) in najbolje ohranjena desna lupina, desna lupina (12/2) z razpoko in poškodovanim ventralnim robom in desna lupina s poškodovanim ventralnim robom (12/3).

Opis: Oblika lupin je ovalna oziroma tipično mitilidna, razpotegnjena po višini. Lupine imajo ozek dorzalen in polkrožen ventralen rob. Vrh je povit in zašiljen, sprednji rob je strm in raven, zadnji rob je zaobljen in položen. Od vrha blizu sprednjega roba poteka ozek greben, ki se proti ventralnemu delu razširi. Površina lupine je prekrita s tankimi radialnimi rebrci.

Tabela 2. Velikost primerkov vrste *Musculus sarmaticus* (Gatujev) iz paleontološke zbirke Prirodoslovnega muzeja Slovenije.

Table 2. Size of specimens of *Musculus sarmaticus* (Gatujev) from the collection of Slovenian Museum of Natural History.

Primerki (Specimens)	Dolžina (Length) mm	Višina (Height) mm	Debelina (Thickness) mm
12/1, T. 1, sl. 6	12	18	½ -5
12/2, T. 1, sl. 7	9	16	½ -4
12/3, T. 1, sl. 8	9	~14	½ -3,5

Primerjava: Hilber (1897: 203, Fig. 21) je iz sarmatijskih plasti najdišča Waldhof južnozahodno od Gradca v Avstriji opisal novo vrsto *Modiola norica*, ki je velikostno in oblikovno zelo blizu vrste *Musculus sarmaticus*. Morda gre celo za isto vrsto?

Pripombe: Rado (1963: 85, Fig. 5) prikazuje ekološke značilnosti posameznih sarmatijskih mehkužcev. Školjka vrste *Musculus sarmaticus* pripada infavni in sodi med limnivore do brakične organizme.

Stratigrafska in geografska razširjenost: Papp (1954: 62) piše, da je vrsta *Musculus sarmaticus* najdena v Dunajski kotlini v sarmatijskih ervilijskih in maktrinih plasteh kar pomeni, da je ta vrsta prisotna skozi celoten sarmatij. Boda (1959: 589) jih opisuje iz sarmatijskih plasti Madžarske. Rado (1963: 84) piše, da je ta školjčna vrsta ugotovljena v Dunajski kotlini, na Madžarskem, v Romuniji in Ukrajini. Kojumdžieva (1969: 57) navaja, da ta školjčna oblika nastopa v Bolgariji v spodnjem in srednjem sarmatiju. Andreescu in Papaianopol (1970: Pl. 1, Tabel. 1) jo prestavljata iz sarmatijskih plasti najdišča valea Şipotelu v Romuniji. Najdena je v vseh sarmatijskih horizontih, najbolj pogostna je v srednjem delu sarmatija. Nicorici (1971: 216) vrsto *Musculus sarmaticus* omenja iz sarmatijskih plasti z območja Vîrciorog v Romuniji. Huică in sod. (1972: 356-357) jo omenjajo iz sarmatijskih ervilijskih in maktrinih plasti Romunije. Papp (1974: 358) piše, da je v sarmatiju razširjena po celotni Centralni Paratetidi. Schultz (2001: 111-114) piše, da je ta vrsta najdena v številnih avstrijskih nahajališčih v različnih sarmatijskih horizontih. Drugod v Centralni Paratetidi je najdena v sarmatijskih skladih Slovenije, Hrvaške, Madžarske, Slovaške, Poljske, Romunije, Bolgarije, Bosne in Srbije. Ugotovljena je tudi v več najdiščih sarmatijskih plasti v Vzhodni Paratetidi. Harzhauser in Piller (2004: 98) omenjajta najdbe vrste *Musculus sarmaticus* iz spodnjesarmatijskih plasti najdišč St. Margarethen in Hummel Quarry v kotlini Eisenstadt – Sopron. Lukeneder in sod. (2011: 771)

prikazujejo primerek vrste *Musculus sarmaticus* iz bessarabijskih plasti najdišča Zavjetnoje na polotoku Krim. Mikuž in Gašparič (2014: 46) omenjata školjko vrste *Musculus sarmaticus* (Gatujev, 1916) iz sarmatijskih plasti najdišča Osek. Mikuž in Gašparič (2015: 48) predstavljata spodnjesarmatijsko školjko *Musculus sarmaticus* iz Oseka v Slovenskih goricah.

Superfamilia Mactroidea Lamarck, 1809
Familia Mactridae Lamarck, 1809
Subfamilia Mactrinae Lamarck, 1809
Genus ***Sarmatimactra*** Korobkov, 1954

Sarmatimactra eichwaldi (Laskarev, 1914)
Tab. 1, sl. 9-12; tab. 2, sl. 1-8

1954 *Mactra vitaliana eichwaldi* Laskarev. – Papp, 90, Taf. 17, Figs. 1-5
1959 *Mactra vitaliana eichwaldi* Laskarev – Boda, 599, táb. 14, figs. 10-18
1969 *Mactra (Sarmatimactra) eichwaldi* Laskarev, 1914 – Kojumdžieva, 19, Tabl. 3, Figs. 5a-5b, 6a-6b, 9a-9b, 10a-10b
1974 *Mactra eichwaldi* Laskarev – Papp, 364, Taf. 16, Figs. 1-5
2003 *Mactra (Sarmatimactra) vitaliana eichwaldi* Laskarev, 1914 – Schultz, 650, Taf. 90, Figs. 17a-17b, 18a-18b, 19a-19b
2008 *Sarmatimactra eichwaldi* (Laskarev, 1914) – Mandic et al., 351, Fig. 7 b
2011 *Sarmatimactra eichwaldi* (Laskarev, 1914) – Harzhauser et al., 172, Fig. 3. 5

Tabela 3. Velikost primerkov vrste *Sarmatimactra eichwaldi* (Laskarev). Primerki z oznako OG so iz paleontološke zbirke Oddelka za geologijo, Univerze v Ljubljani, ostali primerki so iz paleontološke zbirke Prirodoslovnega muzeja Slovenije.

Table 3. Size of specimens of *Sarmatimactra eichwaldi* (Laskarev). Specimens marked with OG are from the paleontological collection of Department of geology, University of Ljubljana, all others are from the paleontological collection of Slovenian Museum of Natural History.

Primerki (Specimens)	Dolžina (Length) mm	Višina (Height) mm	Debelina (Thickness) mm
12/4, T. 1, sl. 9	20	15	½ -5
12/5, T. 1, sl. 10	18	13	½ -4
12/6, T. 1, sl. 11	14	12	½ -4
12/7, T. 1, sl. 12	17	13	½ -4
12/8, T. 2, sl. 1	16	12	½ -4,5
12/9, T. 2, sl. 2	17	13	~ 7
12/10, T. 2, sl. 3	16	12	½ -4
12/11, T. 2, sl. 4	15	12	½ ~4
12/12, T. 2, sl. 5	10	8	½ -3,5
OG-1, T. 2, sl. 6	12	11	½ -4
OG-2, T. 2, sl. 7	16,5	14	½ -4
OG-3, T. 2, sl. 8	24	18	½ ~4

Material: Devet primerkov v sivem nekarbonatnem muljevcu z rastlinskimi ostanki iz PMS. Tri leve lupine (12/4, 12/5 in 12/6), pet desnih lupin (12/7, 12/8, 12/10, 12/11 in 12/12) ter desna lupina s kamenim jedrom leve lupine (12/9). Dodali smo še tri primerke iz paleontološke zbirke Oddelka za geologijo OG-1, OG-2 in OG-3 (tabela 3).

Opis: Lupine so majhne in simetrične, trikotne oblike z dolžinami med 10 in 20 mm ter višinami od 8 do 15 mm. Velik obvršni del z vrhom je blizu sredine lupine. Sprednji rob je kratek, polkrožen in strm, zadnji je bolj raven, položnejši, daljši z vzporedno potekajočim grebenom, spodnji ali ventralen rob je polkrožen. Na površini so vidne številne drobne koncentrične prirastnice.

Stratigrafska in geografska razširjenost: Papp (1954: 90) piše, da ta školjčna vrsta nastopa v sarmatijskih rizojskih in ervilijskih skladih Dunajske kotline. Boda (1959: 599) jo predstavlja iz spodnjesarmatijskih skladov Madžarske. Kojumdžieva (1969: 20) piše, da vrsta nastopa v spodnjem sarmatiju Bolgarije. Papp (1974: 365) omenja, da je pogostna v Centralni Paratetidi v spodnjem sarmatiju, v ervilijskih skladih. Schultz (2003: 651-653) piše, da je vrsta najdena v številnih sarmatijskih lokacijah Avstrije. V drugih delih Paratetide je ugotovljena v sarmatiju na Poljskem, v Romuniji, Moldaviji, Ukrajini, na Madžarskem, Slovaškem, Bolgariji, Bosni, Srbiji in drugod. Mandic in sod. (2008: 351) prikazujejo lupino tovrstne sarmatimaktre iz sarmatijskih skladov severnovzhodnega predela Avstrije. Harzhauser in sod. (2011: 172-173) vrsto *Sarmatimactra eichwaldi* omenjajo iz zgornje ervilijske cone srednjega sarmatija in iz zgornjega sarmatija.

Familia Mesodesmatidae Gray, 1840
Subfamilia Erviliinae Dall, 1895
Genus ***Ervilia*** Tourton, 1822

Ervilia dissita (Eichwald, 1830)
Tab. 2, sl. 9-10

1954 *Ervilia dissita dissita* (Eichwald) – Papp, 88, Taf. 11, Figs. 18-21
1959 *Ervilia dissita dissita* Eichwald – Boda, 597, táb. 13, figs. 5-10
1969 *Ervilia dissita dissita* (Eichwald, 1830) – Kojumdžieva, 27, Tabl. 8, Figs. 1a-1b, 2a-2b, 3
1974 *Ervilia dissita dissita* (Eichwald) – Papp, 366, Abb. 62, Figs. 1-5, 11-14
2003 *Ervilia dissita dissita* (Eichwald, 1830) – Schultz, 681, Taf. 95, Figs. 6a-6c, 7a-7c
2011 *Ervilia dissita* (Eichwald, 1830) – Lukeneder et al., 771, Fig. 3 G_1 – G_2
2011 *Ervilia dissita* (Echwald, 1830) – Harzhauser et al., 172, Fig. 3. 4
2013 *Ervilia dissita* (Eichwald, 1830) – Tămaş et al. , 67, Fig. 2a

Material: Ena poškodovana lupina (12/13) iz PMS v sivem laminiranem muljevcu. Iz paleontološke zbirke Oddelka za geologijo smo dodali še primerek OG-4 (tabela 4).

Opis: Ohranjena je majhna desna lupina z vrhom nekoliko pomaknjenim proti sprednjemu delu. Sprednji rob je kratek in polkrožen, zadnji raven, daljši in položnejši. Zaključni spodnji del zadnjega roba je odlomljen. Spodnji rob je najdaljši in polkrožen. Lupina je rahlo izbočena, na njeni površini so številne zelo tanke prirastne linije. Lupine opisane vrste so običajno zelo majhne, velike vsega nekaj mm.

Tabela 4. Velikost primerkov vrste *Ervilia dissita* (Eichwald). Primerek z oznako OG je iz paleontološke zbirke Oddelka za geologijo, Univerze v Ljubljani, drug primerek je iz paleontološke zbirke Prirodoslovnega muzeja Slovenije.

Table 4. Size of specimens of *Ervilia dissita* (Eichwald). Specimen marked with OG is from the paleontological collection of Department of geology, University of Ljubljana, the other is from the paleontological collection of Slovenian Museum of Natural History.

Primerki (Specimens)	Dolžina (Length) mm	Višina (Height) mm	Debelina (Thickness) mm
12/13, T. 2, sl. 9	8	6	½ -2,5
OG-4, T. 2, sl. 10	10	7	½ -3

Opomba: Rado (1963: 85, Fig. 5) uvršča vrsto *Ervilia dissita* k infavni in med limnivore organizme brakičnega okolja.

Stratigrafska in geografska razširjenost: Papp (1954: 88) piše, da so primerki vrste *Ervilia dissita* najdeni v Dunajski kotlini v sarmatijskih rizojskih in ervilijskih plasteh. Boda (1959: 597) jo opisuje iz sarmatijskih plasti Madžarske. Rado (1963: 84) piše, da so tovrstne ervilije najdene v Dunajski kotlini, na Madžarskem, v Romuniji in Ukrajini. Kojumdžieva (1969: 27) piše, da tovrstne ervilije nastopajo v spodnjem in srednjem sarmatiju Bolgarije. Andreescu in Papaianopol (1970: Tabel. 1) jo omenjata iz sarmatijskih skladov Romunije. Nicorici (1971: 220) predstavlja ervilije iz sarmatijskih plasti Romunije. Muldini-Mamužić in sod. (1974: 95-101) omenjajo ervilije iz sarmatijskih skladov Slovenije, Hrvaške, Bosne in Srbije. Papp (1974: 366) piše, da vrsta *Ervilia dissita* nastopa v sarmatijskih skladih Centralne in Vzhodne Paratetide. Ugotovljene so v skladih z mohrensternijami, v zgornjem delu skladov z ervilijami in v skladih maktra, kjer so že razmeroma redke. Shultz (2003: 683-684) piše, da so ervilije najdene v številnih avstrijskih najdiščih sarmatijskih plasti. Drugod v Centralni Paratetidi je ugotovljena v sarmatijskih skladih Poljske, Slovaške, Romunije, Madžarske, Hrvaške, Bolgarije, Bosne in Slovenije (Slovenske gorice). Našli so jih tudi v sarmatiju Vzhodne Paratetide. Harzhauser in Piller (2004: 98) omenjajta najdbe podvsrte *Ervilia dissita dissita* (Eichwald) iz spodnjesarmatijskih plasti najdišč St. Margarethen in Hummel Quarry v kotlini Eisenstadt – Sopron. Mandic in sod. (2008: 351) jo omenjajo iz sarmatijskih plasti severnovzhodnega predela Avstrije. Lukeneder in sod. (2011: 771) prikazujejo lupino vrste *Ervilia dissita* iz zgornjih ervilijskih plasti najdišča Hauskirchen v Avstriji. Harzhauser in sod. (2011: 172-173) omenjajo vrsto *Ervilia dissita* iz srednjesarmatijskih plasti Dunajske kotline. Tămaş in sod. (2013: 67-69) jo opisujejo iz sarmatijskih plasti vzhodnega predela Romunije. Mikuž in Gašparič (2015: 49) iz spodnjesarmatijskih plasti Oseka v Slovenskih goricah predstavljata školjko vrste *Ervilia dissita*.

Superfamilia Veneroidea Rafinesque, 1815
Familia Veneridae Rafinesque, 1815
Subfamilia Tapetinae H. Adams & A. Adams, 1857
Genus ***Venerupis*** Lamarck, 1818

Venerupis dissita (Eichwald, 1830)
Tab. 2, sl. 11-15

1954 *Irus (Paphirus) gregarius dissitus* (Eichwald). – Papp, 83, Taf. 16, Figs. 6-9
1959 *Irus (Paphirus) gregarius dissitus* (Eichwald) – Boda, 596, táb. 11, figs. 4-8
1974 *Irus (Paphirus) gregarius dissitus* (Eichwald) – Papp, 373, Taf. 15, Figs. 6-9
1998 *Venerupis (Paphirus) gregarius dissitus* (Eichwald) – Schultz, 132-133, Taf. 60, Fig. 2
2005 *Venerupis (Paphirus) gregaria dissita* (Eichwald, 1830) – Schultz, 951, Taf. 142, Figs. 4a-4b, 5a-5b

Material: Tri leve lupine (12/14, 12/15, 12/16) iz PMS v sivem nekarbonatnem sljudnatem peščenem muljevcu z rastlinskimi ostanki in ena cela školjka v kamnini (12/17). Ena cela školjka OG-5 je iz paleontološke zbirke Oddelka za geologijo (tabela 5).

Opis: Lupine so majhne, asimetrične s povsem pomaknjenim vrhom k sprednjemu robu. Vrh je ozek in majhen. Sprednji rob je zelo strm, kratek in polkrožen, zadnji rob je daljši in položnejši, spodnji je najdaljši in blago polkrožen. Lupine so bolj izbočene in tanke. Njihova površina je prekrita s številnimi koncentričnimi prirastnimi linijami.

Tabela 5. Velikost primerkov vrste *Venerupis dissita* (Eichwald). Primerek z oznako OG je iz paleontološke zbirke Oddelka za geologijo, Univerze v Ljubljani, ostali primerki so iz paleontološke zbirke Prirodoslovnega muzeja Slovenije.

Table 5. Size of specimens of *Venerupis dissita* (Eichwald). Specimen marked with OG is from the paleontological collection of Department of geology, University of Ljubljana, all others are from the paleontological collection of Slovenian Museum of Natural History.

Primerki (Specimens)	Dolžina (Length) mm	Višina (Height) mm	Debelina (Thickness) mm
12/14, T. 2, sl. 11	16	13	½ -4
12/15, T. 2, sl. 12	14	12	½ -4
12/16, T. 2, sl. 13	15	13	½ -4,5
12/17, T. 2, sl. 14	12	10	~ 6
OG-5, T. 2, sl. 15	10	8	4,5

Stratigrafska in geografska razširjenost: Papp (1954: 83) piše, da vrsta nastopa v sarmatijskih ervilijskih plasteh Dunajske kotline. Boda (1959:

596) prikazuje več lupin školjke *Venerupis dissita* iz sarmatijskih plasti v okolici Soprona na Madžarskem. Papp (1974: 373) jih omenja iz ervilijskih plasti najdišč vzhodno od Alp in na Madžarskem. Schultz (1998: 132) jo predstavlja iz sarmatijskih ervilijskih plasti Burgenlanda v Avstriji. Harzhauser in Piller (2004: 98) omenjajta najdbe podvsrte *Venerupis gregarius dissitus* (Eichwald) iz spodnjesarmatijskih plasti najdišča Hummel Quarry v kotlini Eisenstadt – Sopron. Schultz (2005: 955) omenja primerke vrste *Venerupis dissita* iz ervilijskih plasti Avstrije, Madžarske, Slovaške, Poljske, Romunije, Moldavije, Hrvaške, Bosne in Srbije. Iz spodnjesarmatijskih plasti najdišča Osek-1 v Slovenskih goricah predstavljata Mikuž in Gašparič (2015: 49) primerek vrste *Venerupis dissita*.

Zaključki

Fosilni mehkužci so najdeni v sivorjavem, sljudnatem in slabo vezanem apnenčevem peščenjaku, v sivem laminiranem muljevcu, v peščenem sljudnatem in nekarbonatnem muljevcu najdišča Osek-1 pri Spodnjem Oseku v Slovenskih goricah (sl. 1a-b).

Ugotovljene vrste mekužcev *Acteocina lajonkaireana* (Basterot, 1825), *Musculus sarmaticus* (Gatujev, 1916), *Sarmatimactra eichwaldi* (Laskarev, 1914), *Ervilia dissita* (Eichwald, 1830) in *Venerupis dissita* (Eichwald, 1830) določajo plastem najdišča Osek-1 sarmatijsko starost. Po zelo majhnih hišicah polža *Acteocina lajonkaireana* (Papp 1954: 60), po številnih primerkih vrste *Sarmatimactra eichwaldi* in po školjčni vrsti *Venerupis dissita* pa sklepamo, da pri Spodnjem Oseku izdanjajo spodnjesarmatijske plasti.

V najdišču Osek-1 je prisoten tudi ooidni horizont, z ooidnimi peski, peščenjaki in apnenci. Ooidni apnenec je prepreden s številnimi votlinicami z odtisi raztopljenih sarmatijskih polžjih hišic. Ooidi kažejo na toplo, plitvo in razgibano morsko do brakično okolje. Nekaj podobnega so registrirali v spodnjem sarmatiju avstrijskih najdišč Hauskirchen, Siebenhirten, Kettlasbrunn in Nexing v severnem delu Dunajske kotline (Lukeneder et al., 2011). To pomeni, da so bile takratne sarmatijske okoljske razmere tudi v bazenu Mura-Zala v Centralni Paratetidi zelo podobne.

Sarmatian molluscs from site Osek-1 in Slovenske gorice, Slovenia

Conclusions

From Osek-1 fossil site we described from fine sandy silt, silty sand and marl a Sarmatian molluscs assemblage with gastropod *Acteocina lajonkaireana* (Basterot, 1825) and four bivalves *Musculus sarmaticus* (Gatujev, 1916), *Sarmatimactra eichwaldi* (Laskarev, 1914), *Ervilia dissita* (Eichwald, 1830) and *Venerupis dissita* (Eichwald, 1830). Small gastropods *Acteocina lajonkaireana* (Papp 1954: 60) and large number of specimens *Sarmatimactra eichwaldi* and *Venerupis dissita* are characteristic for Lower Sarmatian age. From Osek-1 site the oolitic horizons with oolitic limestone, oolitic sand and oolitic grainstone is detected, with abundant dissolved molluscs shells (gastropods and bivalves). Oolitic deposits are typical for Sarmatian beds in Central Paratethys, with best documented sections in Vienna Basin (Lukeneder et al. ,2011). Similar oolitic horizons as at site Osek-1, can be traced also in Neogene of the Styrian Basin and Mura - Zala Basin in the Mura Depression.

Zahvale

Gospodu Franciju Golobu s Ptuja se zahvaljujemo za fosilni inventar iz najdišča Osek-1 pri Spodnjem Oseku, za fotografske usluge se zahvaljujemo sodelavcu Mateju Fistru z Oddelka za geologijo, Naravoslovnotehniške fakultete, Univerze v Ljubljani.

TABLA 1 – PLATE 1

1 *Acteocina lajonkaireana* (Basterot, 1825); I/1, Osek-1, velikost primerka/ size of specimen 7,5 × 3 mm

2 *Acteocina lajonkaireana* (Basterot, 1825); I/2, Osek-1, velikost primerka/ size of specimen 7 × 2,5 mm

3 *Acteocina lajonkaireana* (Basterot, 1825); H/2, Osek-1, velikost primerka/ size of specimen 6,5 × 3 mm

4 *Acteocina lajonkaireana* (Basterot, 1825); H/3, Osek-1, velikost primerka/ size of specimen 6 × 2,5 mm

5 *Acteocina lajonkaireana* (Basterot, 1825); H/1, Osek-1, velikost primerka/ size of specimen 5 × 3 mm

6 *Musculus sarmaticus* (Gatujev, 1916); 12/1, Osek-1, velikost primerka/ size of specimen 12 × 18 × 5 mm

7 *Musculus sarmaticus* (Gatujev, 1916); 12/2, Osek-1, velikost primerka/ size of specimen 9 × 16 × 4 mm

8 *Musculus sarmaticus* (Gatujev, 1916); 12/3, Osek-1, velikost primerka/ size of specimen 9 × 14 × 3,5

9 *Sarmatimactra eichwaldi* (Laskarev, 1914); 12/4, Osek-1, velikost primerka/ size of specimen 20 × 15 × 5 mm

10 *Sarmatimactra eichwaldi* (Laskarev, 1914); 12/5, Osek-1, velikost primerka/ size of specimen 18 × 13 × 4 mm

11 *Sarmatimactra eichwaldi* (Laskarev, 1914); 12/6, Osek-1, velikost primerka/ size of specimen 14 × 12 × 4 mm

12 *Sarmatimactra eichwaldi* (Laskarev, 1914); 12/7, Osek-1, velikost primerka/ size of specimen 17 × 13 × 4 mm

TABLA 1 – PLATE 1


1


2


3


4


5


6


7


8


9


10


11


12

Literatura

Andreescu, I. & Papaianopol, I. 1970: Biostratigrafia depozitelor sarmatiene dintre văile Milcov şi Rîmnicu Sărat. Studii şi cercetări de geol., geofiz., geograf., Ser. geologie, 15/2: 499–512, Pl. 1–8.

Basterot, B. de 1825: Description géologique du bassin tertiaire du sud-ouest de la France. Mém. Soc. Hist. Natur. Paris, 2: 1–100, Pl. 1–7.

Boda, J. 1959: A Magyarországi szarmata emelet és gerinctelen faunája. Annales Inst. Geol. Publ. Hung., 47/3: 567–862, (Táb. 1–44).

Bouchet, P. & J. Rocroi, P. 2005: Classification and Nomenclatur of Gastropod Families. Malacologia, 47/1–2: 1–397.

Chinta, R. 1973: Date noi asupra faunei tortonian-sarmatiene din vestul Depresiunii Transilvaniei. Studii şi cercetări de geol., geofiz., geograf., Ser. geologie, 18/1: 283–287, Pl. 1–2.

Friedberg, W. 1911-1928: Mieczaki Mioceńskie Ziem Polskich. (Mollusca miocaenica Poloniae). Pars 1. Gastropoda et scaphopoda. Nakladem muzeum imienia Dzieduszyckich we Lwowie (Lwów i Poznań): VII, 1–631, Tabl. 1–38.

Fuchs, T. 1875: Über das Auftreten von Miocänschichten vom Charakter der sarmatischen Stufe bei Syrakus. Sitzungsb. Akad. Wiss. mathem.-naturwiss. Kl., Wien, 70: 106–109.

Golikov, A. N. & Starobogatov, Y. J. 1975: Systematics of Prosobranch Gastropods. Malacologia, 15/1: 185–232.

Grateloup, J. P. S. de, 1840: Conchyliologie fossile des terrains Tertiaires du bassin de l'Adour. Tome 1, Univalves, Atlas. Imprimeire de Th. Lafargue, Libraire, (Bordeaux).

Harzhauser, M. 2002: Marine und brachyhaline Gastropoden aus dem Karpatium des Korneuburger Beckens und der Kreuzstettener Bucht (Österreich, Untermiozän). Beitr. Paläont., 27: 61–159, (Taf. 1–12).

Harzhauser, M. 2003: Marine Gastropods, Scaphopods and Cephalopods of the Karpatian in the Central Paratethys. In: Brzobohaty, R., I. Cicha, M. Kováč & F. Rögl (Editors), The Karpatian. A Lower Miocene Stage of the Central Paratethys. Masaryk University (Brno): 193–201, (Pl. 1).

Harzhauser, M., Daxner-Höck, G., Göhlich, U. B. & Nagel, D. 2011: Complex faunal mixing in the early Pannonian palaeo-Danube Delta (Late Miocene, Gaweinstal, Lower Austria). Ann. Naturhist. Mus. Wien, Ser. A, 113: 167–208.

Harzhauser, M. & Kowalke, T. 2002: Sarmatian (Late Miocene) Gastropod Assemblages of the Central Paratethys. Facies, 46: 57–82, (Pl. 9–13).

Harzhauser, M. & Piller, W. E. 2004: The Early Sarmatian – hidden seesaw changes. Cour. Forsch.-Inst. Senckenberg, 246: 89–111, (Pl. 1–3).

Hilber, V. 1897: Die sarmatischen Schichten vom Waldhof bei Wetzelsdorf, Graz SW. Mitt. Naturwiss. Vereines Steiermark, Jg., 33(1896): 182–204, Taf. 1.

TABLA 2 – PLATE 2

1 *Sarmatimactra eichwaldi* (Laskarev, 1914); 12/8, Osek-1, velikost primerka/ size of specimen 16 × 12 × 4,5 mm

2 *Sarmatimactra eichwaldi* (Laskarev, 1914); 12/9, Osek-1, velikost primerka/ size of specimen 17 × 13 × 7 mm

3 *Sarmatimactra eichwaldi* (Laskarev, 1914); 12/10, Osek-1, velikost primerka/ size of specimen 16 × 12 × 4 mm

4 *Sarmatimactra eichwaldi* (Laskarev, 1914); 12/11, Osek-1, velikost primerka/ size of specimen 15 × 12 × 4 mm

5 *Ervilia dissita* (Eichwald, 1830); 12/12, Osek-1, velikost primerka/ size of specimen 10 × 8 × 3,5 mm

6 *Ervilia dissita* (Eichwald, 1830); OG-1, Osek-1, velikost primerka/ size of specimen 12 × 11 × 4 mm

7 *Venerupis dissita* (Eichwald, 1830); OG-2, Osek-1, velikost primerka/ size of specimen 16,5 × 14 × 4 mm

8 *Venerupis dissita* (Eichwald, 1830); OG-3, Osek-1, velikost primerka/ size of specimen 24 × 18 × 4 mm

9 *Ervilia dissita* (Eichwald, 1830); 12/13, Osek-1, velikost primerka/ size of specimen 8 × 6 × 2,5 mm

10 *Ervilia dissita* (Eichwald, 1830); OG-4, Osek-1, velikost primerka/ size of specimen 10 × 7 × 3 mm

11 *Venerupis dissita* (Eichwald, 1830); 12/14, Osek-1, velikost primerka/ size of specimen 16 × 13 × 4 mm

12 *Venerupis dissita* (Eichwald, 1830); 12/15, Osek-1, velikost primerka/ size of specimen 14 × 12 × 4 mm

13 *Venerupis dissita* (Eichwald, 1830); 12/16, Osek-1, velikost primerka/ size of specimen 15 × 13 × 4,5 mm

14 *Venerupis dissita* (Eichwald, 1830); 12/17, Osek-1, velikost primerka/ size of specimen 12 × 10 × 6 mm

15 *Venerupis dissita* (Eichwald, 1830); OG-5, Osek-1, velikost primerka/ size of specimen 10 × 8 × 4,5 mm

Fotografije (Photos): Matej Fister

TABLA 2 – PLATE 2


1


2


3

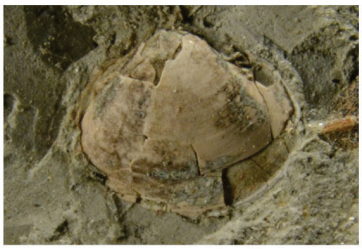
4


5


6


7

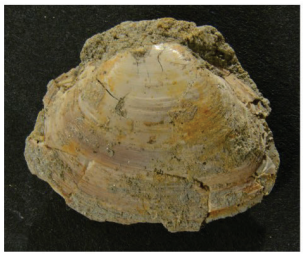
8


9


10


11


12


13


14


15

Hladilová, Š. & Fordinál, K. 2013: Upper Badenian Molluscs (Gastropoda, Bivalvia, Scaphopoda) from the Modra-Kráľová locality (Danube Basin, Slovakia). Mineralia Slovaca, 45: 35–44.

Hörnes, M. 1856: Die Fossilen Mollusken des Tertiaer-Beckens von Wien. Bd. I: Univalven. Abh. Geol. R. A., 3: 1–736, Taf. 1–52.

Hörnes, M., 1870: Die Fossilen Mollusken des Tertiaer-Beckens von Wien. Bd. II, Bivalven. Abh. Geol. R. A., 4: 1-479 + Taf. 1-85.

Huică, I., Hinculov, L. Babucea, Y. & Kokzur, I. 1972: Contributii la cunoaşterea tortonianului şi sarmatianului din zona Minişu de Sus (Bazinul Zarand). Studii şi cercetări de geol., geofiz., geograf., Ser., 17/2: 347–370, (Pl. 1–7).

Kojumdžieva, E. 1969: Fosilite na B`lgarija. VIII, Sarmat. (Les fossiles de Bulgarie. VIII, Sarmatien). B`lgarska akademija na naukite (Sofija): 1–223, (Tab. 1–40).

Lubunescu, V. & Pavnotescu, V. 1970: Contributii la stratigrafia Neogenului din bazinul Caransebş. Dări di seamă ale şedintelor (1968-1969), 4. Stratigrafie, 56: 141–155.

Lukeneder, S., Zuschin, M., Harzhauser, M. & Mandic, O. 2011: Spatiotemporal signals and palaeoenvironments of endemic molluscan assemblages in the marine system of the Sarmatian Paratethys. Acta Paleontologica Polonica, 56/4: 767–784.

Mandic, O., Harzhauser, M., Roetzel, R. & Tibuleac, P. 2008: Benthic mass-mortality events on a Middle Miocene incised-valley tidal-flat (North Alpine Foredeep Basin). Facies, 54: 343–359.

Mikuž, V. & Gašparič, R. 2014: Slovenske gorice in njihove paleontološke posebnosti. In: Rožič, B., Verbovšek, T.& Vrabec, Mi. (eds.): Povzetki in ekskurzije. 4. Slovenski geološki kongres, Ankaran, 8.-10. oktober 2014. Univerza v Ljubljani, Naravoslovnotehniška fakulteta, Ljubljana: 46.

Mikuž, V. & Gašparič, R. 2015: Slovenske gorice in njihove paleontološke posebnosti. Konkrecija, 4: 45–49.

Mioč, P. & Žnidarčič, M. 1989: Tolmač za lista Maribor in Leibnitz. Osnovna geološka karta SFRJ. Zvezni geološki zavod Beograd, Beograd: 60 p.

Muldini-Mamužić, S., Rijavec, L. & Jenko, K. 1974: Das Sarmat in Jugoslawien. In: Papp, A. Marinescu, F.& Seneš, J. (eds.): Chronostratigraphie und Neostratotypen, Miozän der Zentralen Paratethys, Bd. 4, M_5 Sarmatien. Die sarmatische Schichtengruppe und ihr Stratotypus. VEDA, Verlag der Slowakischen Akademie der Wissenschachften, Bratislava: 95–101.

Nicorici, E. 1971: Fauna sarmatiană de la Vîrciorog (Bazinul Vadului). Studii şi cercetări de geol., geofiz., geograf., Ser. geologie, 16/1: 215–232, Pl. 1–7.

Papp, A. 1954: Die Molluskenfauna im Sarmat des Wiener Beckens. Mitt. Geol. Gesselsch., 45: 1–112, Taf. 1–20.

Papp, A. 1974: Die Molluskenfauna der Sarmatischen Schichtengruppe. In: Papp, A. Marinescu, F. & Seneš, J. (eds.): Chronostratigraphie und Neostratotypen, Miozän der Zentralen Paratethys, Bd. 4, M_5 Sarmatien. Die sarmatische Schichtengruppe und ihr Stratotypus. VEDA, Verlag der Slowakischen Akademie der Wissenschachften Bratislava: 318–433, (Taf. 1–19).

Pavšič, J. & Horvat, A. 2009: Eocen, oligocen in miocen v osrednji in vzhodni Sloveniji = The Eocene, Oligocene and Miocene in central and eastern Slovenia. In: Pleničar, M., Ogorelec, B. & Novak, M. (eds.): Geologija Slovenije = The Geology of Slovenia. Geološki zavod Slovenije, Ljubljana: 373–426.

Planjšek, M., Mirtič, B. & Aničić, B. 2002: Naravovarstveno ovrednotenje nahajališč miocenskih sedimentnih kamnin v kamnolomih severovzhodne Slovenije. (Geoconservation evaluation of the sites of Miocene sedimentary rocks in the quarries of north-eastern Slovenia). Geologija, 45/2: 485–492, doi:10.5474/geologija.2002.053

Rado, G. 1963: Contributii la studiul faunei miocene dintre Totoi şi Oarda de sus (Alba Iulia). Analele Universitatii Bucureşti, Ser. Ştiint. Natur. geol. – geograf., 32 (1962): 77–88.

Schultz, O. 1998: Tertiärfossilien Österreichs. Wirbellose, niedere Wirbeltiere und marine Säugetiere. Goldschneck-Verlag (Korb): 1–159.

Schultz, O. 2001: Bivalvia neogenica (Nuculacea – Unionacea). In: Piller, W. E. (ed.): Catalogus Fossilium Austriae. Band 1/Teil 1. Ein systematisches Verzeichnis aller auf österreichischem Gebiet festgestellten Fossilien. Verlag der Österreichischen Akademie der Wissenschaften (Wien): XLVIII, 1–379 + Taf. 1–56.

Schultz, O. 2003: Bivalvia neogenica (Lucinoidea – Mactroidea). In: W. E. Piller (editor), Catalogus Fossilium Austriae. Band 1/ Teil 2. Ein systematisches Verzeichnis aller auf österreichischem Gebiet festgestellten Fossilien. Verlag der Österreichischen Akademie der Wissenschaften (Wien): X, 381–690 + Taf. 57–95.

Schultz, O. 2005: Bivalvia neogenica (Solenoidea – Clavagelloidea). In: W. E. Piller (editor), Catalogus Fossilium Austriae. Band 1/ Teil 3. Ein systematisches Verzeichnis aller auf österreichischem Gebiet festgestellten Fossilien. Verlag der Österreichischen Akademie der Wissenschaften (Wien): V, 691–1067 + Taf. 96–152.

Stancu, J. & Andreescu, E. 1968: Fauna tortoniană din reguinea Rugi – Delineşti (Bazinul Caransebeşului). Studii şi cercetări de geol., geofiz., geograf., Ser. geologie, 13/2: 455–471, Pl. 1–6.

Stancu, J. & Popescu, A. 1970: Studii biostratigrafice şi mineralogice asupra formatiunii tortoniene de pe versantul nord-vestic al masivului Poiana Ruscă (Carpatii Meridionali). Dări di seamă ale şedintelor (1968-1969), 4. Stratigrafie, 56: 165–192.

Strausz, L. 1966: Die miozän – mediterranen Gastropoden Ungarns. Akadémiai Kiadó (Budapest): 1–692, (Taf. 1–79).

Tămaş, D., Tămaş, A. & Popa, M. V. 2013: Early Sarmatian (Middle Miocene) molluscs from Răcăştia (Romania). Acta Palaeont. Romaniae, 9/1: 67–81.

Vadász, E. 1960: Magyarország földtana. Akadémiai Kiadó (Budapest): 1–646, (Táb. 1–51).

Wenz, W. 1938: Gastropoda. Teil 1: Allgemeiner Teil und Prosobranchia. Handbuch der Paläozoologie, 6. Gebrüder Borntraeger (Berlin): 1-1200.

Wenz, W. 1960: Gastropoda. Teil 2, Euthyneura. Zilch, A. (ed.): Gebrüder Borntraeger 1959-1969 (Berlin-Nikolassee): XII, 1–834. In: Schindewolf, O. H. (ed.): Handbuch der Paläozoologie, Band 6, Teil 2.

Zlinská, A. & Fordinál, K. 1995: Spodnosarmatská fauna zo stretavského súvrstvia z okolia Slanskej Huty (východoslovenská panva). Geologické práce, Správy, 100: 71–75, Pl. 25–28.

Žnidarčič, M. & Mioč, P. 1987: Osnovna geološka karta SFRJ, Maribor in Leibnitz 1 : 100 000. Zvezni geološki zavod Beograd.

GEOLOGIJA *58/2*, 233–246, Ljubljana 2015

http://dx.doi.org/10.5474/geologija.2015.019

Isotopic composition of precipitation at the station Portorož, Slovenia – period 2007–2010

Izotopska sestava padavin na postaji Portorož, Slovenija – obdobje 2007–2010

Polona VREČA[1], Ines KRAJCAR BRONIĆ[2] & Albrecht LEIS[3]

[1]Department of Environmental Sciences, Jožef Stefan Institute, Jamova 39, SI–1000 Ljubljana, Slovenia
[2]Ruđer Bošković Institute, Bijenička 54, 10000 Zagreb, Croatia
[3]Institute of Water Resources Management, JOANNEUM RESEARCH, Elisabethstrasse 16/II, 8010 Graz, Austria

Prejeto / Received 17. 11. 2015; Sprejeto / Accepted 7. 12. 2015; Objavljeno na spletu / Published online 30. 12. 2015

Key words: precipitation, isotopes, oxygen, hydrogen, tritium, Portorož, Slovenia
Ključne besede: padavine, izotopi, kisik, vodik, tricij, Portorož, Slovenija

Abstract

The stable isotopic composition of oxygen and hydrogen ($\delta^{18}O$ and $\delta^{2}H$) and the tritium activity (A) were monitored in precipitation at synoptic station Portorož (Slovenia) during the period 2007–2010. Monthly and yearly isotope variations are discussed and compared with those observed over the period 2001–2006 and with the basic meteorological parameters. The mean values for $\delta^{18}O$ and $\delta^{2}H$, weighted by precipitation, are –6.28 ‰ and –41.6 ‰, and these values are 0.35 ‰ and 1.6 ‰ higher but not significantly different than for the period 2001–2006. The reduced major axis (RMA) local meteoric water line ($LMWL_{RMA}$) for the period 2007–2010 is $\delta^{2}H = (8.14 \pm 0.25)\times\delta^{18}O + (8.28 \pm 1.64)$, while the precipitation weighted least square regression (PWLSR) results in $LMWL_{PWLSR}$ $\delta^{2}H = (7.87 \pm 0.28)\times\delta^{18}O + (7.97 \pm 1.87)$. The deuterium excess ($\delta$) weighted mean value is 8.6 ‰ and is 1.2 ‰ lower than in 2001–2006, while the temperature coefficient of $\delta^{18}O$ is 0.21 ‰/°C and is for 0.02 ‰/°C higher than for the previous period. The mean Mediterranean precipitation index (MI) for the period 2007–2010 is 2.3. Lower values of MI and deuterium excess than in the preceding period indicate stronger continental climatic character during observation period, however the differences are not statistically significant. The weighted mean tritium activity is 6.4 TU, which is 0.5 TU lower but not significantly different than in 2001–2006.

Izvleček

V prispevku obravnavamo izotopsko sestavo kisika in vodika ($\delta^{18}O$ in $\delta^{2}H$) ter aktivnosti tricija (A) v mesečnih vzorcih padavin, ki smo jo spremljali na sinoptični postaji Portorož (Slovenija) v obdobju 2007–2010. Analizirali smo mesečne in letne spremembe izotopske sestave padavin in jih primerjali z nizom podatkov za obdobje 2001–2006 ter z osnovnimi meteorološkimi parametri. Srednje tehtane vrednosti $\delta^{18}O$ in $\delta^{2}H$ določene ob upoštevanju izmerjene količine padavin znašajo –6,28 ‰ in –41,6 ‰ in so za 0,35 ‰ oziroma 1,6 ‰ višje kot v obdobju 2001–2006, vendar so razlike statistično neznačilne. Lokalno padavinsko premico ($LMWL_{RMA}$) za obdobje 2007–2010 zapišemo kot $\delta^{2}H = (8{,}14 \pm 0{,}25)\times\delta^{18}O + (8{,}28 \pm 1{,}64)$, ob upoštevanju količine padavin pa kot $LMWL_{PWLSR}$ $\delta^{2}H = (7{,}87 \pm 0{,}28)\times\delta^{18}O + (7{,}97 \pm 1{,}87)$. Srednja tehtana vrednost devterijevega presežka (δ) znaša 8,6 ‰ in je za 1,2 ‰ nižja kot v obdobju 2001–2006, medtem ko je temperaturni koeficient za $\delta^{18}O$ za 0,02 ‰/°C višji kot v primerjalnem obdobju in znaša 0,21 ‰/°C. Srednja vrednost indeksa mediteranskosti padavin (MI) znaša 2,3. Nižje vrednosti MI in devterijevega presežka nakazujejo v opazovanem obdobju bolj kontinentalni značaj podnebja, vendar so razlike statistično neznačilne. Srednja tehtana vrednost tricijeve aktivnosti znaša 6,4 TU in je za 0,5 TU nižja kot v obdobju 2001–2006, a je tudi ta razlika statistično neznačilna.

Introduction

Since initiation of the Global Network of Isotopes in Precipitation (GNIP) by the International Atomic Energy Agency (IAEA) and the World Meteorological Organisation (WMO) in 1958 the importance and need of a systematic collection of data on the isotopic composition, i.e. stable isotopes of oxygen (expressed as $\delta^{18}O$) and hydrogen (expressed as $\delta^{2}H$) and radioactive hydrogen isotope (tritium, ^{3}H), of precipitation across the globe to determine temporal and spatial variations in isotope ratios in precipitation, is steadily increasing. Initially GNIP was focused on monitoring atmospheric thermonuclear test fallout through levels of radioactive tritium and, after 1970, became an important observation network of stable oxygen and hydrogen isotope

composition data for hydrologic investigations of water resources (Internet 1). The past decade has experienced increasing demand for accurate spatial and temporal predictions of point, regional, and continental-scale $\delta^{18}O$ and $\delta^{2}H$ values in precipitation, especially for some regions where little or no GNIP data existed (Terzer et al., 2013). The main reason for steadily increasing application of water isotopes remains their importance in hydrologic and hydrogeologic investigations of water resources, in verification and improvement of atmospheric circulation models and in investigation of regional, global and temporal climates. In addition, it was revealed that the $\delta^{18}O$ and $\delta^{2}H$ values of some plant, animal, and human tissues closely mirrored isotopic patterns of precipitation (Hobson & Wassenaar, 1997; Bowen et al., 2005) and therefore use of stable water isotopes expanded also in ecological, wildlife, food source traceability, and forensic sciences (Terzer et al., 2013).

The only radioactive constituent of water molecule is tritium, ^{3}H, with the half-life of 12.32 yr (Lucas and Unterweger, 2000; Internet 2). It is produced naturally in the upper atmosphere by reaction of cosmic-rays neutron with atmospheric nitrogen (Internet 2). The tritium with atmospheric oxygen subsequently forms tritiated water ($^{1}H^{3}HO$) molecule that in turn reaches the Earth's surface through precipitation. However, most of the tritium present in the atmosphere and hydrosphere is of anthropogenic origin, i.e., tritium was released in atmospheric thermonuclear tests during 1960's, reaching in 1963 several orders of magnitudes higher tritium activity concentration in the atmosphere than the natural levels. After the test ban treaty in 1963, atmospheric tritium activity has been decreasing almost exponentially in the following decades, while during last 10–15 years the mean tritium activity has not been significantly changed (Krajcar Bronić et al., 2006; Vreča et al., 2014; Internet 2). Nowadays, tritium has reached in precipitation levels similar to those occurring before the thermonuclear tests, about 5 TU in central Europe (Internet 2). These low and constant concentrations limit the use of tritium in hydrogeological studies. However, tritium can be used to investigate atmospheric vapour migration under different meteorological conditions, especially if the sources of water vapour differ (Kigoshi & Yoneda, 1970; Unnikrishnan Warier et al., 2013). Due to the water vapour exchange between the atmosphere and the sea (ocean) surface, coastal and oceanic stations show considerably lower tritium activity than the continental stations because the moisture evaporating from the sea/ocean is low in tritium content (Ehhalt, 1971; Vreča et al., 2006). With the more-or-less natural tritium levels in modern precipitation, the technogenic emissions of tritium (from nuclear facilities, or from manufacturing or disposal of luminous consumer products, planned fusion demo facilities) are becoming more and more visible (Hebert, 1990; Rozanski et al., 1991; Matsumoto et al., 2013), and the knowledge of natural tritium distribution remains important from the environmental pollution point of view (Thompson et al., 2015; Ueda et al., 2015).

Regular monitoring of the oxygen and hydrogen isotopic composition of precipitation in the coastal area of SW Slovenia is important not only for studying the isotopic patterns of local meteorological conditions, but also for improvement of the knowledge of the isotopic input signal needed for hydrogeological studies of the large karstic springs used for water supply in the area (Vreča et al., 2007) and other applications. Therefore, monitoring of the isotopic composition of precipitation in Portorož (SW Slovenia) has been performed by the Jožef Stefan Institute (JSI) since 2000 (Vreča et al., 2005, 2006, 2007, 2011). To begin with, monitoring was performed in cooperation with the Slovenian Environment Agency (ARSO), the Ruđer Bošković Institute (RBI; Zagreb, Croatia) and the IAEA (Vreča et al. 2005, 2006). Since 2004 the JSI has also cooperated with Joanneum Research (JR; Graz, Austria). Details on the isotope monitoring until 2006, together with data evaluation, have been reported in Vreča et al. (2005, 2006, 2007, 2011). The isotope data obtained until 2006 for Portorož (Vreča et al., 2005, 2006, 2007, 2011) are also available in the GNIP database. The data were used in different hydrogeochemical investigations of aquifers in Slovenia (Brenčič, 2009; Mezga, 2014; Mezga et al., 2014; Verbovšek & Kanduč, 2015), Croatia (Mandić et al., 2008) and in Italy (Cucchi et al., 2008), as well as in investigations of precipitation (Liotta et al., 2008; Vodila et al., 2011; Michelini, 2013; Vreča et al., 2014; Brenčič et al., 2015, Kovačič, 2015), moisture recycling in Alpine regions (Froehlich et al., 2008) and identification and characterisation of nitrate pollution sources in Marano lagoon in Italy (Saccon et al., 2013).

The main purpose of this paper is to present new results concerning the isotopic composition of precipitation at Portorož for the period 2007–2010 and to compare them with those for the period 2001–2006 (Vreča et al., 2011).

Materials and methods

Sampling

Monthly composite precipitation has been sampled since October 2000 at the synoptic meteorological station Portorož (45°28'N, 13°37'E; 2 m a.s.l.) which is located at the airport and is part of the Slovene national meteorological network maintained by the ARSO (Internet 3). The station is included in the GNIP under the station name Portorož and has the GNIP code 1410500.

Water samples were collected by the staff of the meteorological station from standard precipitation gauge three times daily. After measuring the amount of precipitation the sample was poured

into a 5-litre plastic bottle with a well tight cap to avoid evaporation and kept in a dark place. After bringing the samples to the laboratory the impurities (e.g. dust, particles) were removed from the sample by filtration (Whatman Grade 589, Black Ribbon) before taking aliquots for different isotope analyses. Then a 50 mL glass bottle was filled for the stable isotope analysis of oxygen and hydrogen and the rest of the water was transferred to 0.5 or 1 L high density polyethylene (HDPE) bottles for tritium analysis. During the sampling period April 2007 was very dry with only 2.2 mm precipitation which was not sufficient for isotope analysis.

Meteorological data (amount of precipitation and air temperature) are available from the ARSO (Internet 3).

Stable isotope analysis

The oxygen isotopic composition ($\delta^{18}O$) was measured by means of the water–CO_2 equilibration technique (Epstein & Mayeda, 1953) on a dual inlet isotope-ratio mass spectrometer Finnigan DELTA^{plus} by means of the fully automated equilibration technique at JR until February 2007 (see also Vreča et al., 2011). Since then, a continuous flow isotope-ratio mass spectrometer IsoPrime (GV Instruments, UK) coupled to an automatic water-CO_2 equilibration system MultiFlow was used at the JSI. The isotopic composition of hydrogen was determined on a continuous flow Finnigan DELTA^{plus} XP mass spectrometer with a HEKAtech high-temperature oven, by reduction of water over hot chromium (Morrison et al., 2001) at JR. Results are reported as δ values in per mill (‰) relative to the Vienna-SMOW standard (Coplen et al., 2002). All measurements were carried out together with laboratory standards that were calibrated periodically against international standards, as recommended by the IAEA. Measurement precision was better than ±0.1 ‰ for $\delta^{18}O$ and ±1 ‰ for $\delta^{2}H$.

Tritium activity

Tritium activity (A) in monthly samples was determined at the Tritium Laboratory at the Department of Experimental Physics of the RBI. Results are expressed in Tritium Units (1 TU = 0.118 BqL^{-1}). The gas proportional counting technique (GPC) was used until 2009; since 2010, samples have been measured by the liquid scintillation counting technique (LSC) following electrolytic enrichment (EE), while during 2008 and 2009 both GPC and LSC-EE techniques were used, depending on the available sample quantity. The limit of detection (LOD) was 2.5 TU and 0.5 TU for GPC and LSC-EE techniques, respectively (for details see Barešić et al., 2010, 2011; Krajcar Bronić et al., 2013; Vreča et al., 2014).

Tritium activity in three samples (February, March and April 2010) was determined by the Group for radiochemistry at the Department of Environmental Sciences of the JSI following electrolytic enrichment by liquid scintillation counting (LSC-EE) on a Tri Carb 3170 TR/SL Liquid Scintillation Counter (LSC, Canberra Packard) in accordance with method accredited by Slovenian Accreditation since 2009 (accreditation certificate LP-090). The LOD was 2.9 TU.

Data reduction

The approach of data reduction described by Vreča et al. (2008, 2011, 2014) for Portorož and Ljubljana isotope records 2001–2006 and 2007–2010, was used. Basic descriptive statistics, i.e. mean, minimum and maximum values were determined and the deuterium excess ($d = \delta^{2}H - 8\times\delta^{18}O$; Dansgaard, 1964) was calculated. For the quantitative characterization of the Mediterranean character of yearly precipitation the Mediterranean precipitation index (MI) introduced by Koppany & Unger (1992) was calculated as:

$$MI = (P_{X\text{-}XI} - P_{V\text{-}VI})\times 100/P_{year} \quad (1)$$

where $P_{X\text{-}XI}$ is the sum of precipitation in October and November (in mm), $P_{V\text{-}VI}$ is the sum of precipitation in May and June (in mm) and P_{year} is the annual precipitation (in mm).

Furthermore, mean values weighted by the amount of precipitation were calculated from all monthly data, and then summed over all collected samples, per month, over each season: winter (December, January, February), spring (March, April, May), summer (June, July, August) and autumn (September, October, November), and per year. The minimum required number of data fulfilled the requirement of eight monthly measured samples per year and more than 70 % of total precipitation amount collected per year (IAEA, 1992).

Linear correlations between $\delta^{2}H$ and $\delta^{18}O$ were calculated by methods usually applied in stable isotope studies – the ordinary least squares regression (OLSF) and the reduced major axis (RMA) regression (IAEA, 1992; Hughes & Crawford, 2012). In addition, we applied a precipitation weighted least square regression (PWLSR) method, introduced by Hughes & Crawford in 2012, which takes into account the precipitation amount in particular month. The same approach was used by Vreča et al. (2014) for the 2007–2010 isotope record at Ljubljana. The lines are defined as local meteoric water lines ($LMWL_{OLSF}$, $LMWL_{RMA}$ and $LMWL_{PWLSR}$).

Finally, oxygen-temperature correlation was calculated using air temperature data provided by ARSO from station Portorož for all monthly data and for the mean monthly data from the studied period.

Results and discussion

Meteorological data: Precipitation and temperature

Temporal variations in precipitation and air temperature for the period 2007–2010 are presented in Figure 1. The lowest precipitation was recorded in April 2007 (2 mm) and the highest in September 2010 (249 mm) (Figure 1), which was much greater than the mean September precipitation (118 mm) for the reference period 1981–2010 (Internet 3). In the same months during the period 2007–2010 were minimum and maximum records observed also for Ljubljana (Vreča et al., 2014). Besides in 2010, very high precipitation was recorded also in September 2007 (234 mm, Figure 1), although the total amount of precipitation in 2007 was below the long-term mean (Table 1).

Annual amounts of precipitation and mean annual air temperatures in the period 2007–2010 are summarized in Table 1. The annual precipitation amount varied between 753 mm in 2007 and 1,394 mm in 2010, with a mean value of 1,018 mm (Table 1) which is higher than during the period 2001–2006 (944 mm, Vreča et al., 2011) and also higher than in 1981–2010 (968 mm, Internet 3). In 2010 a record amount of precipitation was registered (1,394 mm), which is 40 % more than on the long-term average (Cegnar, 2011). In the period 2007–2010 mean monthly precipitation was higher for February, March, June, July, September, November and December and lower for other months than in 2001–2006 (Figure 2). Autumn and winter precipitation represent 59 % of annual precipitation which is 5 % higher than in 2001–2006 and 3 % higher than in 1981–2010.

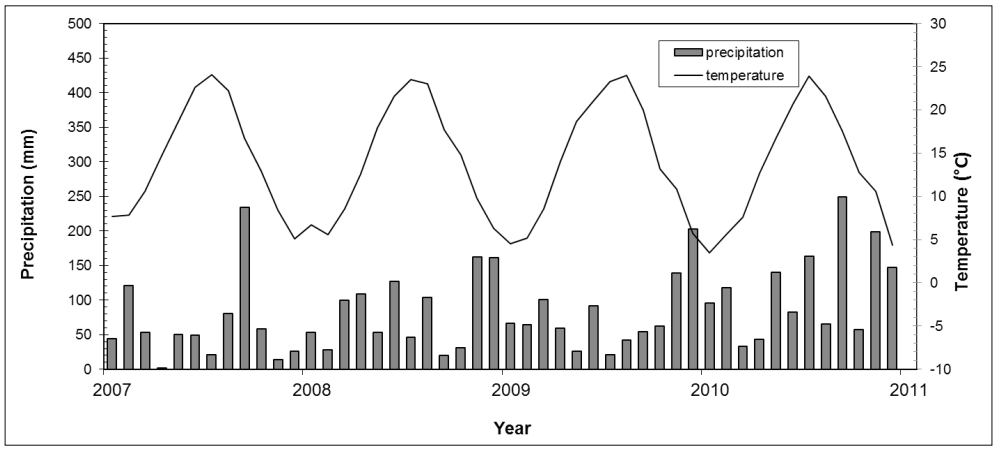

Figure 1. Monthly precipitation and mean monthly air temperature at station Portorož for period 2007–2010.

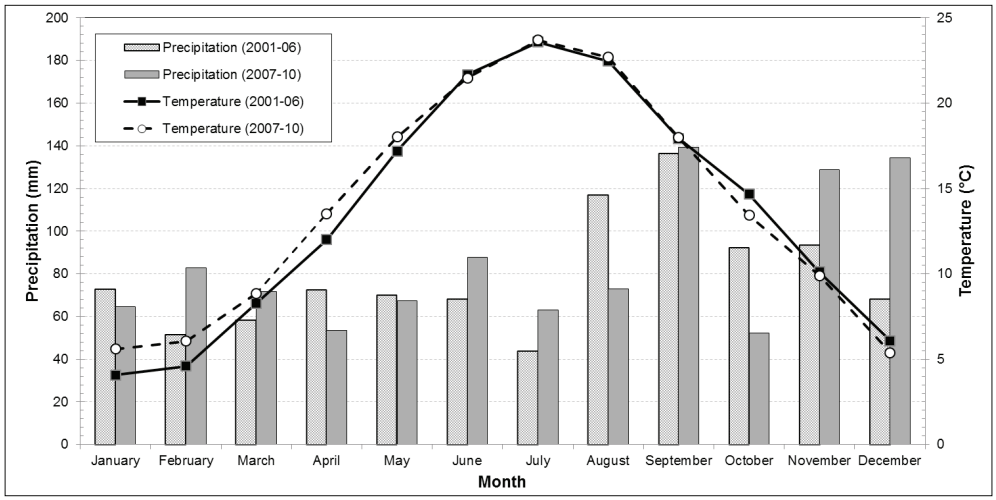

Figure 2. Mean monthly precipitation and mean monthly air temperatures at station Portorož for periods 2001–2006 (Vreča et al., 2011) and 2007–2010.

Table 1. Annual amount of precipitation (P), mean annual air temperature (T) and Mediterranean precipitation index (MI) at station Portorož. * – data for period 2001–2006 (Vreča et al., 2011); ** – data for period 1981–2010 (Internet 2).

Period / Year	P (mm)	T (°C)	MI
2007	753	14.3	–3.6
2008	994	14.0	1.4
2009	932	14.1	9.0
2010	1394	13.1	2.4
mean value 2007–2010	1018 ± 271	13.9 ± 0.5	2.3 ± 5.2
2001–2006 *	944 ± 142	13.6 ± 0.6	5.5 ± 10.2
long-term mean value 1981–2010 **	968	13.2	5.9

The variations in precipitation indicate some changes in climatic character as indicated by change of Mediterranean precipitation index (MI). The MI for the period 2007–2010 varied between –3.6 in 2007 and 9.0 in 2009, with annual mean value of 2.3 (Table 1). This value is much lower than the annual mean during the periods 2001–2006 (5.5), 1981–2010 (5.9) and 1971–2000 (6.1) and indicates at Portorož a stronger Mediterranean climate character than the continental one in the past. However, annual variations are high and therefore the differences between periods 2007–2010 and 2001–2006 are not statistically significant.

Variations of monthly air temperatures are shown in Figure 1. The lowest monthly temperature (3.5 °C) was observed in January 2010 and the highest in July 2007 (24.1 °C) (Figure 1). Similarly as observed in the period 2007–2010 in Ljubljana (Vreča et al., 2014) the warmest year in Portorož was 2007 and the coldest 2010 (Table 1). The mean air temperature for the whole period was 13.9 °C, on average 0.3 °C and 0.7 °C higher than that for 2001–2006 and 1981–2010 (Table 1). Variations of mean monthly air temperature are shown in Figure 2. Deviations up to 1.5 °C from 2001–2006 temperature record were observed in the first half of year.

Long-term mean monthly temperatures for periods 1971–2000 and 1981–2010 show winter minimum in January and summer maximum in July (Internet 3). The difference between maximum and minimum air temperature, which may be taken as a measure of the continentality of the climate (i.e. the larger the difference, the more continental the type of climate) was 18.4 °C and 18.6 °C for 1971–2000 and 1981–2010. During the 2007–2010 the maximum monthly temperature was observed always in July while the minimum was recorded in December (2007), February (2008) or January (2009 and 2010). The difference between maximum and minimum varied from 17.9 °C to 20.4 °C, with a mean of 19.2 °C, and indicates more continental climate at Portorož in investigated period than in the preceding long-term climatological periods. Therefore, both indices of continentality, the MI that takes into account seasonal distribution of precipitation, and the range of temperatures, indicate higher continental influences on the climate in Portorož in the investigated period. These facts, together with the increase in mean annual air temperatures and general decrease in amount of precipitation may indicate modern climatic changes in the area but have to be investigated into more detail in future.

Stable isotope data ($\delta^{18}O$, $\delta^{2}H$ and d)

Results of monthly isotopic composition of precipitation parameters, $\delta^{18}O$, $\delta^{2}H$ and d, are summarized in Table 2. Results are reported to one decimal point for $\delta^{2}H$ and d values and to two for $\delta^{18}O$.

Variations of monthly isotopic composition of precipitation ($\delta^{18}O$, $\delta^{2}H$) from 2007 to 2010 are presented in Figures 3a and 3b. The lowest $\delta^{18}O$ value was observed in January 2010 (–12.20 ‰) and the highest in July 2008 and May 2009 (–2.60 ‰). Variations in $\delta^{2}H$ follow those for $\delta^{18}O$ (Figure 3a), with a minimum $\delta^{2}H$ value of –92.7 ‰ and maximum of –7.1 ‰ observed in January 2010 and July 2008, respectively. The mean $\delta^{18}O$ and $\delta^{2}H$ values for the observed period are –6.08 ‰ and –41.3 ‰ (n = 47), and are more positive than values from 2001 to 2006; i.e., –6.51 ‰ and –43.1 ‰ (n = 74) (Vreča et al., 2011).

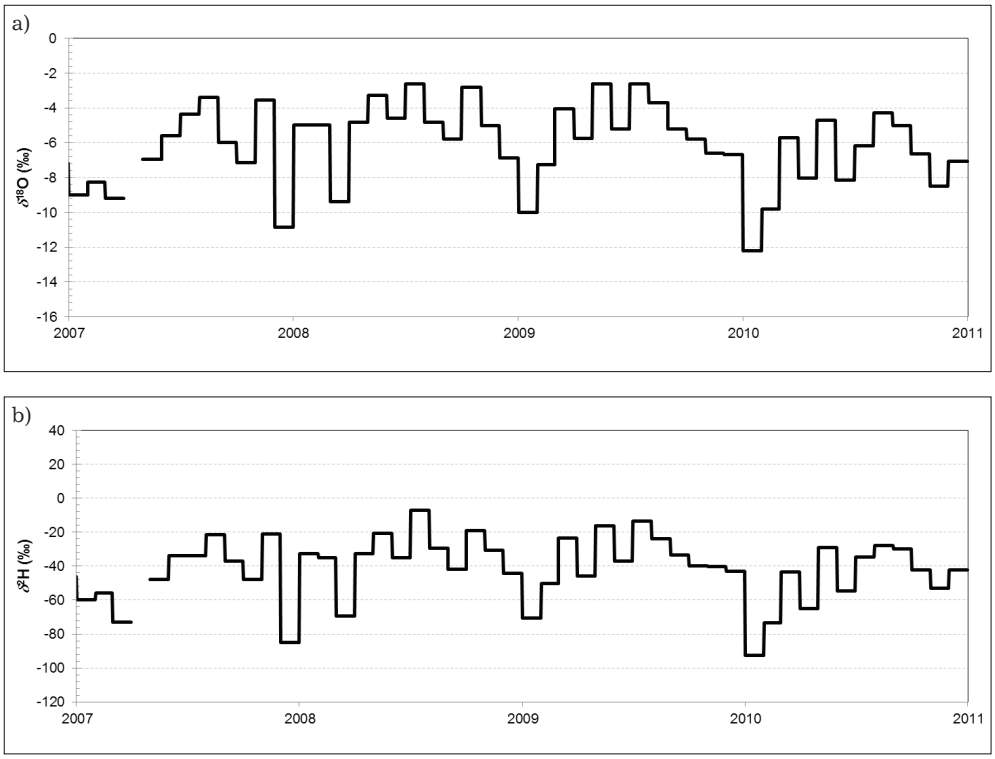

Figure 3. Monthly variations a) of isotopic composition of oxygen ($\delta^{18}O$), b) isotopic composition of hydrogen ($\delta^{2}H$), c) deuterium excess (d) and d) tritium activity (A), in precipitation at station Portorož, 2007–2010.

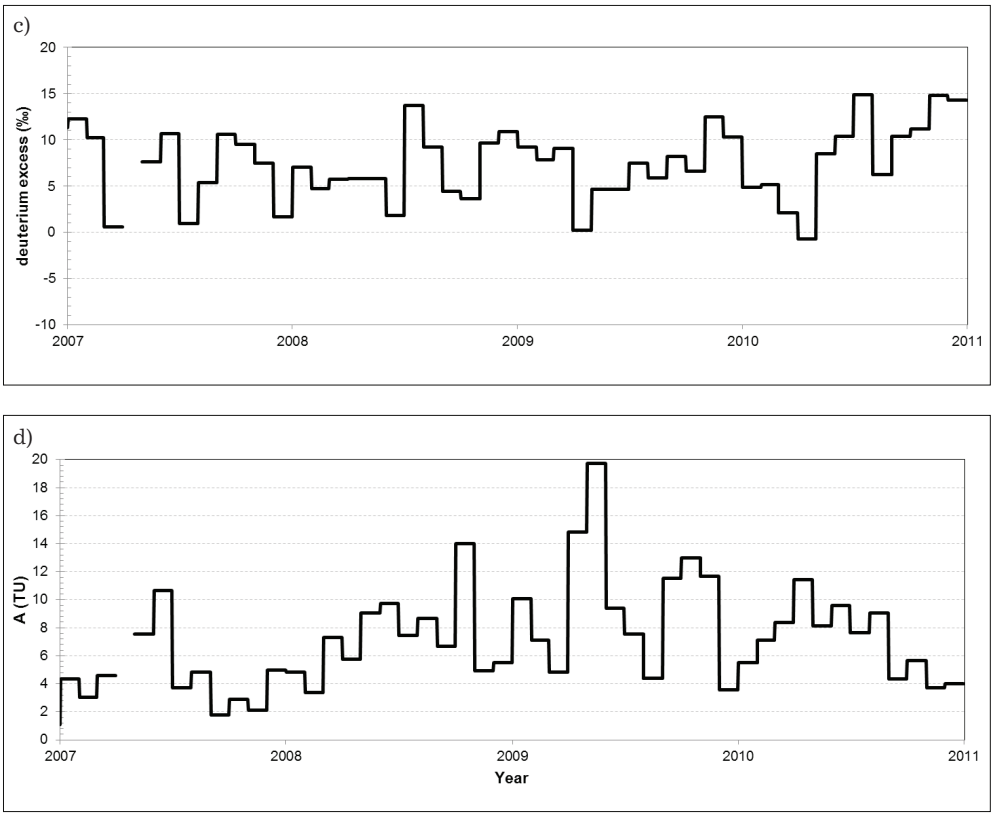

Monthly variations of deuterium excess (*d*) are presented in Figure 3c. The lowest value was obtained for the sample collected in April 2010 (–0.7 ‰, Table 2). The highest *d* values were observed in July 2010 (14.9 ‰) and November 2010 (14.8 ‰). The mean value is 7.4 ‰ (n = 47) (Table 2) and is 1.6 ‰ lower than the mean value of 9.0 ‰ from the period 2001–2006 (Vreča et al., 2011). Most *d* values (72 %, i.e. 34 out of total 47) range between 5 and 15 ‰. No value higher than 15 ‰, typical for Mediterranean-derived precipitation (Cruz-San et al., 1992; Rozanski et al., 1993), was determined indicating different climate conditions as in the period 2001–2006 when more than 10 % of *d* values exceeded 15 ‰ (Vreča et al., 2011). It is known, that *d* values can alter as the air mass moves inland, due to secondary processes such as evaporation from an open surface water body which returns moisture to the air (Craig & Gordon, 1965; Merlivat & Jouzel, 1979; Gat et al., 1994; Gat, 1996). In addition, *d* values can change as precipitation falls through the atmosphere (Gat, 1996; Araguas-Araguas et al., 2000; Peng et al., 2004) or as the precipitation sample sits in the precipitation collector (Harvey, 2005). It was estimated that the initial *d* values should not be less than 3 ‰ and that lower values should be used with caution unless the source of their evaporative enrichment is known (Harvey, 2005). A high proportion (15 %) of *d* values was <3 ‰ (Table 2). These values probably indicate secondary evaporation processes and correspond mainly to months with low precipitation, related to local stormy and windy events in the area or to months with light rainy events, therefore we did not exclude them from evaluation. It is interesting that high *d* values (>13 ‰) were obtained for July 2010 and also July 2008. For both months very intense thunderstorms were characteristic with prevailing south and southwest winds (Internet 3).

Monthly mean $\delta^{18}O$, $\delta^{2}H$ and *d* values, weighted by precipitation amount are summarized in Table 3 and presented in Figures 4 and 5a, where they are compared with the 2001–2006 values (Vreča et al., 2011). The higher $\delta^{18}O$ and $\delta^{2}H$ values in spring and summer months, due to higher air temperatures, constitute a typical seasonal variation which is less pronounced than in Ljubljana (Vreča et al., 2014). Seasonal variations of $\delta^{18}O$ and $\delta^{2}H$ of 5.47 ‰ and 43.1 ‰ (Table 3), respectively, were observed and are smaller than for continental stations like Ljubljana (8.81 ‰ and 53.7 ‰, respectively, Vreča et al., 2014). The lowest $\delta^{18}O$ and $\delta^{2}H$ values are observed in January (Table 3) and are 1.38 ‰ and 9.4 ‰ lower than those for the period 2001–2006. The positive deviations from 2001–2006 calculations are observed for May, June, August and September and can be attributed to higher temperatures and lower amounts of precipitation during sampling period 2007–2010. *d* values range around 8.2 ‰ (Table 3) with the lowest values in April (2.9 ‰) and the highest in July (12.9 ‰) and November (12.4 ‰). Slightly higher *d* values are observed in autumn and winter precipitation, with values above 10 ‰ only in November and December (Figure 5a). Most mean monthly values are lower than for the period 2001–2006, indicating the minor influence of Mediterranean air masses over the region during the observation period.

Table 2. Monthly isotopic composition ($\delta^{18}O$, $\delta^{2}H$, deuterium excess (d) and tritium activity (A)) of precipitation at Portorož for period 2007–2010. n. d. – not determined; GPC – gas proportional counter; LSC – liquid scintillation counter and electrolytic enrichment; JSI – Jožef Stefan Institute; n –number of samples.

Month/ Year	$\delta^{18}O$ (‰)	$\delta^{2}H$ (‰)	d (‰)	A (TU)	Method of tritium activity measurement
01/2007	–9.00	–59.7	12.3	4.3	GPC
02/2007	–8.25	–55.8	10.2	3.1	GPC
03/2007	–9.18	–72.8	0.6	4.6	GPC
04/2007	n. d.	n. d.	n. d.	n. d.	
05/2007	–6.94	–47.9	7.7	7.5	GPC
06/2007	–5.58	–34.0	10.7	10.7	GPC
07/2007	–4.37	–34.0	1.0	3.7	GPC
08/2007	–3.37	–21.6	5.4	4.8	GPC
09/2007	–5.97	–37.2	10.6	1.8	GPC
10/2007	–7.15	–47.7	9.5	2.9	GPC
11/2007	–3.56	–21.0	7.5	2.1	GPC
12/2007	–10.84	–85.0	1.7	5.0	GPC
01/2008	–4.98	–32.8	7.1	4.8	GPC
02/2008	–4.97	–35.0	4.7	3.4	GPC
03/2008	–9.39	–69.4	5.7	7.3	GPC
04/2008	–4.82	–32.8	5.8	5.8	GPC
05/2008	–3.28	–20.5	5.8	9.1	GPC
06/2008	–4.60	–35.0	1.8	9.7	LSC
07/2008	–2.60	–7.1	13.7	7.5	GPC
08/2008	–4.82	–29.4	9.2	8.6	LSC
09/2008	–5.79	–41.9	4.4	6.7	GPC
10/2008	–2.81	–18.8	3.7	14.0	GPC
11/2008	–5.02	–30.5	9.7	4.9	LSC
12/2008	–6.89	–44.2	10.9	5.5	GPC
01/2009	–10.00	–70.8	9.2	10.1	GPC
02/2009	–7.24	–50.1	7.8	7.1	GPC
03/2009	–4.06	–23.4	9.1	4.8	GPC
04/2009	–5.73	–45.6	0.2	14.8	GPC
05/2009	–2.60	–16.1	4.7	19.7	GPC
06/2009	–5.20	–37.0	4.6	9.4	LSC
07/2009	–2.63	–13.6	7.5	7.5	GPC
08/2009	–3.71	–23.8	5.9	4.4	GPC
09/2009	–5.22	–33.6	8.2	11.5	GPC
10/2009	–5.80	–39.8	6.6	13.0	GPC
11/2009	–6.60	–40.3	12.5	11.7	GPC
12/2009	–6.66	–43.0	10.3	3.6	LSC
01/2010	–12.20	–92.7	4.9	5.5	LSC
02/2010	–9.81	–73.3	5.2	7.1	LSC (JSI)
03/2010	–5.70	–43.5	2.1	8.4	LSC (JSI)
04/2010	–8.04	–65.1	–0.7	11.4	LSC (JSI)
05/2010	–4.70	–29.1	8.5	8.1	LSC
06/2010	–8.15	–54.8	10.4	9.6	LSC
07/2010	–6.18	–34.5	14.9	7.6	LSC
08/2010	–4.27	–27.9	6.3	9.1	LSC
09/2010	–5.03	–29.9	10.4	4.3	LSC
10/2010	–6.65	–42.0	11.2	5.7	LSC
11/2010	–8.49	–53.1	14.8	3.7	LSC
12/2010	–7.06	–42.2	14.3	4.0	LSC
min	–12.20	–92.7	–0.7	1.8	
max	–2.60	–7.1	14.9	19.7	
mean	–6.08	–41.3	7.4	7.2	
n	47	47	47	47	

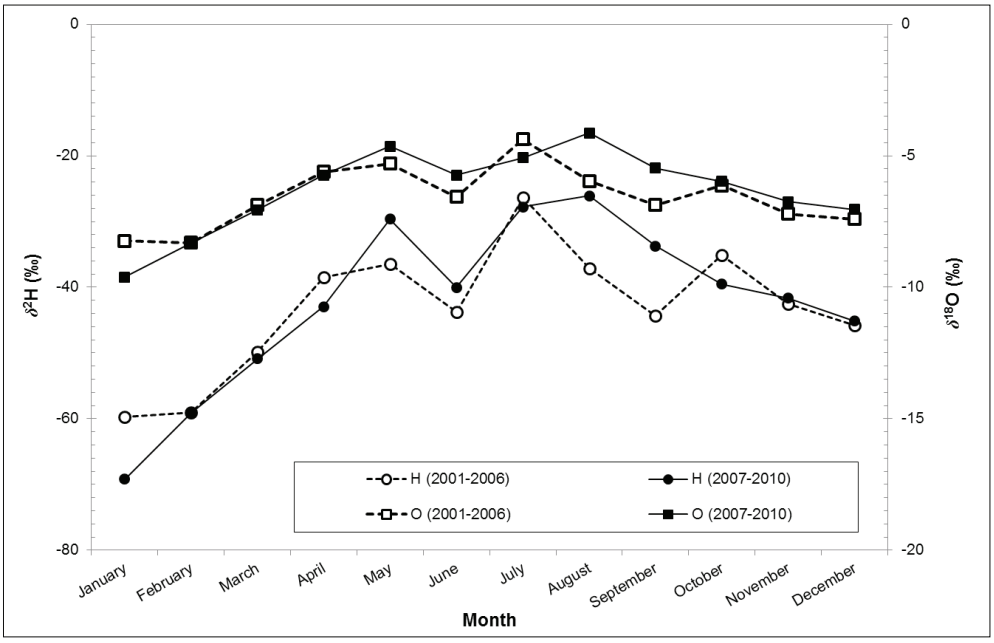

Figure 4. Monthly weighted mean $\delta^{18}O$ (in legend O) and $\delta^{2}H$ (in legend H) for periods 2001–2006 (Vreča et al., 2011) and 2007–2010 at station Portorož.

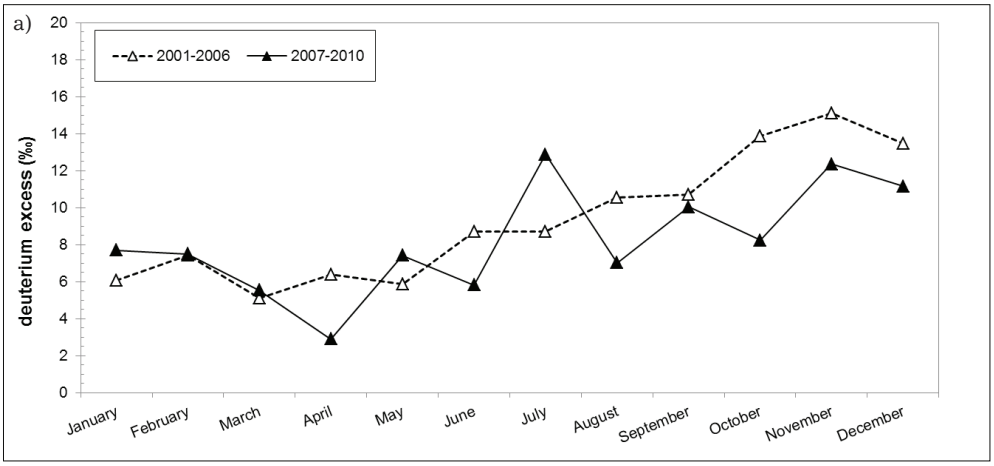

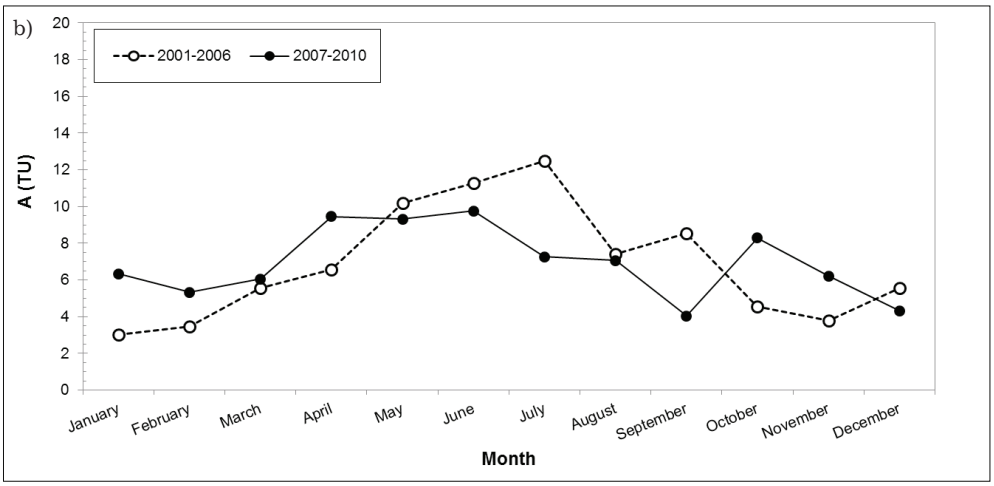

Figure 5. Monthly weighted mean a) deuterium excess (*d*) and b) tritium activity (A) for periods 2001–2006 (Vreča et al., 2011) and 2007–2010 at station Portorož.

Seasonal mean $\delta^{18}O$, $\delta^{2}H$ and *d* values weighted by amount of precipitation are summarized in Table 4. The lowest $\delta^{18}O$ and $\delta^{2}H$ values are typical of those in winter and the highest of those in summer and autumn. The *d* values for all seasons are <10 ‰ and confirm lower Mediterranean-derived precipitation influence than for the period 2001–2006 (Vreča et al., 2011).

Annual mean $\delta^{18}O$, $\delta^{2}H$ and *d* values, weighted by amount of precipitation for the period 2007–2010 are summarized in Table 5. The $\delta^{18}O$ and $\delta^{2}H$ values show an overall increase by 0.35 ‰ and 1.6 ‰ compared to the period 2001–2006 (Table 5), while the weighted mean *d* values show an overall decrease by 1.2 ‰. However, changes are not statistically significant different. The maximum

annual weighted mean $\delta^{18}O$ and $\delta^{2}H$ values were observed in 2008, when the smallest difference between maximum and minimum air temperature (i.e. 17.9 °C) was recorded and precipitation was higher during the spring-summer season. Consequently spring-summer precipitation with higher isotopic composition contributed more to the annual weighted mean. Similar pattern was observed in Ljubljana (Vreča et al., 2014). The lowest annual weighted mean $\delta^{18}O$ and $\delta^{2}H$ values were observed in 2010 and can be attributed to the lowest mean annual air temperature (13.1 °C) during 2007–2010, lower temperature than the long-term records (Table 1), a cold January and December and the highest precipitation (1,394 mm). The highest annual weighted mean *d* value was observed in 2010 (Table 5) and is related mainly to the Mediterranean-derived precipitation in the autumn (Table 2). The lowest annual weighted mean *d* value was observed for 2008.

Table 3. Monthly weighted mean $\delta^{18}O$, $\delta^{2}H$, deuterium excess (*d*) values and tritium activity (A) for period 2007–2010. n – number of samples.

Month	n	$\delta^{18}O$ (‰)	$\delta^{2}H$ (‰)	*d* (‰)	A (TU)
January	4	–9.61	–69.2	7.7	6.3
February	4	–8.33	–59.1	7.5	5.3
March	4	–7.05	–50.9	5.5	6.1
April	3	–5.73	–43.0	2.9	9.5
May	4	–4.63	–29.7	7.4	9.3
June	4	–5.73	–40.0	5.8	9.7
July	4	–5.08	–27.8	12.9	7.3
August	4	–4.14	–26.1	7.0	7.1
September	4	–5.47	–33.7	10.0	4.0
October	4	–5.97	–39.5	8.2	8.3
November	4	–6.75	–41.6	12.4	6.2
December	4	–7.04	–45.2	11.2	4.3
	min	–9.61	–69.2	2.9	4.0
	max	–4.14	–26.1	12.9	9.7
2007–2010 monthly weighted mean		–6.29	–42.1	8.2	7.0

Table 4. Seasonal weighted mean $\delta^{18}O$, $\delta^{2}H$, deuterium excess (*d*) values and tritium activity (A) for period 2007–2010. n – number of samples.

Season	n	$\delta^{18}O$ (‰)	$\delta^{2}H$ (‰)	*d* (‰)	A (TU)
Winter	12	–8.01	–54.8	9.3	5.1
Spring	11	–5.84	–41.3	5.5	8.1
Summer	12	–5.03	–32.0	8.2	8.2
Autumn	12	–5.04	–31.5	8.9	5.3

Table 5. Annual weighted mean $\delta^{18}O$, $\delta^{2}H$, deuterium excess (*d*) values and tritium activity (A). n – number of samples. * – data for period 2001–2006 (Vreča et al., 2011).

Year	n	$\delta^{18}O$ (‰)	$\delta^{2}H$ (‰)	*d* (‰)	A (TU)
2007	11	–6.67	–44.9	8.5	3.9
2008	12	–5.40	–35.8	7.4	7.0
2009	12	–5.96	–39.5	8.3	8.6
2010	12	–7.06	–46.2	10.2	6.2
	min	–7.06	–46.2	7.4	3.9
	max	–5.40	–35.8	10.2	8.6
2007–2010 annual weighted mean		–6.28 ± 0.74	–41.6 ± 4.8	8.6 ± 1.2	6.4 ± 2.0
2001–2006 annual weighted mean*		–6.63 ± 0.45	–43.2 ± 3.9	9.8 ± 1.5	6.9 ± 2.1

Local meteoric water lines

The local meteoric water lines (LMWLs) for the period 2007–2010 were calculated using different types of linear regression analysis. The ordinary least squares regression (OLSF) regression line ($LMWL_{OLSF}$) for Portorož is:

$$\delta^2H = (7.96 \pm 0.28)\times\delta^{18}O + (7.15 \pm 1.81);\ r = 0.98,\ n = 47 \quad (2)$$

The reduced major axis (RMA) regression line ($LMWL_{RMA}$) is:

$$\delta^2H = (8.14 \pm 0.25)\times\delta^{18}O + (8.28 \pm 1.64);\ r = 0.98,\ n = 47 \quad (3)$$

For the precipitation amount recorded at Portorož, the precipitation weighted least square regression (PWLSR) line ($LMWL_{PWLSR}$) is:

$$\delta^2H = (7.87 \pm 0.28)\times\delta^{18}O + (7.97 \pm 1.87);\ r = 0.99,\ n = 47 \quad (4)$$

For comparison with $LMWL_{PWLSR}$ for the 2007–2010 we calculated also the $LMWL_{PWLSR}$ for the 2001–2006 isotope record at Portorož (Vreča et al., 2011) and the PWLSR line ($LMWL_{PWLSR(2001–2006)}$) is:

$$\delta^2H = (7.80 \pm 0.27)\times\delta^{18}O + (8.52 \pm 1.85);\ r = 0.96,\ n = 71 \quad (5)$$

All regression lines have similar values (within uncertainties) for both the slope and the intercept values.

The slopes of LMWLs obtained are close to the LMWLs for the period 2001–2006 (Vreča et al., 2011) and to those at Ljubljana for the period 2007–2010 (Vreča et al., 2014). All slopes are also close to the slope 8 of Global Meteoric Water Line (GMWL) of Craig (1961) and to that calculated from the GNIP database for the period 1961–2000 by Gourcy et al. (2005).

Oxygen – temperature correlation

The linear correlation between $\delta^{18}O$ in monthly samples and mean monthly air temperature at Portorož, T, for the period 2007–2010 (Figure 6) is:

$$\delta^{18}O = 0.21\times T - 8.94;\ r = 0.61,\ n = 47 \quad (6)$$

The linear correlation between monthly weighted $\delta^{18}O$ values and mean monthly air temperature at Portorož, $T_{monthly}$, for the period 2007–2010 (Figure 6) is:

$$\delta^{18}O = 0.20\times T_{monthly} - 9.03;\ r = 0.86;\ n = 12 \quad (7)$$

The correlations obtained differ slightly in their intercept values and have the higher slope as that for the records 2001–2003 and 2001–2006 (Vreča et al., 2006, 2011). The slope of about 0.20 ‰/°C is between those typical of continental and maritime stations (Rozanski et al., 1993) but indicates a more continental climate influence than during the period 2001–2003 (Vreča et al., 2006), lower than the one estimated for the same period for Ljubljana (Vreča et al., 2014) and close to an average isotope temperature gradient of 0.25 ‰/°C for groundwater in Slovenia estimated by Mezga et al. (2014).

Tritium activity

Results of monthly tritium activity (A) of precipitation are summarized in Table 2. We present also two numerical results below the LOD (September and November 2007) for the purpose of statistical analysis. Amount of precipitation weighted mean monthly, seasonal and annual values are summarized in Tables 3, 4 and 5. Variations of tritium activity in monthly precipitation during the sampling period 2007–2010 are presented in Figure 3d. Maximum value was observed in May 2009 (19.7 TU, Table 2), similarly as in Ljubljana (Vreča et al.,

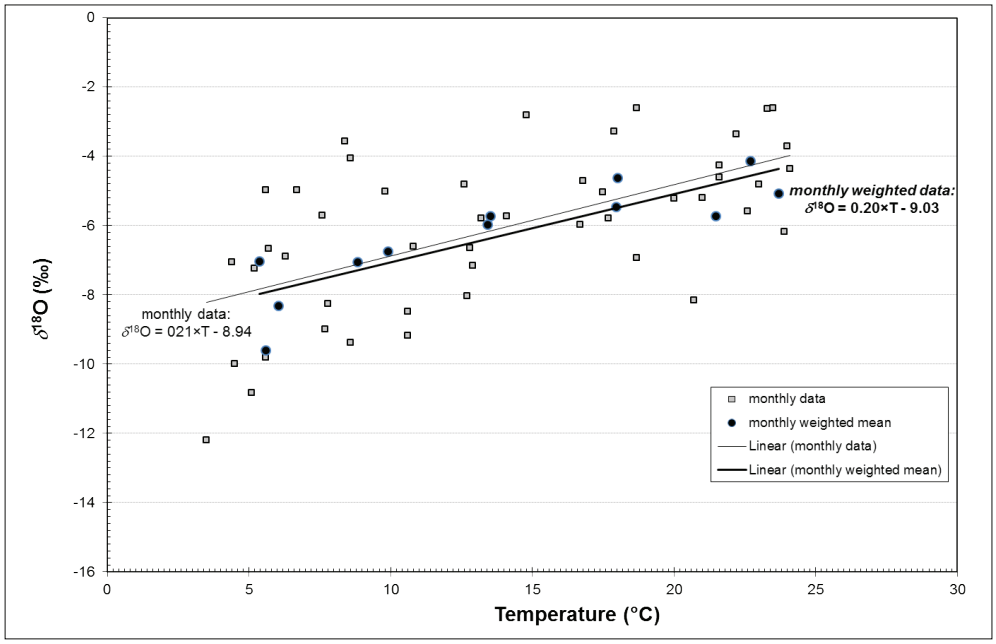

Figure 6. Correlation between $\delta^{18}O$ of monthly samples and monthly air temperature in the period 2007–2010 (open symbol), and monthly weighted mean $\delta^{18}O$ values and mean monthly air temperature for the same period (full symbols).

2014). In May 2009 high air temperatures were recorded, precipitation was lower than the long-term mean and most precipitation fell during two thunderstorms (Internet 3). Therefore, the relatively high tritium activity may indicate the influence of continental effect and re-evaporation of tritium from the continental land surfaces. The minimum (1.8 TU, <LOD) was recorded in September 2007. Seasonal fluctuations typical of stations of the Northern hemisphere (Rozanski et al., 1991) are observed for 2007 and 2010, with lower tritium activities in autumn and winter and higher ones in spring and summer (Figure 3d), while in 2008 we observed maximum in October and in 2009 three peaks were recorded in January, May and October. Similar patterns of ^{3}H were observed also for Ljubljana (Vreča et al., 2014) and Zagreb (Krajcar Bronić, unpublished data). The seasonality is evident also by about 3 TU difference between autumn-winter and spring-summer precipitation (Table 4). Monthly weighted mean A values are presented in Table 3 and in Figure 5b. Maximum value was observed in June (9.7 TU) and the minimum in September (4.0 TU) and December (4.3 TU) (Table 3), which is slightly different than in the period 2001–2006 (Figure 5b). The differences are related to different climate conditions (see Meteorological data: Precipitation and temperature) during periods 2001–2006 and 2007–2010. The mean tritium activity in the studied period is 7.2 TU (Table 2) and is the same as in the period 2001–2006 (Vreča et al., 2011). The weighted mean annual A is 6.4 TU and is 0.5 TU lower than for the 2001–2006 record (Table 5) but not significantly different.

The weighted mean tritium activity at the Portorož station (6.4 TU) is 2.1–2.6 TU lower than the mean tritium activity for the same period at the continental stations Ljubljana and Zagreb (8.5 TU and 9.0 TU, Vreča et al., 2014) and is related to the coastal position of the station. Similar difference (1.7–2.5 TU) between Portorož and continental stations was also observed for a short-term period 2001–2003 (Vreča et al., 2006).

A good correlation between mean monthly deuterium excess (d) and tritium activity (A) has been obtained with a slope of –0.35 ‰/TU ($r = 0.52$, $n = 12$) indicating that during the period 2007–2010 higher d values were associated with lower A values (Table 3) that correspond to precipitation that has been formed by moisture evaporated from the Adriatic Sea (Froehlich et al., 2008).

Conclusions

The results of the water isotopic composition (δ^{18}O, δ^{2}H, d and A) of precipitation collected at Portorož in the period 2007–2010 are presented and compared with the data from the period 2001–2006. Isotope data corroborate conclusions derived from the analysis of the meteorological data about the change in climate setting in the Portorož area: more positive δ^{18}O and δ^{2}H mean values reflect an increase in temperature, while lower deuterium excess (d) values together with the lower MI values indicate a change in air mass trajectory towards more continental influence. However, the time period of isotope data records is relatively short and is influenced by year-to-year differences in weather conditions.

The results presented are important for further scientific and practical applications in hydrology and hydrogeology, and in climatology. Taking into account the characteristic geographic diversity of Slovenia, which influences considerably the climate and the isotopic composition of precipitation, a more detailed investigation of the complete 10-year isotope data set (2001–2010) for Portorož needs to be performed. The LMWLs obtained for 10-year isotope record will be useful above all in investigating the karst hydrological systems in Slovenia that are fed directly by precipitation. Finally, a mathematical model that enables estimation of δ^{18}O and δ^{2}H values for the precipitation generated at distinctive atmospheric circulation patterns proposed by Brenčič et al. (2015) will be applied to separate data with different air mass origins.

Acknowledgements

The authors express their gratitude to the staff of the Slovenian Environment Agency at the meteorological station Portorož for their valuable help in sampling and M. Demšar for help with meteorological data. Special thanks are due to S. Žigon, S. Lindbichler, J. Barešić, A. Rajtarić, B. Svetek and V. Stibilj for their valuable help with analyses. Investigations were supported financially in the frame of projects P1-0143 and BI-HR/09-10-32 by the Slovenian Research Agency and by the Ministry of Education, Science and Sports of the Republic of Croatia in the frame of project 098-0982709-2741.

References

Araguas-Araguas, L., Fröhlich, K. & Rozanski, K. 2000: Deuterium and oxygen-18 isotope composition of precipitation and atmospheric moisture. Hydrol. Process., 14/8: 1341–1355, doi:10.1002/1099-1085(20000615)14:8<1341::AID-HYP983>3.0.CO;2-Z.

Barešić, J., Horvatinčić, N., Krajcar Bronić, I. & Obelić, B. 2010: Comparison of two techniques for low-level tritium measurement – gas proportional and liquid scintillation counting. Third European IRPA Congress: Radiation protection - science, safety and security, Proceedings, Full papers of poster presentations. Helsinki, Finland: P12-21-1-P12-21-5: 1988 – 1992. Internet: http://www.irpa2010europe.com/pdfs/Proceedings_-_Third_European_IRPA_Congress_2010.pdf (02.12.2015)

Barešić, J., Krajcar Bronić, I., Horvatinčić, N., Obelić, B., Sironić, A. & Kožar-Logar, J. 2011: Tritium activity measurement of water samples using liquid scintillation counter and

electrolytical enrichment. Proceedings of the 8th Symposium of the Croatian Radiation Protection Association, Krk, 13 – 15 April, 2011, Ed. by Krajcar Bronić, I., Kopjar, N., Milić, M., Branica, G. HDZZ, Zagreb, 2011, 461-467.

Bowen, G.J., Wassenaar, L. I. & Hobson, K. A. 2005: Global application of stable hydrogen and oxygen isotopes to wildlife forensics. Oecologia, 143/3: 337–348, doi:10.1007/s00442-004-1813-y.

Brenčič, M. 2009: Hydrogeochemistry of Coastal Carbonate Aquifer in Lucija-Portorož (Gulf of Trieste, Northern Adriatic Sea, Slovenia). Acta Carsologica, 38/2: 179–196, doi:10.3986/ac.v38i2-3.122.

Brenčič, M., Kononova, N. & Vreča, P. 2015: Relation between isotopic composition of precipitation and atmospheric circulation patterns. J. Hydrol., 529/3:1422–1432, doi:10.1016/j.jhydrol.2015.08.040.

Cegnar, T. 2011: Climate in Slovenia in 2010. UJMA 25: 17–27. (in Slovene)

Coplen, T.B., Hopple, J.A., Böhlke, J.K., Peiser, H.S., Rieder, S.E., Krouse, H.R., Rosman, K.J.R., Ding, T., Vocke, Jr., R.D., Revesz, K.M., Lamberty, A., Taylor, P, & De Bièvre, P. 2002: Compilation of minimum and maximum isotope ratios of selected elements in naturally occurring terrestrial materials and reagents: U.S. Geological Survey Water-Resources Investigations Report 01-4222,01-4222: 98 p.

Craig, H. 1961: Isotope variations in meteoric waters. Science, 133: 1702-1703, doi:10.1126/science.133.3465.1702.

Craig, H. & Gordon, L. 1965: Deuterium and Oxygen-18 Variations in the Ocean and the Marine Atmosphere. In: Tongiorgi, E. (Ed.): Stable Isotopes in Oceanographic Studies and Paleotemperatures. Cons. Naz. di Rech., Spoleto, Italy, 9–130.

Cruz-San, J., Araguas-Araguas, L., Rozanski, K., Benavente, J., Cardenal, J., Hidalgo, M. C., Garcia-Lopez, S., Martinez-Garrido, J. C., Moral, F. & Olias, M. 1992: Sources of precipitation over South-Eastern Spain and groundwater recharge – An isotopic study. Tellus, 44B: 226–236.

Cucchi, F., Franceschini, G. & Zini, L. 2008: Hydrogeochemical investigations and groundwater provinces of the Friuli Venezia Giulia Plain aquifers, northeastern Italy. Environ. Geol., 55: 985–999, doi: 10.1007/s00254-007-1048-4.

Dansgaard, W. 1964: Stable isotopes in precipitation. Tellus, 16/4: 436–468, doi: 10.1111/j.2153-3490.1964.tb00181.x.

Ehhalt, D.H. 1971: Vertical profiles and transport of HTO in the troposphere. J. Geophys. Res., 76: 7351–7367.

Epstein, S. & Mayeda, T.K. 1953: Variations of ^{18}O content of waters from natural sources. Geochim. Cosmochim. Acta, 4/5: 213–224, doi:10.1016/0016-7037(53)90051-9.

Froehlich, K., Kralik, M., Papesch, W., Rank, D., Scheifinger, H. & Stichler, W. 2008: Deuterium excess in precipitation of Alpine regions - moisture recycling. Isot. Environ. Health. Stud., 44/1: 61–70, doi:10.1080/10256010801887208.

Gat, J. R., Bowser, C. J. & Kendall, C.1994: The Contribution of Evaporation from the Great Lakes to the Continental Atmosphere: Estimate Based on Stable Isotope Data. Geophys. Res. Lett., 21/7: 557–560, doi:10.1029/94GL00069.

Gat, J.R. 1996: Oxygen and hydrogen isotopes in the hydrologic cycle. Annu. Rev. Earth. Planet Sci, 24: 225–262.

Gourcy, L.L., Groening, P.K. & Aggarwal, P.K. 2005: Stable oxygen and hydrogen isotopes in precipitation. In: Aggarwal, P.K., Gat, J.R. & Froehlich, K. (Eds.): Isotopes in the water cycle: past, present and future of a developing science. Dordrecht: Springer, 39–51.

Harvey, F.E. 2005: Stable hydrogen and oxygen isotopic composition of precipitation in northeastern Colorado. J. Am. Water Resour. Assoc., 41/2: 447–460, doi:10.1111/j.1752-1688.2005.tb03748.x

Hebert, D. 1990: Technogenic tritium in Central Europeanprecipitation.Isot.Environ.Health.Stud., 26/2: 592–595, doi:10.1080/10256019008622441.

Hobson, K.A. & Wassenaar, L.I. 1997: Linking brooding and wintering Grounds of neotropical migrant songbirds using stable hydrogen Isotopic analysis of feathers. Oecologia, 109: 142–148.

Hughes, C.E. & Crawford, J. 2012: A new precipitation weighted method for determining the meteoric water line for hydrological applications demonstrated using Australian and global GNIP data. J. Hydrol., 464–465: 344–351, doi:10.1016/j.jhydrol.2012.07.029.

IAEA 1992: Statistical treatment of environmental isotopes in precipitation. Technical Report Series No. 331, IAEA, Vienna: 781 p.

Kigoshi, K. & Yoneda, K. 1970: Daily variation in the tritium concentration of atmospheric moisture. J. Geophys. Res., 75: 2981–2984, doi:10.1029/JC075i015p02981.

Koppany, G. & Unger, J. 1992: Mediterranean Climatic Character in the Annual March of Precipitation. Acta Climatologica, 24–26: 59–71.

Kovačič, K. 2015: Radioactive isotopes in ground waters of Slovenia. Dissertation, Nova Gorica, XV, 127 p. Internet: http://repozitorij.ung.si/Dokument.php?id=3167&lang=slv (date 29/10/2015)

Krajcar Bronić, I., Vreča, P., Horvatinčić, N., Barešić, J. & Obelić, B. 2006: Distribution of hydrogen, oxygen and carbon isotopes in the atmosphere of Croatia and Slovenia, Arhiv za higijenu rada i toksikologiju, 57: 23–29.

Krajcar Bronić, I., Barešić, J., Sironić, A. & Horvatinčić, N. 2013: Stability analysis of systems for preparation and measurement of ^{3}H and ^{14}C (In Croatian with English Abstract). In: Knežević, Ž., Majer, M. & Krajcar Bronić, I. (Eds.): Proceedings of the 9th Symposium of the

Croatian Radiation Protection Association, Krk, 10 – 12 April, 2013, HDZZ, Zagreb, 495–501.

Liotta, M., Bellissimo, S., Favara, R. & Valenza, M. 2008: Isotopic composition of single rain events in the central Mediterranean. J. Geophys. Res. 113: D16304, doi:10.1029/2008JD009996.

Lucas, L. L. & Unterweger, M. P. 2000: Comprehensible Review and Critical of the Half-life of Tritium. Journal of Research of the National Institute of Standards and Technology, 105–4: 541–549.

Mandić, M., Bojić, D., Roller-Lutz, Z., Lutz, H.O. & Krajcar Bronić, I. 2008: Note on the spring region of Gacka River (Croatia). Isot. Environ. Health. Stud., 44/2: 201–208.

Matsumoto, T., Maruoka, T., Shimoda, G., Obata, H., Kagi, H., Suzuki, K., Yamamoto, K., Mitsuguchi, T., Hagino, K., Tomioka, N., Sambandam, C., Brummer, D., Klaus, P.M. & Aggarwal, P. 2013: Tritium in Japanese precipitation following the March 2011 Fukushima Daiichi Nuclear Plant accident. Sci. Total Environ., 445–446: 365–370, doi:10.1016/j.scitotenv.2012.12.069.

Merlivat, L. & Jouzel, J. 1979: Global Climate Interpretation of the Deuterium-Oxygen 18 Relationship for Precipitation. J. Geophys. Res., 84(C8): 5029–5033, doi:10.1029/JC084i C08p05029.

Mezga, K. 2014: Natural hydrochemical background and dynamics of groundwater in Slovenia. Dissertation, Nova Gorica, XVI: 226 p. Internet: http://www.ung.si/~library/doktorati/okolje/37Mezga.pdf (date 11/08/2014)

Mezga, K., Urbanc, J. & Cerar, S. 2014: The isotope altitude effect reflected in groundwater: a case study from Slovenia. Isot. Environ. Health. Stud., 50/1: 33–51, doi:10.1080/10256016.2013.826213.

Michelini, M. 2013: Studio geochimico-isotopico delle precipitazioni del Friuli-Venezia Giulia. Dissertation, Trieste: 123 p. Internet: http://www.openstarts.units.it/dspace/bitstream/10077/8666/1/Studio%20geochimico%20isotopico%20delle%20precipitazioni%20del%20Friuli%20Venezia%20Giulia.pdf (date 05/11/2015).

Morrison, J., Brockwell, T., Merren, T., Fourel, F. & Phillips A.M. 2001: On-line high-precision stable hydrogen isotopic analyses on nanoliter water samples. Anal. Chem., 73/15: 3570–3575, doi:10.1021/ac001447t.

Peng, H., Mayer, B., Harris, S. & Krouse, H. R. 2004: A 10-yr record of stable isotope ratios of hydrogen and oxygen in precipitation at Calgary, Alberta, Canada. Tellus, 56B: 147–159, doi:10.1111/j.1600-0889.2004.00094.x.

Rozanski, K., Gonfiantini, R. & Araguas-Araguas, L. 1991: Tritium in the global atmosphere: distribution patterns and recent trends. Journal of Physics G: Nuclear and Particle Physics, 17: 523–536, doi:10.1088/0954-3899/17/S/053.

Rozanski, K., Araguas-Araguas, L. & Gonfiantini, R. 1993: Isotopic patterns in modern global precipitation. Geophys. Monogr. 78: 1–36, doi:10.1029/GM078p0001.

Saccon, P., Leis, A., Marca, A., Kaiser, J., Campisi, L., Böttcher, M.E., Savarino, J., Escher, P., Eisenhauer, A. & Erbland, J. 2013: Multi-isotope approach for the identification and characterisation of nitrate pollution sources in the Marano lagoon (Italy) and parts of its catchment area. Appl. Geochem. 34: 75–89, doi:10.1016/j.apgeochem.2013.02.007.

Terzer, S., Wassenaar, L. I., Araguas-Araguas, L. & Aggarwal, P. 2013: Global isoscapes for $\delta^{18}O$ and $\delta^{2}H$ in precipitation: improved prediction using regionalized climatic regression models. Hydrol. Earth syst. Sci., 17: 4713–4728, doi:10.5194/hess-17-4713-2013.

Thompson, P.A., Kwamena, N.-O.A., Ilina, M., Wilk, M. & Clark, I.D. 2015: Levels of tritium in soils and vegetation near Canadian nuclear facilities releasing tritium to the atmosphere: implications for environmental models. J. Environ. Radioact. 140: 105-113, doi:10.1016/j.jenvrad.2014.11.009

Ueda, S., Hasegawa, H., Kakiuchi, K., Ochiai, S., Akata, N. & Hisamatsu, S. 2015: Nuclear accident-derived ^{3}H in river water of Fukushima Prefecture during 2011–2014. J. Environ. Radioact. 146: 102–109,

Unnikrishnan Warier, C., Praveen Babu, M., Manjula, P. & Shahul Hameed, A. 2013: Spatial and temporal variations of natural tritium in precipitation of southern India. Curr. Sci. India 105: 242–249.

Verbovšek, T. & Kanduč, T. 2015: Isotope Geochemistry of Groundwater from Fractured Dolomite Aquifers in Central Slovenia. Aquat. Geochem., 1-21, doi: 10.1007/s10498-015-9281-z.

Vodila, G., Palcsu, L., Futó, I. & Szántó, Zs. 2011: A 9-year record of stable isotope ratios of precipitation in Eastern Hungary: Implications on isotope hydrology and regional palaeoclimatology. J. Hydrol., 400: 144–153, doi:10.1016/j.jhydrol.2011.01.030.

Vreča, P., Kanduč, T., Žigon, S. & Trkov, Z. 2005: Isotopic composition of precipitation in Slovenia. In: Gourcy, L. (Ed.): Isotopic composition of precipitation in the Mediterranean basin in relation to air circulation patterns and climate, 157-172, IAEA-TECDOC-1453, IAEA, Vienna.

Vreča, P., Krajcar Bronić, I., Horvatinčić, N. & Barešić, J. 2006: Isotopic characteristics of precipitation in Slovenia and Croatia: Comparison of continental and maritime stations. J. Hydrol., 330/3–4: 457–469, doi:10.1016/j.jhydrol.2006.04.005.

Vreča, P., Brenčič, M. & Leis, A. 2007: Comparison of monthly and daily isotopic composition of precipitation in the coastal area of Slovenia. Isot. Environ. Health. Stud., 43/4: 307–321, doi:10.1080/10256010701702739.

Vreča, P., Krajcar Bronić, I., Leis, A. & Brenčič, M. 2008: Isotopic composition of precipitation in Ljubljana (Slovenia). Geologija, 51/2: 169–180, doi:10.5474/geologija.2008.018.

Vreča, P., Krajcar Bronić, I. & Leis, A. 2011: Isotopic composition of precipitation in Portorož (Slovenia). Geologija, 54/1: 129–138, doi:10.5474/geologija.2011.010.

Vreča, P., Krajcar Bronić, I., Leis, A. & Demšar, M. 2014: Isotopic composition of precipitation at the station Ljubljana (Reaktor), Slovenia – period 2007–2010. Geologija, 57/2: 217–230, doi:10.5474/geologija.2014.019.

Internet resources:

Internet 1: http://www-naweb.iaea.org/napc/ih/IHS_resources_gnip.html (15/11/2015)

Internet 2: http://www-naweb.iaea.org/napc/ih/documents/global_cycle/vol%20II/cht_ii_05.pdf (02/12/2015)

Internet 3: http://meteo.arso.gov.si/ (10/11/2015)

GEOLOGIJA *58/2*, 247–260, Ljubljana 2015

http://dx.doi.org/10.5474/geologija.2015.020

Computer aided method for colour calibration and analysis of digital rock photographs

Računalniško podprta metoda za barvno umerjanje in analizo digitalnih fotografij kamnin

Matic POTOČNIK[1], Bojan KLEMENC[1], Franc SOLINA[1] & Uroš HERLEC[2]

[1]FRI, UL, Večna pot 113, SI–1000 Ljubljana, maticpotocnik@gmail.com, bojan.klemenc@fri.uni-lj.si
[2]NTF, UL, Aškerčeva cesta 12, Ljubljana, uros.herlec@gmail.com

Prejeto / Received 11. 10. 2014; Sprejeto / Accepted 4. 12. 2015; Objavljeno na spletu / Published online 30. 12. 2015

Key words: digital photography, colour calibration, colour analysis, digital rock photograph colour analysis, Munsell colour system

Ključne besede: digitalna fotografija, barvno umerjanje, barvna analiza, barvna analiza digitalnih fotografij kamnin, barvni sistem Munsell

Abstract

The methods used in geology to determine colour and colour coverage are expensive, time consuming, and/or subjective. Estimates of colour coverage can only be approximate since they are based on rough comparison-based measuring etalons and subjective estimation, which is dependent upon the skill and experience of the person performing the estimation. We present a method which accelerates, simplifies, and objectifies these tasks using a computer application. It automatically calibrates the colours of a digital photo, and enables the user to read colour values and coverage, even after returning from field work. Colour identification is based on the Munsell colour system. For the purposes of colour calibration we use the X-Rite ColorChecker Passport colour chart placed onto the photographed scene. Our computer application detects the ColorChecker colour chart, and finds a colour space transformation to calibrate the colour in the photo. The user can then use the application to read colours within selected points or regions of the photo.

The results of the computerised colour calibration were compared to the reference values of the ColorChecker chart. The values slightly deviate from the exact values, but the deviation is around the limit of human capability for visual comparison. We have devised an experiment, which compares the precision of the computerised colour analysis and manual colour analysis performed on a variety of rock samples with the help of geology students using Munsell Rock-color Chart. The analysis showed that the precision of manual comparative identification on multi-coloured samples is somewhat problematic, since the choice of representative colours and observation points for a certain part of a sample are subjective. The computer based method has the edge in verifiability and repeatability of the analysis since the application the original photo to be saved with colour calibration, and tagging of colour-analysed points and regions.

Izvleček

Metode, ki se v geologiji uporabljajo za določanje barv in barvne pokritosti, so drage, zamudne in/ali subjektivne. Ocena barvne zastopanosti ali pokritosti je lahko le zelo približna, saj temelji na grobih primerjalnih etalonih in subjektivni oceni, ki je odvisna od izurjenosti in izkušenj ocenjevalca. Predstavljamo metodo, ki te naloge pospeši, poenostavi in objektivizira s pomočjo računalniške aplikacije, ki na zajeti digitalni fotografiji z uporabo računalniškega vida samodejno umeri barve in uporabniku tudi kasneje, po terenskem delu, omogoča odčitavanje barvnih odtenkov. Barvna identifikacija temelji na barvnem sistemu Munsell. Za barvno umerjanje uporabljamo umerjevalno barvno lestvico X-Rite ColorChecker Passport, ki jo uporabnik postavi v območje zajema fotografije kamnine. Računalniška aplikacija, ki smo jo razvili, na zajeti fotografiji zazna barvno lestvico ColorChecker in poišče transformacijo barvnega prostora, s katero fotografijo barvno umerimo. Uporabnik lahko nato s pomočjo aplikacije po barvnem sistemu Munsell odčita barvo v izbranih točkah in izbranih področjih na fotografiji.

Rezultate računalniško podprtega barvnega umerjanja smo primerjali z referenčnimi vrednostmi barvne lestvice ColorChecker. Rezultati umerjanja kažejo, da računalniška metoda umeri dovolj natančno točne barvne vrednosti, tako da je barvno odstopanje blizu meje, ki jo človek še lahko razloči. Za primerjavo smo opravili poskus, pri katerem smo na raznovrstnih primerkih kamnin primerjali natančnost računalniške barvne analize z ročnimi barvnimi primerjalnimi analizami študentov geologije s pomočjo lestvice Munsell Rock-color Chart. Ugotovili smo, da nastopajo velike razlike v odčitkih predvsem pri raznobarvnih kamninah zaradi subjektivnosti izbora najbolj reprezentativnih barv za posamezni analizirani kos kamnine oziroma lege reprezentativnih primerjalnih točk. Prednost računalniške metode je tako v preverljivosti in ponovljivosti analize, saj aplikacija omogoča shranjevanje originalne in barvno umerjene fotografije ter označitve lege posamične analizirane točke in območja opravljanja barvne analize.

Introduction

The methods used in geology to determine colours are: (a) verbal description, which is dependent upon the skill and visual perception of the person performing it, and is thus subjective, (b) measurement using a spectrophotometer, which is time consuming, expensive and impractical for field work, and (c) comparison based comparative determination using a colour chart (e.g. Munsell Rock Colour chart), which can be time consuming, especially for rocks with many colour shades, and is not always appropriate for field work since the colour patches are sensitive to weather and environmental conditions.

Estimates of colour coverage can only be approximate, since they are based on rough comparison-based measuring etalons and is also dependent upon the skill and experience of the person performing the assessment. Statistical assessment of colour "classes" is possible if points on a regular grid are used to count occurrences of each "class", but this method is also time consuming and thus expensive, and not commonly used.

With more objective colour values and statistically significant rock colour coverage analyses we could extract much more significant and consequently valuable rock data parameters.

We introduce a method, which greatly accelerates and simplifies these tasks, and makes them more objective. We have developed a computer application for automatic colour calibration of digital photographs made either during field work, or in the laboratory, which allows the user to accurately identify colours in the Munsell colour system; a standard used in geology for colour determination. We use the X-Rite ColorChecker Passport reference colour chart in combination with computer vision and colour calibration algorithms. This enables completely automated colour calibration of digital photographs. Colour calibration is a necessary step, since it greatly improves the quality of the colour information by diminishing the various effects, such as weather, illumination, the photographic equipment used, etc.

Before capturing a digital photograph, the ColorChecker chart needs to be placed into the photograph capture area of the rock we wish to analyze. To ensure a good baseline and thus improve the accuracy of results, the illumination should be as uniform as possible. Additional lighting or camera flash can be used to achieve this, if natural illumination conditions are not favourable or if the angle of sunlight produces shadows.

Existing methods for colour calibration used in professional photography are either manual or semi-automatic and are more focused on providing the photographer with tools to achieve the best aesthetic effect, not necessarily the most correct colour information (Van Hurkman, 2013). The photographers also use the calibration tools differently, since they capture one image with the colour chart, and then (keeping other parameters as similar as possible) capture the images they have actually set out to photograph. The existing tools are shaped by this mode of work, and are not well suited for the use case covered by the application we have developed, i.e. completely automatic colour calibration and a user interface focused on objective analysis rather than aesthetics.

The computer application we developed uses the ASIFT algorithm (Yu & Morel, 2011) to detect the ColorChecker chart on the captured photograph, and then determines a transformation of the CIE Lab colour space, which then colour-calibrates the photograph. The user is then able to read out the colour values in selected points and regions. Approximate measuring of distances on the photograph is also possible, if we assume the objects are in the same plane as the ColorChecker chart.

Differences in colour of rocks and soils is the result of differences in qualitative and quantitative mineral composition and, in particular, in the presence and quantity of the pigment minerals (most common are lepidocrocite, goethite and hematite). Mineral and chemical composition determination requires complex and time consuming sampling and more costly analyses. Unfortunately the number of such analyses is limited by available funds. Due to the fact that colour is one of the basic properties/attributes of rock, which is noticed macroscopically in the field, an objective capture is very important and useful.

Rocks within some lithologic units are unicoloured, which means, that the variability of colour values is within a very narrow range of colour hue. In such cases field researchers do not compare their colour with the colour chart on every outcrop, but rather assign the same colour value on the basis of previous observation experiences. This shortens observation and time needed for comparison, but they can unwittingly neglect differences in the lateral colour variability within the same lithostratigraphic unit and lose part of the information. Huge variability of colour within the same lithostratigraphic unit of clastic sedimentary rocks reflects differences in their microenvironment of their origin (sedimentation energy) resulting into grain-size differences and also differences in the mineral composition, porosity and permeability of the sedimentary clastic rocks and consequently onto differences in the oxygen availability during diagenetic processes. This influences the oxidation state of the pigment minerals.

Multicoloured lithostratigraphic units contain several indirect colour information on grain size, mineral composition and genetic environment and rock diagenetic processes. A number of determined colours is fully left to the subjective decision of the observer, who will usually, due to the time needed for a full procedure, only determine a few characteristic colours based on their needs or a regional similarity approach. A more objective capture of the colour range and colour coverage would undoubtedly offer a lot of additional information.

The processes of magmatic and metamorphic rocks genesis also result in their different mineral and grain size composition and consequently a different colour range and coverage.

As much as possible objective and detailed colour analysis can offer very useful additional information which enable simple and significant statistical comparison between rock samples and rock outcrops within the same lithostratigraphic units and between the different ones.

The proposed computer aided method of colour calibration and analysis is based on the Munsell, CIE XYZ and CIE Lab colour models and calculates colour distances within them and a short overview of these models follows.-

CIE 1931 XYZ Colour Model

CIE XYZ, which was standardized in 1931, was the first mathematically defined colour model that still serves as the basis for newer models and as the linking model used to convert colour values from one model to another.

The model is comprised of three components: X, Y, and Z which were modelled after the human visual system with its three types of cone cells. Experimental data determined how strongly each type of cone cell responds to some wavelength of light, and from the response the colour matching functions $\bar{x}(\lambda)$, $\bar{y}(\lambda)$ and $\bar{z}(\lambda)$ (Schanda, 2007) were derived. A spectrophotometer is a device for measuring material reflectance values at different wavelengths. If we integrate the reflectance measurements with the colour matching functions we get the colour values for the components X, Y, and Z respectively.

The values also vary depending on the illuminant used to perform the measurements which is also defined as a function of λ. The International Commission on Illumination (CIE) has also provided several standard illumination sources. Unless otherwise specified the values in this article use the D65 standard illuminant which is modelled after natural daylight on Earth.

Spectrophotometers are used in laboratories, but are impractical for field work and are very expensive devices. Further drawbacks of their use is a small operating range, usually a few millimeters, the inability to directly measure colour coverage, sampling is required, and the inability to measure rough uneven surfaces (Ruiz & Pereira, 2014).

Munsell colour system

The Munsell colour system (Munsell, 1905) was developed by prof. Albert H. Munsell with the goal of creating a perceptually uniform system. Perceptual uniformity means that an equal change of a colour component anywhere inside the system means approximately the same perceptual difference to a human observer. Colour in the Munsell system is determined by three components: hue, value, and chroma.

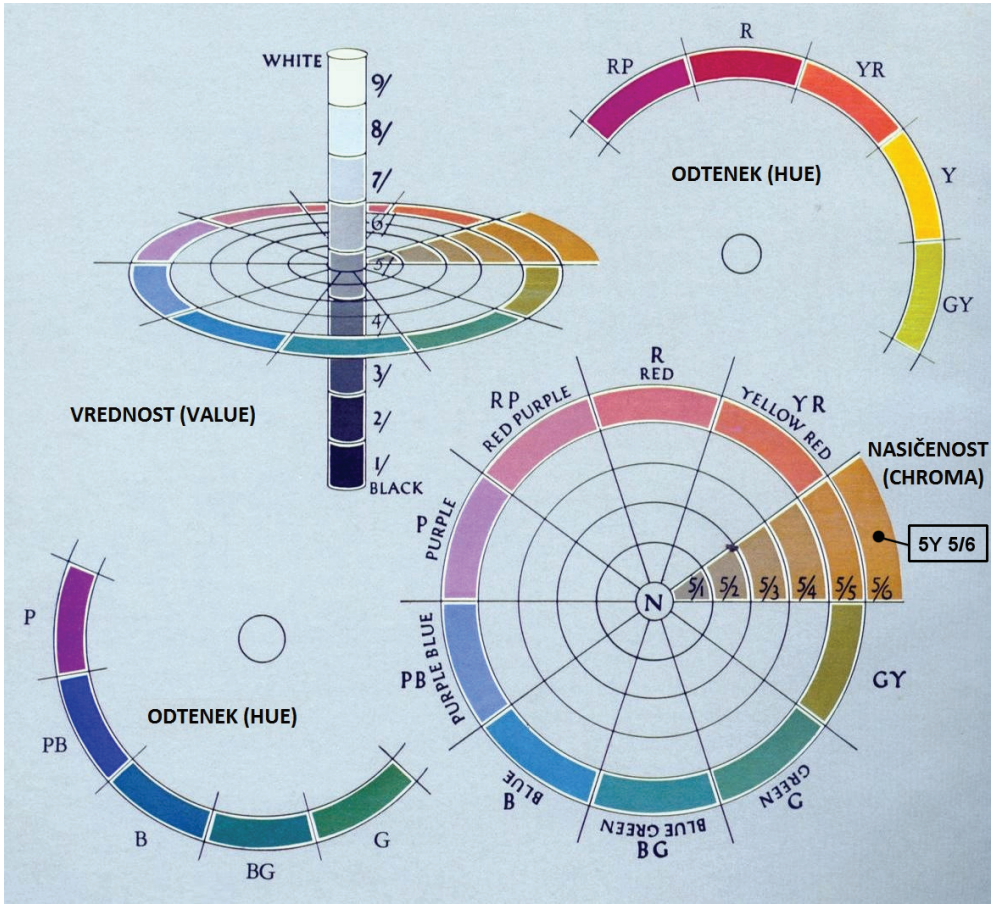

Fig. 1. Three-dimensional illustration of the Munsell colour system.

The first component, "Hue", is given as number from 0 to 10, and a one or two letter abbreviation of the hue name. Apart from the colour hues in Fig. 1, there is also a special abbreviation N, which stands for neutral and is reserved for grey shades. "Value" determines the lightness of a colour on a scale from 0 (black) to 10 (white). The third component, "chroma" determines the saturation and has no upper bound in theory, but in practice it is limited by the pigments that can be manufactured. A neutral colour has a chroma value of 0, the highest value we find in the Rock and Soil charts is 8 and 20 would mean a very saturated colour.

The advantages of the Munsell system are intuitive components, and a long tradition of use in industry, art, and science. The drawback is that it is not a mathematically defined colour model, and is connected to the mathematically defined models only by tables of measurements (RIT Munsell Color Science Laboratory), which makes exact calculation and conversion difficult.

Use of Munsell colour system in Geology

The Munsell system has a long tradition of use in geology. In 1948 the Geological Society of America (GSA) released the first Rock-color Chart based on the Munsell system. In 1949 the Munsell Color Company collaborated with the United States Department of Agriculture (USDA) to release the first "Munsell Soil-color Chart". These are books of colour charts intended for comparative determination of colour values of rocks and soil. Both books are still available in updated editions and still in widespread use. They have effectively become the standard for colour communication in geology.

Munsell colour charts are used both for geological field work and work in a laboratory. The comparative method is a lot more precise and objective than verbal descriptions of colours, but is still somewhat subjective and inaccurate, because the books contain a limited number of colour patches, and because of the limitations of the human visual system to accurately distinguish colour differences. Munsell Soil-color Chart (X-Rite, Inc., 2009c) contains nine pages, which cover colours with hues from 5R to 5Y at various values of value and chroma components, and four additional pages; one with a few colours with hue values 10Y and 5GY, two pages with low-chroma colours for gleysols, and one page with colours with a high value component. The colours on pages are sorted in two dimensions by value and chroma, so the user can gain a feel for the colours with a particular hue, and can in some cases decide to visually interpolate and assign a colour not depicted in the chart. Rock-color Chart (X-Rite, Inc., 2009b) contains only three pages with the most common rock colours. The colours are not sorted by any of the Munsell system components, which prevents visual interpolation.

Each page of colour chart contains up to 42 colour patches, usually fewer, since some pigments are more expensive or difficult to produce. Each colour patch has a hole to allow direct comparison of the patch with the rock or soil for which the colour is being determined. Next to each colour page is a page with the Munsell values and colour names in the ISCC-NBS system, according to the mapping defined in (Kelly & Judd, 1976). The design purpose of ISCC-NBS was to improve the accuracy of colour descriptions by constraining the language to a set of colour names and a few standard adjectives (e.g. dark, vivid, very pale), and to define which parts of the Munsell system correspond to which colour descriptions.

Fig. 2. Munsell Soil-color and Munsell Rock-color charts.

CIE Lab colour model

The International Commission on Illumination (CIE) accepted the CIE Lab colour model in 1976. A colour in CIE Lab is defined by three components: L* – lightness, a* – red/green, and b* – blue/yellow. CIE Lab was designed to be perceptually uniform on all three components at once, and is mathematically defined, which makes it very appropriate for colour computation.

Measuring colour distance

When working with colour, e.g. in print, or industrial design, a common task is tolerancing - checking if colours are acceptably close to some predefined standard. A colour distance measure, where, to the human eye, the same distance means the same amount of change, is very useful, since it can be used for all the colours used. In this section we will mention three formulas for colour distance (Schanda, 2007), which have been implemented in our computer application.

Since CIE Lab was designed with good perceptual uniformity on all components at once, the first colour distance measure CIE is simply the Euclidean distance of the per component deltas of two colours:

$$\Delta E^*_{76} = \sqrt{\Delta L^{*2} + \Delta a^{*2} + \Delta b^{*2}}$$

Later it was found that CIE Lab is not completely perceptually uniform, so in 1994 CIE Lab confirmed a new formula CIE , which was based on a large amount of experimental data collected by the automotive industry. This formula is defined on CIE LCH - a colour model related to CIE Lab, with the same L* component and C* – chroma, and H* – hue, which are simply polar definitions of a* and b*.

$$\Delta E^*_{94} = \sqrt{\left(\frac{\Delta L^*}{k_L S_L}\right)^2 + \left(\frac{\Delta C^*_{ab}}{k_C S_C}\right)^2 + \left(\frac{\Delta H^*_{ab}}{k_H S_H}\right)^2}$$

In the year 2000 CIE released another formula, CIE , which experimentally works very well for small colour distances, but has some mathematical discontinuities which skew the results at larger distances (Sharma et al., 2005).

$$\Delta E^*_{00} = \sqrt{\left(\frac{\Delta L'}{k_L S_L}\right)^2 + \left(\frac{\Delta C'}{k_C S_C}\right)^2 + \left(\frac{\Delta H'}{k_H S_H}\right)^2 + R_T \frac{\Delta C'}{k_C S_C} \frac{\Delta H'}{k_H S_H}}$$

Another difficulty we had when working with CIE is that the formula takes a lot more computing time. Because of these issues we use CIE for most tasks, and CIE where the expected difference is small.

For an easier interpretation of later results, let us provide some context to the values from these formulas. The limit at which the average human observer barely distinguishes two colours if laid next to each other is 2.3. This value is called the just noticeable difference (JND) (Mahy et al., 1994). The approximate distance between neighbouring grey shades on the ColorChecker chart is 15. The average of distances between pairs of nearest colour values on the Munsell Rock-color chart is 5.4 (highly saturated colours a bit farther apart, and colours with low saturation a bit nearer).

Development of the application

ColorChecker colour calibration chart

ColorChecker colour chart was developed in 1976 by the Macbeth company (today part of X-Rite company) (McCamy et al., 1976). The chart is used for the colour calibration of different devices (e.g. cameras, printers, displays). ColorChecker colour chart contains four lines with six colour patches, 24 patches in all. Patches have precisely defined colour values which can be used to check the quality of colour reproduction or colour acquisition. The first two lines contain approximations of some common natural hues (e.g. human skin, greenery, blue sky) and intermediate hues (e.g. orange, yellow-green). The third line represents the extreme points of the RGB (red, green, blue) colour system and CMY (cyan, magenta, yellow) colour system. The fourth line contains 6 patches of grey that can be used for calibration of lightness and white balance.

For the usage in our application we chose the X-Rite ColorChecker Passport (X-Rite, Inc., 2009a), shown in Figure 3, instead of the classical variant of ColorChecker since it better suits our requirements. This version of the colour chart is suitable for field work in geology since it is smaller than the classical version and has a hard plastic casing. Concerning the accuracy of colours one of the larger colour charts with more colour patches (e.g. ColorChecker Digital SG, IT8) would be more appropriate for laboratory work. The advantage of a smaller format of the colour chart is that its size better suits the size of rock samples and thus enables us to capture the samples in a higher resolution. For many samples an even smaller colour chart of 3 cm × 2 cm would be convenient.

The X-Rite ColorChecker Passport colour chart contains two additional calibration charts compared to the classic ColorChecker chart – a special section with a large grey patch for white balance and a section named Creative Enhancement Target (CET). CET contains 28 patches: 8 highly saturated colour patches, 2 lines of 6 patches for visual white balance and 4 very light grey and 4 very dark grey patches for detection of overexposure and underexposure. This colour chart is not meant for automatic colour calibration, which may be the reason

why there is no data on official colour values of the patches available in the literature or on the internet. However, we have found unofficial spectrophotometric measures (Myers, 2010) which we used to help evaluate the calibration quality of our method.

Detection of the ColorChecker colour chart - ASIFT algorithm

Precise detection of patches on the ColorChecker is very important since the calibration process depends on the measured colour values. For detection of the ColorChecker colour chart we used Affine Scale Invariant Feature Transform or ASIFT (Yu & Morel, 2011).

SIFT (Lowe, 2004) is a computer vision algorithm which extracts features that can be used for various tasks in computer vision, e.g. object detection (Lowe, 1999), panorama stitching (Agarwala et al., 2006), automatic 3D modelling (Vergauwen & Van Gool, 2006) and gesture recognition (Scovanner et al., 2007). Features detected by SIFT are resistant to scaling, translation, and to some degree rotation. ASIFT is a simple extension of SIFT where combinations of rotation and shearing transformations are applied multiple times on the image. SIFT features are extracted from the transformed image and transformed back to the original image coordinate space. Using this process we get a larger number of features that are also more robust under affine transforms. According to a recommendation by Yu & Morel, 2011, it is sufficient to use 6 shears and rotations from 0° to 180° depending on degree of shearing – in all 42 transformations.

Fig. 3. X-Rite ColorChecker Passport colour calibration chart that is used by our application.

Colour chart detection

To detect a particular object with the ASIFT algorithm we need an image of the object, we then extract SIFT features from both images, the image where we want to detect the object and the image of the object. Detection is performed by finding the best correspondence between the SIFT features of both images. Figure 4 shows lines connecting the corresponding pairs of ASIFT points. Squares on the photo show the centre of the patches. On the bottom left we see the aligned image of the detected object (colour chart) and squares with averaged colours inside the detected patches.

Fig. 4. Visualization of ASIFT on a photograph of X-Rite ColorChecker Passport (right hand side) and reference X-Rite ColorChecker Passport colour patch image (upper left hand side).

The method is sufficiently general to be used for other colour charts as well. The only part we would need to change is the colour chart image and the arrangement of the patches as they appear on a particular colour chart. For the purpose of evaluating the quality of calibration we have added the option to detect the CET colour chart on the ColorChecker Passport.

Colour calibration of photographs

The aim of photograph colour calibration is to bring the colour values of the photograph as close as possible to values we would measure on the surfaces we are photographing. Calibration could be attempted completely programmatically without the colour chart by extracting the necessary information from the metadata and the image itself (e.g. conditions under which the photograph was taken and the equipment used) and infer the actual colours in the photograph. Because this procedure cannot guarantee accuracy we have decided on calibration using a colour chart.

Colour calibration can be done using ColorChecker colour calibration chart that is put in the photographed scene. To assure best results the lighting of both the colour chart and the rock should be as uniform as possible (X-Rite, Inc., 2009a) and with a sufficiently wide spectrum. We can achieve that by using additional lighting or the camera flash. If we use natural light the direction and the intensity of the light should be as much as possible similar on both the rock and the chart.

During the calibration process the application first detects the ColorChecker colour chart on the photograph. Then average colour values are extracted from the chart and the distances from the reference colour values for the chart are calculated. Thus we get a calibration vector in CIE Lab colour space for each colour patch. The calibration could be done in another colour space as well but CIE Lab is very suitable for this purpose because of its good perceptual uniformity.

The issue of overfitting

We are generalizing on the basis of a quite small amount of data, so we have to take care not to overfit the algorithm (Hastie et al., 2009). With simple calibration methods overfitting may appear because of the uneven colour distances between colour patches, since parts of the colour space represented by more patches are weighted more. When using more complex methods we also have to take care, that the algorithms do not transform the colours in a way that does not correspond to physical reality. In calibration with translation the overfitting was avoided by using leave-one-out cross validation (Hastie et al., 2009), where the colour patch, for which the value is being predicted, is not used in the prediction. In calibration with a linear combination some resilience against overfitting is provided by the fact that the patches on the ColorChecker chart contain both the extreme and central points in the colour space, and since the space is perceptually uniform, a linear method is not likely to overfit.

Calibration with translation

The first method for colour calibration that we implemented finds a single colour vector in the CIE Lab space, which minimizes the CIE ΔE^*_{00} distance between the average colour value on the detected colour patches $\widehat{C\bar{C}_i}$ and the reference values $C\bar{C}_i$. Using the ColorChecker chart, we have n = 24 patches, but the method works with any number of patches.

$$\vec{C} = (L, a, b)$$
$$\overrightarrow{C'} = \vec{C} + \vec{v}$$

Where $\vec{v}$ is a vector which minimizes the following expression:

$$min \sum_{i=1}^{n} \Delta E^*_{00}(Corr(\widehat{C\bar{C}_i}),\ C\bar{C}_i)$$

As mentioned, the CIE Lab space is not perfectly perceptually uniform, furthermore, the photograph capturing process is not perfect and introduces various changes to the colour space (e.g. contrast, fringing, over- or underexposure), which require more advanced methods of correction. However the method is simple so we implemented it to compare it with other methods.

This method can also be used in conjunction with other methods, since it cannot skew the colour space, however, it should not be used after a calibration method which is more robust against overfitting.

Calibration with a weighted average

The method of calibrating with the weighted average of calibration vectors $\vec{C}c_i$, , computes the weighted average using two weighting coefficients u_{i_k}. The value of the first coefficient is determined using an evolutionary algorithm before calibration, while the value of the second coefficient $d_i(\vec{C})$ is a function of the distance between the colour being calibrated $\vec{C}$ and the colour patch $\widehat{C\bar{C}_i}$.

For the first u_{i_k} weights we have $3 \cdot n$ normalized weights, which determine the importance of each component (L, a, and b) of each colour patch. If the colour value of some patch deviates greatly from the reference value (e.g. because of a damaged patch, over- or underexposure, shadows, partly occluded patch), or put another way: if the other patches offer a better calibration in the part of the colour space the current patch occupies, then its weight will be smaller. These weights are determined before the calibration with an evolutionary search algorithm.

$$\vec{C} = (L, a, b), \quad \overrightarrow{C'} = (L', a', b')$$
$$\vec{C}c_i = (Lc_i, ac_i, bc_i) = CC_i - \widehat{CC_i}$$
$$d_i(\vec{C}) = 1 - \frac{\Delta E^*_{94}(\vec{C},\ \widehat{CC_i})}{max_{j=1}^{n} \Delta E^*_{94}(\vec{C},\ \widehat{CC_i})}$$
$$L' = L + \sum_{i=1}^{n} Lc_i \cdot u_{i_L} \cdot d_i(\vec{C})$$
$$a' = a + \sum_{i=1}^{n} ac_i \cdot u_{i_a} \cdot d_i(\vec{C})$$
$$b' = b + \sum_{i=1}^{n} bc_i \cdot u_{i_b} \cdot d_i(\vec{C})$$

The algorithm starts with all weights set to $\frac{1}{n}$, and then iteratively makes random changes, and computes the fitness function to see if the new set of weights is better than the previous one. The fitness function works according to the leave-one-out cross validation strategy. This means the algorithm is used n times, and one patch is left out of the calibration each time. The value of the remaining patch is calibrated each time, and the output of the fitness function is the average of colour distances ΔE^*_{00} from the calibrated patch colour value to the reference colour value.

The second weight coefficient $d_i(\vec{C})$ is a function of the colour being calibrated. The colour patches which are further away in the colour space are weighted less than those nearby. The CIE ΔE^*_{94} formula was used, since the colour differences are expected to be large, which makes the use of CIE ΔE^*_{00} inappropriate.

Calibration with a linear combination

This calibration method computes each calibrated component as a linear combination of the old component values in CIE Lab. Again, the task is to find the coefficients where the distance between the calibrated patches and their respective reference values is minimal.

$$\vec{C} = (L, a, b), \quad \overrightarrow{C'} = (L', a', b')$$
$$L' = L \cdot u_{L_1} + a \cdot u_{a_1} + b \cdot u_{b_1} + u_1$$
$$a' = L \cdot u_{L_2} + a \cdot u_{a_2} + b \cdot u_{b_2} + u_2$$
$$b' = L \cdot u_{L_3} + a \cdot u_{a_3} + b \cdot u_{b_3} + u_3$$

The meaning of components a and b in CIE Lab is the balance between red and green, and yellow and blue. We can add some more strength to the method by choosing different coefficients for the positive and negative side of the a and b axes:

$$u_{a_n}(a) = \begin{cases} u^+_{a_n} & a > 0, \\ 0 & a = 0, \\ u^-_{a_n} & a < 0; \end{cases}$$
$$u_{b_n}(b) = \begin{cases} u^+_{b_n} & b > 0, \\ 0 & b = 0, \\ u^-_{b_n} & b < 0; \end{cases}$$

As shown later, this improves the results somewhat, but since it is still a linear transformation there should be no problems with skewing the colour space. The exception would be if the colour value of some patch deviated greatly from the reference values. This could be avoided by leaving out the patches which deviate the most. However this could lead to overfitting, or bad calibration results in cases, where some part of the colour space on the captured photograph really was quite far from the reference values. The method for calibration with a weighted average is more robust against this kind of problem.

Apart from this, we have only noticed one more interesting glitch, later found not to be limited to this method. The cyan patch found in the third row of the ColorChecker calibration chart has Lab values which fall outside the range of colours presentable in the RGB colour system which is used in digital photography. This means there is some colour clamping upon conversion from CIE Lab back to RGB. We have noticed this effect on an image which had strong JPEG compression artifacts, which the clamping had amplified. If the RGB colour system supported a wider range, the red component of RGB would need to be negative, but this issue is not too problematic, since the CIE ΔE^*_{00} distance between the actual and clamped value is only 2.2, and the application performs the calculations and user readouts in the CIE Lab colour space, so the glitch was noticeable only on screen, and upon saving back to JPEG.

User interface

The application user interface is simple and contains only the necessary components for swift, accurate and repeatable colour analysis. The interface was built using the Scala Swing library. In figure 5 the original photograph can be seen on the left including annotation points for the colour charts ColorChecker, and Creative Enhancement Target. On the right side the colour calibrated photo with some manually added annotations is shown. The results of colour analysis at these points and areas are presented in the text field on the right. Additionally the photograph metadata and annotation data can be saved to a file. To ease working with the calibrated photograph, we can choose to hide the original photograph.

If the user only wants to check particular photograph colour values, they can click on the desired points. If the shift key is held when moving the mouse pointer around the photograph, the colour values under the mouse cursor are continually printed out on the right. An area on the photograph can be selected holding the control key and dragging the mouse. The application then prints the average colour value and percentage of coverage of individual Munsell colour values. In the annotation mode colour values of currently selected points and areas are printed out on the right side.

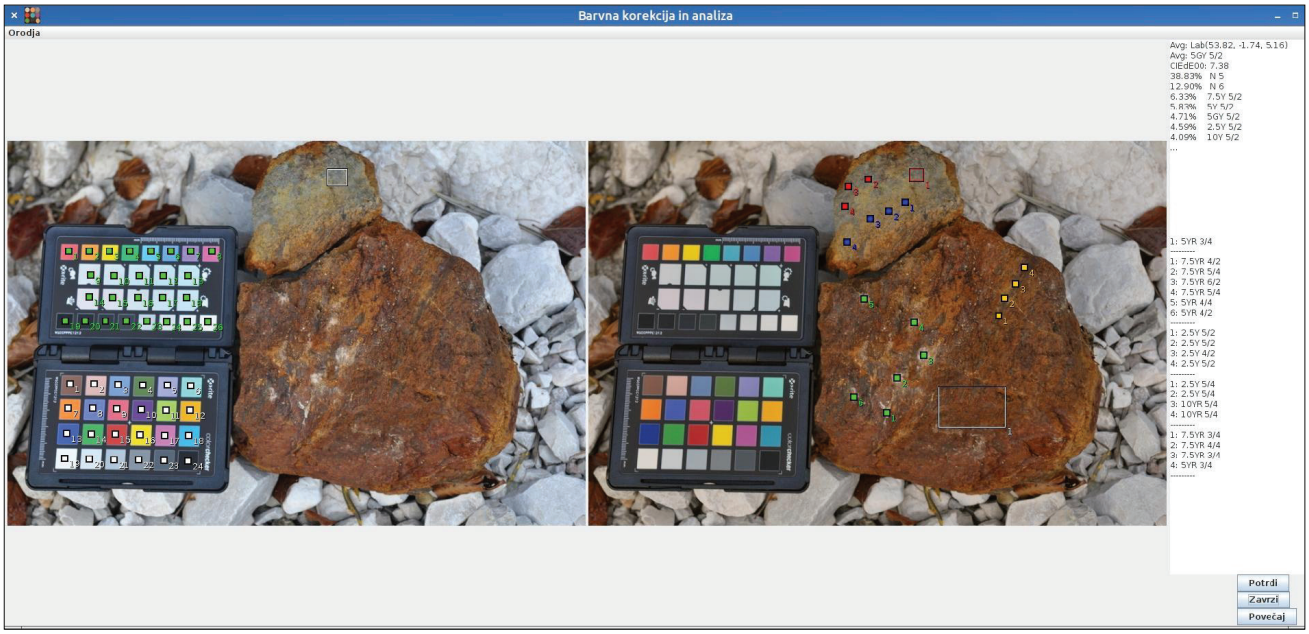

Fig. 5 User interface of the developed application.

Results

Measuring the accuracy of colour calibration

A good colour calibration is necessary to precisely determine the colour values. Therefore we evaluated the accuracy of the calibration procedure. We estimated the accuracy with statistical analysis of deviations between measured and reference colour values of two colour charts. We first compiled a statistic for the ColorChecker colour chart. This could be problematic as this data also served as the basis of fitting the parameters for the calibration procedure. In the case of a too strong fit (overfitting), we would not be able to detect it. Therefore we chose to additionally evaluate the colour deviations on the upper eight patches of the Creative Enhancement Suite (CET) colour chart. We have to reiterate that the reference colour values used for CET colour chart are not provided by the colour chart manufacturer, which could cause deviations. However, the deviations should be small since the values we use were acquired with accurate spectrophotometric measuring (Myers, 2010).

We used two sets of digital photographs for evaluation. The first set contains 40 different photographs taken under non-controlled conditions – outdoors (field work) and indoors – and therefore contains a mixture of different light conditions (direct sunlight, cloudy weather, indirect lighting in shadows, camera flash, indoor lighting etc.) taken with a variety of digital photographic cameras.

The second set of photographs contains 10 digital photographs, which were taken using the geological sample collection of Faculty of Natural Sciences and Engineering, University of Ljubljana. This set of photographs was taken under good lighting conditions on a white surface using camera flash illumination. Both sides of the colour chart (ColorChecker and CET) were positioned and lit as consistently as possible in every photograph.

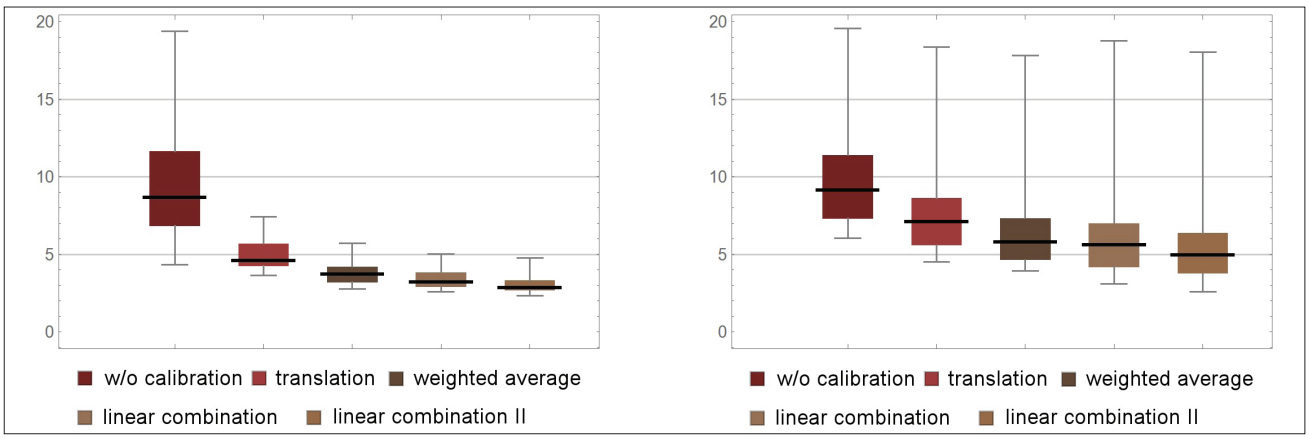

Fig. 6. Boxplot of deviation from reference colour values (0) on ColorChecker (left) in CET (right) colour charts for photographs captured under outdoor field work conditions.

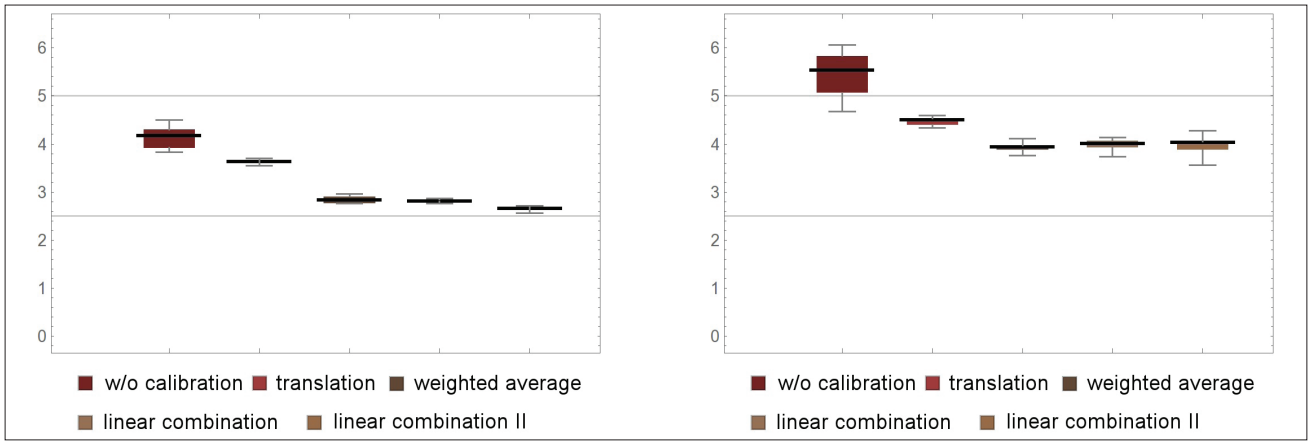

Fig. 7. Boxplot of deviation from reference colour values (0) on ColorChecker (left) in CET (right) colour charts for photographs captured under laboratory conditions.

As we can see in figures 6 and 7 the colour calibration lowers deviations and distances in almost every case and thus enhances the quality of colour information. First column in the figures represents the distances of measured uncalibrated colour values from the reference values. Other columns show colour distances after different colour calibration procedures, which were presented in the colour calibration section.

In the photos captured in non-controlled conditions we can see a large difference between the values shown on the left and right in Figure 6. This is likely the consequence of different illumination on the two colour charts in the photographs, therefore we once again stress the importance of uniform lighting, i.e. usage of additional lighting or camera flash when photographing. For photographs taken under laboratory conditions in figure 7 the colour deviations between detected and reference values are much lower and the interval is narrower. It is interesting that all values, even in the uncalibrated first column on the left graph in figure 7 are lower compared to the right graph in figure 7. This may be the consequence of deviation between the official values for ColorChecker colour chart and the unofficial values for the CET colour chart.

On the basis of the above measurements of deviation from the reference values, we can assess that by using the proposed computer-aided method under good lighting conditions we can calibrate colours almost as precise as an average human being can differentiate between different shades of colours (Mahy et al., 1994). Moreover for photographs captured in non-controlled conditions, we can greatly improve the quality of colour information.

Comparative analysis

In the second part of the evaluation we compared the results of manual colour analysis of rock samples by students of geology using a Munsell Rock-color Chart. From the geological rock sample collection of Department of geology of Faculty of Natural Sciences and Engineering, University of Ljubljana, we selected 10 rock samples (Table 1) and photographed them on a level white surface using camera flash (Fig. 8). Captured images were colour calibrated with the second linear combination procedure, which performed best in the assessment. Then we selected and determined the colour values of representative parts of each sample using the application.

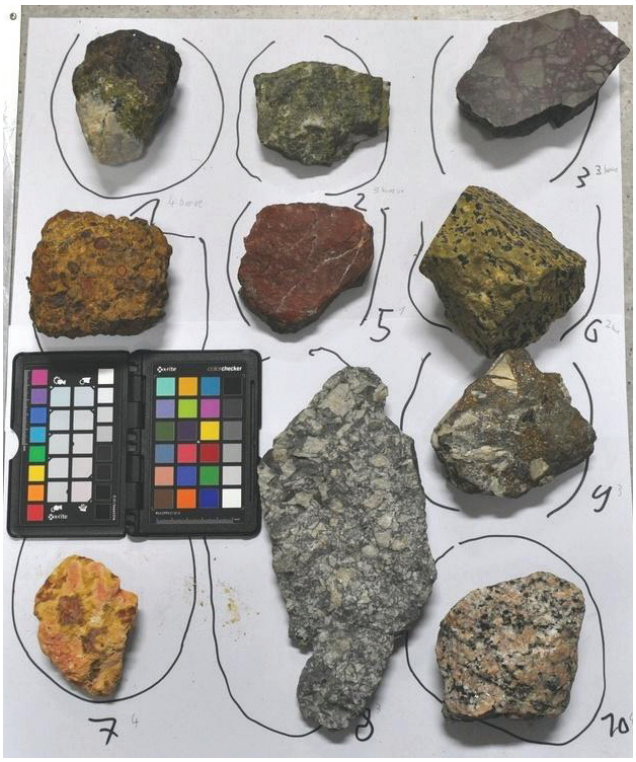

Fig. 8. Rock samples that were colour analysed in the comparison experiment.

With the help of eight volunteer geology students we conducted an experiment. We enumerated and put 10 rock samples on the laboratory table and we specified how many different colours have to be determined for each sample (Fig. 8). The students were instructed to determine the set number of colours based on the importance and colour coverage using their domain knowledge. The students had the

appropriate experiences for the task, since they have already been trained to determine colour using comparison methods in laboratory and outdoor field working conditions. It turned out that not every student determined the colours on the same part of the multi-coloured rock samples and consequently the order and colour labels did not match. The result is somewhat worse compared to the expected precision of colour value discrimination precision of the average human. The experiment has shown that the selection of measuring points on rock surface is subjective. In some cases it was difficult to infer which part of rock is described by a given colour value. Table 1 summarizes the determined colour labels for all samples. The last column shows the average of average CIE ΔE00* distance between the determined colour values in each group.

Table 1. Results of manual comparative rock colours determination on selected rock samples. From high average distances between individual readings it is obvious the subjective selection of the points of observation/comparison by the observers.

no.	sample	colour - mineral composition	estimated compared colours, number of students with the same estimation in brackets	average of average intermeasure distances in CIE
1	mineralised skarn – contact-metamorphic rock	white – calcite	5Y 8/1 (3), N8 (3), 5GY 8/1, N7	8.71
		green – epidote	10Y 5/4 (5), 10Y 7/4 (2), 10Y 6/6	8.79
		red – granate	10R 2/2 (2), 10R 3/4, 5YR 3/4, 5R 2/2, 10R 6/2	16.97
		black – ore mineral magnetite	N2 (5), N3 (2), 5Y 2/1	5.23
2	hidrothermaly altered fine-grained magmatic rock	white – quartz	5Y 8/1 (2), N9 (2), 5B 9/1, 5G 8/1, N7, N8	11.88
		dark green – chlorite	10GY 5/2 (3), 10G 4/2 (2), 10Y 4/2	8.65
		light green – epidote	5GY 7/4 (3), 10Y 6/6 (2), 10Y 5/4, 5GY 7/2	10.39
3	mercury ore in carbonate host rock from the Idrija mine	red – cinnabarite	5R 3/4 (4), 5R 2/6 (2), 5R 4/6 (2)	7.60
		grey – dolomite	5Y 6/1 (4), 5Y 6/2, 5Y 4/1, N7, N5	10.96
		black – pirobitumen	N1 (4), 5R 3/4, 10YR 2/2, 5GY 4/1	14.80
4	aluminium ore – bauxite	brown – goethite	N2, N3 (2), N4, 10YR 2/2 (2), 5YR 3/2 (2),	10.35
		yellow – lepidokrokite	10R 6/2, 5YR 5/6 (2), 10YR 6/6 (2), 10YR 8/6, 10YR 5/4, 5YR 2/2	20.22
		red – hematite	5R 4/6, 10R 3/4 (5), 10R 8/2, 10R 4/6	15.13
5	red hematitized limestone	red: hematite in limestone build of calcite; white: vein of pure calcite	10R 3/4 (3), 5R 4/6 (2), 5R 3/4 (2), 10R 5/4	8.76
6	chrome ore	green – serpentinite	10Y 5/4 (3), 10Y 7/4 (2), 5Y 7/6, 5Y 4/4, 5Y 6/4	13.36
		black – ore mineral chromite	N2 (4), N1, 5Y 2/1, 5G 2/1	6,53
7	aluminium ore	brown pigment– goethite	10R 6/6 (2), 10R 7/4 (5), 5R 6/6	5.81
		yellow pigment – lepi-dokrokite	5Y 8/4, 10YR 8/6 (7)	2.17
		red pigment – hematite	10R 4/6, 5R 6/6, 10R 3/4 (5), 10R 5/4	12.05
8	carbonate host rock mineralised with lead and zinc	black – ore mineral galenite	N5 (3), N4 (2), N3 (2), 5G 4/1	10.96
		brown – ore mineral sphalerite	5Y 8/1 (5), 5GY 8/1 (2), N9	5.71
		white – dolomite	5Y 7/2 (3), 5Y 6/1 (2), 5GY 8/1 (2)	8.18
9	silicified carbonate rock mineralised by zinc	brown – ore mineral sphalerite	5Y 5/2, 10YR 6/6 (4), 5YR 3/4, 10YR 2/2, 5YR 5/6	18.75
		white – dolomite partly replaced by quartz	5Y 8/1 (2), N5, N7, 5G 8/1, 10YR 4/2, 5Y 6/1 (2)	18.80
10	coarse - grained igneous rock	white – plagioclase	N9 (7), 5Y 8/1	3.37
		pink – K feldspath	5R 7/4, 10R 8/2, 5R 8/2, 5YR 8/4, 10R 7/4 (2), 5YR 6/4, 5YR 8/4	10.24
		grey – quartz	N5 (2), N6 (2), N7 (3), 5Y 8/1	11.48
		black – biotite	N1 (4), N2 (3), 5G 2/1	5.45

Sample no. 3 is the only cut and polished sample. The values for red agree well, however for grey and black the students chose less saturated hues, i.e. purer grey and black. A possible explanation for this is that the surrounding red colour influenced the students' perception of grey and black. Such phenomena of human visual perception are acknowledged by Sharma & Bala, 2002. We chose sample no. 5 for its relatively uniform coloration and therefore we instructed the students to determine only one colour value – in this case the subjectivity of choosing the measuring location is smaller. Samples no. 4 and 9 proved to be problematic as the students chose many different colour values. Sample no. 9 was problematic for the application as well since it contains small fragments of brown mineral sphalerite which somewhat reflects light – in this case it would be better to photograph the sample without using the flash and in a very high resolution to be able to analyse individual fragments. It would be necessary to examine and determine the optimal conditions for photographing samples that are reflecting light to different degrees.

Let us name a few other problems we noticed during the experiment. One of the students turned the colour chart the other way around and read the wrong colour values, however he noticed the mistake after finishing the first sample and corrected the results. One of the noted colour values was not a valid value in the Munsell system. Two of the students marked two different rock samples with the same number, however we managed to determine which sample they belong to in both cases by examining the remaining data. Some samples were missing a few of the colour values and there was one sample with one value more than the requested number of values. When transcribing the written data into the computer we made a few mistakes that were identified and corrected after proofreading. Colour analysis with the help of the application would solve most of the subjective causes for problems.

If we count the number of measures for each sample we can see that every colour is on average represented by four different Munsell colour values. If all the students took the measures on the same points of the rock sample and if we eliminate some of the other errors that occurred in the data, the average would likely be reduced. However, it is necessary to stress that the students were motivated volunteers who did the colour determinations in a well-lit room. We believe that the values acquired during field work would be much more varied, since we have to take into account the weather, and changing light conditions.

Discussion

Estimation of colour value and colour coverage for multicoloured objects in geology is very subjective especially in field work due to lack of time and unpredictable weather and lighting conditions. Objectivity is higher when these parameters are estimated on the samples brought from field work to the laboratory, where there are fewer time constraints and the lighting conditions are better. Moreover there is no precipitation, humidity is low and there is less chance to make the colour chart dirty or otherwise degrade its quality. The presented computer application is useful in both environments. During field work it enables very quick acquisition of the observed object's colours information, while the analyses can be done later in the laboratory or office with the use of the proposed application when there is more time available.

The computer application also substantially enhances and improves the work in the laboratory.

We propose to include colour calibrated photographs into the archives along with the samples or other objects of observation.

Further development of the application can take several directions. We can implement it as a web and/or mobile application suited for field work use. Digital photography is inexpensive and enables photographic documentation of all important rock outcrops on the route of field observation, which could result in several hundred observed outcrops and samples daily. With the synchronous capture of digital photographs of rocks outcrops and samples combined with the GPS coordinates the user can map rock colour variability in the area.

In areas where rock colour is distinctive of a specific part of the lithostratigraphic succession (lithostratigraphic unit) we can use the quality rock colour information as basic lithology recognition parameters, which in turn enable us to construct geological maps together with the use of structural and tectonic elements.

For further processing of the acquired data we can use additional statistical approaches (e.g. clustering) and with the help of crowdsourcing we can build a database containing colours of rock and mineral types, which could aid computer rock identification.

The proposed method is most useful for recognition of lithostratigraphic units, which contain varieties of clastic sedimentary and mixed carbonate-clastic sedimentary rock varieties. We believe that most of such lithostratigraphic units could be distinguished and recognised on the basis of the proposed method of colour analysis.

Conclusions

Munsell Rock-color Chart and Munsell Soil-color Chart for soils have already been used for precise comparative determination of rock and mineral colours for some decades. Determining colour values of multicoloured rocks in the field with the manual method is very time consuming

and consequently expensive. This is especially so in detrimental weather conditions when colour charts could get wet and/or dirty, making comparison inconvenient and can severely degrade the quality of the standard chart used for comparison. Conventional colour charts are relatively expensive, so every additional purchase in order to replace a dirty chart is an additional unplanned cost.

In search for the best compromise between time used for colour determination and quality of colour determination for multicoloured objects, each observer chooses their own set of representative points. This was found to be more or less subjective and did not necessarily result in colour values, which were representative for the observed outcrop or for a rock fragment, taking into account the surface area of a specific colour.

Surface colour representation and coverage is often very subjectively estimated. Determination of colour surface coverage on the basis of a statistically representative number of evenly distributed points on the analysed surface is too time consuming and consequently too expensive and usually omitted. This results in subjectivity and an incorrect estimation of various visible rock characteristics.

Digital cameras have become a standard tool for documenting geological and other field observations. Besides various other information found in digital photographs, they can be also used as an objective source of colour values and their areal coverage on the captured objects, if the digital photographs are properly calibrated.

To provide fast, objective and repeatable colour values determination we have developed a computer application, which provides automatic colour calibration of digital photographs on the basis of a standard colour chart ColorChecker, systematically added onto the photographed surface. It automatically identifies colours within the Munsell colour system, and calculates colour surface/areal representativity coverage and logs the details of executed analyses (positions of measured points and areas saved along with calibrated images).

For digital photograph colour calibration we implemented the detection of the ColorChecker and Creative Enhancement Suite colour charts, which are a part of the ColorChecker Passport produced by the X-Rite Company. It is easy to add support for any other models or types of colour charts, if needed, as the used approach for detection and calibration is general and can be used for any of them.

We have implemented four methods for computer colour calibration, which use evolutionary algorithms to determine the best coefficients for each method.

Methods for colour calibrations have improved the quality of colour information on practically all the digital photographs used in the assessment. In some test photographs, taken in non-controlled conditions, there was quite a big deviation of colour values from the reference values for the Creative Enhancement Target, which was not used in calibration (fig. 6). The deviation is likely a consequence of uneven natural lighting, so it is necessary that during the capture of the digital photographs, the colour chart and the outcrop, rock or any other object of photography, is as evenly illuminated as possible (e.g. by using camera flash). The test photographs were taken in very varied conditions on purpose, so the effectivity of the method could be tested.

The assessment results of the colour calibration methods we implemented also show that under laboratory conditions the colour distances from reference colour values are low and around the limit which still can be recognised by human vision. For the photographs taken under non-controlled conditions the average colour distances are larger, but still quite low and within acceptable limits.

Results of the comparison between the proposed automatic and the existing manual/comparative methods have shown, that manual/comparative colour determination is subjective and error-prone, even in stable laboratory conditions with no time pressure and with optimal lighting conditions.

The user interface of the developed computer application enables colour value determination at selected points and calculation of colour value coverage and average colour of a broader selected area. Selected annotation points and areas, and the detail of calibration are saved inside the metadata of photographs, which enables full repeatability, and verifiability of the analyses at a later date.

The described method is not limited to the field of geology and can be used in other areas, where colour determinations and colour areal representativity determination is a common task and objects of observation are of appropriate size to add a calibration colour chart into the scene, for example in soil science, archeology, biology, architecture, painting, art history etc.

References

Agarwala, A., Agrawala, M., Cohen, M., Salesin, D. & Szeliski, R. 2006: Photographing long scenes with multi-viewpoint panoramas. ACM Trans. Graph., 25/3: 853–861, doi:10.1145/1141911.1141966.

Hastie, T., Tibshirani, R. & Friedman, J. 2009: The Elements of Statistical Learning: Data Mining, Inference, and Prediction, Second Edition, Springer.

Kelly, K. & Judd, D. 1976: Color: Universal Language and Dictionary of Names, U.S. Department of Commerce, National Bureau of Standards.

Lowe, D. 2004: Distinctive Image Features from Scale-Invariant Keypoints. International Journal of Computer Vision, 60/2: 91–110, doi:10.1023/B:VISI.0000029664.99615.94.

Lowe, D. 1999: Object recognition from local scale-invariant features. In 1150–1157, doi:10.1023/B:VISI.0000029664.99615.94.

Mahy, M., Van Eycken, L. & Oosterlinck, A. 1994: Evaluation of Uniform Color Spaces Developed after the Adoption of CIELAB and CIELUV. Color Research & Application, 19/2: 105–121, doi:10.1111/j.1520-6378.1994.tb00070.x.

McCamy, C.S., Marcus, H. & Davidson, J.G. 1976: A color-rendition chart. J. Appl. Photogr. Eng., 2/3: 95–99.

Munsell, A. 1905: A color notation, G. H. Ellis Company.

Myers, R.D. 2010: ColorChecker Passport Technical Review, revision 3.

RIT Munsell Color Science Laboratory Munsell Renotation Data. Internet: http://www.cis.rit.edu/research/mcsl2/online/munsell.php (3. 10. 2014)

Ruiz, J.F. & Pereira, J. 2014: The colours of rock art. analysis of colour recording and communication systems in rock art research. Journal of Archaeological Science, 50: 338–349, doi:10.1016/j.jas.2014.06.023.

Schanda, J. 2007: Colorimetry: understanding the CIE system, Wiley.

Scovanner, P., Ali, S. & Shah, M. 2007: A 3-dimensional sift descriptor and its application to action recognition. In: Proceedings of the 15th international conference on multimedia 357–360. MULTIMEDIA '07, New York, NY, USA: ACM, doi:10.1145/1291233.1291311.

Sharma, G. & Bala, R. 2002: Digital Color Imaging Handbook, Taylor & Francis.

Sharma, G., Wu, W. & Dalal, E.N. 2005: The CIEDE2000 color-difference formula: implementation notes, supplementary test data, and mathematical observations. Color research and application, 30/1: 21–30, doi:10.1002/col.20070.

Van Hurkman, A. 2013: Color correction handbook: professional techniques for video and cinema 2nd ed., Berkeley, CA, USA: Peachpit Press.

Vergauwen, M. & Van Gool, L. 2006: Web-based 3D reconstruction service. Mach. Vision Appl., 17/6: 411–426, doi:10.1007/s00138-006-0027-1.

X-Rite, Inc. 2009a: ColorChecker Passport User Manual. Internet: http://www.xrite.com/documents/manuals/en/ColorCheckerPassport_User_Manual_en.pdf (3. 10. 2014)

X-Rite, Inc. 2009b: Munsell Rock-color Charts with genuine Munsell color chips.

X-Rite, Inc. 2009c: Munsell Soil-color Charts with genuine Munsell color chips.

Yu, G. & Morel, J.M. 2011. ASIFT: An Algorithm for Fully Affine Invariant Comparison. Image Processing On Line 2011, doi:10.5201/ipol.2011.my-asift.

Nova knjiga

Goran Schmidt, 2015: **Slovenska rudarska poročila iz rudišča Belščica v Karavankah s preloma 18. in 19. stoletja za Sigismonda (Žiga) Zoisa.** *Diplomatični in kritični prepis, interpretacija v sodobni slovenščini in komentar poročil o delovanju rudnika Žirovnica, ki sta jih med letoma 1797 in 1805 pisala rudarska nadzornika Lukas in Vincenc Polc; v Dodatku Geslovnik s komentarjem.* Thesaurus memoriae Fontes 11, Zgodovinski inštitut Milka kosa ZRC SAZU, Ljubljana: 494 str.

O zgodovini rudarjenja na slovenskem ozemlju obstaja mnogo zapisov, a nova monografija postavlja visoka merila tudi tej tematiki. Dr. Goran Schmidt je s svojim sistematičnim pristopom tako arhivskih virov, kot tudi terenskih pregledov podal obsežen pregled o zgodovini, delovanju in tudi geologiji nekdanjega rudišča Belščica izpod Stola v Karavankah. Monografija je zastavljena pregledno, kjer avtor predstavi nekaj značilnosti takratnih Zoisovih rudnikov. Sledi predstavitev poročil o rudišču Belščica, kjer poizkuša avtor locirati tudi omenjane rudne jame in predstavi avtorje arhivskih poročil in njihovo obliko. V enem od poglavij avtor predstavi rudarska poročila tudi z vidika jezikoslovja.

Iz poročil je bilo mogoče razbrati izjemno veliko informacij, ki jih v publikaciji lahko prebiramo pod poglavji o organizaciji dela in delokrogih na rudišču. Sledijo zapisi o tehnologiji pridobivanja rude, od rudniških načrtov, rudniških jam in rovov, odkopnih tehnik ter vse do količine izkopane rude. V geološkem delu publikacije najdemo zanimiva stara poimenovanja posameznih rud, kamnin, lege rudnih teles kot tudi problematike vdorov vode in plinov v rudniških rovih. Posebno, kratko poglavje je namenjeno tudi rudniku Žirovnica, ki je eden redkih rudnikov z ohranjenimi arhivskimi podatki skozi celotni čas delovanja. Največji del publikacije obsegajo diplomatični prepisi in kritični prepisi poročil.

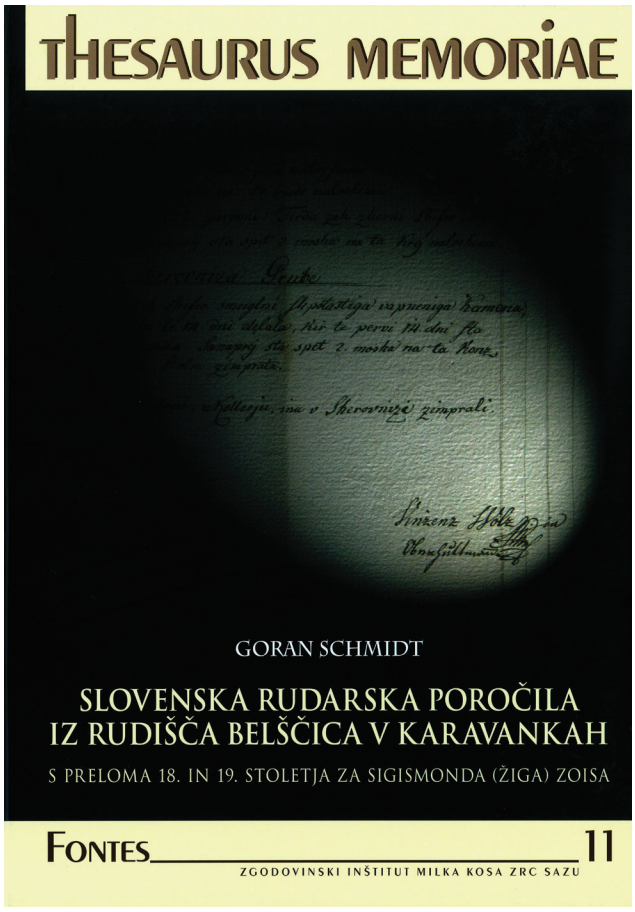

Pričujoča publikacija je opremljena tudi s slikovnimi dodatki, ki dejansko stanje rudarske dediščine najbolje izpričujejo fotografije zarušenih rovov in nekaterih drugih rudarskih del. Obsežnejšo slikovno gradivo bi pripomoglo k še boljši predstavitvi rudišča. Avtor je z nekaterimi sodelavci na koncu pripravil tudi geslovnik, kjer pojasnjuje mnoge posebne besede in besedne sklope in jih kritično opredeli. Prav geslovnik predstavlja izjemen prispevek k razumevanju in raziskovanju rudarske zgodovine, tudi nesnovne. Pregled literature in virov je obsežen, a še vedno pomanjkljiv, saj manjka nekaj pomembnejših avtorjev oziroma publikacij. Med njimi lahko izpostavimo dela Alfonsa Müllnerja, ki ni opisoval samo železarstva in rudnikov železa na Kranjskem, ampak tudi druge kovinske rudnike Kranjske v reviji Argo. Gotovo tudi geološka poročila Friedricha Tellerja in drugih geologov podajajo še več informacij o geološki zgradbi in zato lažji interpretaciji obdelanih poročil. Izmed kartografskih virov pa pogrešamo omembe Jožefinskih vojaških kart, nastalih med leti 1806-1869, kjer so na ozemlju pod Stolom natančno označene rudniške jame in rudišče.

Monografija *Slovenska rudarska poročila iz rudišča Belščica v Karavankah na prelomu 18. in 19. stoletja za Sigismonda (Žiga) Zoisa* gotovo ne bo edina izpod peresa dr. Gorana Schmidta, saj kot poznavalec deluje na tem področju vrsto let. Ta publikacija je dober pokazatelj pomanjkanja podobnih del v zelo pestri rudarski zgodovini, ki je že desetletja zapostavljena. Seveda je teoretični del potrebno nadgraditi in dokumentirati tudi z terenskimi podatki, kar je gotovo tudi želja avtorja monografije in drugih raziskovalcev, saj snovna dediščina rudarstva izjemno hitro izginja nazaj v nedrja narave.

Matija Križnar

GEOLOGIJA *58/2*, 262, Ljubljana 2015

8. Hidrogeološki kolokvij

Ljubljana 3. 12. 2015

Mihael BRENČIČ[1,2]

[1]Oddelek za geologijo, NTF, UL, Aškerčeva cesta 12, SI– 1000 Ljubljana;
email: mihael.brencic@ntf.uni-lj.si
[2]Geološki zavod Slovenije, Dimičeva ul. 14, SI–1000 Ljubljana

Tudi tokrat je hidrogeološki kolokvij potekal v soorganizaciji Katedre za aplikativno geologijo - Oddelka za geologijo Naravoslovnotehniške fakultete in Slovenskega komiteja mednarodnega združenja hidrogeologov – SKIAH, prav tako kot lani, tudi letos v tednu Univerze v Ljubljani. Dogodek je bil sestavljen iz dveh delov. V prvem delu so bile podeljene nagrade SKIAH, v drugem delu, imenovanem Rim po Rimu pa so bila predstavljena predavanja in tudi večina posterjev, ki so jih v mesecu septembru imeli slovenski hidrogeologi v Rimu, na 42. hidrogeološkem kongresu.

Z letošnjim letom je SKIAH uvedel podeljevanje nagrad za pomembne dosežke na področju hidrogeologije. Nagrado Franceta Drobneta za mladega hidrogeologa je prejela dr. Nina Rman z Geološkega zavoda Slovenije za svojo doktorsko disertacijo z naslovom »Analysis of the extraction of thermal water from low enthalpy geothermal resources in sedimentary basins: a case study of the Mura-Zala sedimentary basin« (Izkoriščanje termalne vode iz nizko entalpijskega geotermalnega vira v sedimentnem bazenu na primeru Mursko-zalskega sedimentnega bazena). Dr. Rman že ima zavidljivo raziskovalno bibliografijo, ki jo je na kratko povzela v predstavitvenem predavanju z nekoliko humornim naslovom »Odkrivanje tople vode ... «. Nagrado Dušana Kuščerja za življenjsko delo na področju hidrogeologije je prejel dr. Ljubo Žlebnik, ki je skoraj celotno svojo profesionalno kariero posvetil hidrogeologiji. Dr. Žlebnik sodi med pionirje kvantitativne hidrogeologije v Sloveniji, pomembno pa je zaznamoval tudi hidrogeologijo na območju nekdanje Jugoslavije. Ukvarjal se je z zelo širokim spektrom hidrogeoloških raziskav, med katerimi bi lahko izpostavili aplikativne raziskave za številne elektroenergetske objekte in regionalne hidrogeološke raziskave. Je tudi zelo plodovit pisec znanstvenih in strokovnih del, nekatera med njimi so danes za slovensko hidrogeologijo pomembna referenčna dela. Dr. Žlebnik je v zahvalnem govoru na kratko orisal svojo kareiro ter se ozrl na začetke izvajanja kvantitativnih terenskih poizkusov v kvartarnih vodonosnikih. Nagrade je podelil predsednik SKIAH mag. Zlatko Mikulič ob sodelovanju dr. Katice Drobne in Nuše Kuščer.

V drugem delu kolokvija so sledila štiri predavanja. Prvo predavanje z naslovom »Ocenjevanje obnovljive in razpoložljive količine podzemne vode za načrtovanje upravljanja voda« avtorjev Mikulič, Uhan, Janža in Andjelov, je predstavil mag. Zlatko Mikulič. V predavanju so bila predstavljena zakonodajna izhodišča za upravljanje s podzemno vodo na območju Slovenije in metodološki pristopi, ki se jih v Sloveniji uporablja za ocenjevanje količinskega stanja podzemne vode.

Drugo predavanje z naslovom »Geokemični procesi v podzemni vodi Velenjskega premogovnega bazena« avtorjev Kanduč, Samardžija, Grassa, Verbovšek, Vižintin, Supovec, Papež in Lenart, je predstavil dr. Timotej Verbovšek. Avtorji so se lotili podrobne analize geokemičnih značilnosti različnih podzemnih voda na širšem območju Velenja. Pri delu so bile uporabljene analize zelo širokega spektra, od klasičnih kemijskih analiz, do izotopskih analiz vode. Predstavljeni preliminarni rezultati kažejo na zelo raznoliko genezo in napajalno zaledje posameznih vodonosnikov.

Tretje predavanje z naslovom »Ranljivost vodnih virov z vidika podnebnih sprememb v jugovzhodni Evropi« avtorjev Čenčur Curk, Vrhovnik, Verbovšek, Corsini, Simonfy, Tahy, Dimkic, Nachtnebel, Hernegger, je predstavila dr. Barbara Čenčur Curk. Rezultati, ki jih je podala predavateljica so bili pridobljeni v okviru evropskega projekta CC-Ware, ki je potekal v okviru regionalne iniciative Jugovzhodna Evropa. Projekt se je ukvarjal z aktualno problematiko vpliva podnebnih sprememb na oskrbo s pitno vodo. Avtorji projekta so na podlagi različnih podnebnih scenarijev izdelali dolgoročne napovedi razpoložljivih količin pitne vode v vodnih virih na širšem prostoru jugovzhodne Evrope. Analize so pokazale, da so najbolj ranljive mediteranske države na jugu Evrope, države centralne Evrope, kot sta Slovenija in Avstrija, pa večjih problemov ne pričakujeta.

Četrto predavanje z naslovom »Regionalni tok podzemne vode v krasu« je predstavil dr. Mihael Brenčič. Pri toku podzemne vode v krasu še vedno obstajajo številni odpri problemi, ki so povezani z raztekanjem in koncentracijo odtoka. V predavanju so bila predstavljena teoretična izhodišča na podlagi katerih lahko nekatere značilnosti toka podzemne vode v krasu razložimo s pomočjo koncepta regionalnega toka in enotskega bazena po Tothu.

Dogodek je potekal v izredno sproščenem vzdušju h kateremu sta pomembno prispevala oba nagrajenca. Prav tako so predavanja in posterji, ki so jih slovenski hidrogeologi prestavili na hidrogeološkem kongresu v Rimu, pokazali, da je v Sloveniji hidrogeološka stroka zelo aktivna in da se lahko s svojimi rezultati enakovredno kosa s hidrogeološko stroko in znanostjo v tujini.

GEOLOGIJA *58/2*, 263-264, Ljubljana 2015

5. Svetovni geotermalni kongres v Melbournu (Avstralija)

19. – 24. 4. 2015

Dušan RAJVER

Geološki zavod Slovenije, Dimičeva ul.14, SI–1000 Ljubljana; e-mail: dusan.rajver@geo-zs.si

V Melbournu se je aprila 2015 v centru MCEC odvijal 5. svetovni geotermalni kongres. Melbourne je glavno mesto zvezne države Viktorija in drugo največje avstralsko mesto s 3,5 milijoni prebivalcev. Svetovni geotermalni kongresi se v organizaciji Mednarodnega geotermalnega združenja (IGA) odvijajo vsakih pet let. Prejšnji kongresi so bili leta 2010 v Indoneziji (Nusa Dua, Bali), leta 2005 v Turčiji (Antalya), leta 2000 na Japonskem (v krajih Beppu in Morioka), prvi pa leta 1995 v Italiji (Firence). Pred letom 1995 so se odvijali Mednarodni simpoziji o razvoju in izkoriščanju geotermalnih virov pod okriljem Združenih narodov. Prvi tovrsten simpozij je bil leta 1970 v Italiji (Pisa). Naslednji simpoziji so postali za svetovno javnost zanimivejši, saj so sledili prvemu svetovnemu naftnemu šoku leta 1973 in so šli vštric s pospešenim iskanjem alternativnih virov energije. Tako je leta 1975 sledil drugi simpozij v San Francisku. Leta 1980 svetovnega simpozija ni bilo. Leta 1985 in 1990 pa so pod okriljem ameriškega sveta za geotermalne vire (Geothermal Resources Council) organizirali Mednarodni simpozij o geotermalni energiji, obakrat na Havajih.

Tokratni kongres sta organizirali dve državi, Avstralija in Nova Zelandija, udeležilo se ga je okoli 1600 udeležencev, od tega 1300 na samem kongresu. Sosklicatelja kongresa sta bili državni geotermalni združenji Avstralije in Nove Zelandije, pod glavnim sponzorstvom filipinske družbe Energy Development Corporation, tema kongresa pa je bila: »Views from down under – geothermal in perspective« (»Pogledi od tam spodaj - geotermalna v perspektivi«). Nova Zelandija je danes s 1005 MW_e peta na svetu po instalirani moči geotermalnih elektrarn in s 7000 GWh v letu 2014 celo četrta na svetu po proizvedeni elektriki iz teh elektrarn, v neposredni rabi geotermalne energije pa je na prav tako odličnem 14. mestu (8621 TJ ali 2395 GWh v letu 2014). Avstralija ima sicer le eno elektrarno na geotermalno energijo, ki je razvita na principu »izboljšanega (spodbujenega) geotermalnega sistema« (EGS), z instalirano močjo 1,1 MW_e. V neposredni rabi geotermalne energije (194,4 TJ v letu 2014) pa je sicer šele na 52. mestu med 82 državami, ki so poročale o neposredni rabi, vendar z dobrimi pogoji za nadaljnjo rast. Lahko rečemo, da sta obe državi svetovni kongres upravičeno organizirali s primerno predstavitvijo sodobnega stanja v razvoju in izkoriščanju geotermalne energije.

Kongres je bil predvsem v primerjavi s tistim leta 2010 v Indoneziji nekoliko slabše obiskan zaradi velike oddaljenosti in s tem povezanih stroškov. Po drugi strani pa je bil letošnji kongres največji doslej po številu sprejetih referatov, s 30% porastom v številu le-teh glede na kongres leta 2010. To je rezultat širitve svetovne dejavnosti v raziskavah in rabi geotermalne energije, kakor tudi porasta v popularnosti kongresa samega. Za ta kongres je bilo sprejeto 1346 referatov iz 89 držav, od teh je bilo 1076 predavanj v 12 vzporednih sekcijah, 270 pa kot posterji.

Pod okriljem kongresa se je odvijalo več kratkih pred- in po-kongresnih tečajev (Gutiérrez-Negrín, 2015). Štirje od petih pred-kongresnih tečajev so se odvijali na Univerzi Victoria v Melbournu. To so bili: (1) – *Drilling, completion and testing of geothermal wells*, (2) – *Electricity generation from low-temperature geothermal resources*, (3) – *Reservoir engineering and reservoir management*, in (4) – *Scaling and corrosion in geothermal development*. Tečaj (5) – *Reducing drilling costs – from exploration to field management* je financirala Svetovna banka ter se je odvijal v Melbournu. Edini tečaj po kongresu *Geothermal policy and implementation – The New Zealand example* se je odvijal v Taupo-ju (Nova Zelandija). Aktualne geotermalne téme, izjemni predavatelji in aktivna izmenjava mnenj udeležencev tečajev je pripomogla k uspešnosti tečajev, kar je zelo dvignilo uspešnost kongresa v celoti. Pred kongresom sta bili izvedeni tudi dve strokovni ekskurziji, 4-dnevna v državi Victoria in 1-dnevna v okolici Melbourna, po kongresu pa še tri 3-dnevne ekskurzije po severnem otoku Nove Zelandije.

Kongres v Melbournu je bil priča ponovnega zagona v geotermalnem razvoju, če primerjamo stanje le tega v obdobju treh mejnikov (tabela 1). Od kongresa WGC 2005 dalje je skupno 88 držav prikazalo oz. poročalo o izkoriščanju geotermalne energije: za proizvodnjo elektrike ali za neposredno rabo ali za oboje. Več podrobnosti o stanju neposredne rabe in proizvodnje elektrike iz geotermalne energije pa sledi v bodočem članku.

Kam so osredotočeni glavni napori v raziskavah in razvoju, se vidi iz števila prevladujočih tém z vsaj 50 ali več referati na CD zborniku: geofizika (109), inženiring geotermalnih rezervoarjev (108), geokemija (99), raziskave (92), geologija (85), ocenitev virov (80), sedanje stanje izkoriščanja po državah (77), proizvodnja elektrike (74), EGS (59) in geotermalne toplotne črpalke (56). Znova se je izkazalo, da so posredne in površinske metode (geofizika, geokemija in geologija) zelo pomembne v raziskavah in upravljanju geotermalnih virov. Številni referati o raziskavah kažejo kako dejavno

Tabela 1. Stanje izkoriščanja geotermalne energije v svetu; navedena so leta, v katerih je bilo poročano na kongresih (Bertani, 2015; Lund & Boyd, 2015).

Leto	2005	2010	2015
		Proizvodnja elektrike	
Instalirana kapaciteta (MW_e)	8933	10716	12635
Proizvedena elektrika (GWh/leto)	55709	67246	73549
Koeficient izkoristka	0,71	0,72	0,72?
Število držav	23	24	26
		Neposredna raba	
Instalirana kapaciteta (MW_t)	28269	50583	70329
Izkoriščena energija (TJ/leto)	273372	438071	587786
Koeficient izkoristka	0,31	0,27	0,27
Število držav	72	78	82

je iskanje novih virov. Še nikoli ni bilo na kongresu toliko referatov osredotočenih na EGS sisteme, čeprav so poglavitne težave, vezane na vrtanje in stimulacijo rezervoarja, nekako zavlekle razvoj te tehnologije.

Glede izkoriščanja geotermalne energije v Sloveniji znaša instalirana kapaciteta za neposredno rabo skoraj 188 MW_t, letna izkoriščena geotermalna energija pa skoraj 1265 TJ ali 351,4 GWh (stanje na 31. dec. 2014), vključno z geotermalnimi toplotnimi črpalkami (posodobljeno po Rajver et al., 2015). Prispevek geotermalnih toplotnih črpalk znaša 120,6 MW_t oziroma 618 TJ/leto. Različne vrste uporabe zajemajo: individualno ogrevanje prostorov, daljinsko ogrevanje, klimatizacijo/hlajenje, ogrevanje rastlinjakov, kopanje in plavanje z balneologijo, taljenje snega ter geotermalne toplotne črpalke.

Iz Slovenije se je kongresa udeležil le pisec tega prispevka, ki je predstavil dva referata (Rajver et al., 2015a; Rajver et al., 2015b), ostala dva referata, v katerih so avtorji sodelavci Geološkega zavoda Slovenije, pa sta predstavila M. O'Sullivan iz univerze v Aucklandu oziroma G. Goetzl iz avstrijskega geološkega zavoda (Rman et al., 2015; Prestor et al., 2015). V centru MCEC je med kongresom potekala še razstava nekaterih najbolj znanih razvojnih inštitucij ter proizvajalcev in serviserjev raziskovalne in proizvodne opreme (za vrtine, cevovode, toplotne postaje, itd.) v geotermalnih raziskavah in razvoju ter izkoriščanju geotermalne energije. Naslednji svetovni geotermalni kongres bo leta 2020 na Islandiji, še prej pa bo septembra 2016 že naslednji evropski geotermalni kongres v Strasbourgu.

Viri

Bertani, R. 2015: Geothermal power generation in the World, 2005-2010 Update Report. Proceedings, World Geothermal Congress 2015, Melbourne, Australia, IGA, 19 p.

Gutiérrez-Negrín, L.C.A. 2015: The World Geothermal Congress 2015. IGA's Melbourne Declaration. IGA News, 100: 2–5.

Lund, J. W. & Boyd, T. L. 2015: Direct utilization of geothermal energy 2015 Worldwide review. Proceedings, World Geothermal Congress 2015, Melbourne, Australia, IGA, 31 p.

Prestor, J., Szőcs, T., Rman, N., Nádor, A., Černák, R., Lapanje, A., Schubert, G., Marcin, D., Benkova, K. &, Götzl, G. 2015: Benchmarking – Indicators of sustainability of thermal groundwater management. Proceedings, World Geothermal Congress 2015, Melbourne, Australia, IGA, 12 p.

Rajver, D., Prestor, J. & Tinti, F. 2015a: Comparison of geological and shallow geothermal characteristics of some Adriatic regions in the Circum-Adriatic countries (LEGEND project). Proceedings, World Geothermal Congress 2015, Melbourne, Australia, IGA, 15 p.

Rajver, D., Rman, N., Lapanje, A. & Prestor, J. 2015b: Geothermal development in Slovenia: Country update report 2010-20149. Proceedings, World Geothermal Congress 2015, Melbourne, Australia, IGA, 14 p.

Rman, N., Lapanje, A., Prestor, J., O'Sullivan, M.J. & Brenčič, M. 2015: Effects of regional production of thermal water on low-temperature geothermal aquifers in north-east Slovenia. Proceedings, World Geothermal Congress 2015, Melbourne, Australia, IGA, 11 p.

GEOLOGIJA *58/2*, 265-267, Ljubljana 2015

Akademik, zasl. prof. dr. Matija Drovenik – zadnje slovo

Z žalostjo in velikim spoštovanjem se poslavljamo od dragega profesorja, sodelavca, akademika in zaslužnega profesorja, doktorja znanosti. univ. inženirja rudarstva Matije Drovenika.

Življenje prof. dr. Matije Drovenika se je začelo v Ljubljani 14. februarja 1927. Tu je obiskoval osnovno šolo in gimnazijo. Kot sedemnajstletnega dijaka so ga julija 1944 zaradi sodelovanja v NOB aretirali in poslali v Nemčijo v taborišče Dachau in potem Rabstein. Po osvoboditvi se je vrnil domov in jeseni 1945 maturiral ter se vpisal na takratni Rudarski oddelek Tehniške visoke šole. Zaradi zanimanja za geološko stroko, znanja in vestnosti je že kot študent delal kot pomožni asistent na katedri za mineralogijo, petrografijo in nauk o rudiščih. Leta 1951 je prejel Prešernovo nagrado in naslednje leto z odliko diplomiral.

Leta 1953 je začel pot rudnega geologa v vzhodni Srbiji v Boru. Stik s slovensko geološko stroko je ohranjal s pisanjem člankov, predvsem o borskem rudišču, v reviji Geologija. Za delo Prispevek k poznavanju kamnin Timočkega eruptivnega masiva mu je 1960 ljubljanska univerza priznala habilitacijo in mesto univerzitetnega učitelja. Ker pa v Ljubljani ni imel stanovanja, je z družino ostal v Boru. Leta 1961 je na Univerzi v Ljubljani doktoriral z delom Geološko-petrološka študija širše okolice rudnika Bor (Vzhodna Srbija). Ko so istega leta v Boru ustanovili rudarsko-metalurško fakulteto, se je zaposlil kot izredni profesor in bil hkrati glavni geolog borskega bazena. Svoje znanje je preverjal in dopolnjeval na obiskih v tujini – v Franciji, Bolgariji, Sovjetski zvezi, Romuniji in Nemčiji. Med letoma 1963 in 1965 je bil v Alžiriji svetnik v direkciji za rudarstvo in geologijo.

Po vrnitvi v Slovenijo se je zaposlil na ljubljanski univerzi na takratni Fakulteti za naravoslovje in tehnologijo (FNT). Postal je predstojnik Inštituta za geologijo FNT ter strokovni sodelavec Geološkega zavoda in RUDIS-a. Leta 1970 je bil izvoljen za izrednega profesorja za predmete Mikroskopiranje rud in premogov, Raziskovanje in ocena nahajališč mineralnih surovin ter Teksture in strukture rud. Raziskovalno se je posvečal metalogenezi Slovenije, zlasti rudišču Idrija. Za razpravo o pogojih nastanka tega rudišča je skupaj z Ivanom Mlakarjem leta 1973 prejel nagrado Sklada Borisa Kidriča. Zvest pa je ostal tudi raziskovanju petrogeneze in orudenja v Boru. Bil je med prvimi geologi, ki so nastanek orudenj ugotavljali s takrat popolnoma novo metodo stabilnih žveplovih izotopov.

Kot mednarodno priznani strokovnjak je leta 1967 proučeval bakrova rudišča v Čilu in Kolumbiji. S sodelavci je sestavil program za raziskovanje polimetalnih rudišč v Pontidih v Turčiji in kasneje tudi sam sodeloval pri raziskavah na tem območju. Leta 1973 je bil gost Nacionalne akademije znanosti ZDA, kjer se je seznanjal s pogoji nastanka ter geološko zgradbo bakrovih, svinčevo-cinkovih ter molibdenovih rudišč. Med leti 1972 in 1976 je večkrat obiskal severnoitalijanska in avstrijska Pb-Zn rudišča in jih primerjal z orudenjem v Mežici.

Od ustanovitve Raziskovalne skupnosti Slovenije se je ukvarjal z organizacijo znanstveno-raziskovalnega dela na področju geologije. Bil je pobudnik raziskovalnega projekta Mezozoik v Sloveniji, ki je bil takrat največji združevalni geološki projekt pri nas. Leta 1971 je bil predsednik organizacijskega komiteja 2. mednarodnega simpozija o rudnih nahajališčih v Alpah in bil naslednje leto izvoljen za svetnika Društva za geologijo mineralnih nahajališč (Society for Geology Applied to Mineral Deposits). Istega leta je postal tudi član uredniškega odbora revije Geologija.

Leta 1977 je bil prvič in leta 1982 ponovno izvoljen v naziv rednega profesorja. Leta 1978 je postal dopisni in 1987 redni član SAZU v razredu za naravoslovne vede. Med letoma 1992 in 1999 je bil glavni tajnik SAZU.

V mnogočem je oral strokovno ledino. Med drugim je v Sloveniji vzpostavil delovanje Unescovega Mednarodnega programa za vede o Zemlji IGCP (International Geologic Correlation Programme). Bil je prvi predsednik nacionalnega odbora IGCP in ga je uspešno vodil celih 20 let, od leta 1978 pa vse do 1997. Ves čas si je prizadeval za vključitev čim večjega števila mladih raziskovalcev v projekte IGCP, predvsem pa za pravično razdeljevanje skromnih finančnih sredstev za mednarodno sodelovanje med vse raziskovalce. Zavedal se je, da geologija nima nacionalnih meja, in da je drobce spoznanj o našem planetu potrebno neprekinjeno združevati v enoten svetovni mozaik. Svoje bogato znanje in izkušnje je kot namestnik vodje mednarodnega projekta ter kot koordinator za Slovenijo skupaj s sodelavci vtkal v projekt IGCP št. 6: Korelacija diagnostičnih značilnosti rudišč baznih kovin v dolomitih in apnencih. Poleg tega je sodeloval še v treh projektih IGCP. Delo je v soavtorstvu z M.

Pleničarjem in F. Drovenikom okronal z monografijo Nastanek rudišč v SR Sloveniji, ki predstavlja katekizem za mikroskopijo rudnih mineralov pri nas. Kot rezultat tega dela je Oddelku za geologijo in vsem prihajajočim generacijam študentov zapustil neprecenljivo zbirko poliranih preparatov. Sistematizirani so po nahajališčih in poleg slovenskih predstavljajo tudi številna tuja rudišča. Prof. dr. Matija Drovenik je ostal častni član nacionalnega odbora IGCP do konca.

Akademik zaslužni prof. dr. Matija Drovenik je napisal 52 znanstvenih člankov, pet učbenikov, bil mentor dvema doktorandoma, trem magistrantom in 16 diplomantom. Poleg tega ni nikdar odrekal pomoči diplomantom pri drugih mentorjih.

Za svoje delo je prejel številna priznanja – red dela z zlatim vencem, plaketo Rudarsko-topilniškega bazena Bor, zahvalnico Tehniške fakultete v Boru, Univerze v Beogradu, Zoisovo plaketo ter Lipoldovo plaketo Geološkega zavoda Slovenije.

Profesor Drovenik je rad pripovedoval o doživetjih iz svojega vsebinsko polnega življenja; iz časov svojega dela v borskem rudniku, iz strokovnih potovanj po štirih celinah, obiskov mnogih mineralnih nahajališč in znanstvenih inštitucij po svetu. V izjemnem spominu mu je ostalo izpopolnjevanje v Parizu pri mineralogu Jeanu Orcelu. Poudarjal je, koliko mu dolguje. O nečem pa ni rad govoril, o svoji izkušnji iz nacističnih taborišč. »V lagerju je bilo tako hudo«, je dejal nekoč, »da tega ni mogoče povedati - in ne pozabiti. Čeprav bi si to želel«.

Življenje mu tudi v nadaljnjem ni prizanašalo z bolečimi udarci usode. Po vrnitvi v Ljubljano iz Alžirije je umrl v cvetu let sin Matiček. Od te tragične izgube si vsa družina ni nikoli več povsem opomogla. Bolečina je bila prehuda. Vendar se Matija ni vdal, ni popustil. V življenju je hudo vračal z dobrim. V vsem svojem delovanju, od pedagoškega dela, znanstvenega raziskovanja, administrativnih dolžnosti v šoli, stanovskih organizacijah, vodenja raziskovalne dejavnosti, Unescovih geoloških programov, do reševanja povsem osebnih težav kolegov in študentov, se je izrazito odlikoval po delavnosti, občutku za pravičnost, natančnost, inovativnost in nepristranskost. Za njegove dosežke ga je UL imenovala za zaslužnega profesorja. O njegovem zavzemanju za etiko v raziskovalni dejavnosti priča tale zgled, ki zadeva njegov zadnji znanstveni članek o Boru iz leta 2006. V njem je, prizadet zaradi tamkajšnjega nekritičnega privzetja modela borskega nahajališča od drugod, tega argumentirano zavrnil na osnovi svojih rezultatov, pridobljenih s skrbnim proučevanjem geoloških razmer v rudišču. Poštenje v znanosti pomeni izvajati zaključke samo iz nepristransko pridobljenih, preverjenih opazovanj. V tem duhu je vzgajal tudi svoje študente. O uspešnosti priča bogata bera njihovih odličnih raziskovalnih in drugih delovnih dosežkov. Marsikakšna pedagoška in raziskovalna ureditev, ki jo je vzpostavil, živi dalje, marsikaj pa se je obrnilo drugače, kot si je zamislil, zlasti pozneje, ko se je upokojil.

Med svojimi študenti je bil eden najbolj priljubljenih profesorjev; pa ne toliko zaradi snovi same, kolikor zaradi žara in jasnosti s katerima je predaval, prizadevajoč si, da bi ga lahko vsi razumeli in mu sledili. Redki so bili, ki jih njegovo navdušenje ni prevzelo. Izredno nevsiljivo je znal ohranjati ravnotežje med sproščenim, rahlo humornim vzdušjem ter potrebno akademsko resnostjo. Kolikokrat se je med predavanji, ko je prišel do imena kakšnega kraja, ustavil in nas povprašal – pa veste kje je Chuquicamata? Seveda nismo vedeli, in že je hitel risati po tabli obris Južne Amerike in dodal še lastne izkušnje iz obiska tega dela sveta. Suhoparni podatki so se spremenili v zanimivo zgodbo in znanje se je kar samo usedlo v naše glave. V nas je znal vzbuditi zanimanje za opazovanje, povezovanje in razmišljanje. Pri mikroskopiji rud smo komaj čakali, da nam dodeli težji preparat in nam s tem da priznanje, da je opazil, koliko smo že sposobni videti in razumeti. Verjetno nihče od nas nikoli ne bo pozabil skritega mackinawita. Čeprav smo ga izredno spoštovali, se ga nismo nikoli bali. Prej nas je bilo sram, če ob vsem žaru in predanosti, ki ju je vložil v predavanja in vaje, nismo pokazali zadostnega znanja. Do nas se nikoli ni obnašal le kot profesor, prej kot blag, a strog in pravičen oče. Ko je neke mrzle zime odpovedalo centralno ogrevanje in se je mikroskopirnica spreminjala v ledenico, vaj seveda ni odpovedal, poskrbel pa je, da so nam postregli s čajem.

Kljub čedalje hujšim zdravstvenim težavam zaradi zahrbtne bolezni se je še do pred nekaj leti ukvarjal z znanstvenim delom na področju svoje priljubljene vede - geologije mineralnih nahajališč.

Bolezen je napredovala, izgubil je tudi življenjsko družico, gospo Majdo. Obolél za pljučnico, je 30. oktobra 2015 za vedno zaprl svoje trudne oči. Končalo se je bogato življenje vélikega človeka.

Profesor Drovenik bo vedno ostal prisoten v spominu vseh, ki nas je učil, njegovo bogato znanje pa je našlo pot tudi do novih generacij. Za seboj je zapustil sled, ki je čas ne more izbrisati. Njegovo delo bo ostalo priča vélikega raziskovalca.

Nina Zupančič
Simon Pirc
Mirka Trajanova

Akademik prof. dr. Matija Drovenik – pomembnejša tiskana bibliografija

Drovenik, M. 1953: O izvoru rudnih mineralov v borskem rudišču. Geologija, 1: 225–242.

Drovenik, M. 1955: Kontaktno metamorfni pojavi in orudenenje območja Potoj Čuka - Valja Saka. Geologija, 3: 151–180.

Drovenik, M. 1958: Bakrovo rudišče Gornja Lipa. Geologija, 4: 63–78, 2 karti.

Drovenik, M. 1959: Prispevek k poznavanju kamenin timočkega eruptivnega masiva. Geologija, 5: 11–30.

Drovenik, M. & Sclar, Ch. B. 1960: Lazarevićite, a new cubic copper - arsenic sulfide from Bor, Jugoslavia. Bulletin of the Geological Society of America, 71: 1050–9747.

Drovenik, M. 1961: Geološko-petrološka studija širše okolice Rudnika Bor, vzhodna Srbija. Doktorska disertacija, Ljubljana: 344 str.

Drovenik, M., Antonijević, I. & Mičić, I. 1962: Novi pogledi na magmatizam i geološku gradju Timočke eruptivne oblasti. Vesnik. Serija A, Geologija, 20: 67–92.

Drovenik, M. 1966: Mineralni sastav i geneza odlomaka sa bakarskim sulfidima u piroklastitima šire okoline rudnika Bor. Rudarsko-metalurški zbornik, 13: 407–427.

Drovenik, M., Djordjević, M., Antonijević, I. & Mičić, I. 1967: Les rôches magmatiques de la région éruptive de Timok. Acta geologica Hungarica, 11: 115–129.

Drovenik, M. 1968: Psevdomorfoze rudnih mineralov po rastlinskih drobcih v bakrovem rudišču Škofje. Rudarsko-metalurški zbornik, 15: 141–146.

Drovenik, M. 1968: Razvoj magmatskih in piroklastičnih kamenin v okolici bakrovega rudišča Bor. Geologija, 11: 5–127.

Drovenik, M., Leskovšek, H., Pezdič, J. & Štrucl, I. 1970: Izotopska sestava žvepla v sulfidih nekaterih jugoslovanskih rudišč. Rudarsko-metalurški zbornik, 17: 153–173.

Mlakar, I. & Drovenik, M. 1971: Strukturne in genetske posebnosti idrijskega rudišča. Geologija, 14: 67–126.

Drovenik, M. 1972: Prispevek k razlagi geokemičnih podatkov za nekatere predornine in rude Slovenije. Rudarsko-metalurški zbornik, 19: 145–167.

Drovenik, F. & Drovenik, M. & Grad, K. 1972: Kupferführende Gödener Schichten Sloweniens. Geologija, 15: 95–107.

Mlakar, I. & Drovenik, M. 1972: Geologie und Vererzung der Quecksilberlagerstätte Idrija. Geologija, 15: 47–62.

Drovenik, M., Leskovšek, H. & Pezdič, J. 1974/75: Izotopski sastav sumpora o rudnim ležištima Timočke eruptivne oblasti. Rudarsko-metalurški zbornik, 21: 319–362.

Drovenik, M., Čar, J. & Strmole, D. 1975: Langobardske kaolinitne usedline v idrijskem rudišču. Geologija, 18: 107–155.

Drovenik, M., Duhovnik, J. & Pezdič, J. 1976: Izotopska sestava žvepla v sulfidih rudnih nahajališč v Sloveniji. Rudarsko-metalurški zbornik, 23/ 2–3, 193–246.

Drovenik, M. 1978: Mikroskopiranje rud in premogov. 1. del, Mikroskopiranje rud.: FNT, VTOZD Montanistika, Ljubljana, Odsek za geologijo, 198 str., ilustr., graf. prikazi.

Drovenik, M. 1978: Mikroskopiranje rud in premogov: tabele za določevanje mineralov v odsevni svetlobi. FNT, VTOZD Montanistika, Ljubljana, Odsek za geologijo, 45 str.

Drovenik, M. 1978: Mikroskopiranje rud in premogov. 2. del, Mikroskopiranje premogov. FNT, VTOZD Montanistika, Odsek za geologijo, Ljubljana: 84 str., ilustr., graf. prikazi.

Drovenik, M. 1979: Prilog poznavanju geneze bakrovih ležišta i rudnih pojava u crvenim permskim peščarima SR Slovenije i SR Srbije: II. deo. Rudarsko-metalurški zbornik, 26: 363–382.

Drovenik, M., Štrucl, I. & Pezdič, J. 1980: Izotopska sestava žvepla v svinčevo-cinkovih nahajališčih severnih Karavank: Del II. Rudarsko-metalurški zbornik, 27: 413–436.

Drovenik, M. 1979: Prilog poznavanju geneze bakrovih ležišta i rudnih pojava u crvenim permskim peščarima SR Slovenije i SR Srbije: I. deo. Rudarsko-metalurški zbornik, 26: 139–153.

Drovenik, M. & Pezdič, J. 1980: Izotopska sestava žvepla v rudnih mineralih svinčevo-cinkovega nahajališča Sasa. Rudarsko-metalurški zbornik, 27: 241–47.

Drovenik, M., Štrucl, I. & Pezdič, J. 1980: Izotopska sestava žvepla v svinčevo-cinkovih nahajališčih severnih Karavank: Del I. Rudarsko-metalurški zbornik, 27: 179–197.

Drovenik, M., Pleničar, M. & Drovenik, F. 1980: Nastanek rudišč v SR Sloveniji. Geologija, 23/1: 1–157.

Drovenik, M., Duhovnik, J. & Pezdič, J. 1981: Cinkovo-svinčevo rudišče Zavrh. Rudarsko-metalurški zbornik, 28: 152–276.

Drovenik, M. 1981: Mineral deposits in Permian and Triassic beds of Slovenia (Yugoslavia). V: Schneider, H.J. (ur.): Mineral deposits of the Alps and of the Alpine epoch in Europe: proceedings of the IV. ISMIDA, Berchtesgaden, October 4-10, Special publication of the Society for Geology Applied to Mineral Deposits, Berlin, 3: 9.

Drovenik, M. 1983: Ali je bakrovo rudišče Bor res nastalo v zgornjekrednem vulkanskem kompleksu? Rudarsko-metalurški zbornik, 30: 139–149.

Drovenik, M., Pezdič, J. & Rakić, S. 1983: Izotopska sestava žvepla v piritu iz vrtine ZB-24 Plavica, Zletovsko-kratovsko vulkansko območje. Rudarsko-metalurški zbornik, 30: 69–76.

Drovenik, M. 1984: Nekaj misli k razpravam o triadnih magmatskih kameninah na Slovenskem. Rudarsko-metalurški zbornik, 31: 335–384.

Drovenik, M. 1984: Mineral deposits of Permian beds of Slovenia, Yugoslavia. Permophiles, 8: 5–6.

Drovenik, M. 1984: Nahajališča premogov, nafte in zemeljskega plina. VDO Fakulteta za naravoslovje in tehnologijo, VTOZD Montanistika, Ljubljana, III, 94 str., IV, 129 str., ilustr.

Drovenik, M. 1984: Nahajališča mineralnih surovin. Fakulteta za naravoslovje in tehnologijo, Ljubljana, IV, 375 str., ilustr.

Drovenik, M. 1985: Significance of the Triassic igneous-tectonic activity for the origin of the Slovenian mineral deposits (Pomen triadne magmatsko-tektonske aktivnosti za nastanek rudišč v Sloveniji. V: Grafenauer, S., Pleničar, M. & Drobne, K (ur.): Zbornik Ivana Rakovca, Slovenska akademija znanosti in umetnosti, Razprave, 26: 343–360.

Drovenik, M. 1985: O anhidritu iz bakrovega ležišča Bor. Rudarsko-metalurški zbornik, 32: 173–194.

Drovenik, M. & Pungartnik, M. 1987 Nastanek cinkovo-svinčevega rudišča Topla in njegove značilnosti. Geologija, 30: 245–314.

Drovenik, M. 1988: Dodatek k „Sistematski mineralogiji". Ljubljana: Fakulteta za naravoslovje in tehnologijo, VTOZD Montanistika,. 70 str., ilustr.

Drovenik, M., Pezdič, J. & Pungartnik, M. 1988: Izotopska sestava žvepla v sulfidih cinkovo svinčevega rudišča Topla. Razprave, 29: 113–128.

Drovenik, M. 1989: Pomen Idrije za vedo o rudiščih. Idrijski razgledi, 34/1–2: 12–16, ilustr.

Skaberne, D. & Drovenik, M. 1988: Tirkiz in halloysit iz bakrovega rudišča Veliki Krivelj, vzhodna Srbija. Rudarsko-metalurški zbornik, 35/1–4: 37–41.

Drovenik, M., Dolenec, T., Režun, B. & Pezdič, J. 1990: O živosrebrovi rudi iz rudnega telesa Grübler v Idriji. Geologija, 33, 397–446.

Drovenik, M. 1992: Prispevek k poznavanju rudnih klastov iz rudnega telesa Novo okno v bakrovem rudišču Bor. Geologija, 35: 287–318, ilustr.

Mlakar, I., Skaberne, D. & Drovenik, M. 1992: O geološki zgradbi in orudenju v karbonskih kameninah severno od Litije. Geologija, 35: 229–286.

Drovenik, M. 2005: Origin of Bor and other copper deposits in its surroundings (east Serbia) Razprave, 46/1: 5–81, ilustr., fotogr., tab., graf. prikazi.

Drovenik, M. & Grafenauer, S. 2010: Letopis Slovenske akademije znanosti in umetnosti, (1922-2010), 61: 220–222, portret.

Navodila avtorjem

GEOLOGIJA objavlja znanstvene in strokovne članke s področja geologije in sorodnih ved. Revija od leta 2000 izhaja dvakrat letno. Članke recenzirajo domači in tuji strokovnjaki z obravnavanega področja. Ob oddaji člankov avtorji predlagajo **tri recenzente**, vendar pa si uredništvo pridržuje pravico do izbire recenzentov po lastni presoji. Avtorji morajo članek popraviti v skladu z recenzentskimi pripombami ali utemeljiti zakaj se z njimi ne strinjajo.

Avtorstvo: Za izvirnost podatkov, predvsem pa mnenj, idej, sklepov in citirano literaturo so odgovorni avtorji. Z objavo v GEOLOGIJI se tudi obvežejo, da ne bodo drugje objavili prispevka z isto vsebino.

Jezik: Članki naj bodo napisani v angleškem, izjemoma v slovenskem jeziku, vsi pa morajo imeti slovenski in angleški izvleček. Za prevod poskrbijo avtorji prispevkov sami.

Vrste prispevkov:

Izvirni znanstveni članek
Izvirni znanstveni članek je prva objava originalnih raziskovalnih rezultatov v takšni obliki, da se raziskava lahko ponovi, ugotovitve pa preverijo. Praviloma je organiziran po shemi IMRAD (**I**ntroduction, **M**ethods, **R**esults, **A**nd **D**iscussion).

Pregledni znanstveni članek
Pregledni znanstveni članek je pregled najnovejših del o določenem predmetnem področju, del posameznega raziskovalca ali skupine raziskovalcev z namenom povzemati, analizirati, evalvirati ali sintetizirati informacije, ki so že bile publicirane. Prinaša nove sinteze, ki vključujejo tudi rezultate lastnega raziskovanja avtorja.

Strokovni članek
Strokovni članek je predstavitev že znanega, s poudarkom na uporabnosti rezultatov izvirnih raziskav in širjenju znanja.

Diskusija in polemika
Prispevek, v katerem avtor ocenjuje ali dokazuje pravilnost nekega dela, objavljenega v Geologiji, ali z avtorjem strokovno polemizira.

Recenzija, prikaz knjige
Prispevek, v katerem avtor predstavlja vsebino nove knjige.

Oblika prispevka: Besedilo pripravite v urejevalniku Microsoft Word. Prispevki naj praviloma ne bodo daljši od 20 strani formata A4, v kar so vštete tudi slike, tabele in table. Le v izjemnih primerih je možno, ob predhodnem dogovoru z uredništvom, tiskati tudi daljše prispevke.

Članek oddajte uredništvu vključno z vsemi slikami, tabelami in tablami v elektronski obliki po naslednjem sistemu:
- *Naslov članka (do 12 besed)*
- *Avtorji (ime in priimek, naslov, e-mail naslov)*
- *Ključne besede (do 7 besed)*
- *Izvleček (do 300 besed)*
- *Besedilo*
- *Literatura*
- *Podnaslovi k slikam in tabelam*
- *Tabele, Slike, Table*

Citiranje: V literaturi naj avtorji prispevkov praviloma upoštevajo le tiskane vire. Poročila in rokopise naj navajajo le v izjemnih primerih, z navedbo kje so shranjeni. V seznamu literature naj bodo navedena samo v članku omenjena dela. Citirana dela, ki imajo DOI identifikator, morajo imeti ta identifikator izpisan na koncu citata. Za citiranje revije uporabljamo standardno okrajšavo naslova revije. Med besedilom prispevka citirajte samo avtorjev priimek, v oklepaju pa navajajte letnico izida navedenega dela in po potrebi tudi stran. Če navajate delo dveh avtorjev, izpišite med tekstom prispevka oba priimka (npr. Pleničar & Buser, 1967), pri treh ali več avtorjih pa napišite samo prvo ime in dodajte et al. z letnico (npr. Mlakar et al., 1992). Citiranje virov z medmrežja v primeru, kjer avtor ni poznan, zapišemo (Internet 1). V seznamu literaturo navajajte po abecednem redu avtorjev.

Imena fosilov (rod in vrsta) naj bodo napisana poševno, imena višjih taksonomskih enot (družina, razred, itn.) pa normalno. Imena avtorjev taksonov naj bodo prav tako napisana normalno, npr. *Clypeaster pyramidalis* Michelin, *Galeanella tollmanni* (Kristan), Echinoidea.

Primeri citiranja članka:

Mali, N., Urbanc, J. & Leis, A. 2007: Tracing of water movement through the unsaturated zone of a coarse gravel aquifer by means of dye and deuterated water. Environ. geol., 51/8: 1401–1412, doi:10.1007/s00254-006-0437-4.

Pleničar, M. 1993: *Apricardia pachiniana* Sirna from lower part of Liburnian beds at Divača (Triest-Komen Plateau). Geologija, 35: 65–68.

Primer citirane knjige:

Flügel, E. 2004: Mikrofacies of Carbonate Rocks. Springer Verlag, Berlin: 976 p.

Jurkovšek, B., Toman, M., Ogorelec, B., Šribar, L., Drobne, K., Poljak, M. & Šribar, Lj. 1996: Formacijska geološka karta južnega dela Tržaško-komenske planote – Kredne in paleogenske kamnine 1: 50.000 = Geological map of the southern part of the Trieste-Komen plateau – Cretaceous and Paleogene carbonate rocks. Geološki zavod Slovenije, Ljubljana: 143 p., incl. Pls. 23, 1 geol. map.

Primer citiranja poglavja iz knjige:

Turnšek, D. & Drobne, K. 1998: Paleocene corals from the northern Adriatic platform. In: Hottinger, L. & Drobne, K. (eds.): Paleogene Shallow Benthos of the Tethys. Dela SAZU, IV. Razreda, 34/2: 129-154, incl. 10 Pls.

Primer citiranja virov z medmrežja:

Če sta znana avtor in naslov citirane enote zapišemo:
Čarman, M. 2009: Priporočila lastnikom objektov, zgrajenih na nestabilnih območjih. Internet: http://www.geo-zs.si/UserFiles/1/File/Nasveti_lastnikom_objektov_na_nestabilnih_tleh.pdf (17. 1. 2010)

Če avtor ni poznan zapišemo tako:
Internet: http://www.geo-zs.si/ (22. 10. 2009)

Če se navaja več enot z medmrežja, jim dodamo še številko
Internet 1: http://www.geo-zs.si/ (15. 11. 2000)
Internet 2: http://www.geo-zs.si/ (10. 12. 2009)

Slike, tabele in table: Slike (ilustracije in fotografije), tabele in table morajo biti zaporedno oštevilčene in označene kot sl. 1, sl. 2 itn., oddane v formatu TIFF, JPG ali EPS z ločljivostjo 300 dpi. Le izjemoma je možno objaviti tudi barvne slike, vendar samo po predhodnem dogovoru z uredništvom. Obvezno je treba upoštevati zrcalo revije **172 x 235 mm**. Večjih formatov od omenjenega zrcala GEOLOGIJE ne tiskamo na zgib, je pa možno, da večje oziroma daljše slike natisnemo na dveh straneh (skupaj na levi in desni strani) z vmesnim »rezom«. V besedilu prispevka morate omeniti vsako sliko po številčnem vrstnem redu. Dovoljenja za objavo slikovnega gradiva iz drugih revij publikacij in knjig, si pridobijo avtorji sami. Table pripravite v formatu zrcala naše revije.

Če je članek napisan v slovenskem jeziku mora imeti celotno besedilo, ki je na slikah in tabelah tudi v angleškem jeziku. Podnaslovi naj bodo čim krajši.

Korekture: Te opravijo avtorji člankov, ki pa lahko popravijo samo tiskarske napake. Krajši dodatki ali spremembe pri korekturah so možne samo na avtorjeve stroške.

Prispevki so prosto dostopni na spletnem mestu: http://www.geologija-revija.si/

Oddajanje prispevkov:

Avtorje prosimo, da prispevke pošljejo na naslov uredništva:
GEOLOGIJA
Geološki zavod Slovenije
Dimičeva ulica 14, 1000 Ljubljana
bernarda.bole@geo-zs.si ali urednik@geologija-revija.si

Uredništvo Geologije

Instructions for authors

Scope of the journal: GEOLOGIJA publishes scientific papers which contribute to understanding of the geology of Slovenia or to general understanding of all fields of geology. Some shorter contributions on technical or conceptual issues are also welcome. Occasionally, a collection of symposia papers is also published.
All submitted manuscripts are peer-reviewed by at least two specialists. When submitting their paper, authors should recommend at least **three reviewers**. Note that the editorial office retains the sole right to decide whether or not the suggested reviewers are used. Authors should correct their papers according to the instructions given by the reviewers. Should you disagree with any part of the reviews, please explain why. Revised manuscript will be reconsidered for publication.

Author's declaration: Submission of a paper for publication in Geologija implies that the work described has not been published previously, that it is not under consideration for publication elsewhere and that, if accepted, it will not be published elsewhere.

Language: Papers should be written in English or Slovene, and should have both English and Slovene abstracts.

Types of papers:

Original scientific paper
In an original scientific paper, original research results are published for the first time and in such a form that the research can be repeated and the results checked. It should be organised according to the IMRAD scheme (**I**ntroduction, **M**ethods, **R**esults, **A**nd **D**iscussion).

Review scientific paper
In a review scientific paper the newest published works on specific research field or works of a single researcher or a group of researchers are presented in order to summarise, analyse, evaluate or synthesise previously published information. However, it should contain new information and/or new interpretations.

Professional paper
Technical papers give information on research results that have already been published and emphasise their applicability.

Discussion paper
A discussion gives an evaluation of another paper, or parts of it, published in GEOLOGIJA or discusses its ideas.

Book review
This is a contribution that presents a content of a new book in the field of geology.

Style guide:
Submitted manuscripts should not exceed 20 pages of A4 format (12 pt typeface, 1 line-spacing, left justification) including figures, tables and plates. Only exceptionally and in agreement with the editorial board longer contributions can also be accepted.
Manuscripts submitted to the editorial office should include figures, tables and plates in electronic format organized according to the following scheme:
- *Title (maximum 12 words)*
- *Authors* (*full name and family name, postal address and e-mail address)*
- *Key words (maximum 7 words)*
- *Abstract (maximum 300 words)*
- *Text*
- *References*
- *Figure and Table Captions*
- *Tables, Figures, Plates*

References: References should be cited in the text as follows: (Flügel, 2004) for a single author, (Pleničar & Buser, 1967) for two authors and (Mlakar et al., 1992) for multiple authors. Pages and figures should be cited as follows: (Pleničar, 1993, p. 67) and (Pleničar, 1993, fig. 1). Anonymous internet resources should be cited as (Internet 1). Only published references should be cited. Manuscripts should be cited only in some special cases in which it also has to be stated where they are kept. Cited reference list should include only publications that are mentioned in the paper. Authors should be listed alphabetically. Journal titles should be given in standard abbreviated form. A doi identifier, if there is any, should be placed at the end as shown in the first case.
Taxonomic names should be in italics, while names of the authors of taxonomic names should be in normal, such as *Clypeaster pyramidalis* Michelin, *Galeanella tollmanni* (Kristan), Echinoidea.

Articles should be listed as follows:
Mali, N., Urbanc, J. & Leis, A. 2007: Tracing of water movement through the unsaturated zone of a coarse gravel aquifer by means of dye and deuterated water. Environ. geol., 51/8: 1401–1412, doi:10.1007/s00254-006-0437-4.
Pleničar, M. 1993: *Apricardia pachiniana* Sirna from lower part of Liburnian beds at Divača (Triest-Komen Plateau). Geologija, 35: 65–68.

Books should be listed as follows:
Flügel, E. 2004: Mikrofacies of Carbonate Rocks. Springer Verlag, Berlin: 976 p.
Jurkovšek, B., Toman, M., Ogorelec, B., Šribar, L., Drobne, K., Poljak, M. & Šribar, Lj. 1996: Formacijska geološka karta južnega dela Tržaško-komenske planote – Kredne in paleogenske kamnine 1: 50.000 = Geological map of the southern part of the Trieste-Komen plateau – Cretaceous and Paleogene carbonate rocks. Geološki zavod Slovenije, Ljubljana: 143 p., incl. Pls. 23, 1 geol. map.

Book chapters should be listed as follows:
Turnšek, D. & Drobne, K. 1998: Paleocene corals from the northern Adriatic platform. In: Hottinger, L. & Drobne, K. (eds.): Paleogene Shallow Benthos of the Tethys. Dela SAZU, IV. Razreda, 34/2: 129-154, incl. 10 Pls.

Internet resources should be listed as follows:
Known author and title:
Čarman, M. 2009: Priporočila lastnikom objektov, zgrajenih na nestabilnih območjih. Internet: http://www.geo-zs.si/UserFiles/1/File/Nasveti_lastnikom_objektov_na_nestabilnih_tleh.pdf (17. 1. 2010)
Unknown authors and title:
Internet: http://www.geo-zs.si/ (22.10.2009)

When more than one unit from the internet are cited they should be numbered:
Internet 1: http://www.geo-zs.si/ (15.11. 2000)
Internet 2: http://www.geo-zs.si/ (10.12. 2009)

Figures, tables and plates: Figures (illustrations and photographs), tables and plates should be numbered consequently and marked as Fig. 1, Fig. 2 etc., and saved as TIFF, JPG or EPS files and submitted at 300 dpi. Colour pictures will be published only on the basis of previous agreement with the editorial office. The maximum size of full-page illustrations and tables is **172 x 235 mm**. Larger formats can only be printed as a double-sided illustration (left and right) with a cut in the middle. All figures should be referred to in the text and should normally be numbered in the sequence in which they are cited. The approval for using illustrations previously published in other journals or books should be obtained by each author.
When a paper is written in Slovene it has to have the entire text which accompanies illustrations and tables written both in Slovene and English. Figure and table captions should be kept as short as possible.

Proofs: One set of page proofs (as pdf files) will be sent by e-mail to the corresponding author. Corrections are made by the authors. They should correct only typographical errors. Short additions and changes are possible but should be paid by the authors.

Geologija is an open access journal, all pdfs can be downloaded from the website: http://www.geologija-revija.si/en/

Submission: Authors should submit their papers to the address of the editorial office:

GEOLOGIJA
Geological Survey of Slovenia
Dimičeva ulica 14, 1000 Ljubljana, Slovenia
bernarda.bole@geo-zs.si or urednik@geologija-revija.si

The Editorial Office

GEOLOGIJA

št.: 58/2, 2015
www.geologija-revija.si

ISSN 0016-7789

Geološki zavod Slovenije
Geological Survey of Slovenia
www.geo-zs.si